Accessing the Records of Methane Passage in Ancient Sediments

Ruth A. Martin

A dissertation
submitted in partial fulfillment of the
requirements for the degree of

Doctor of Philosophy

University of Washington

2010

Program Authorized to Offer Degree:
Department of Earth and Space Sciences

TABLE OF CONTENTS

LIST OF FIGURES

LIST OF TABLES

Acknowledgements

I gratefully acknowledge the support of the following people and organizations.

My supervisor, Liz Nesbitt, who is a treasured mentor, role model and friend.

Kathy Campbell, University of Auckland, also a treasured friend, who freely shared her enormous expertise in the field of methane seeps, and was responsible for organizing my trip to New Zealand.

Marta Torres, Oregon State University also for sharing her formidable knowledge of the subject and providing inspiration through example.

Many others who collaborated and/or advised on various aspects of this work, including

Gary Klinkhammer, Oregon State University
Jens Greinert, Royal Netherlands Institute for Sea Research
Stefan Sommer, Matthias Haeckel, Peter Linke, IFM Geomar, Kiel, Germany

The members of my committee

Jody Bourgeois
Roger Buick
Eric Steig
Debbie Kelley

all of whom brought much to the table and contributed to my growth as a scholar.
Ron Eng for camaraderie.

Charlotte Schreiber for her willingness to read and critique much of this dissertation.

Andy Schauer, David Mucciarone, Andy Ungerer, Jude Swales and Ed Hare for their expert assistance with geochemical analyses, illustrations and SEM imaging.

Funding sources

University of Washington Department of Earth and Space Sciences

Geological Society of America

Cushman Foundation for Foraminiferal Research

American Association of Petroleum Geologists

North American Micropaleontologic Society

German Ministry of Education (BMBF)

Marsden Fund Council, the Royal Society of New Zealand

And, of course, the many un-named friends and colleagues who helped make this such an amazing experience.

DEDICATION

This dissertation is dedicated to my heroes, with deepest gratitude

My beloved husband, Gerald Martin

My awesome children and their equally awesome spouses and children

Caroline, Pete, Noah and Riley

Eliza, Alexis and Gabbie

Jessica and Jayson

David and Elizabeth

My wonderful parents

John and Ruth Stenmark

My also wonderful siblings and niece

Pam, John, Sally, Torrey

Chapter 1. Introduction

The problem investigated in this study is:
How is the passage of methane recorded in marine sediments, and how do we access the archives?

The goal of this project was to use integrated data from the tests of foraminifera and authigenic carbonates, both fossil and Recent, as a proxy to unravel the history of methane influence on marine sediments, particularly near the sediment/water interface.

Specific objectives were to:

1. assess the interaction of foraminifera and seep-fluids with respect to foraminiferal assemblages and biomineralization;
2. integrate carbon and oxygen isotope data from foraminifera and authigenic carbonates in order to form a more complete picture of fluid-flow and methane sources within the sediments;
3. use SEM imaging and Mg/Ca ratios to identify and characterize diagenetic alterations that may be caused by seep fluids.

The hypothesis driving the study is that foraminifera respond to the presence of methane-influenced fluids through changes in the species composition of their assemblages and in the isotopic and geochemical composition of their calcium carbonate shells. The latter may be in their primary mineralization, or as nucleation centers for the deposition of inorganic carbonate during early diagenesis.

Hydrocarbons accumulate in the Earth's geosphere and are released into the oceans and atmosphere, driven by geologic and tectonic events that modify the character of sedimentary basins over time. On marine continental margins, faulting and over-pressured sedimentary pore-fluids can initiate fluid movement from depth to manifest as seafloor hydrocarbon seepages or frozen methane-ice (gas hydrates). Cold hydrocarbon seeps are receiving a great deal of international attention for a number of reasons. Gas hydrates are implicated in submarine slope instability as hydrates form and dissociate, resulting in slumping, landslides, or "frost-heave"

effects (Paull et al., 1996; Maslin et al., 1998). Dissociation of methane hydrates on a global scale has been implicated as a possible cause of sudden climate change (Kennett et al., 2003; Hill et al., 2004). The extreme high sulfide, low oxygen environments of cold seeps also support luxurious and unique ecosystems that yield valuable insights into adaptations in these environments and possibly the beginnings of life on Earth (Sassen and MacDonald, 1998; Levin, 2005). The economic community also has a robust interest in cold seeps as it seeks new, commercially viable, environmentally sustainable energy sources.

An understanding of the mechanisms of formation and transport of hydrocarbon-influenced fluids is critical to all of the above endeavors. The Cascadia Margin in the eastern Pacific and the Hikurangi Margin off the east coast of North Island, New Zealand are two of six margins world-wide (the others are in western Indonesia, the Makran coast of Pakistan and Iran, Barbados, and the eastern Aleutians) that have developed anomalously thick sedimentary sequences and have older parts of the sedimentary sequence preserved on-shore. They are, therefore, ideal for the investigation of the timing and spatial distribution of hydrocarbon accumulation and migration. For this investigation, material from Recent seeps from the Hikurangi Margin and fossil seeps from the Cascadia margin accretionary prism is being used to establish a baseline and test the usefulness of the proxy in the fossil record.

1.1 Cold hydrocarbon seeps and associated processes

1.1.1 Cold seeps

Cold hydrocarbon seeps are seafloor sites of H_2S- and CH_4-rich fluid flow generally at ambient temperatures resulting from the accumulation and burial of organic matter. They are ubiquitous on continental margins, occurring in widespread and diverse geologic settings from shallow to deep water in active and passive tectonic regimes. Cold methane seeps in the modern marine environment were first reported from carbonate cements in barrier and beach sands of the Chandeleur Islands off the Louisiana coast (Roberts and Whelan, 1975).

Subsequently, dense communities of organisms resembling those found at hydrothermal vents were observed at active seepage areas along the base of the Florida Escarpment (Paull et al., 1984) and in subduction-related settings offshore of Oregon and Washington (Suess et al., 1985). Since then, modern seeps have been described from most continental shelves, especially from localities around the Pacific Rim. Fossil seeps are also now well-known from marine sedimentary strata of Europe, Japan, California, and Washington (Majima et al. 2005; Campbell, 2006) (Figure 1.1).

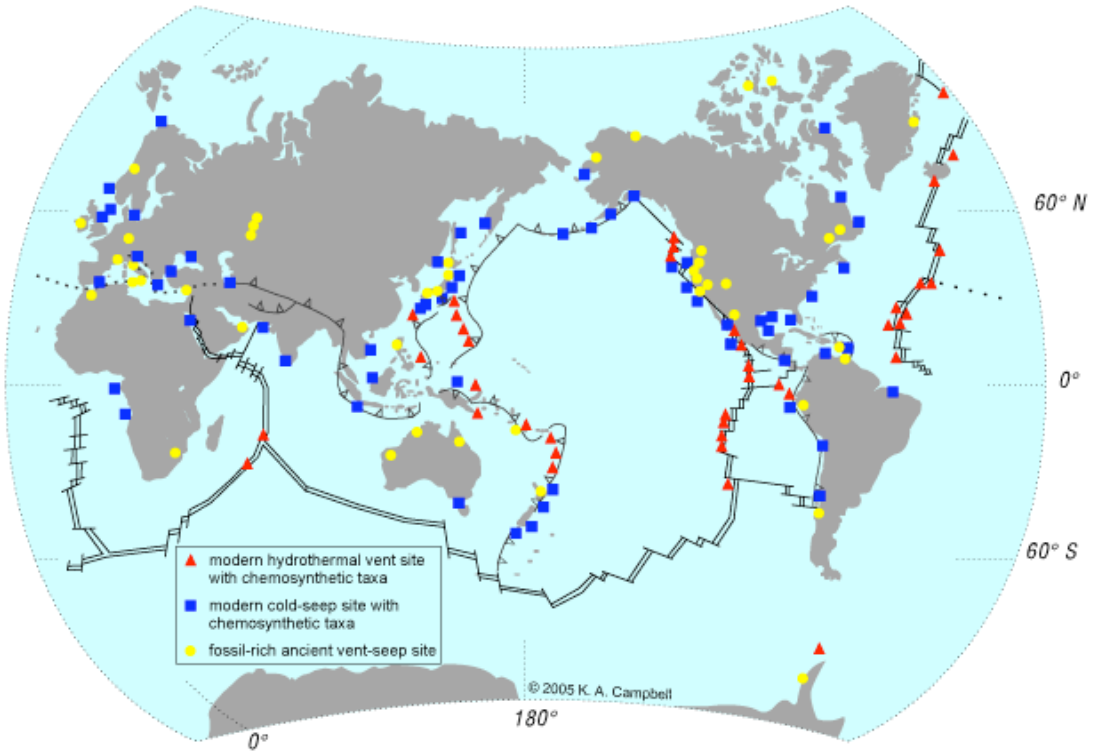

Figure 1.1. Global distribution of hydrothermal vents, cold seeps and fossil seeps and vents. Note cold seeps distributed along all types of tectonic margins. Used with permission of K.A. Campbell.

Methane in the marine environment can be generated microbially, thermogenically, or abiogenically. Methanogenesis can take place at various depths in the sediment, in many cases only a few centimeters below the sediment-water interface (Claypool and Kaplan, 1974). When sediment overpressuring, changes in

sea level or tectonic regime, or altered deposition rates occur, accumulated hydrocarbons migrate through the sediments along faults, through permeable sediments, via diapirs or other pathways to be released into the oceans and atmosphere. Before reaching the sediment/water interface, however, the majority of methane gas is oxidized by a consortium of methane-oxidizing archaea and sulfate-reducing bacteria. This process is extremely efficient; less than 5% of the methane generated in submarine sediments is discharged into the water column (Sommer et al., 2006).

Migration of hydrocarbons through sediment can leave behind robust geological signatures. Where temperature and pressure conditions are favorable, gas hydrates form in the sediments, trapping hydrocarbons in a lattice of ice. Estimates of the reserves of methane in these hydrates range from 210 Gt (Milkov et al., 2003) to 1500 Gt (Kvenvolden, 1999), potentially rendering them a valuable source of commercial energy and a possible agent of catastrophic climate change (e.g. Kennett et al., 2000).

The oxidation of methane in pore water and at the sediment surface results in oversaturation of carbonate, leading to the precipitation of distinctive authigenic carbonates. These range from massive chemoherms (e.g. Aharon, 1994; Tiechert et al., 2005) to plumbing features such as chimneys and burrow infillings, and to small nodules and blebs characteristic of more diffuse seepage (Campbell, 2006). These carbonates can form at many depths in the sediment, from the zone of methanogenesis up to the surface, and they frequently display morphologies and mineralogies characteristic of the zone in which they form (Greinert et al., 2001).

In addition to these inorganic features, cold seeps support a unique assemblage of chemosymbiotic organisms. For nutrition, these organisms rely on the oxidation of reduced sulfur and methane by their microbial symbionts. The most common invertebrate taxa in Recent seeps are polychaetes of the genera *Lamellibrachia, Escarpia, Alaysia*, bathymodiolid mussels (*Bathymodiolus*), and vesicomyid clams (*Calyptogena, Vesicomya*). In addition, some seep sites include thyasirid, solemyid, and lucinid bivalves, pogonophoran worms, and abyssochrysid and provannid

gastropods as well as a number of non-seep-restricted gastropods and decapod crustaceans (Tunnicliffe, 1992; Sibuet and Olu, 1998; Levin, 2005). Indeed, many seeps display a zonation of biota that reflects sulfide concentrations and fluxes in the sediment. For example, in areas of high sulfide flux, cold seeps on Hydrate Ridge sustain mats of the thiotrophic bacteria *Beggiatoa*. Surrounding this, with lower sulfide fluxes, is a zone of the bivalve *Calyptogena*, and further away, with sulfide fluxes orders of magnitude lower than the *Calyptogena* zone, lie beds of the solemyid clam *Acharax.* It is thus postulated that sulfide flux accounts for faunal distributions in diverse geological settings (Suess et al., 2001; Sahling et al., 2002). Figure 2.2 schematically represents the development of cold seeps and associated features on an active tectonic margin.

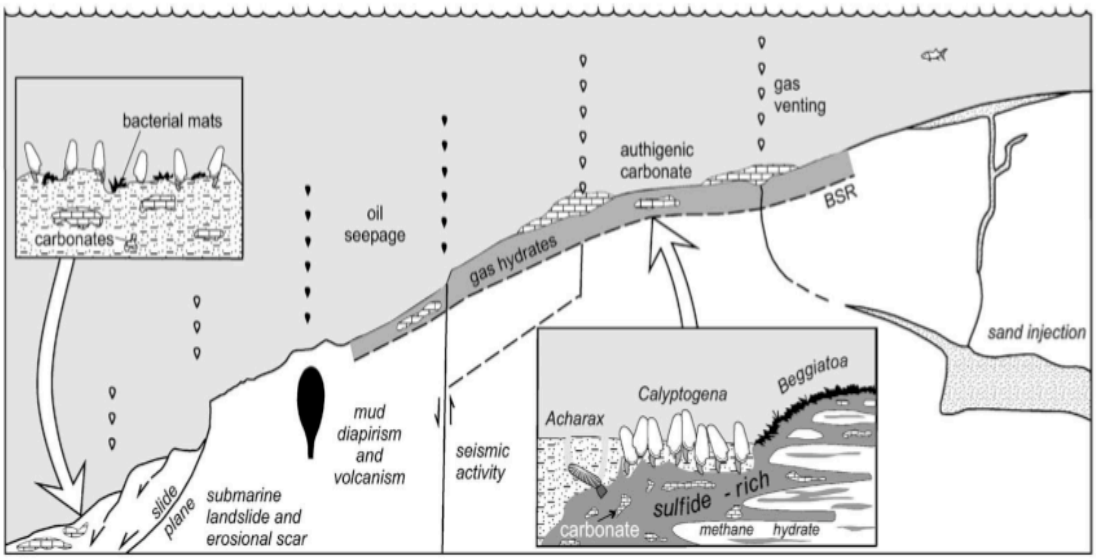

Figure 1.2. Diagram representing the links between fluid migration pathways, gas hydrate distribution, carbonate precipitation and endemic seep communities on an active tectonic margin. Note zonation of communities due to changing sulfide configurations. Modified from Campbell, 2006.

generally form from methane-supersaturated fluids at pressures >60 bars and temperatures <4°C. Although largely bound by temperature and pressure (Figure

1.3), other factors such as salinity, types and concentrations of gases present, and inhibitors and catalysts in the system influence the stability of gas hydrates (Suess, in review).

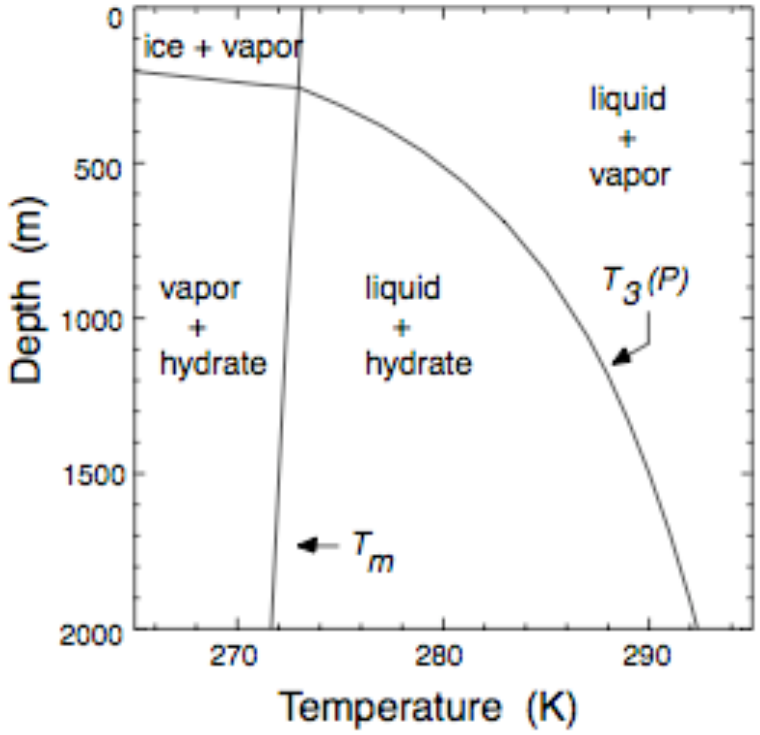

Figure 1.3. Phase diagram for methane-water mixture. $T_3(P)$ is the boundary between the regions of methane hydrate stability and instability. T_m is the melting temperature of pure water. From Buffet, 2000.

In general, hydrates form well below the sediment surface, however, in a number of areas such as the Blake Ridge (Atlantic Ocean), Hydrate Ridge (Cascadia Margin), and the Hikurangi Margin (New Zealand), they are found at or near the sediment surface (e.g. Suess, et al. 1999, Buffet, 2000; Lorenson & Collett, 2000). Although they develop preferentially along bedding planes (with occasional cross-cutting), they do not occupy the original sediment pore space. Instead they fill secondary pore space such as fractures, or creates it own pore space by fracturing or wedging apart the sediment framework (Suess et al., 2001).

Evidence for the presence of gas hydrates is sometimes direct, as when they are recovered in cores or other samples (e.g. Lorenson & Collett, 2000; Treude et

al., 2003), however this rarely maintains the original characteristics of the hydrates and thus limits the data that can be collected (Suess et al., 2001). Most evidence, therefore, is gathered indirectly, the most common and reliable indicator being seismic evidence in the form of a prominent Bottom Simulating Reflector (BSR). Marking the boundary between high velocity hydrate-rich sediment and low velocity hydrate-free sediment, the BSR occurs at the base of the hydrate stability zone and roughly parallels the topography of the sediment surface (Figure 1.4).

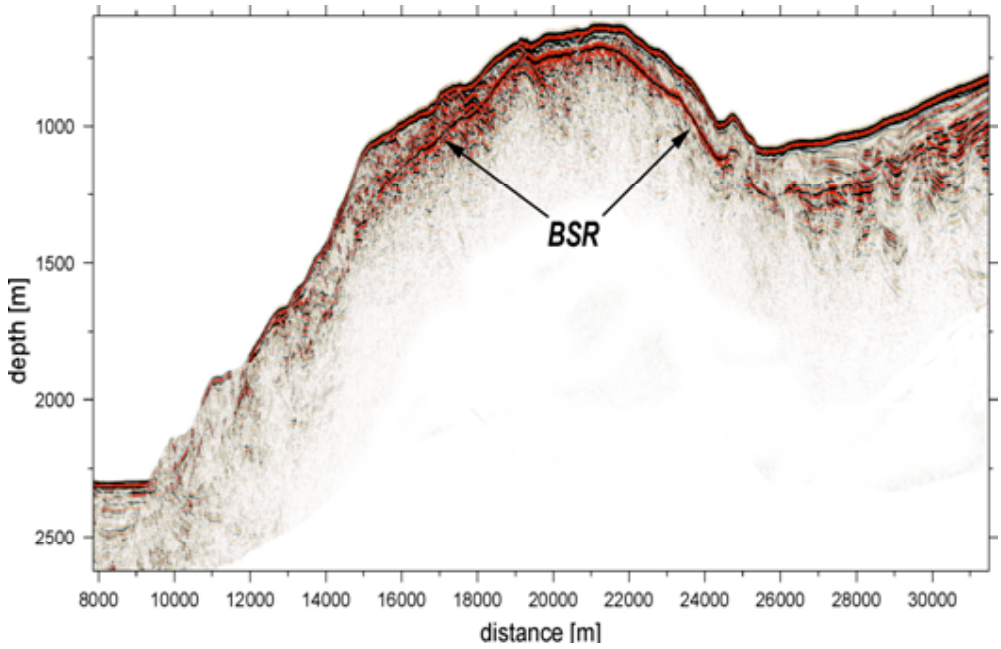

Figure 1.4. Seismic profile at Hydrate Ridge, Cascadia margin, showing prominent bottom simulating reflector indicating the base of the hydrate stability zone. Image courtesy J. Greinert.

Indirect chemical evidence is gathered based on $d^{18}O$ and chloride anomalies. These result from the preferential incorporation of ^{18}O and exclusion of chloride during the formation of gas hydrates (e.g. Suess et al., 2001).

Primary economic interest in gas hydrates is due to their ability to store large volumes of hydrocarbons within their lattices. Methane is the most common gas in these hydrates; at Hydrate Ridge, Bohrmann et al. (1998) found CH_4

constituted 97.4% of the gas in hydrates, with hydrogen sulfide constituting 2.6% and CO_2, C_2H_6, and C_3H_8 occurring in small amounts.

1.1.2 Methanogenesis and methanotrophy

Particulate organic matter in terrestrial, aquatic and marine environments is subjected to physical and chemical alteration, or diagenesis, as it is buried. The sediments containing this organic matter become reservoirs for many elements, and global biogeochemical cycles depend on the balance between sequestration and remobilization of these elements. The fates of the elements involved are inextricably linked, and are generally microbially mediated.

Methane is one end-product of diagenetic alteration of organic matter, and although it consumes a relatively small fraction (~1%) of the total organic carbon present in shallow, organic-rich sediments (Whiticar, 1999), the processes of methanogenesis and methanotrophy receive considerable attention. There are several reasons for this. First, various forms of hydrocarbons contribute the major portion of economic energy sources, and new, commercially viable, environmentally sustainable energy sources are continually being sought. Second, methane is a significant greenhouse gas, and has been implicated as an agent in both climate change and in the original oxygenation of the Earth's atmosphere (Catling et al., 2001). Third, methanogenic and methanotrophic processes are of interest to microbiologists because of the relative simplicity of their reactions. Finally, methanogenesis and methanotrophy are indicators of the diagenetic state of a particular depositional setting (Whiticar, 1999).

Methanogenesis takes place in a number of environments and by several different processes including thermal maturation of organic matter (thermogenic methanogenesis), microbial methanogenesis, and abiotic methanogenesis. Each process imparts a distinctive carbon isotopic fractionation to its end product. This isotopic signature allows distinction between the different sources of methane.

Microbial methanogenesis occurs in anaerobic environments in marine, fresh-water, and terrestrial settings. Methanogens are a phylogenetically diverse group of anaerobic archaea characterized by a highly restricted energy metabolism that is limited to the formation of methane using CO_2, and H_2 as well as other substrates such as formate, methanol, and/or acetate (Thauer et al., 2008). Because they are anaerobic, methanogens cannot tolerate significant pO_2, nitrate, or nitrite and are confined to anoxic environments (Claypool and Kaplan, 1974; Whiticar, 1999, Thauer, 2008). Five orders of methanogenic archaea have been identified: Methanopyrales, Methanococcales, Methanobacteriales, Methanomicrobiales and Methanosarcinales. The first four orders utilize CO_2 and H_2, but except for one species (*Methanosphaera stadtmanae*), they cannot grow on acetate, formate or methylamines. Methanosarcinales utilize acetate, methanol and methylamines, but are restricted in their growth on CO_2 and H_2.

Microbial methanogenesis occurs in anoxic environments where concentrations of sulfate, nitrate, Mn(IV) and Fe(III) are low. Where these are plentiful, methanogens are out-competed by organisms using anaerobic respiration. Methanogenic pathways are classified according to the preferred substrate; the primary pathways are hydrogenotrophic, acetotrophic, and methylotrophic (Whiticar, 1999). In addition, pathways are classified in ecological terms as competitive or non-competitive. Competitive pathways are those that are also utilized by other microbes such as sulfate-reducing bacteria (SRB). Competitive substrates include CO_2, with a net reaction represented by

$CO_2 + 4H_2 \rightarrow CH_4 + 2H_2O$,

acetate, net reaction

$CH_3COOH \rightarrow CH_4 + CO_2$,

and formate (Whiticar, 1999).

Where sulfate is abundant in the water column or sediment, methanogenesis is severely limited, as SRB outcompete methanogens for available organic carbon or hydrogen. This typically occurs in marine sediments where sulfate concentrations are greater than 200 μM. Once the available sulfate is depleted, the SRB become

inactive and methanogenesis proceeds, primarily utilizing CO_2 reduction. In fresh water environments, sulfate is generally low, eliminating competition from SRB. In this case, methanogenesis proceeds wherever conditions are anaerobic and a suitable substrate is present.

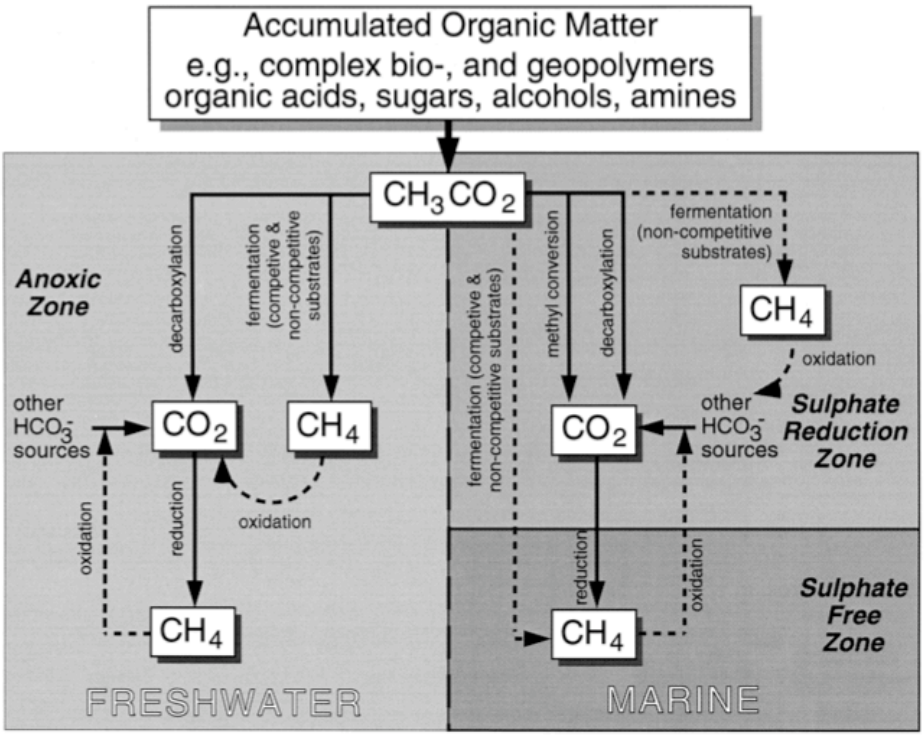

Figure 1.5. Schematic diagram showing methanogenic pathways in marine and terrestrial environments. From Whiticar, 1999.

Non-competitive pathways for methanogenesis include the acetotrophic and methylotrophic pathways, which are both fermentative. The substrates utilized in this process are primarily methanol and methylated amines, as well as some organic sulphur compounds. A typical fermentation reaction is represented by $CH_3\text{-}A + H_2O \rightarrow CH_4 + CO_2 + A\text{-}H$. Non-competitive pathways occur most frequently in wetlands, for example swamps, marshes and rice paddies (Whiticar, 1999). Marine and freshwater methanogenic pathways are illustrated schematically

in Figure 1.5. In sulfate-rich zones of the marine environment, most organic compounds are metabolized by non-methanogens and added to the bicarbonate pool. At the same time, methane consumption in the same zone results in the loss of methane and keeps the methane concentration low. Below the sulfate reduction zone (where sulfate has been severely depleted) methanogenesis begins using competitive pathways.At temperatures exceeding 50°C, non-biological thermocatalytic reactions produce methane accompanied by higher hydrocarbons such as ethane, propane and butane (Claypool and Kaplan, 1974). Thermogenic methanogenesis produces methane through thermal cracking of organic matter, first to oil and with higher maturity to hydrocarbon gases. The high temperatures required to initiate this reaction necessitates deep burial of the parent organic matter. The depth at which the necessary temperature is achieved is dependent upon the tectonic regime in the source area. Thermogenic methanogenesis is thus common in, but not limited to, active tectonic margins, where organic matter is subjected to elevated temperatures in the subduction zone.

Abiogenic methane, synthesized from carbon monoxide or carbon dioxide, has been identified in a number of settings worldwide, including hydrothermal environments, Precambrian shields and metamorphic provinces (Berndt et al., 1996; Horita and Berndt, 1999; Lollar et al., 2006). In the absence of catalysts, abiogenic methanogenesis proceeds extremely slowly. Experimental evidence, however, indicates the presence of iron or other transition metals can catalyze and hasten abiogenic methane synthesis. Under conditions simulating those encountered during the serpentinization of ultramafic rocks, methane formed rapidly when catalyzed with a Ni-Fe alloy via the reaction

$$HCO_3^- + 4H_2 \rightarrow CH_4 + OH^- + 2H_2O$$ (Horita and Berndt, 1999).

The process considered responsible for most abiogenic methanogenesis is Fischer-Tropsch (FT) synthesis, in which CO_2 is converted to hydrocarbon gas by reaction with H_2. In situations such as the serpentinization of ultramafic rocks, H_2 is generated as Fe(II) is from olivine is converted by aqueous reaction to Fe(III) in magnetite. Other products of this process are brucite ($Mg(OH)_2$) and (rarely)

awaruite (Ni_3Fe). Magnetite plays a dual role in this process as its formation not only provides a source of H_2, but also catalyzes the FT reaction (Berndt et al., 1996).

Isotope data are reported in standard δ notation as follows:

$\delta_x = [R_{sample}/R_{standard} - 1]10^3$ ‰

where R is the ^{13}C /^{12}C (or D/H) ratios relative to the PDB or SMOW standards. A number of factors influence the final isotopic signature of methane produced by any process. These include the isotopic signature of the substrate, equilibrium fractionation between methane and other compounds, and kinetic effects associated with methane formation. Ranges of C and H isotopic values for microbial, thermogenic and abiogenic gases are shown in Figure 1.6.

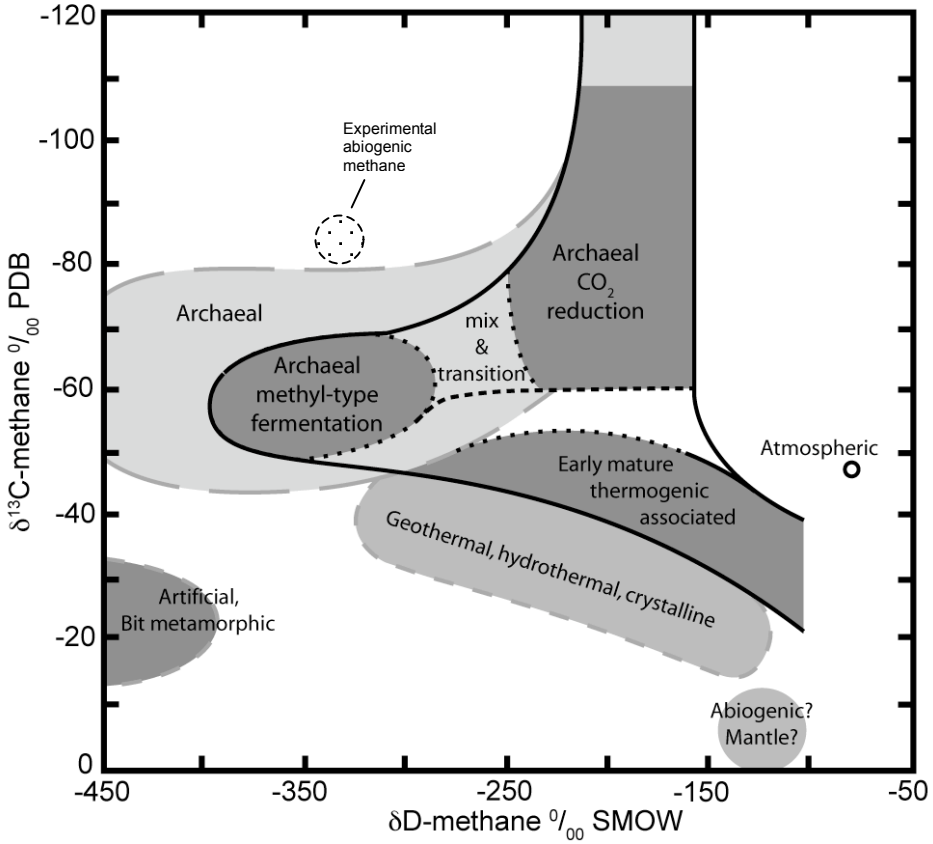

Figure 1.6. CD-diagram for classification of microbial and thermogenic natural gas by the combination of $\partial^{13}C$ and $\partial^{4}D_{CH4}$ information. From Whiticar, 1999.

In methane generated microbially, $\delta^{13}C$ values range between -50‰ and -110‰ PDB, although the $d^{13}C$ signatures in fresh water and marine microbial CH_4 differ. Marine CH_4 is typically more depleted in ^{13}C and more enriched in deuterium than freshwater CH_4. Methanogenic pathways differ in the two environments, with CO2reduction dominating in the marine environments and methylated substrates more important in freshwater. The two pathways can be inferred from the C and H isotope data (Whiticar, 1999). The variation and overlap in C and H isotope values shown in Figure 1.6 are explained by three factors, 1) kinetic isotope fractionation by methanogens; 2) mixtures of pathways or CH_4 types; and 3) variations in the C and H signatures of the precursor substrates.

Thermogenic methane, with $\delta^{13}C$ values between -50‰ and -20‰, is enriched in ^{13}C relative to microbial CH_4 (Figure 1.6). The differences are attributed to precursor compounds, kinetic effects, and the higher temperatures of thermal methanogenesis. The separation between the isotopes of the parent and daughter ($\delta^{13}C_{CH4} - \delta^{13}C_{org}$) ranges from 30‰ to 0‰. In addition, kerogen types influence the final $\delta^{13}C$ values, as hydrogen-rich kerogentypes I and II often generate CH_4 with more negative $\delta^{13}C$ than type III (Whiticar, 1999). Hydrogen isotopic values are less useful in classifying origins of natural gases as thermogenic δD_{CH4} values (-275‰ to -100‰) overlap with those of microbial CH_4 and thus cannot be used as a single defining parameter (Figure 1.6).

Stable isotope values for abiogenic methane are generally much heavier than those of either microbial or thermogenic methane (Figure 1.6). Values for abiogenic methane range between 0‰ PDB and -20‰ PDB, with most falling around -15‰ PDB to -18‰ PDB. Thus abiogenic methane should be readily distinguishable from thermogenic and biogenic methane. Experiments by Horita and Berndt (1999), however, generated abiogenic methane under hydrothermal conditions that carried $d^{13}C$ values as depleted as -60‰ PDB, well within the range of thermogenic and microbial methanogenesis. Thus, careful attention to context is necessary for clearly distinguishing between gases of organic and inorganic origin.

In general, compounds with lower isotopic mass diffuse and react more readily than those with higher masses, thus ^{12}C reacts more readily than does ^{13}C. For example, during CH_4 formation in the Saanich Fjord off British Columbia, $H^{12}CO_3^-$ was removed 7% faster than $H^{13}CO_3^-$ (Claypool and Kaplan, 1974). The magnitude of the fractionation depends on the pathway. Enrichment in acetate fermentation $\delta^{13}C_{CH4} - \delta^{13}C_{acetate}$ is 25‰ to 35‰. For CO_2 reduction, the difference is far greater, $\delta^{13}C_{CH4} - \delta^{13}C_{CO2} > 55‰$. In a closed system, the mass balance of the reaction is described by the Rayleigh functions in the general forms

$$R_{r,t} = R_{r,i} f^{(\tilde{a}-1)}$$

and

$$R_{p,t\ t} = R_{r,i}(1 - f^{\tilde{a}-1} f)$$

where $R_{r,x}$ is the isotope ratio of the precursor substrate accumulating initially (i) and at time t and $R_{p,x}$ is the isotope ratio of the accumulating product. f is the fraction of the initial substrate remaining at time t, and a is the kinetic isotope fractionation factor. The actual location of the fractionation, for example at the membrane or at an enzymatic locus, is uncertain. The isotope separation between substrate and product is expressed as the isotope separation factor

$e_C \approx 10^3 \ln a_C \approx 10^3(a_C - 1) \approx \delta^{13}C_{CO2} - \delta^{13}C_{CH4}$.

As fractionation proceeds in a Rayleigh distillation system, depletion of the substrate results in considerable variation in isotope values, and as the substrate is exhausted $\delta^{13}C_{CH4} \approx \delta^{13}C_{org}$.

Temperature effects on isotope fractionation are not fully understood. Increased temperature has been demonstrated to increase the amount of CH_4 generated (Conrad and Schutz, 1988). It is unclear, however, whether this affects the kinetic isotope effect (KIE). There is evidence of a general trend to lower fractionations with increasing temperature as demonstrated by Whiticar and Faber (1986) and shown in Table 1.1. These results suggest that the KIE decreases with increasing temperature.

Table 1.1

Effect of temperature on the magnitude of carbon isotope effects associated with methanogenesis by carbonate reduction

Location/bacterium	Temperature (°C)	ε_C CO_2–CH_4	References
Bransfield Strait (Antarctic)	−1.3	86 to 95	Whiticar and Suess (1990)
Methanosarcina barkeri	20	77	Whiticar, Müller, Blaut (unpublished data)
	37	58	
Thermoautotrophicum	65	34 to 40	Fuchs et al. (1979)
Hyperthermophil	110	40	Whiticar, Stetter, Huber (unpublished data)

From Whiticar, 1999

Another factor affecting isotope fractionation is the substrate concentration. In CO_2 reduction, above a critical CO_2 concentration, the isotope separation (e) remained constant, but dropped dramatically as the substrate was depleted (Zyakun, 1992). It is likely that this is due primarily to a "reservoir effect" in which the isotopic signature of the product approaches that of the substrate due to exhaustion of the substrate and removal of the lighter isotope.

Hydrogen isotope effects in methanogenesis are not well understood. Substantial enrichment in ^1H occurs as hydrogen is transferred to methane; the partitioning is present regardless of the pathway, but the magnitude of the enrichment may depend on the precursor. Factors such as different CH_4 pools may also influence dD,, even including the mixing of thermogenic and microbial CH_4.

Oxidation of CH_4 is of global significance, reducing the impact of CH_4 on the atmospheric carbon budgets by orders of magnitude. Microbial oxidation of CH_4 can be aerobic or anaerobic, with the former most common in freshwater or soils (Whiticar, 1999). Anaerobic oxidation results in as much as 5 – 20% of the net modern atmospheric CH_4 flux being consumed by a population of prokaryotes (Valentine and Reesburgh, 2000).

Methanotrophs are characterized by their ability to utilize CH_4 as their sole C source. Although most methanotrophs inhabit areas of normal temperature and pH, recent investigations have identified thermoacidophilic methanotrophs from extreme environments such as volcanic mud pots in Italy (*Acidimethylosilex fumarilicum,* temp. 55ºC, pH 0.8), a geothermal area in New Zealand (*Methylokorus infernorum*, temp. 60º, pH 1.0-6.0) and an acidic hot spring in Kamchatka, Russia (*Methyloacida kamchatkaensis,* temp. 55ºC, pH 3.5) (Semrau et al., 2008).

Methanotrophy in marine sediments acts as a barrier to CH_4 release into the water column and atmosphere as methanotrophs oxidize up to 100% of CH_4 before it reaches the sediment-water interface (Boetius and Suess, 2004; Sommer et al., 2006; Catling et al., 2007). Indeed, Luff and Wallman (2003) found anaerobic oxidation of methane (AOM) to be so efficient the flow rate of CH_4 must be >100 cm/y for free gas to break through the sediment surface into the water column. Anaerobic methanotrophs are not well understood, but are phylogenetically related to anaerobic methanogens and are grouped into three "clades": ANME-2, related to Methanosarcinales (Figure 1.7a), ANME-1, related to Methanosarcinales and Methanomicrobiales (Figure 1.7b), and ANME-3, closely related to Methanococcoides. These archaea operate as consortia, living in dense aggregates with sulfate-reducing bacteria (Figure 1.7c). The sulfate reducing bacteria (SRB) are a small, anaerobic branch of Deltaproteobacteria including the genera *Desulfosarcina* and *Desulfococcus*. The average archaea/SRB consortium consists of an inner sphere containing ~100 archaeal cells partially or fully surrounded by about 200 cells of SRB which form an outer shell of one or two layers (Figure 3c) (Boetius et al., 2000).

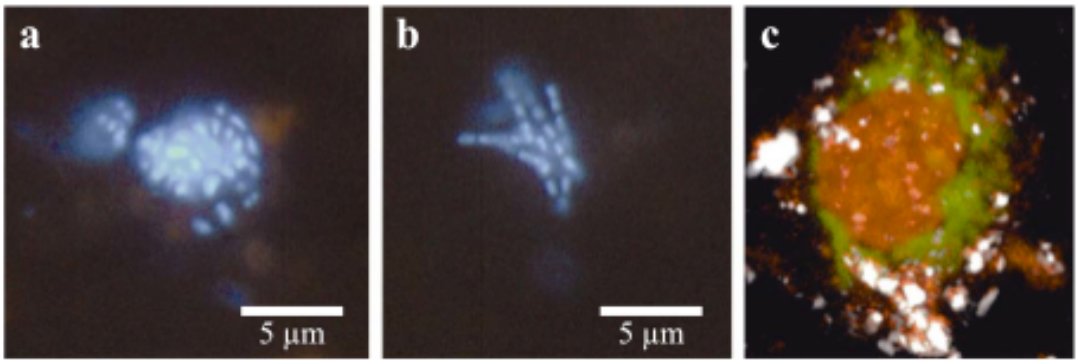

Figure 1.7. Microphotograph of methanotrophic archaea (a) ANME-2 aggregate stained with DAPI; (b) ANME-1 stained with DAPI; and (c) CLS image of aggregate stained with fluorescent oligonucleotides specifically targeting archaea (red) and sulfate-reducing bacteria (green) and calcite mineral reflection (white). From Boetius and Suess, 2004.

Methanotrophy and sulfate reduction are described by the net reaction

$CH_4 + SO_4^{2-} \rightarrow HCO_3^- + HS^- + H_2O$,

where sulfate is the electron acceptor and CH_4 the donor. The sulfide released in this reaction fuels luxurious growths of chemoautotrophic organisms in cold seeps and hydrothermal vents worldwide. For example, taxa found in cold methane seeps at Hydrate Ridge, off the coast of Oregon, include the giant sulfide-oxidizing bacteria *Beggiatoa* sp., the symbiotic vesicomyid clams *Calyptogena pacifica* and *C.kilmeri,* and the solemyid clam *Acharax sp.*; these can contribute up to 35g C m^{-2} in sea-floor sediments (Boetius and Suess, 2004).

The microbial consumption of CH_4 is accompanied by a KIE that enriches residual CH_4 in the heavier isotopes; the fractionation is more pronounced for the carbon isotopes than for the hydrogen isotopes. Methanotrophs select the lighter isotope of carbon first, however the isotope separation (e_C) of methanotrophy is considerably less than that of methanogenesis, varying between 5 and 10‰ (occasionally as high as 20‰), whereas that for methanogenesis is ~95‰ (Whiticar, 1999). The greatest enrichment in ^{13}C occurs in residual CH_4 as it leaves the zone of methanotrophy (Figure 1.8).

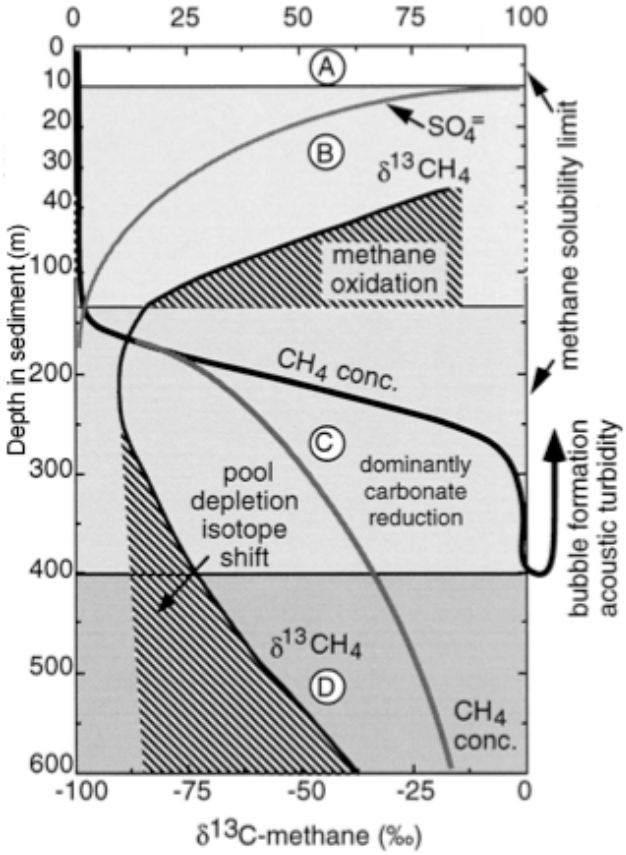

Figure 1.8 Comparison of CH_4 concentration with $\delta^{13}C$ values for residual CH_4 and CO_2 during methanotrophy. Solid black line = CH_4 concentration, dotted line = $\delta^{13}C$ of CO_2, dashed line = $\delta^{13}C$ of

Methanogenesis and methanotrophy play a vital role

in mobilizing carbon that would otherwise remain sequestered in organic matter. The two processes are not always easily separated, often appearing to occur in the same place, perhaps even performed by the same organisms (Martin et al., 2008).

1.2 Cold seep carbonates

Residual carbonate produced during methanogenesis and carbonate resulting from methanotrophy can be incorporated into authigenic and, possibly, biogenic carbonates. These seep carbonates become the repository for information regarding the methanogenic and methanotrophic history of cold seeps.

1.2.1 Authigenic carbonates

Authigenic carbonates are abundant, if not defining, features of cold methane seeps (Aharon, 1994; Greinert et al., 2001; Luff et al., 2004; Orphan et al., 2004; Campbell, 2006; Naehr et al., 2007; Paull et al., 2007). Carbonates formed in cold seeps act as sinks for methane carbon, and as such, play a crucial role in the global carbon cycle through the regulation of ocean-atmosphere carbon fluxes (Whiticar, 1999). As methane migrates through sediment toward the sea floor, a number of processes may factor into the formation of authigenic carbonates, including aerobic oxidation of methane, anaerobic oxidation of methane, and sulfate reduction of organic matter. Aerobic oxidation of methane:

$CH_4 + 2O_2 \rightarrow CO_2 + 2H_2O$

however, is more important in the water column and results in increased acidification, thus promoting dissolution of carbonate. Anaerobic oxidation of methane (AOM):

$CH_4 + SO_4^{2-} \rightarrow HCO_3^- + HS^- + H_2O$

increases alkalinity in the water. This process incorporates isotopically depleted carbon from methane into the bicarbonate, making it available for precipitation in authigenic carbonates. Sulfate reduction:

$2CH_2O + SO_4^{2-} \rightarrow 2HCO_3^- + H_2S^-$

also increases alkalinity, but it is more widely disseminated than AOM and is less effective in the formation of carbonates (Paull et al., 2007). Factors controlling the

precipitation of carbonate are not well understood, but may include the delivery of cations, Ca, Mg, and to a lesser extent Fe and Mn, from the overlying water, the rate of AOM producing alkalinity, and chemical reactions at the mineral surface (Greinert et al., 2001; Luff and Wallmann, 2003).

Evidence is unequivocal that the precipitation of carbonates at cold seeps is largely mediated by the processes involved in the microbial consumption of methane. Working with carbonates from Eastern Mediterranean mud volcanoes, Aloisi et al. (2002) used phylogenetic and lipid analyses to demonstrate the link between supersaturation of bicarbonate and microbial consumption of methane. In their study of seep carbonates at Hydrate Ridge, Teichert et al. (2005) used visual and petrographic inspection to investigate chemoherm aragonites. They discovered thrombolitic fabrics in cryptocrystalline aragonite phases and microbial filaments in microcrystalline phases. Both of these are regarded as demonstrating the essential role played by microbes in the precipitation of seep carbonates (Teichert et al. 2005). Also working at Hydrate Ridge, (Leefmann et al., 2008) used miniaturized biosignature analysis to study the lipid biomarkers from different phases of carbonate precipitation and identify the organisms associated with each phase. They found that >90% of the lipids related to AOM were concentrated in one mineral phase – a whitish-colored aragonite. Their biomarker analyses indicated that ANME-2 archaea were largely responsible for the formation of this mineral phase, with a smaller contribution from ANME-1 archaea. Working on carbonates from the Kidd mud volcano in the Gulf of Cadiz, Stadnitskaia et al. (2008) analyzed lipid biomarkers and 16s rRNA gene sequences and concluded that the carbonate crust formed in two phases and grew downward. The first phase (top part of the crust) showed a dominance of ANME-2 archaea, whereas the second phase grew downward and indicated reduced methane flux and a dominance of ANME-1 archaea. Finally, Luff and Wallman (2003) determined that approximately 14% of carbonate generated by AOM was removed by precipitation of authigenic carbonates and that a layer of carbonate ~1 m thick had been deposited at Hydrate Ridge over a period of 20,000 years.

Carbonates in cold seeps can take a number of different forms, distinguished by their morphologies, mineralogies, and isotopic compositions (Greinert et al., 2001; Han et al., 2004; Teichert et al., 2005). These forms are 1) chemoherm carbonates; 2) seepage-associated concretions/nodules/ pavements; 3) gas-hydrate-associated concretions/nodules/pavements; and 4) dolomitic concretions (Greinert et al., 2001; Aloisi et al., 2002; Han et al., 2004; Teichert et al., 2005). Chemoherms are large, free-standing, typically pinnacle-shaped carbonate bodies that form at the seafloor surface and protrude into the water column. They incorporate the shells of seep-specific bivalves and other organisms along with clasts in an aragonite cement and have an anomalously depleted ^{13}C signal (Aharon, 1994; Teichert et al., 2005). Their large communities of chemosynthetic organisms contradict their above-the-seafloor (oxic water) location of formation, but this is explained by Teichert et al. (2005) as shown in Figure 1.9. In this model, the chemoherm actively grows only at the surface covered with the AOM consortia and sulfur-oxidizing bacteria.

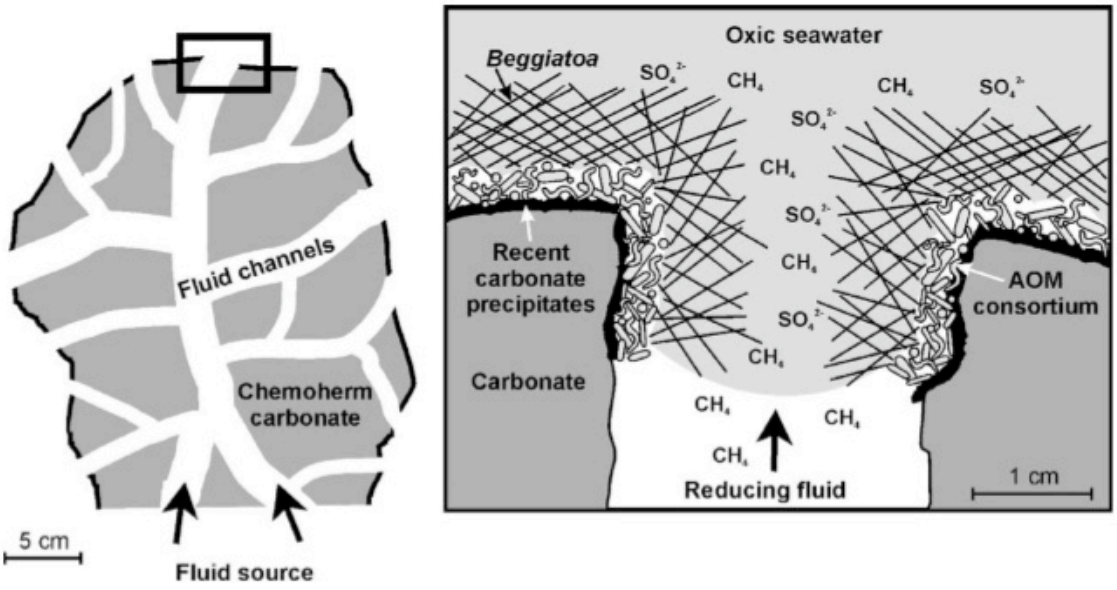

Figure 1.9 Schematic representation of chemoherm growing into water column above methane seep. The methane-oxidizing consortium lives in the anoxic environment under bacterial mats and supplies sulfide for the bacteria as well as carbonate for chemoherm building. Modified from Teichert et al. (2005)

Figure 1. The development of chemoherms above the seafloor. Diagram at left depicts a typical chemoherm with numerous fluid-flow channels. Box outlines area shown at right. In this model, a veneer of anoxia provides the setting for AOM, which supports luxurious growths of sulfur oxidizing bacteria (in this case *Beggiotoa*) and promotes precipitation of carbonate. Modified from Teichert et al., 2005.

Concretions and nodules can form near the surface or deeper in the seep system, and are distinguished by their mineralogies and isotopic compositions. All can be exhumed and exposed at the seafloor surface, or they can be structurally modified (e.g. brecciated) by such processes as gas hydrate dissociation or tectonism (Greinert et al., 2001). Pavements and crusts commonly form above dissociating gas hydrates, where AOM of the newly-released methane gas provides bicarbonate over a widespread area. Figure 1.10 schematically represents the zones in which the different seep carbonates form.

Aragonite, high-Mg calcite and dolomite are the principal calcium carbonate lithologies among authigenic seep carbonates (Bohrmann et al., 1998; Greinert et al., 2001; Luff and Wallmann, 2003; Paull et al., 2007). Each mineralogy is characteristic of a particular zone within the seep system; 1) the oxic zone, 2) the sulfate reduction zone, 3) the upper part of the zone of methanogenesis, and 4) the lower part of the zone of methanogenesis (Greinert et al., 2001) (Figure 1.10). Aragonite tends to dominate at shallow depths at near-sea-water temperatures (Naehr et al., 2000; Greinert et al., 2001; Luff & Wallmen, 2002). Its common association with authigenic pyrite, however, precludes an oxic environment of formation (Naehr et al., 2000). In cold seeps, dolomite is formed in the zone of methanogenesis or in the transition zone between methanogenesis and sulfate reduction, both zones in which the Mg/Ca ratio is high, sulfate is reduced or absent, and pH and alkalinity are increased ((Mazzullo, 2000; Greinert et al., 2001). The zone of methanogenesis may be tens of meters below the sea floor, or may be pushed upward to within a few centimeters of the surface such that the different types of carbonate are juxtaposed. For example, on the Jaco Scarp off Costa Rica, Han et al., (2004) found aragonitic chemoherms growing into the water column from a base of dolostone hardground.

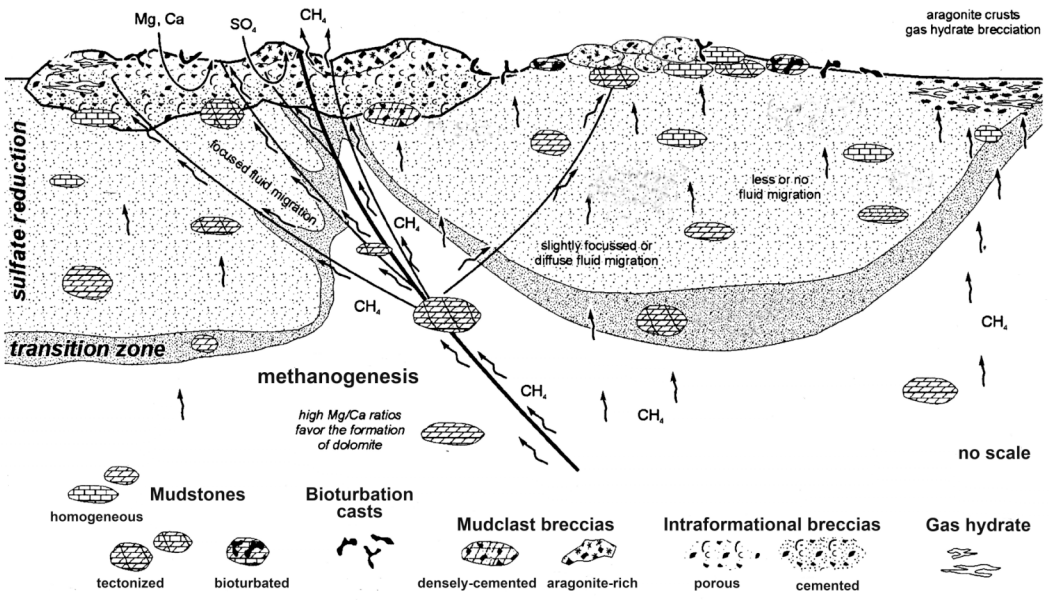

Figure 1.10 Schematic depicting zones of formation of different types and lithologies of seep carbonates. Modified from Greinert et al., 2001.

Carbon incorporated into authigenic carbonates at cold seeps may be derived from a variety of sources: 1) microbial or thermogenic methane, 2) sedimentary organic carbon, 3) marine biogenic carbonate, and 4) dissolved inorganic carbon in sea water (Naehr et al., 1998). Each of these has a distinctive carbon isotopic signature that can be used to identify carbon sources and to characterize the fluid flow. Microbial methane carries a $d^{13}C$ signature < –50‰ PDB, thermogenic methane has a signature of -30‰ PDB to –50‰ PDB, sedimentary organic carbon carries a signature of ~ –25‰ PDB, while marine dissolved inorganic carbon has $d^{13}C$ values ~0‰ PDB (Naehr et al., 1998; Whiticar, 1999). The $d^{13}C$ signature of a seep carbonate is often a mixture of these different carbon sources, with the final $d^{13}C$ signature dependent on the original sources and the amount of mixing. Carbonates are only labeled as methane-derived when their $d^{13}C$ signature is < –25‰ PDB (Paull et al., 2007), or when their values are highly enriched due to residual CO_2 from microbial methanogenesis (up to +34‰ PDB) (Budai et al., 2002; Torres and Kastner, 2009).

In their study of carbonates from Hydrate Ridge, Greinert et al. (2001) discriminated six different geochemical environments of carbonate formation based on lithologies and isotopic composition. Group A consisted primarily of dolomite and carried $d^{13}C$ values of ~10‰ PDB, indicating formation within the zone of methanogenesis utilizing residual, isotopically enriched CO_2. On the other hand, carbonates formed at or near the surface (Group E) were dominated by aragonite and high Mg calcite had $d^{13}C$ values ranging between –38‰ PDB and –55‰ PDB, typical of methane-induced carbonate precipitates. The range of $d^{13}C$ values is due to the mixture of carbon from various sources such as AOM of different methane pools, and marine organic carbon.

1.2.2 Foraminiferal biomineralization

Biomineralization is the process by which organisms interact with their environment to form minerals. The products of biomineralization are usually composites of organic and mineral components, and many have unusual morphologies as well as distinctive isotopic and minor/trace element compositions (Weiner and Dove, 2003). Biomineralization occurs in two distinct modes: biologically induced and biologically controlled. Biologically induced mineralization is exemplified by prokaryotes and other organisms that exert little control over mineralization. Such biogenic products display considerable heterogeneity in their morphologies and composition (Weiner and Dove, 2003). In biologically controlled mineralization, cellular activities control and direct the nucleation, morphology, growth, and the final location of the mineral deposited. Biologically controlled mineralization is subdivided into extracellular and intracellular mineralization. In extracellular mineralization, the organism uses organic material to delimit an external site where the mineral will be deposited. At this site, the organism must establish and maintain supersaturation of the necessary anion. The cations are concentrated inside the cell, then exported to the external region by active pumping or by diffusion. Examples of this process are foraminiferal shell construction and cartilage mineralization. Intracellular biomineralization occurs in special vesicles entirely within the cell, and produces

the highest degree of control over the final product. Minerals produced this way may leave the cell as a single unit, or as "pre-fabricated" structures. Echinoderms produce large structures this way, and intracellular mineralization is employed by some plants, which then retain the structures internally (Weiner and Dove, 2003).

Calcium carbonate minerals are the most abundant biogenic minerals, followed by phosphates; other notable biogenic minerals include sulfates and sulfides, oxides, and metals (Weiner and Dove, 2003). In fact, calcification in the modern ocean is almost entirely biogenic, with planktic foraminifera alone contributing 32-80% of the $CaCO_3$ deposited in the deep oceans (Erez, 2003). Within the class Foraminifera, the majority, or 11 out of 15 extant orders, construct their tests (shells) of calcium carbonate (Hansen, 1999). Of these, one order, the Carterinida, utilize concentrically laminated ovoid spicules held in place by organic material. The Miliolida, a primitive calcareous order, construct their tests of rods of high magnesium calcite formed intracellularly then exported by exo-cytosis (Erez, 2003). The rods have no particular arrangement, but the shell may be covered with a shiny veneer of calcite needles, resulting in a shiny, porcellaneous appearance. The majority of calcareous foraminifera, however, use low magnesium calcite in their shell construction, though some may approach six to seven mole % Mg (Erez, 2003). In addition, most calcareous foraminifera utilize lamellar construction, which places a new layer of calcium carbonate over all exposed chambers in the foraminifera as each new chamber is formed. This can be either a single layer (monolamellar) or a double layer separated by an organic "wall" (bilamellar) (Figure 1.11).

During precipitation of the secondary calcite layer, Mg must be excluded, because ordinary sea water contains 5x more Mg than Ca. Erez, (2003) suggested excess Mg is either trapped in vacuoles within the cytoplasm or is sequestered in the delimited seawater space surrounding the shell while low magnesium calcite is precipitated in the secondary layer.

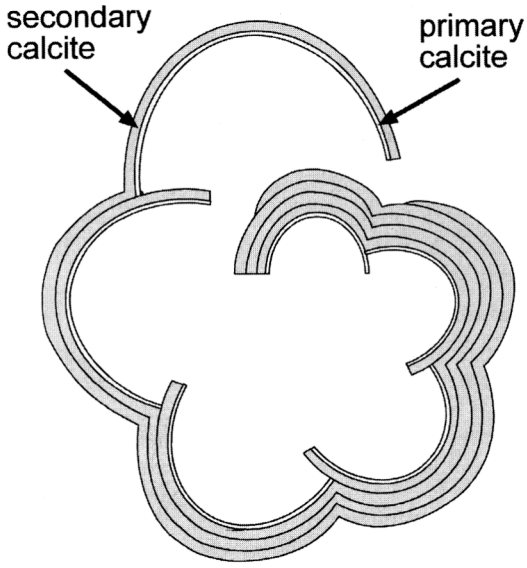

Figure 1.11. Schematic depicting bilamellar wall structure in calcareous foraminifera. The first thin layer, or primary calcite, consists of high Mg calcite. Secondary calcite is low Mg calcite and forms the bulk of the shell. From Erez, 2003.

It is their calcareous shells, easily fossilized and extracted from ancient sediments, that have rendered foraminifera so useful in stratigraphic and paleoenviromental studies. In particular, they are used widely in paleotemperature studies and in paleoecologic reconstructions (Pearson et al., 2001; Lear et al., 2002; Kennett et al., 2003). They must, however, be used with caution, because biomineralization processes do not necessarily obey the thermodynamic laws controlling the inorganic precipitation of calcite. This frequently results in disequilibrium between the chemistry of sea water and that of the foraminiferal calcite. To complicate the situation further, disequilibrium may be inconsistent within different parts of the shell and for different parameters (e.g. isotopic, Mg, Sr) and between species of the same genus. Causes of this "vital effect" are not clearly understood, but have been attributed to, among other things, the rate of calcification, the incorporation of metabolic products into the shell, and poor understanding of the microhabitat surrounding the foraminifer (Grossman, 1984; Grossman, 1987; Erez, 2003). Despite this, foraminiferal species considered to be faithful recorders of environmental parameters have been identified, and are used as proxies in reconstructions. For example, *Uvigerina* spp., and *Cassidulina* spp., are used in isotopic studies of DIC in bottom waters, whereas *Globobulimina* spp. are used as proxies for the composition of pore waters (Grossman, 1987).

Foraminifera in modern cold seeps have been studied at locations on tectonically active and passive margins, including Blake Ridge, Atlantic Ocean

(Robinson et al., 2004; Panieri and Sen Gupta, 2008); Gulf of Mexico (Sen Gupta and Aharon, 1994; Sen Gupta et al., 1997; Robinson et al., 2004; Sen Gupta et al., 2007; Lobegeier and Sen Gupta, 2008); the North Sea (Jones, 1993); coastal California (Rathburn et al., 2000; Bernhard et al., 2001; Rathburn et al., 2003); Hydrate Ridge, eastern Pacific (Torres et al., 2003; Heinz et al., 2005); the Rockall Trough, Irish Sea (Panieri, 2005); Japan (Akimoto et al., 1994); the Barents Sea (Mackensen et al., 2006); the Adriatic Sea (Panieri, 2003; Panieri, 2006); the SW Barents Sea (Wollenburg and Mackensen, In press); and off New Zealand (Martin et al., 2009). Foraminifera from Cenozoic seeps have been investigated from the Miocene of Italy (Barbieri and Panieri, 2004) and the Eocene through Pliocene of the Cascadia Margin of the eastern Pacific (Martin et al., 2005; Martin et al., 2007). All of these studies found that, unlike seep invertebrate fauna, there are no foraminiferal species that are endemic to seeps.

Foraminifera found in cold seeps respond to the presence of methane in pore waters by recording a depleted and highly variable $\delta^{13}C$ signal in their calcite tests (Hill et al., 2003; Rathburn et al., 2003; Hill et al., 2004; Martin et al., in press). In non–seep sediments, the $\delta^{13}C$ value of benthic foraminiferal tests varies within a narrow range: for example, the range of $\delta^{13}C$ values in non–seep specimens of the species *Uvigerina peregrina* is typically between 0.2‰ to 0.4‰ PDB (Rathburn et al., 2003). In foraminiferal tests from modern seeps, however, $\delta^{13}C$ values are considerably more variable. Analyses of single foraminiferal apecimens indicate that the isotopic variation is large even within the same species. For instance, from seeps in the Santa Barbara channel, the epifaunal $d^{13}C$ values for *Cibicides mckannai* varied between –0.37‰ and –2.28‰ PDB, and the infaunal *Pyrgo* sp. recorded values between –0.01‰ and –25.23‰ PDB (Hill et al., 2003). From this, it is clear that foraminiferal test carbonate is capable of recording excursions of depleted ^{13}C in ambient seawater and interstitial waters. $d^{13}C$ values of foraminiferal carbonate in modern seeps are, however, not in equilibrium with ambient pore water (e.g Rathburn et al., 2003; Torres et al., 2003; Martin et al., in press). In fossil seeps, $\delta^{13}C$ values for some species, particularly the infaunal

Globobulimina pacifica, Nonionella stella, and *Pyrgo* spp. exhibited $\delta^{13}C$ as low as -55‰ PDB, certainly within the range of archaeal (microbial or biogenic) methane (Martin et al., 2007).

The reason for the high variability and apparent isotopic disequilibrium in seep foraminifera is not completely understood. The variability is almost certainly due in part to the heterogeneity of the micro-environments in cold seep sediments, brought about by mixing of carbon sources and the fine scale tortuosity of fluid-flow pathways. The isotopic disequilibrium may have a number of explanations. Chief among these is the question of whether foraminifera actually live and calcify in methane seeps. Numerous studies have concluded that various species of foraminifera live in seeps (e.g. Sen Gupta et al., 1997; Bernhard et al., 2001; Hill et al., 2003; Rathburn et al., 2003; Heinz et al., 2005; Mackensen et al., 2006; Panieri and Sen Gupta, 2008). Most of these studies relied on Rose Bengal stain to identify living organisms, and this is known to stain cytoplasm weeks after the death of the organism. In their study, Bernhard et al. (2001) compared Rose Bengal with adenosine triphosphate assay (ATP), and ultrastructural studies and concluded that foraminifera did, indeed live in methane seeps. If this is the case, two questions are still unanswered: how do aerobic foraminifera survive in the dys-anoxic seep environment, and why are their shells apparently not in isotopic equilibrium with the surrounding pore waters? A possible answer to the first question is provided by Bernhard and Bowser (2008) who investigated the reason for an unusually large number of peroxisomes present in seep foraminifera and speculated that in some foraminifera, the peroxisomes convert environmentally and metabolically produced H_2O_2 into water and oxygen, and the latter is used in foraminiferal respiration. Assuming foraminifera do live in seeps, the reason for their isotopic disequilibrium is still enigmatic. In their study of laminated sediments in the Santa Barbara Basin, (Bernhard and Bowser, 1999) suggested foraminifera may migrate into and out of seeps, which would result in isotopic disequilibrium. Sen Gupta et al. (1997) observed a thickened organic lining in *Cassidulina neocarinata* in Gulf of Mexico seeps, leading them to speculate that the foraminifer might become dormant during

periods of environmental stress. A final possibility is simply a lack of understanding of the micro-habitats in which the foraminifera actually live, and that may not be reflected in the comparatively large-scale sampling of pore waters. This study was undertaken to utilize the carbonate shells of benthic foraminifera to develop a proxy for identifying and characterizing methane seepage in ancient sediments. Foraminifera and authigenic carbonates were recovered from late Eocene through early Pliocene sediments of the Cascadia accretionary margin and modern seeps from the Hikurangi margin of New Zealand. The investigation concentrated on foraminiferal assemblage data, isotopic data from both foraminiferal shells and authigenic carbonates and Mg/Ca ratios of carbonates. The most significant findings to date are:

1. consistent with modern seep foraminifera, no endemic seep foraminiferal species were identified;
2. in both modern and ancient seeps, foraminiferal $d^{13}C$ values are more variable and depleted than those in normal marine water;
3. in some cases, seep foraminiferal $d^{13}C$ is depleted enough to identify it as derived from microbial methanogenesis; in other cases it is well within the range of thermogenic methanogenesis, or may be attributable to a mixture of sources;
4. Mg/Ca ratios, obtained using an innovative flow-through system, identified diagenetic alteration as well as pristine shell carbonate in fossil foraminifera, and also distinguished multiple phases of mineralization in some shells;
5. comparison of foraminiferal isotopic and elemental ratios with those of authigenic carbonates indicates that during post-depositional alteration, foraminifera become nucleation centers for diagenetic mineralization, and the resulting elemental ratios mimic those of the authigenic carbonates;

6. further refinement, in particular, the addition of other isotopic ($^{87}Sr/^{86}Sr$) and elemental ratios (Ba/Mg) will result in a sensitive, fine-scale proxy that will yield high-resolution results.

This proxy has the potential to lead to a more detailed understanding of methane seep processes as well as their interconnection with tectonism, climate events, and, possibly, new economic resources. In addition, the proxy may prove to be a useful addition to paleoclimate studies by determining the degree of alteration in foraminiferal samples and identifying those that will yield the most meaningful results.

Notes to Chapter 1

Aharon, P., 1994. Geology and biology of modern and ancient hydrocarbon seep vents: An introduction. Geo-Marine Letters, 14: 69-73.

Akimoto, K., Tanaka, T., Hattori, M. and Hotta, H., 1994. Recent benthic foraminiferal assemblages from the cold seep communities - A contribution to the methane gas indicator. In: R. Tsuchi (Editor), Pacific Neogene Events in Time and Space. University of Tokyo Press, Tokyo, pp. 11 - 25.

Aloisi, g. et al., 2002. CH_4-consuming microorganisms and the formation of carbonate crusts at cold seeps. Earth and Planetary Science Letters, 203: 195-203.

Barbieri, R. and Panieri, G., 2004. How are benthic foraminiferal faunas influenced by cold seeps? Evidence from the Miocene of Italy. Palaeogeography, Palaeoclimatology, Palaeoecology, 204: 257-275.

Berndt, M.E., Allen, D.E. and Seyfried, W.E.J., 1996. Reduction of CO_2 during serpentinization of olivine at 300^{o}C and 500 bar. Geology, 24(4): 351-354.

Bernhard, J.M. and Bowser, S.S., 1999. Benthic foraminifera of dysoxic sediments: chloroplast sequestration and functional morphology. Earth-Science Reviews, 46(1-4): 149-165.

Bernhard, J.M. and Bowser, S.S., 2008. Peroxisome proliferation in foraminifera inhabiting the chemocline: An adaptation to reactive oxygen species exposure? Journal of Eukaryotic Microbioloby, 55(3): 135-144.

Bernhard, J.M., Buck, K.R. and Barry, J.P., 2001. Monterey Bay cold-seep biota: Assemblages, abundance, and ultrastructure of living foraminifera. Deep-Sea Research Part I-Oceanographic Research Papers, 48: 2233-2249.

Boetius, A. et al., 2000. A marine microbial consortium apparently mediating anaerobic oxidation of methane. Nature, 407: 623-626.

Boetius, A. and Suess, E., 2004. Hydrate Ridge: a natural laboratory for the study of microbial life fueled by methane from near-surface gas hydrates. Chemical Geology, 205: 291-310.

Bohrmann, G., Greinert, J., Suess, E. and Torres, M., 1998. Authigenic carbonates from the Cascadia subduction zone and their relation to gas hydrate stability. Geology, 26(7): 647-650.

Budai, J.M., Martin, A.M., Walter, L.M. and Ku, T.C.W., 2002. Fracture-fill calcite as a record of microbial methanogenesis and fluid migration: a case study from the Devonian Antrim Shale, Michigan Basin. Geofluids, 2: 163-183.

Buffet, B. A., 2000. Clathrate Hydrates. Annual Review of Earth and Planetary Sciences, 28: 477-507.

Cameron, E.M., 1982. Sulfate and sulfate reduction in early Precambrian oceans. Nature, 296: 145-148.

Campbell, K.A., 2006. Hydrocarbon seep and hydrothermal vent palaeoenvironments and palaeontology: Past developments and future research directions. Palaeogeography, Palaeoclimatology, Palaeoecology, 232(2-4): 362-407.

Catling, D.C., Zahnle, K.J. and McKay, C.P., 2001. Biogenic methane, hydrogen escape, and the irreversible oxidation of Early Earth. Science, 293: 839-843.

Claypool, G.E. and Kaplan, I.R., 1974. The origin and distribution of methane in marine sediments. In: I.R. Kaplan (Editor), Natural Gases in Marine Sediments. Plenum, New York, pp. 99-139.

Conrad, R. and Schutz, H., 1988. Methods of studying methanogenic bacteria and methanogenic activities in aquatic envitonments. In: B. Austin (Editor), Methods in Aquatic Bacteriology. Wiley, Chichester, U.K., pp. 301-343.

Erez, J., 2003. The source of ions for biomineralization in Foraminifera and their implications for paleoceanographic proxies. In: P.M. Dove, J.J. De Yoreo and S. Weiner (Editors), Biomineralization. Reviews in Mineralogy and Geochemistry. Mineralogical Society of America, Washington, pp. 115-149.

Greinert, J., Bohrmann, G. and Suess, E., 2001. Gas hydrate-associated carbonates and methane-venting at Hydrate Ridge: classification, distribution, and origin of authigenic lithologies. In: C.K. Paull and W. Dillon (Editors), Natural Gas Hydrates: Occurrence, Distribution, and Detection. American Geophysical Union, Washington, D.C., pp. 99-113.

Grossman, E.L., 1984. Carbon isotopic fractionation in live benthic foraminifera—comparison with inorganic precipitate studies. Geochimica et Cosmochimica Acta, 48: 1505-1512.

Grossman, E.L., 1987. Stable isotopes in modern benthic foraminifera: a study of vital effect. Journal of Foraminiferal Research, 17(1): 48-61.

Han, X., Suess, E., Sahling, H. and Wallmann, K., 2004. Fluid venting activity on the Costa Rica margin: new results from authigenic carbonates. International Journal of Earth Sciences, 93: 596–611.

Hansen, H.J., 1999. Shell construction in modern calcareous foraminifera. In: B.K. Sen Gupta (Editor), Modern Foraminifera. Kluwer, Dordrecht/Boston/London, pp. 57-70.

Heinz, P., Sommer, S., Pfannkuche, O. and Hemleben, C., 2005. Living benthic foraminifera in sediments influenced by gas hydrates at the Cascadia convergent margin, NE Pacific. Marine Ecology Progress Series, 304: 77-89.

Hill, T.M., Kennett J.P. and Spero, H.J., 2003. Foraminifera as indicators of methane-rich environments: A study of modern methane seeps in Santa Barbara Channel, California. Marine Micropaleontology, 49: 123-138.

Hill, T.M., Kennett, J.P. and Spero, H.J., 2004. High-resolution records of methane hydrate dissociation: ODP site 893, Santa Barbara Basin. Earth and Planetary Science Letters, 223: 127-140.

Horita, J. and Berndt, M., 1999. Abiogenic methane formation and isotopic fractionation under hydrothermal conditions. Science, 285: 1055-1057.

Jones, R.W., 1993. Preliminary observations on benthonic foraminifera associated with biogenic gas seeps in the North Sea. In: D.G. Jenkins (Editor), Applied Micropaleontology. Kluwer Academic Publishers, Dordrecht, pp. 69-91.

Kastner, M. 2001, Gas hydrates in convergent margins: Formation occurrence, geochemistry and global significance. In: C.K. Paull and W.P. Dillon, (Editors), Natural Gas Hydrates: Occurrence, Distribution and Detection, Geophysical Monograph 124, AGU, Washington, D.C.: 67-86.

Kennet, J.P., Cannariato, K.G., Hendy, I.L., Behl, R.J., 2000. Carbon isotopic evidence for methane hydrate instability during Quaternary interstadials. Science, 288: 128-133.

Kennett, J.P., Cannariato, K.G., Hendy, I.L. and Behl, R.J., 2003. Methane Hydrates in Quaternary Climate Change: The Clathrate Gun Hypothesis. AGU Special Publication, 54, 216 pp.

Kvenvolden, K.A., 1999. Potential effects of gas hydrates on human welfare. National Academy of Science Proceedings, 96: 3420-3426.

Leefmann, T. et al., 2008. Miniaturized biosignature analysis reveals implications for the formation of cold seep carbonates at Hydrate Ridge. Biogeosciences, 5: 731-738.

Levin, L.A., 2005. Ecology of cold seep sediments: Interactions of fauna with flow, chemistry, and microbes. Oceanography and Marine Biology, an Annual Review,

Lobegeier, M.K. and Sen Gupta, B.K., 2008. Foraminifera of hydrocarbon seeps, Gulf of Mexico. Journal of Foraminiferal Research, 38(2): 93-116. 43: 1-46.

Lollar, B.S. et al., 2006. Unravelling abiogenic and biogenic sources of methane in the Earth's deep surface. Chemical Geology, 226: 328-339.

Lorenson, T.D., Collett, T.S., 2000. Gas content and composition of gas hydrate from sediments of the southeastern North American continental margin. In: C.K. Paull et al., (Editors), Proceedings of the Ocean Drilling Program, Scientific Results, 164: 47-46.

Luff, R. and Wallmann, K., 2003. Fluid flow, methane fluxes, carbonate precipitation and bigeochemical turnover in gas hydrate-bearing sediments at Hydrate Ridge, Cascadia Margin. Geochimica et Cosmochimica Acta, 67: 3403-3421.

Luff, R., Wallmann, K. and Aloisi, G., 2004. Numerical modeling of carbonate crust formation at cold vent sites: significance for fluid and methane budgets and chemosynthetic biological communities. Earth and Planetary Science Letters, 221: 337-353.

Mackensen, A., Wollenburg, J. and Licari, l., 2006. Low $d^{13}C$ in tests of live epibenthic and endobenthic foraminifera at a site of active methane seepage. Paleoceanography, 21: PA2022, doi:10.1029/2005PA001196,2006.

Majima, R., Nobuhara, T. and Kitazaki, T., 2005. Review of fossil chemosynthetic assemblages in Japan. Palaeogeography, Palaeoclimatology, Palaeoecology, 277: 86 - 123.
Martin, W., Baross, J., Kelley, D., Russell, M.J., 2008. Hydrothermal vents and the origin of life. Nature Reviews: Microbiology, 6:805-814.
Martin, R.A., Nesbitt, E.A. and Campbell, K.A., 2005. Benthic foraminiferal characterization of two Cenozoic cold seeps, Cascadia accretionary margin, Third International Symposium on Hydrothermal Vent and Seep Biology, Scripps.
Martin, R.A., Nesbitt, E.A. and Campbell, K.A., 2007. Carbon stable isotopic composition of benthic foraminifera from Pliocene cold methane seeps, Cascadia accretionary margin. Palaeogeography, Palaeoclimatology, Palaeoecology, 246: 260-277.
Martin, R.A., Nesbitt, E.A. and Campbell, K.A., in press. The effects of anaerobic methane oxidation on benthic foraminiferal assemblages and stable isotopes on the Hikurangi Margin of eastern New Zealand. Marine Geology.
Maslin, M., Mikkelsen, N., Vilela, C., Haq, B., 1998. Sea-level- and gas-hydrate-controlled catastrophic sediment failures of the Amazon Fan. Geology 26: 1107-1110.
Mazzullo, S.J., 2000. Organogenic dolomitization in peritidal to deep-sea sediments. Journal of Sedimentary Research, 70(1): 10-23.
Milkov, A.V. et al., 2003. In situ methane concentrations at Hydrate Ridge, offshore Oregon: New constraints on the global gas hydrate inventory from an active margin. Geological Society of America Bulletin, 31(10): 833-836.
Naehr, T.H. et al., 2007. Authigenic carbonate formation at hydrocarbon seeps in continental margins. Deep-Sea Research II, 54: 1268-1291.
Naehr, T.H. et al., 1998. Authigenic carbonates from the Cascadia subduction zone and their relation to gas hydrate stability. Geology, 26(7): 647 - 650.
Orphan, V.J. et al., 2004. Geological, geochemical, and microbiological heterogeneity of the seafloor around methane vents in the Eel River Basin, offshore California. Chemical Geology, 205: 265-289.
Panieri, G., 2003. Benthic foraminifera response to methane release in an Adriatic Sea pockmark. Rivista Italiana di Paleontologia e Stratigrafia, 109(3).
Panieri, G., 2005. Benthic foraminifera associated with a hydrocarbon seep in the Rockall Trough (NE Atlantic). Geobios, 38(2): 247-255.
Panieri, G., 2006. Foraminiferal respoonse to an active methane seep environment: A case study from the Adriatic Sea. Marine Micropaleontology, 61: 116-130.
Panieri, G. and Sen Gupta, B.K., 2008. Benthic foraminifera of the Blake Ridge hydrate mound, Western North Atlantic Ocean. Marine Micropaleontology, 66(2): 91-102.
Paull, C.K., Juli, A.J.T., Toolin, L.J. and Linick, T., 1984. Stable isotope evidence for chemosynthesis in an abyssal seep community. Nature, 317: 709-711.
Paull, C.K., Buelow, W.J., Ussler, W., III, Borowski, W.S., 1996. Increased continental-margin slumping frequency during sea-level lowstands above gas hydrate-bearing sediments. Geology, 24: 143-146.
Paull, C.K. et al., 2007. Authigenic carbon entombed in methane-soaked sediments from the northeastern transform margin of the Guaymas Basin, Gulf of California. Deep-Sea Research Part II, 54: 1240-1267.
Pearson, P.H. et al., 2001. Warm tropical sea surface temperatures in the Late Cretaceous and Eocene epochs. Nature, 413: 481-488.
Rathburn, A.E., Levin, L.A., Held, Z. and Lohmann, K.C., 2000. Benthic foraminifera associated with cold methane seeps on the northern California margin: Ecology and stable isotopic composition. Marine Micropaleontology, 38: 247-266.
Rathburn, A.E. et al., 2003. Relationships between the distribution and stable isotopic composition of living benthic foraminifera and cold methane seep biogeochemistry in Monterey Bay, California. Geochemistry, Geophysics, Geosystems, 4(12): 1106, doi:10.1029/2003GC000595, 2003.
Roberts, H. and Whelan, T.W.I., 1975. Methane-derived carbonate cements in barrier and beach sands of a subtropical delta complex. Geochimica et Cosmochimica Acta, 19: 1085-1089

Robinson, C.A., Bernhard, J.M., Levin, L.A., Mendoza, G.F. and Blanks, J., 2004. Surficial hydrocarbon seep infauna from the Blake Ridge (Atlantic Ocean, 2150 m) and the Gulf of Mexico (690-2240 m). P.S.N.Z.: Marine Ecology, 25(4): 313-336.

Sahling, H., Rickert, D., Lee, R.W., Linke, P. and Suess, E., 2002. Macrofaunal community structure and sulfide flux at gas hydrate deposits from the Cascadia convergent margin, NE Pacific. Marine Ecology Progress Series, 231: 121-138.

Sassen, R. and MacDonald, I., 1998. Bacterial methane oxidation in sea-floor gas hydrate: Significance to life in extreme environments. Geology, 26: 851-854.

Semrau, J.D., DiSpirito, A.A. and Murrell, J.C., 2007. Life in the extreme: thermoacidophilic methanotrophy. Trends in Microbiology, 16(5): 190-193.

Sen Gupta, B.K. and Aharon, P., 1994. Benthic foraminifera of bathyal hydrocarbon vents of the Gulf of Mexico: Initial report on communities and stable isotopes. Geo-Marine Letters, 14: 88-96.

Sen Gupta, B.K., Platon, E., Bernhard, J.M. and Aharon, P., 1997. Foraminiferal colonization of hydrocarbon-seep bacterial mats and underlying sediment, Gulf of Mexico slope. Journal of Foraminiferal Research, 27(4): 292-300.

Sen Gupta, B.K., Smith, L. and Lobegeier, M., 2007. Attachment of Foraminifera to vestimentiferan tubeworms at cold seeps: Refuge from seafloor hypoxia and sulfide toxicity. Marine Micropaleontology, 62: 1-6.

Stadnitskaia, A. et al., 2008. Carbonate formation by anaerobic oxidation of methane: Evidence from lipid biomarker and fossil 16S rDNA. Geochimica et Cosmochimica Acta, 72: 1824-1836.

Suess, E. et al., 2001. Sea floor methane hydrates at Hydrate Ridge, Cascadia Margin. In: C.K. Paull and W.P. Dillon (Editors), Natural Gas Hydrates: Occurrence, Distribution and Detection. American Geophysical Union Geophysical Monograph, Washington, D.C., pp. 87-98.

Shen, Y., Buick, R. and Canfield, D.E., 2001. Isotopic evidence for microbial sulphate reduction in the early Archaean era. 410: 77-81.

Sibuet, M. and Olu, K., 1998. Biogeography, biodiversity and fluid dependence of deep-sea cold-seep communities at active and passive margins. Deep-Sea Research II, 45: 517-567.

Sommer, S. et al., 2006. Efficiency of the benthic filter: Biological control of the emission of dissolved methane from sediments containing shallow gas hydrates at Hydrate Ridge. Global Biogeochemical Cycles, 20(GB2019): doi:10.1029/2004GB002389.2006.

Suess, E., Carson, B., Ritger, S.D., Moore, J.C., Jones, M.L., Kulm, L.D., Cochrane, G.R., 1985. Biological communities at vent sites along the subduction zone off Oregon, in: Jones, M.L., ed., The hydrothermal vents of the eastern Pacific: An Overview. Biological Society of Washinton Bulletin 6: 475-484

Thauer, R. K., Kaster, A.-K., Seedorf, H., Buckel, W., Hedderick, R., 2008. Methanogenic archaea: ecologically relevant differences in energy conservation. Nature Reviews Microbiology, 6: 579-591.

Teichert, B.M.A., Bohrmann, G., Suess, E., 2005. Chemoherms on Hydrate Ridge – Unique microbially-mediated carbonate build-ups growing into the water column. Paleogeography, Paleoclimatology, Paleoecology, 227: 67-85.

Torres, M. et al., 2003. Is methane venting at the seafloor recorded by the d13C of benthic foraminifera shells? Paleoceanography, 18: 1062-1075.

Torres, M.E. and Kastner, M., 2009. Data report: clues about carbon cycling in methane-bearing sediments using stable isotopes of the dissolved inorganic carbon. Proceedings of the Integrated Ocean Drilling Program, 311.

Treude, T., Boetius, A., Knittel, K., Wallmann, K. and Jorgensen, B.B., 2003. Anaerobic oxidation of methane above gas hydrates at Hydrate Ridge, N.E. Pacific Ocean. Marine Ecology Progress Series, 264: 1-14.

Tunnicliffe, V., 1992. The nature and origin of the modern hydrothermal vent fauna. Palaios, 7: 338-350.

Valentine, D.L. and Reesburgh, W.S., 2000. New perspectives on anaeroic methane oxidation. Environmental Microbiology, 2(5): 477-484.

Weiner, S. and Dove, P.M., 2003. An overview of biomineralization processes and the problem of the vital effect. In: P.M. Dove, J.J. De Yoreo and S. Weiner (Editors), Biomineralization. Reviews in Mineralogy and Geochemistry. Mineralogical Society of America, Washington, pp. 1-29.

Whiticar, M.J., 1999. Carbon and hydrogen isotope systematics of bacterial formation and oxidation of methane. Chemical Geology, 161: 291-314.

Whiticar, M.J. and Faber, E., 1986. Methane oxidation in sediment and water column environments - isotope evidence. Organic Geochemistry, 10: 759-768.

Wollenburg, J.E. and Mackensen, A., In press. The ecology and distribution of benthic foraminifera at the Hakon Mosby muc volcano (SW Barents Sea slope). Deep-Sea Research I – Oceanographic Research Papers, 56: 1336-1370.

Zyakun, A.M., 1992. Isotopes and their possible use as biomarkers of microbial products. In: R. Vially (Editor), Microbial Gas. Editions Technip, Paris, pp. 27-46.

Chapter 2. Carbon Stable Isotopic Composition Of Benthic Foraminifera From Pliocene Cold Methane Seeps, Cascadia Accretionary Margin

Summary

Cold methane seep carbonates preserve the distinctive carbon stable isotope signatures of their ambient pore waters, thus facilitating the identification of methane sources and fluid migration pathways. This study employs an isotopic indicator from microfossils in a diffuse fossil seep for the recognition and characterization of methane seepage in the rock record. Benthic foraminifera from the Pliocene Quinault Formation, western Washington State, are plentiful and provide a temporal link between modern and more ancient seeps. Stable carbon isotope analyses of individual foraminiferal tests revealed a clear distinction between seep and non-seep foraminifera. Infaunal species *Globobulimina pacifica* and *Nonion basispinatum* collected from seep samples exhibited $\delta^{13}C$ values that were highly variable and often strongly depleted: values ranged from −33.1‰ to −55.3‰ PDB in *G. pacifica* and from +2.1‰ to −42.9‰ PDB in *N. basispinatum.* The epifaunal species *Cibicidoides mckannai*, though less depleted, also showed considerable variability with $\delta^{13}C$ values ranging from +1.7‰ to −3.1‰ PDB. In contrast, non-seep specimens were much more enriched and variable: non-seep specimens of *N. basispinatum* displayed $\delta^{13}C$ values clustering between −0.5‰ and −1.5‰ PDB, while non-seep specimens of *C. mckannai* yielded a range of +1.1‰ to +1.8‰ PDB. SEM analyses and oxygen isotope values of foraminiferal tests indicated minimal diagenetic alteration. $\delta^{13}C$ values from authigenic blebs (small nodules with wispy, indistinct boundaries) ranged from +8.7‰ to −38.4‰ PDB. By combining these inorganic carbonate data with the foraminiferal values, the association of seep-specific bivalves, and the present-day leakage of thermogenic methane from the nearby Garfield gas mound, we conclude that these foraminifera precipitated their tests in the presence of methane-derived carbon. Thus they record

pore-water ^{13}C depletion and syndepositional fluid-flow pathways near the sediment/water interface in a seep system active 3.4 mya and continuing onshore and offshore today. The range and degree of ^{13}C depletion in the Pliocene microfossils is due to the heterogeneity of seepage caused by different methane sources (i.e. thermogenic and biogenic), the tortuosity of fluid migration pathways reaching the seafloor sediments, and mixing of seep fluids with dissolved inorganic carbon (DIC) and marine organic carbon.

1. Introduction

Biogeographic and stratigraphic distribution of chemosynthesis-based ecosystems in marine sedimentary basins reflect positions of hydrocarbon accumulation and advection. The present study investigates methane-seep carbon isotope signatures in fossil foraminifera from Pliocene accretionary wedge sediments of the northeast Pacific margin, and evaluates whether foraminiferal characteristics found in Recent seeps (e.g. Sen Gupta et al., 1997; Hill et al., 2003; Rathburn et al., 2003) are applicable to ancient settings. Fossil methane seeps of middle Eocene to Pliocene age in California, Oregon and Washington have been identified on the basis of their macrofaunal assemblages, which contain typical hydrothermal vent and hydrocarbon seep taxa, including fossil siboglinid (pogonophoran annelid) tubeworms, solemyid, modiolid and vesicomyid bivalves, and provannid and peltospirid gastropods (Campbell, 1989, 1992; Squires and Goedert, 1991; Rigby and Goedert, 1996; Goedert and Benham, 1999; Goedert et al., 2000). Foraminifera from the Pliocene Quinault Formation of western Washington State were chosen for this study for several reasons. First, the marine strata contain macrofaunal and lithological evidence of methane seepage (Campbell, 1992) as well as a substantial assemblage of benthic foraminifera (Rau, 1970). Second, the Pliocene age of the formation provides a convenient temporal link between modern and more ancient seep sites. Third, diagenetic overprinting is minimal, because of the young age, shallow burial, and fossil preservation in siliciclastic sediments (sandy mudstone to muddy sandstone), rather than in

calcareous chemoherms. Specifically, the goals of this study are to establish whether the foraminifera from the Quinault Formation preserve robust seep signatures that can be used to characterize seepage, and if these signatures are similar to those found in foraminifera of modern seeps.

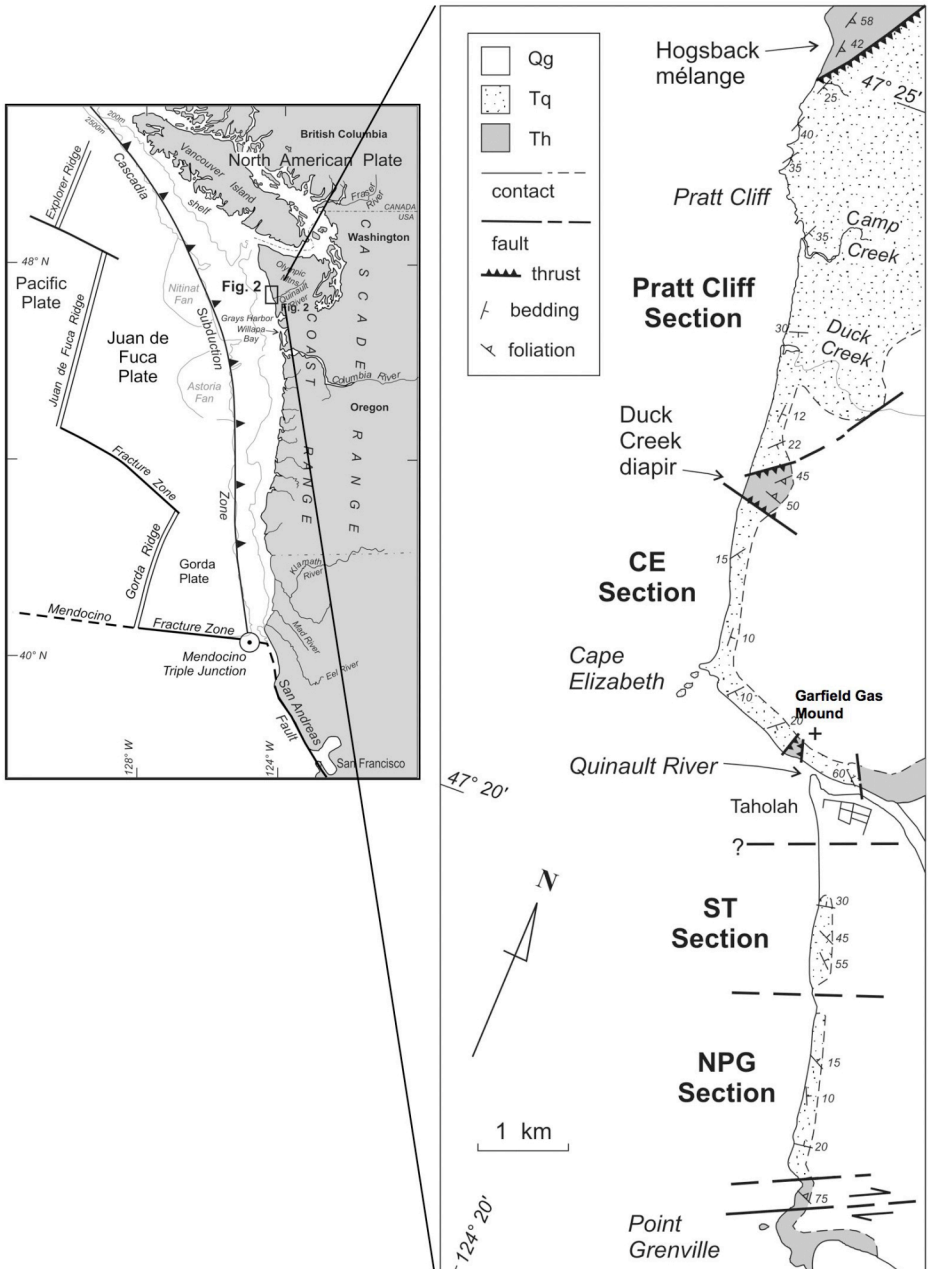

Figure 2.1. Tectonic map of northeastern Pacific convergent margin showing the positions of the Juan de Fuca ridge, the Cascadia subduction zone, and the Pliocene Quinault forearc strata (inset). Positions of the four sections of the Quinault Formation and the Garfield Gas Mound are shown in the inset. Modified from Campbell et al., 2006, page 3.

2. Background

Cold methane seeps occur in widespread and diverse geologic settings; from shallow to deep water, and from tectonically active to passive continental margins (Campbell, 2006). They are seafloor sites of CH_4- and H_2S - rich fluid flow at ambient temperatures, and are characterized by a distinctive suite of organisms, including chemoautotrophic microbes, siboglinid tubes, and seep-specific bivalves (Sibuet and Olu, 1998; Levin and Michener, 2002). Cold methane seeps in the modern marine environment were first reported from carbonate cements in barrier and beach sands of the Chandeleur Islands off the Louisiana coast (Roberts and Whelan, 1975). Subsequently, dense communities of organisms resembling those found at hydrothermal vents were observed at active seepage areas along the base of the Florida Escarpment (Paull et al., 1984) and in subduction-related settings offshore of Oregon and Washington (Suess et al., 1985). Fossil seeps are also now well-known, particularly from marine sedimentary strata of Italy, Japan, California, and the northeast Pacific margin (Goedert and Squires, 1990; Campbell and Bottjer, 1993; Aharon, 1994; Goedert and Benham, 1999; Goedert et al., 2000: Campbell et al., 2002; Goedert et al., 2003; Barbieri and Panieri, 2004; Majima et al., 2005). Recent seep sites often show distinctive zonation of organisms that reflects the distribution of sulfide in the sediment. For example, on Hydrate Ridge, off the Oregon coast, Sahling et al. (2002) note zonation with the cheomautotrophic, mat-forming bacteria *Beggiatoa* sp. directly overlying gas hydrates where maximum concentrations of hydrogen sulfide venting occur. As surface concentrations of sulfide decrease away from central vent areas, *Beggiatoa* gives way to vesicomyid bivalves and finally to solemyid bivalves. Similar zonation has been found in seeps in Monterey Bay (Rathburn et al., 2003). In the Quinault Formation, cold seep macrofauna are represented by scattered occurrences of the solemyid bivalve *Acharax ventricosa* with few *Calyptogena pacifica* and *Modiolus* sp., surrounded by a zone of *Lucinoma annulata* and *Yoldia (Cnesterium) scissurata* (Campbell, 1992; Nesbitt and Campbell, 2004a). Hence,

Pliocene Quinault seeps were zones of relatively low sulfide concentration. Methane-charged fluid flow in the Quinault Formation was either extremely diffuse or not sustained long enough for the development of voluminous carbonates nor for the establishment of large communities of characteristic seep macrofauna (Nesbitt and Campbell, 2004b).

Methanogenesis, both biogenic and thermogenic, produces characteristic strongly depleted stable carbon isotope signatures that range from –50‰ to –30‰ PDB (PeeDee belemnite standard) for thermogenic methane, and –110‰ to –50‰ PDB for biogenic methane (Claypool and Kaplan, 1974; Whiticar, 1999). Carbonates formed using methane-derived carbon sources preserve these distinctive isotopic signatures and become indicators of past fluid activity (Campbell et al., 2002).

Foraminifera in modern cold seeps have been studied at locations including Blake Ridge, Atlantic Ocean (Robinson et al., 2004), Gulf of Mexico (Sen Gupta and Aharon, 1994; Sen Gupta et al., 1997; Robinson et al., 2004), the North Sea (Jones, 1993), coastal California (Bernhard et al., 2001), Hydrate Ridge, Oregon (Torres et al., 2003; Heinz et al., 2005), the Rockall Trough, Irish Sea (Panieri, 2005), off Japan (Akimoto et al., 1994), and the Barents Sea (Mackensen et al., 2006). All of these studies found that, unlike seep macrofauna, there are no foraminiferal species that are endemic to seeps. In addition, foraminiferal densities and diversity in modern seeps do not show consistent trends. In some cases, density was low relative to comparable non-seep sites (e.g. Sen Gupta et al., 1997, Bernhard et al., 2001); in others densities were similar in seep and non-seep samples (e.g. Rathburn et al., 2003). In two studies, statistical analyses resulted in the identification of diagnostic assemblages (Akimoto et al., 1994, and Panieri, 2005).

The possibility of using stable isotopes of benthic foraminifera as indicators for the past presence of methane in marine sediments was proposed during an investigation of a late Quaternary core from ODP site 680 B off Peru (Wefer et al., 1994). It is hypothesized that seep foraminifera respond to the presence of methane

in pore waters by recording a depleted and variable $\delta^{13}C$ signal in their calcite tests (Hill et al., 2003, 2004; Rathburn et al., 2003;). In non-seep sediments, the $\delta^{13}C$ value of foraminiferal tests varies within a narrow range: for example, the range of variation in non-seep specimens of *Uvigerina peregrina* is typically between 0.2‰ to 0.4‰ (Rathburn et al., 2003). In foraminifera from modern seeps, however, $\delta^{13}C$ values are considerably more variable. Single species bulk samples from Santa Barbara Channel seeps recorded $\Delta\delta^{13}C$ ($\delta^{13}C_{max} - \delta^{13}C_{min}$) between species ranging from –0.9‰ to –20.13‰ PDB (Hill et al., 2003). Analyses of individual specimens from seeps indicate that the isotopic variation is large even within a single species. For instance, *Cibicides mckannai* varied between –0.37‰ and –2.28‰ PDB, and *Pyrgo* sp. recorded values between –0.01‰ and –25.23‰ PDB (Hill et al., 2003). Thus, foraminiferal carbonate is capable of recording excursions of depleted ^{13}C in ambient seawater and interstitial waters and these can be used to identify seep sites and methane sources.

3. Geologic setting

The Quinault Formation is an ancient forearc sequence on the Cascadia convergent margin, exposed in seacliff sections along a 10 km stretch of coastline north of Point Grenville, Washington (Figure 2.1). Outcrops are accessible only at lowest low tide, and some are continually wave-washed. Inland, outcrops are sparse and poorly exposed, typically covered by vegetation or Quaternary alluvium. Offshore exploratory drilling on the Washington shelf has encountered rocks equivalent in age to Quinault strata (Rau, 1970). The Pliocene age of the formation is based on foraminifera and macrofauna (Rau, 1970; Campbell and Nesbitt, 2000). Quinault strata are underlain by the middle Miocene Hoh rock assemblage, an ancient accretionary prism in fault contact with and, in places, diapirically intruded into the overlying Quinault forearc sediments (Orange and Campbell, 1997; Campbell et al., 2006). This thick accretionary wedge of organic-rich sediments that accumulated on the Washington shelf and slope during the Cenozoic was subjected to compression and compaction as the Juan de Fuca Plate subducted

beneath North America, resulting in reduced sediment porosities, elevated pore pressures, and fluid de-watering (Rau, 1970; Orange and Campbell, 1997; Stewart et al., 2003). Conduits for the migration of fluids, and thus the formation of seeps, were provided by faults, diapirs, and permeable sediments.

With a total thickness of 3000 m, the Quinault Formation outcrops in four sections which, though internally contiguous, are not preserved in stratigraphic sequence. Each section is bounded by faults or Hoh diapirs (Campbell and Nesbitt, 2000), and emplaced in relatively coherent blocks by "tectonic surfing" associated with subduction translation and emplacement (Stewart et al., 2003). Sedimentary structures and fauna indicate these sediments were deposited in a shallowing basin, ranging from outer shelf to estuarine/fluvial (Rau, 1970; Campbell and Nesbitt, 2000; Campbell et al., 2006). Ancient methane seep-carbonate deposits (cf. Campbell, 1992) occur in the marine shelf section exposed north and south of Pratt Cliff (Figure 2.2). Paleontological and sedimentological evidence imply that this section was deposited in mid-to-outer shelf depths (Rau, 1970; Campbell et al., 2006). Initially, one seep deposit was identified by Campbell (1992) on the basis of five criteria: tectonic and geologic setting, depositional and sedimentological context, carbon isotopic signatures, fossil megafaunal assemblage, and similarity to adjacent seeps on the modern Cascadia shelf and slope. Subsequently, several more fossil seeps have been discovered and identified in the Pratt Cliff section on the basis of seep-specific mollusks and anomalous carbonates (Figure 2.2).

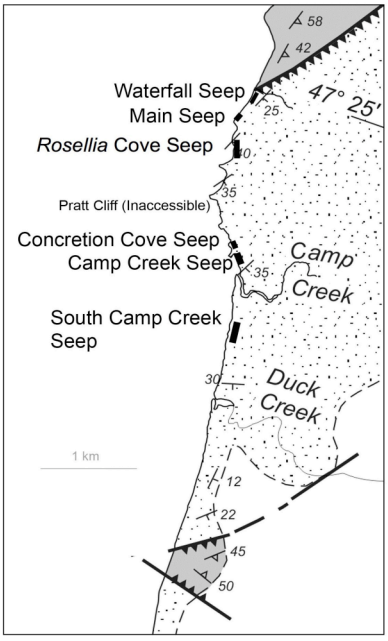

Figure 2.2. Fossil seep sites in the Pratt Cliff section of the Quinault Formation, western Washington State. Individual seeps are indicated by black rectangles. Modified from Campbell et al., 2006, page 4.

4. Methods

Foraminiferal samples were collected in the outcrops of the north and south Pratt Cliff sections as indicated in Table 2.1 and Figure 2.2. Unweathered samples were collected fromlocations that contained evidence of diffuse methane seepage as well as from sites that did not contain such evidence. Seep indicators include fossils of chemoautotrophic organisms such as the bivalves *Calyptogena pacifica, Acharax ventricosa*, and *Lucinoma annulata* and patches of carbonate nodules (physically distinct from surrounding sediments, having discrete boundaries) and carbonate blebs (indistinct, wispy, diffuse boundaries) (Campbell and Nesbitt, 2004; Nesbitt and Campbell, 2004b). In addition, crystals of glendonite, a calcite pseudomorph of the low temperature hydrated calcium carbonate mineral ikaite, were common in the ancient seep localities but were not found in non-seep sites. Thus they were used in conjunction with the other seep indicators. Dry sediment samples (150 grams) were washed through nested 180, 124, and 63 μm sieves, and dried at room temperature. The 63 μm fraction was reserved. The >124 μm fraction

was picked and the foraminifera identified. Where possible, 300 specimens were picked; if this was not possible, the entire >124 μm fraction was picked.

Table 2.1. Burke Museum locality data for Quinault Formation sample sites.

Burke Museum Number	Location	Burke Museum Number	Location
B6858	Camp Creek seep	B6835	Non-seep South Pratt Cliff
B6860	Camp Creek seep	B6837	Non-seep South Pratt Cliff
B6861	Camp Creek seep	B6838	Non-seep South Pratt Cliff
B6862	Camp Creek seep	B6840	Non-seep South Pratt Cliff
B6863	Camp Creek seep	B6841	Non-seep South Pratt Cliff
B6864	Camp Creek seep	B6842	Non-seep South Pratt Cliff
B6865	Camp Creek seep	B6843	Non-seep South Pratt Cliff
B6866	Camp Creek seep	B6845	Non-seep North Pratt Cliff
B6868	Camp Creek seep	B6846	Non-seep North Pratt Cliff
B6869	Camp Creek seep	B6848	Non-seep North Pratt Cliff
B6871	Camp Creek seep	B6857	Non-seep North Pratt Cliff
B6877	Concretion Cove seep	B6874	Non-seep South Pratt Cliff
B6849	Main seep	B6883	*Rosselia* Cove seep
B6850	Main seep	B6839	South Camp Creek Seep
B6851	Main seep	B6875	South Camp Creek seep
B6852	Main seep	B6876	South Camp Creek seep
B6884	Main seep	B6854	Waterfall seep
B6885	Main seep	B6855	Waterfall seep
B6886	Main seep	B6856	Waterfall seep
B6831	Non-seep South Pratt Cliff	B6872	Waterfall seep
B6832	Non-seep South Pratt Cliff	B6873	Waterfall seep
B6834	Non-seep South Pratt Cliff		

Carbon and oxygen isotope analyses were conducted on foraminiferal tests from both seep and non-seep sites, bivalve shells, and authigenic carbonates.

Analyses were performed on individual foraminifera or, if the species was very small, on two or three individuals. The species used for isotope analyses were chosen based on three criteria. First, where possible, species that occur in modern seeps were used in this study. Second, the species chosen were common in a variety of samples. Finally, it was decided to use representatives of foraminifera from different microhabitats. Thus, *Globobulimina auriculata, G. pacifica, Cibicidoides mckannai, Epistominella pacifica,* and *Nonionella stella* were chosen because they are found in Recent cold seeps and/or severely dysoxic environments (Bernhard et al., 1997; Hill et al., 2003; Rathburn et al., 2003; Martin et al., 2004).

Foraminifera are motile organisms, capable of changing position within sediments in response to varying environmental conditions. In their study, Linke and Lutz (1993) concluded that foraminiferal migration within sediments was a food acquisition strategy. Moodley et al. (1998) and Geslin et al. (2004) found that varying oxygen concentration caused foraminifera to move to their favored habitat. Moreover, Geslin et al. (2004) discovered that one species, *Globobulimina affinis,* which is closely related to *G. pacifica* (Corliss, 1985), actually migrates preferentially to dysoxic/anoxic conditions. Thus, different species of foraminifera, although able to migrate within sediments, still have a preferred microhabitat (McCorkle et al., 1997; Geslin et al., 2004). Therefore, for the study of Quinault seep foraminifera, species were chosen to represent microhabitats in which they have most often been reported in the literature (Corliss, 1985; Corliss, 1991; Rathburn and Corliss, 1994; McCorkle et al., 1997). Consequently, *C. mckannai* represents an epifaunal habitat, although Hill, et el. (2003) reports this can be a transitional epi-to-infaunal taxon. *G. pacifica* and *G. auriculata* represent a deep infaunal habitat, and five other species, *Cassidulina reflexa, Epistominella. pacifica, Nonion basispinatum, Nonionella stella,* and *Uvigerina* sp.*,* are representative of shallow infaunal habitats.

To inspect foraminifera for post-depositional alteration, specimens were examined carefully with a light microscope and five representative individuals from each site were examined with a scanning electron microscope (SEM). Isotope

analyses were performed at the Stanford University Stable Isotope Laboratory on a Finnegan Kiel III carbonate device interfaced with a MAT 252 IRMS. Based on multiple analyses of the NBS 19 standard, precision was <0.05‰ for $\delta^{18}O$ and <0.03‰ for $\delta^{13}C$. Results are reported in delta notation ($\delta^{18}O$ and $\delta^{13}C$) relative to the PDB standard, where $\delta = (R_{sample}/R_{standard} - 1)\ 1000$.

The Shannon Weiner diversity index (H) and Simpson's index (λ) were used as measures of the biodiversity of seep and non-seep faunas (see Buzas, 1979). Both of these indices take into account the richness and evenness of the species assemblage. In addition to diversity indices, foraminiferal density was calculated by dividing the number of foraminifera per sample by the weight of dry sediment picked.

5. Results

At low magnification, SEM images (Figure 2.3A, B) would indicate the foraminiferal tests are free of overgrowths and the pores are open with well-defined edges. However, examination at higher magnification (Figure 2.3C,D,E) reveal that tests appear to display some authigenic overgrowth, particularly on exterior surfaces. Comparing these images with those of Millo et al. (2005) illustrates that the foraminifera have been affected to some extent by early diagenesis. Electron Dispersive Spectroscopy (EDS) showed that the overgrowths are calcium carbonate. Oxygen isotope values of Quinault bivalve shells, inorganic carbonates (Table 2.3), and foraminiferal tests (Table 2.4) are within a normal range for marine carbonate and are thus in agreement with the SEM images in suggesting that diagenetic alteration is minimal (cf. Barbieri and Panieri, 2004; Aharon and Sen Gupta, 1994).

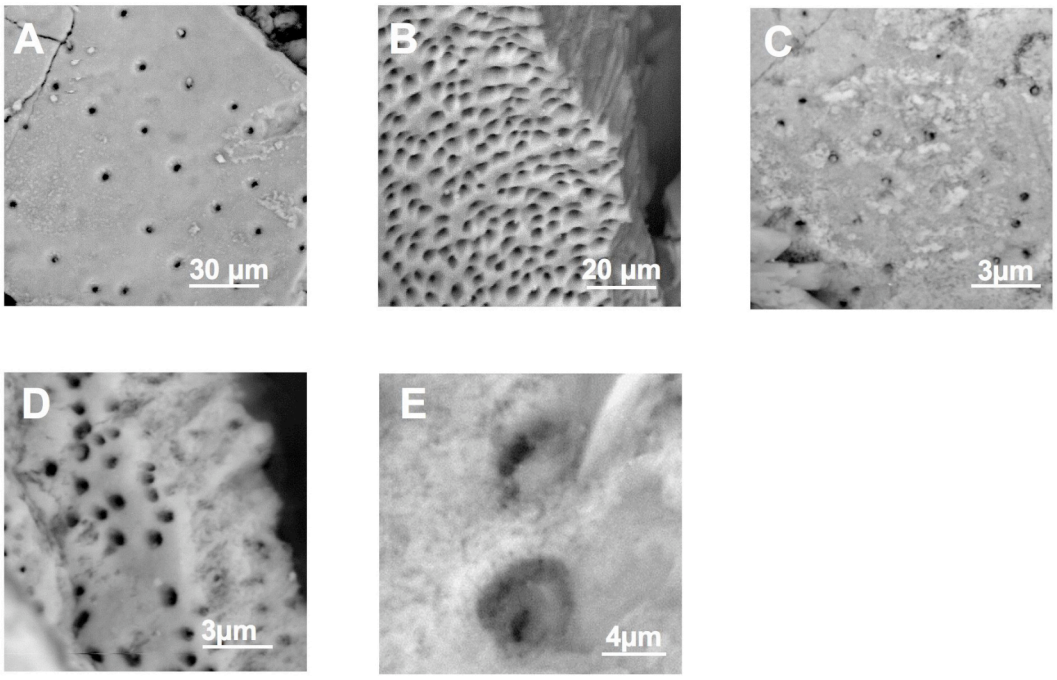

Figure 2.3. SEM images of exterior and interior walls of seep foraminifera. (A) *Globobulimina pacifica*. (B) *Nonion basispinatum*. (C) *Nonionella stella*, exterior wall. (D) *N. stella*, interior wall. (E) *G. pacifica*, exterior wall.

5.1 Foraminiferal assemblage composition

Fifty-one species of foraminifera from 33 genera were identified from the Quinault Formation (Table 2.2). However the assemblage was dominated by individuals of three genera, *Cibicides, Cibicidoides,* and *Globobulimina*, which together totaled 30% of the fauna. Two species of *Cibicides* were present, *C. conoideus*, and *C. fletcheri,* while *Cibicioides* was represented by *C. mckannai.* Although *C. fletcheri* appeared in more samples than the other two species, it was never more than a minor constituent of the assemblage. In contrast, both *C. conoideus* and *C. mckannai* were major contributors to the assemblage in several samples (Figure 2.4A).

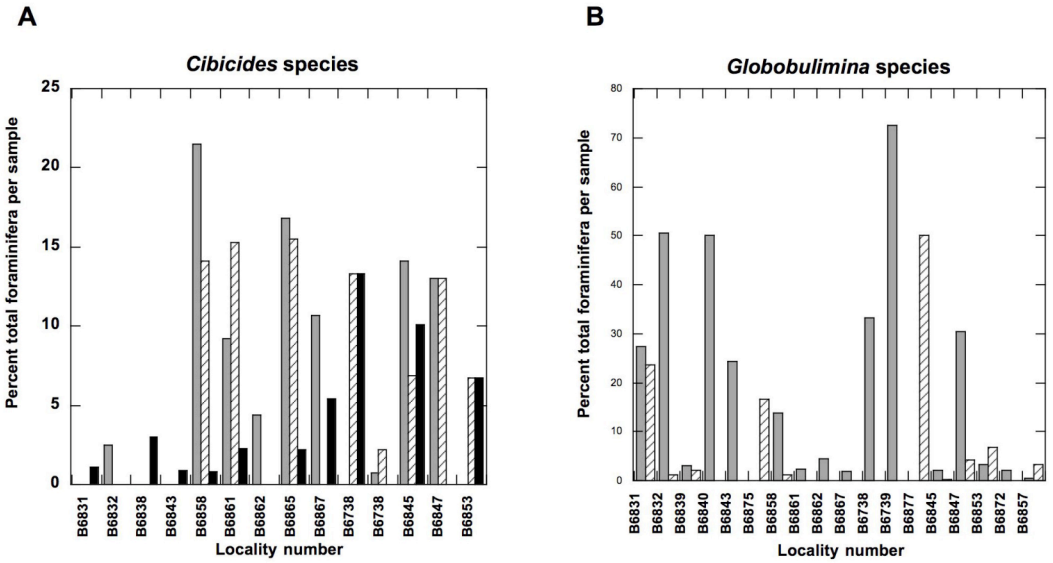

Figure 2.4. Comparison of abundances of the *Cibicides, Cibicidoides* and *Globobulimina* species in samples from the Pratt Cliff section of the Quinault Formation. Key: Figure 4A, gray bar = *Cibicides conoideus*, striped bar = *Cibicidoides mckannai*, black bar = *Cibicides fletcheri.* Figure 4B, gray bar = *Globobulimina auriculata*, striped bar = *G. pacifica.*

The globobuliminids were represented by two species, *Globobulimia auriculata* and *G. pacifica* (Figure 2.4B). Both species were well-represented in some samples, but *G. auriculata* was the most common foraminiferal species in the entire Quinault assemblage, totaling 10.1% of the fauna. Although neither *Epistominella pacifica* nor *Nonionella stella* was an abundant constituent of the faunal assemblage, their occurrences are significant because both are known to be tolerant of low-oxygen environments and *E. pacifica* has been found in Recent cold seep sediments (Bernhard et al., 2001; Hill et al., 2003; Rathburn et al., 2003).

Table 2.2. Foraminiferal species found in the Pratt Cliff section of the Quinault Formation.

Angulogerina semitrigona (Galloway & Wissler)	*Haplophragmoides* sp.
Anomalinoides quinaultensis Rau	*Islandiella islandica* Norvang
Bolivina advena Cushman	*Islandiella limbata* Cushman & Hughes
Bucella inusitata Anderson	*Islandiella translucens* Cushman & Hughes
Bulimina subacuminata Cushman & R.E. Stewart	*Lagena cf. pliocenica timmsana* Cushman & Gray
Bulimina subcalva Cushman & K.C. Stewart	*Lagena* sp.
Buliminella bassendorfensis Cushman & Parker	*Melonis barleeanus* Williamson
Buliminella curta Cushman	*Neogloboquadrina pachyderma (*Ehrenberg)
Buliminella elegantissima d'Orbigny	*Nonion basispinata* (Cushman & Moyer)
Cassidulina reflexa Galloway & Wissler	*Nonion goudkopfi* Kleinpell
Cibicides conoideus Galloway & Wissler	*Nonionella stella* Cushman & Moyer
Cibicides mckannai Galloway & Wissler	*Oolina borealis* Loeblich & Tappan
Cibicides fletcheri Galloway & Wissler	*Oolina melo* d'Orbigny
Cribrostomoides sp.	*Pullenia salisburyi* R.C. & K.C. Stewart
Cyclammina cf. constrictimargo R.C. & K.C. Stewart	*Pullenia cf. miocenica* Kleinpell
Elphidium micrograniulosum (Galloway & Wissler)	*Pyrgo cf. murrhina* Schwager
Epistominella pacifica (Cushman)	*Quinqueloculina akneriana* d'Orbigny
Eponides healdi R.C. & K.C. Stewart	*Quinqueloculina* sp.
Fursenkoina californiensis ticensis Cushman & Kleinpell	*Orbulina universa* d'Orbigny
Gavelinopsis sp.	*Textularia* sp.
Globobulimina auriculata Bailey	*Uvigerina hootsi* Rankin
Globobulimina pacifica Cushman	*Uvigerina juncea* Cushman & Todd
Globigerina bulloides d'Orbigny	*Uvigerina subperegrina* Cushman & Kleinpell
Globigerina quinqueloba Natland	*Uvigerina senticosa* Cushman
Globorotalia crassaformis (Galloway & Wissler)	*Valvulineria* sp.
Globorotalia cf. scitula Brady	

In the Quinault Formation, the average densities of seep and non-seep foraminiferal assemblages (>124μm fraction) were quite different (Figure 2.5A). The number of foraminifera per gram of dry sediment in seep samples ranged from 0 to 187 individuals/gm, with an average of 73.8. In non-seep samples, the range was from 0 to 522, with an average of 125.2 individuals/gm of dry sediment. Despite the difference in averages, samples barren or nearly barren of foraminifera occurred in both seep and non-seep sites. Diversity indices calculated for the Quinault assemblages show that the seep and non-seep assemblages are similar (Figure 2.5B,C). The average Simpson's index for seep samples is 0.32 and for non-seep samples is 0.30, while the average Shannon-Wiener index for non-seep

samples is 2.52, and for seep samples it is 2.38. Thus there is little diversity distinction between the foraminiferal assemblages in the two environments.

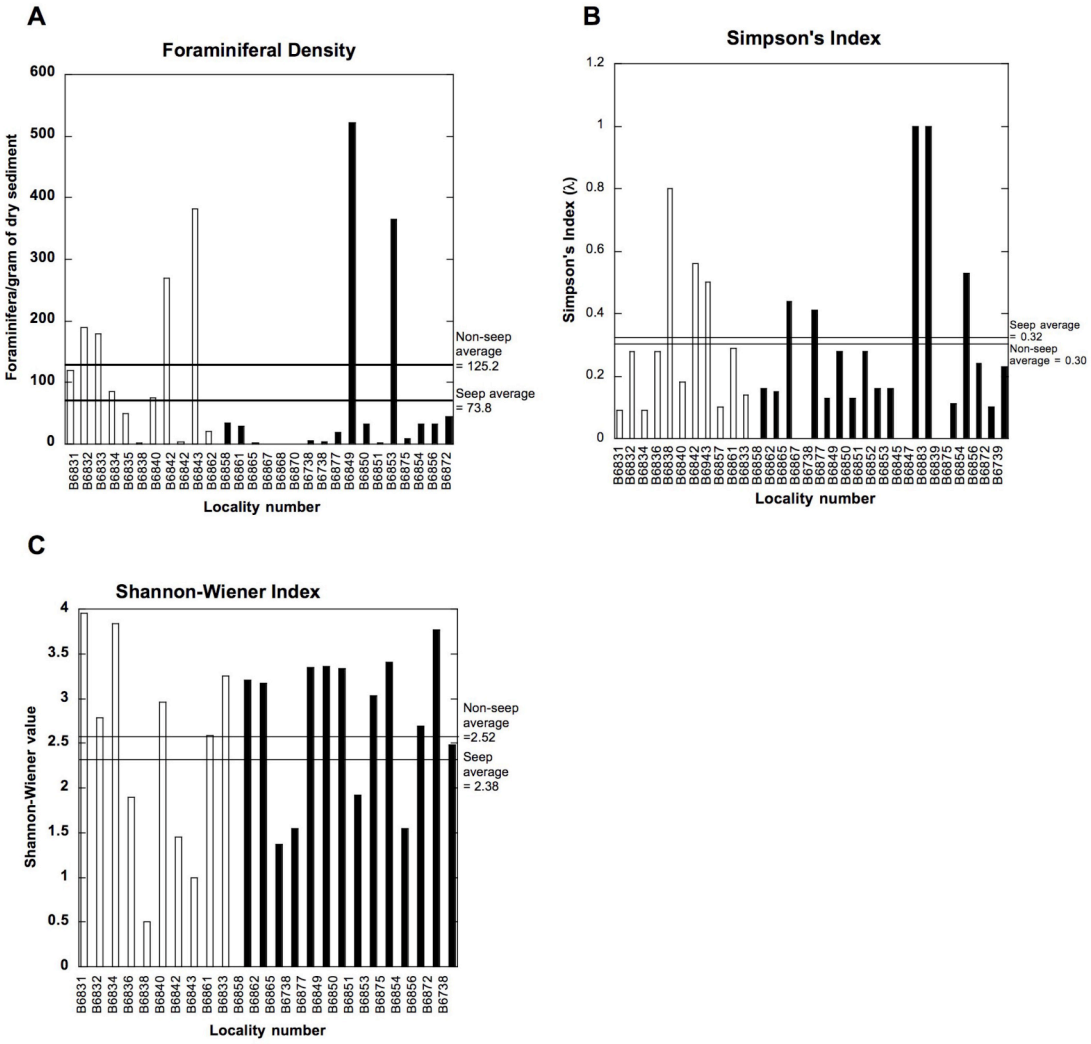

Figure 2.5. Density and diversity plots for foraminiferal assemblages. (A) Foraminiferal density measured as number of foraminifera per gram of dry sediment. (B) Simpson's diversity index. (C) Shannon Wiener diversity index. Key: white bars = non-seep samples, black bars = seep samples.

5.2 Stable isotopes

5.2.1 Autochthonous sedimentary carbonates

The measured carbon and oxygen isotope values obtained from blebs, shell and burrow infillings, and glendonite carbonates are summarized in Table 2.3 and Figure 2.6. The inorganic carbonates analyzed show significant variation in ^{13}C values. A single highly enriched value of +8.7‰ PDB was recorded in one bleb

from Camp Creek Seep; other seep samples exhibited depleted $\delta^{13}C$ values ranging from –14‰ to –38.4‰ PDB with no apparent distinctions among seep localities (Figure 2.6A). Micritic carbonate infilling of bivalve shells and burrow fillings were significantly depleted in ^{13}C (<–30‰ PDB). The greatest depletion (–38.4‰ PDB) occured in a nodule from South Camp Creek Seep. Carbonate $\delta^{13}C$ values from bivalve shells (Figure 2.7) were variable, ranging from +3.47‰ PDB in the epifaunal species *Acila empirensis,* to more depleted values in the infaunal species *Lucinoma annulata* (–25.06‰ PDB) and *Acharax ventricosa* (–32.66‰ PDB).

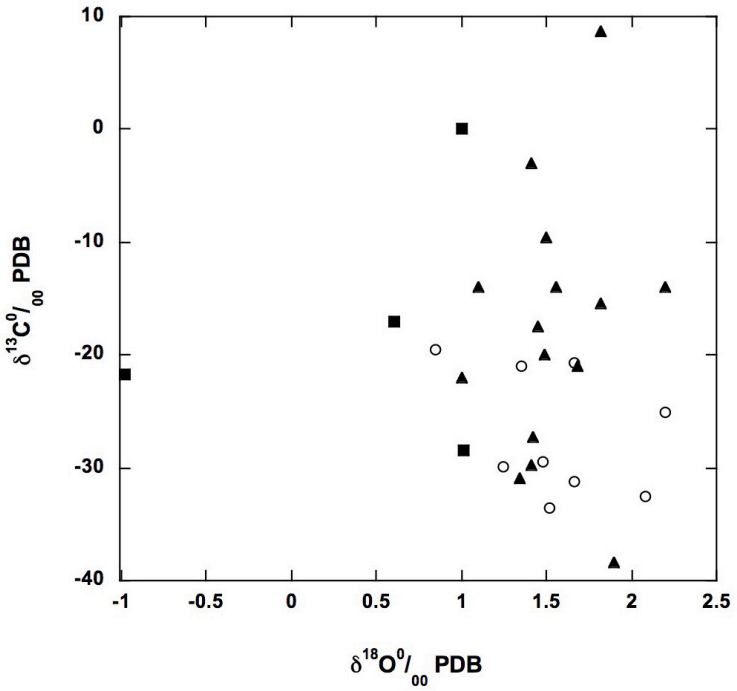

Figure 2.6. Graph of $\delta^{13}C$ vs. $\delta^{18}O$ for inorganic carbonates from the Quinault Formation. Key: ▲ = blebs (small carbonate nodules with diffuse, indistinct boundaries). ○ = burrow and shell carbonate infillings. ■ = glendonite crystals.

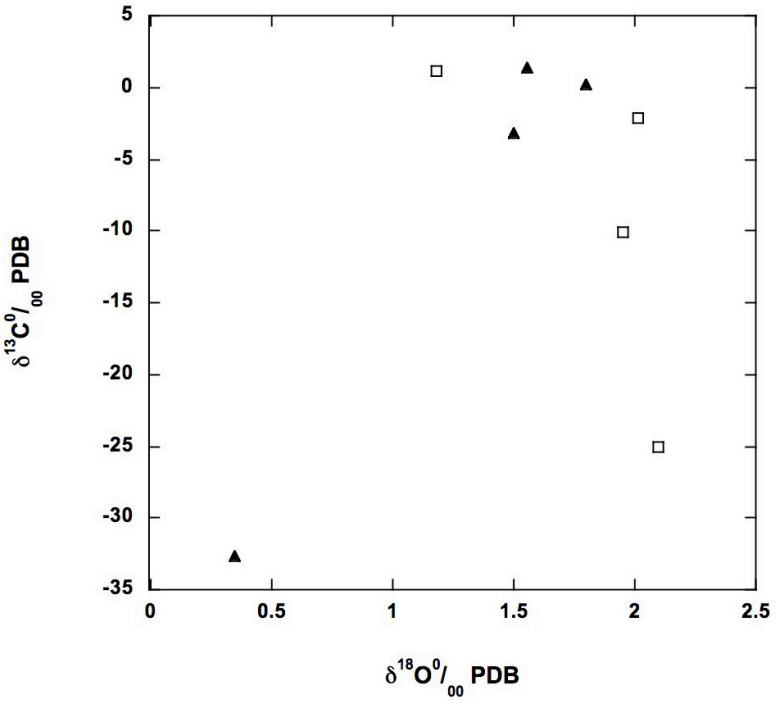

Figure 2.7. Graph of $\delta^{13}C$ vs $\delta^{18}O$ for bivalve shells. Key: ▲ = *Acharax ventricosa.* □ = *Lucinoma annulata.*

Table 2.3. Stable isotope values for authigenic carbonates and bivalve shells.

Species name or carbonate type	Seep name	Burke Museum locality number	$d^{13}C$ $^{0}/_{00}$ PDB	$d^{18}O$ $^{0}/_{00}$ PDB
Bleb	Camp Creek	B6858	-22	1.007
Bleb	Camp Creek	B6858	8.7	3.301
Bleb	Waterfall	B6855	-29.773	1.407
Bleb	Main	B6831	-20.998	1.686
Bleb	Main	B6831	-14.003	1.557
Bleb	Main	B6851	-34.528	1.098
Bleb	Main	B6839	-9.557	0.422
Bleb	Main	B6839	-3.046	1.480
Bleb	Camp Creek	B6858	-27.287	1.423
Bleb	Camp Creek	B6958	-19.947	1.492
Bleb	Waterfall	B6886	-30.902	1.340
Bleb	Camp Creek	B6833	-15.378	1.820
Bleb	Main	B6738	-14.000	2.200
Bleb	Main	B6738	-17.440	1.450
Bleb	SCC	B6839	-38.413	-1.870
Burrow fill	Main	B6739	-25.020	2.200
Burrow fill	Main	B6738	-29.520	1.480

Table 3. (*continued)*

Table 2-3 (*continued)*

Species name or carbonate type	Seep name	Burke Museum locality number	$d^{13}C$ ‰ PDB	$d^{18}O$ ‰ PDB
Burrow fill	Main	B6739	-32.610	2.080
Glendonite	Camp Creek	B6870	-28.5	1.011
Glendonite	Rosselia Cove	B6886	-17.1	0.602
Glendonite	Main	B6843	-21.708	-0.979
Acharax shell fill	Main	B6739	-33.570	1.520
Acharax shell fill	Main	B6739	-19.520	0.850
Acharax shell fill	Main	B6738	-31.210	1.660
Acharax shell fill	Main	B6738	-20.630	1.660
Acharax shell fill	Main	B6738	-29.870	1.250
Acharax shell fill	Main	B6739	-21.000	1.350
Acharax ventricosa shell	Main	B6850	-32.664	0.349
Acharax ventricosa shell	Main	B6851	-3.204	1.497
Acharax ventricosa shell	Waterfall	B6886	1.431	1.558
Acharax ventricosa shell	Main	B6739	0.190	1.790
Acila empirensis shell	Main	B4959	2.934	2.370
Acila empirensis shell	Main	B4959	0.365	0.631
Acila empirensis shell	Camp Creek	B6739	3.465	2.554
Acila empirensis shell	Main	B4959	2.750	2.419
Lucinoma annulata shell	Main	B6851	-10.073	1.954
Lucinoma annulata shell	Main	B6831	1.156	1.180
Lucinoma annulata shell	Main	B6739	-25.064	2.096
Lucinoma annulata shell	Main	B6739	-2.150	2.013
Lucinoma annulata shell	Main	B6739	1.400	1.950
Yoldia scissurata shell	Camp Creek	B6739	2.234	1.917
Yoldia scissurata shell	Main	B6739	2.608	0.894
Yoldia scissurata shell	Main	B6831	1.506	1.859

5.2.2 Stable isotopes of foraminiferal carbonate

The isotope data for foraminiferal carbon isotopes are summarized in Table 2.4 and Figure 2.8. A clear distinction between the isotopic values of seep and non-seep foraminifera was revealed. $\delta^{13}C$ values for non-seep individuals clustered near 0‰ PDB and showed little variation. For example, $\delta^{13}C$ values for non-seep specimens of *Cassidulina reflexa* (Figure 2.8C) spanned from 1.1‰ to 1.8‰ PDB, and for *Nonion basispinatum* (Figure 2.8D) they extended from 0.5‰ to 1.1‰ PDB. Both of these are infaunal taxa. Non-seep specimens of *Cibicidoides mckannai* (Figure 2.8A), an epifaunal species, yielded a $\delta^{13}C$ range of 1.2‰ to 1.9‰ PDB. In contrast, $\delta^{13}C$ values from seep individuals were considerably more depleted and variable. In seep sites, *C. reflexa* displayed values ranging from –

11.5‰ to 1.4‰ PDB, *N. basispinatum* from −21.8‰ to −11.7‰ PDB, and *C. mckannai* from −4.4‰ to 1.7‰ PDB. Two deep infaunal species found only in seep sites exhibited tests that were extremely variable and depleted. *Globobulimina pacifica* (Figure 2.8E) had $\delta^{13}C$ values ranging from −55.3‰ to −37.2‰ PDB, and values for *Nonionella stella* (Figure 2.8F) ranged between −42.9‰ and −10.7‰ PDB.

Isotope results for the deep infaunal species *Globobulimina auriculata* (Figure 2.8B) were more ambiguous than those for other foraminifera in this study. Seep and non-seep individuals were not as clearly differentiated as other species. Non-seep individuals of *G. auriculata* showed more variability in their $\delta^{13}C$ values than did other species, varying between +0.2‰ and −1.77‰ PDB. Seep individuals, however, are even more variable and depleted than non-seep *G. auriculata,* with $\delta^{13}C$ values ranging from −0.73‰ to −3.31‰ PDB. Two individuals of *G. auriculata* displayed ^{18}O values more depleted than other carbonates (−5.4‰ and −8.1‰ PDB). Neither of these individuals was among those examined with the SEM. This species has a thin, fragile test, was often found crushed and distorted, and was difficult to clean. It is likely that incomplete cleaning is responsible for the anomalously low $\delta^{18}O$ values and the lack of clear differentiation between seep and non-seep $\delta^{13}C$ values for *G. auriculata.*

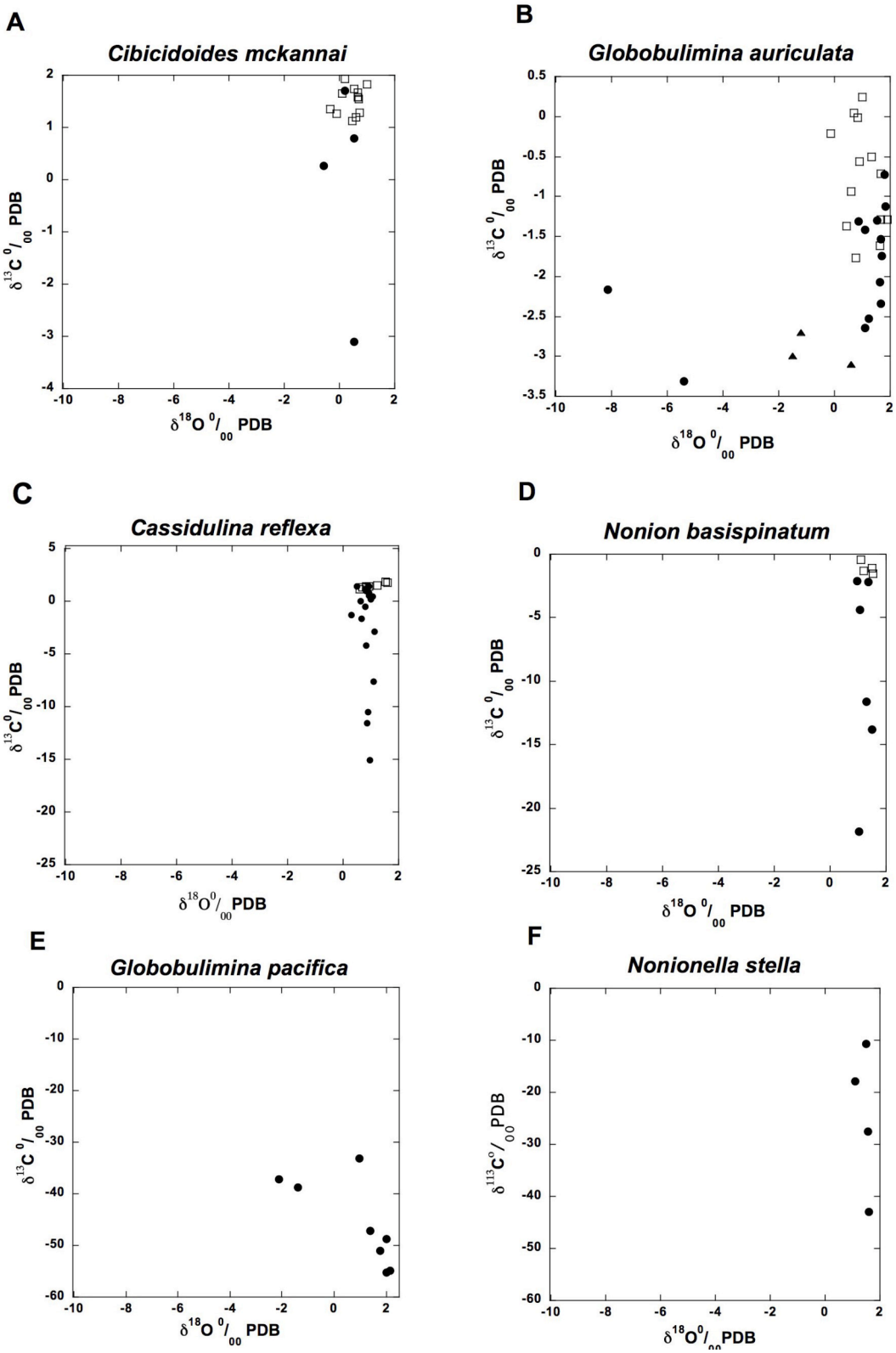

Figure 2.8. Graphs of $\delta^{13}C$ vs $\delta^{18}O$ for foraminiferal test carbonates. **Note:** The y-axis scale is different for each pair of graphs in order to better display the variability in the different species. Key: ● = seep individuals, □ = non-seep individuals, ▲ = pooled analyses.

6. Discussion

6.1 Foraminiferal assemblage

Fossil assemblage analysis and sedimentological evidence indicate that this section of the Quinault Formation was deposited in depths not exceeding wave and flood base, a maximum depth of approximately 200m (Campbell et al., 2006). This is also the depth of the shelf break off present-day Washington and Oregon. The foraminiferal assemblage of the Quinault Formation is in agreement with this depth assessment. The majority of its constituents, including *Globobulimina ariculata, G. pacifica, Cibicides conoideus, C. fletcheri, Cibicidoides mckannai,* and *Islandiella* spp*.,* all have depth distributions which fall within this range (Ingle, 1980). The assemblage does not include shallow intertidal or estuarine taxa, nor those inhabiting bathyal depths. Any extensive transport of material would also be recognized by characteristic sedimentary structures, but these are not evident here.

A number of investigations have focused on the assemblage composition and isotope geochemistry of benthic foraminifera in modern cold seep environments (Akimoto et al., 1994; Sen Gupta and Aharon, 1994; Sen Gupta et al., 1997; Rathburn et al., 2000; Hill et al., 2003; Rathburn et al., 2003; Martin et al., 2004; Mackensen, 2006). Although our understanding of factors controlling foraminiferal populations in these environments is incomplete, we can use the results from investigations of modern seeps to guide the interpretation of fossil data. The composition,density and diversity of the foraminiferal assemblages from the Pliocene Quinault Formation seeps are consistent with those from modern seeps. All species occurring in the Quinault seep assemblages also occur in non-seep environments. However, several of the Quinault species, specifically the deep infaunal *Globobulimina auriculata, G. pacifica,* and the shallow infaunal *Epistominella pacifica,* are known from modern seep studies to occur in dysoxic or anoxic environments (Bernhard et al., 2001; Rathburn et al. 2000, 2003). In addition, the epifaunal species *Cibicidoides mckannai* is a persistent and conspicuous constituent of foraminiferal populations in Recent methane seeps in the Santa Barbara Channel, California (Hill et al., 2003). The reason for the

perseverance of foraminifera in the harsh microchemical environment of methane seep sediments is not fully understood, but clearly they have inhabited such environments since at least the Pliocene. Most foraminifera are mobile and can change their positions laterally and vertically if they need to seek a better location (Alve and Bernhard, 1995; Moodley et al., 1998; Geslin et al., 2004). The benefit seeps afford to foraminifera probably lies in the food source provided by abundant bacteria (Torres et al., 2003). Regardless, foraminifera must employ some strategy or possess considerable ecological plasticity to survive in these extreme environments (Rathburn et al., 2003). It has been suggested that foraminifera in dysoxic environments lower their metabolism and retreat into inactivity for a considerable period of time (Bernhard, 1992). Sen Gupta et al. (1997) observed a thickened organic lining in *Cassidulina neocarinata* found in seeps, and speculated that the lining might allow the foraminifer to become dormant during adverse periods. Another possibility for survival of benthic foraminifera in extreme environments such as seeps is the sequestering of chloroplasts in the cytoplasm of living foraminifera. Some foraminifera, such as infaunal species *Nonionella stella* and *Buliminella elegantissima*, were found to contain abundant, intact chloroplasts that occurred throughout the test (Bernhard and Bowser, 1999). These authors, studying laminated sediments in the Santa Barbara Basin, suggested that chloroplast-sequestering foraminifera may not be permanent residents of dys/anoxic sediments, but may instead migrate into and out of them. This would explain the isotopic disequilibrium of the tests that has been observed between foraminifera and their surrounding pore waters (e.g. Erez, 2003). Finally, it is possible that foraminifera inhabiting cold seeps may employ symbionts to provide their metabolic needs. Symbiosis is well-known among larger, tropical foraminifera and planktic species (Lee and Anderson, 1991; Hallock, 1999). *Buliminella tenuata* in the Santa Barbara Basin appears to have endosymbiotic bacteria of an unknown phylogenetic affinity (Bernhard, 1996). Furthermore, *Virgulinella fragilis* obtained from cores in the oxygen-depleted, sulfide-enriched Cariaco Basin, Venezuela,

contained chloroplasts that were clustered in the center of the cell, and accompanied by rod-shaped endobionts around the periphery (Bernhard, 2003).

Within modern cold seeps, biotic density enrichment is commonly observed in bacteria, some other protists, bivalves and nematodes (Levin, 2005) but not in foraminifera (Bernhard et al., 2001). Seeps from the California margin have foraminiferal densities similar to their non-seep counterparts, and in some cases density may be reduced (Bernhard et al., 2001, Rathburn et al., 2000, 2003). Consistent with this, the Quinault Formation foraminiferal density is reduced in seep samples compared to their non-seep counterparts. Likewise, diversity, although not widely studied in modern seeps, appears to be only slightly reduced from non-seep to seep sites (Robinson et al., 2004). Foraminiferal diversity in the Quinault Formation follows the same trend. Both diversity indices used in this study show the assemblages from seeps vs. non-seeps to be remarkably similar. However, the interpretation of statistical data in fossil samples must take into consideration the variability in preservation owing to depositional and fossilization processes. Preservation of foraminiferal assemblages in the Quinault Formation was most certainly influenced by the sedimentological regime. The Pliocene shelf was subjected to episodic storms and floods alternating with periods of quiescence and intense bioturbation (Campbell et al., 2006). These conditions undoubtedly affected the accumulation of foraminifera in the sediments and must account for much of the variability of foraminiferal distribution, density and diversity. Within the Quinault seeps, variability in microhabitats would have been particularly marked, which is corroborated by macrofaunal and trace fossil evidence (Nesbitt and Campbell, 2004b). Thus, the density and diversity of the fossil foraminiferal assemblages in the Quinault Formation are relicts of both the environmental conditions at the time the foraminifera were alive, and of taphonomic biases occurring during sediment accumulation and burial.

6.2 Stable Isotopes

The extremely negative carbon isotope values of some of the inorganic carbonates, particularly the blebs, suggest the influence of carbon derived from a source other than seawater or marine organic carbon (Figure 2.9).

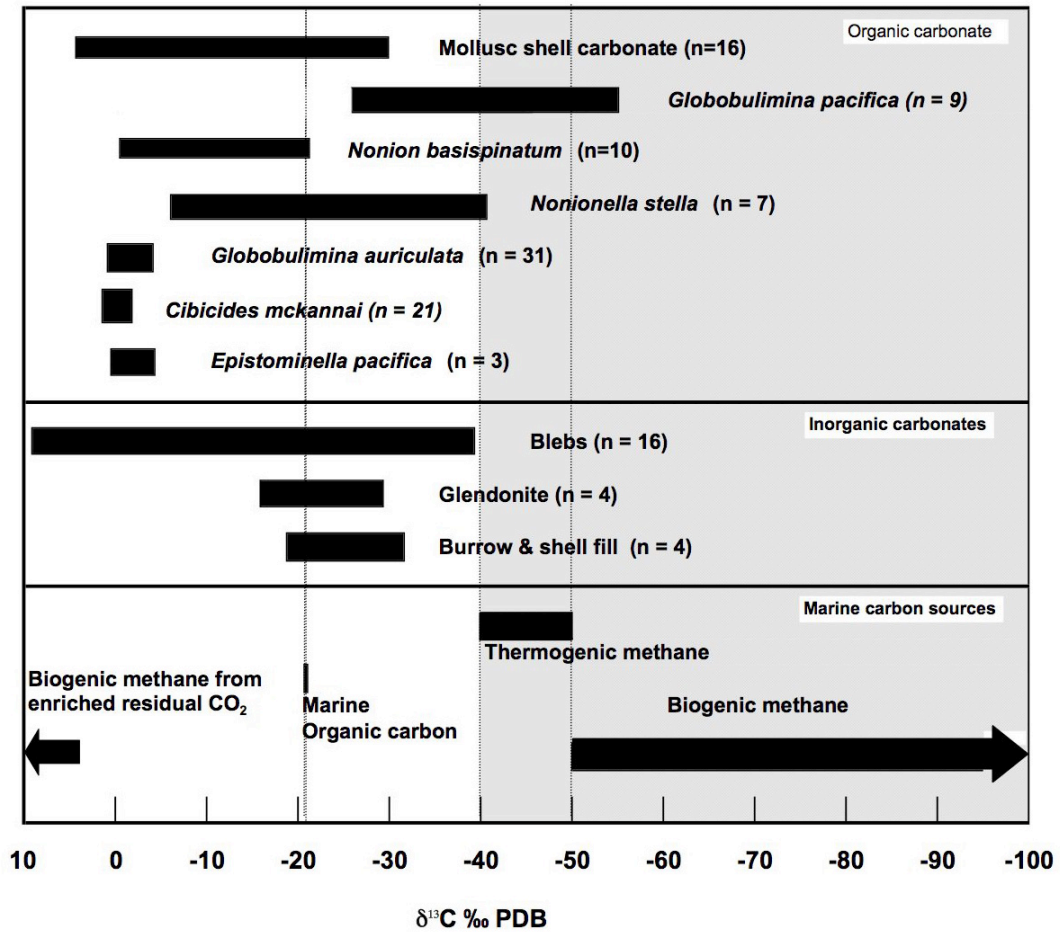

Figure 2.9. $\delta^{13}C$ ranges for biogenic and abiogenic carbonates from the Pratt Cliff section of the Quinault Formation (Pliocene) compared with ranges for carbon sources in the modern marine environment. n = the number of analyses for each category.

Seawater normally has $\delta^{13}C$ values within a few per mil of 0 ‰ PDB, while marine organic carbon yields values of about –20‰ to –22 ‰ PDB (Paull et al., 1984). The wide range of $\delta^{13}C$ values in the Quinault nodules is probably due to a combination of causes. Mixtures of gas pools from different sources including thermogenic and biogenic methane could be responsible (Whiticar, 1999), as could

the mixture of methane-derived HCO_3 with bicarbonate from sulfate reduction and oxidation of organic matter. This likely explains the variability of $\delta^{13}C$ values of the bivalve shell carbonates. In particular, *Acharax ventricosa* and *Lucinoma annulata* are both burrowers that utilize the metabolic products of their chemosymbionts for nutrition (Felbeck, 1983; Distel, 1998). They do, however, maintain contact with the sea floor and pump oxygenated water in order to perform respiration. In calcifying their shells, they incorporate carbon derived from the anaerobic oxidation of methane (AOM), sulfate reduction, and ambient sea water, accounting for the variation and depletion in their $\delta^{13}C$ signatures. The remaining bivalves are surface-dwellers, and thus appear to have been only minimally influenced by ^{13}C-depleted pore waters, if at all.

Carbon isotope data for the Pliocene Quinault foraminifera display the same general trends recorded by various studies of similar taxa in Recent seeps; in particular, $\delta^{13}C$ values from seep foraminifera are more depleted and variable than values from non-seep foraminifera. Post-depositional diagenetic alteration probably had an influence on the isotope values of the Quinault foraminifera. SEM images of exterior and interior test surfaces indicate some degree of calcitic overgrowth. In their study of foraminiferal tests of the southwestern Greenland Sea, Millo et al. (2005) concluded that depleted ^{13}C contributed by methane caused distinct shifts in the $\delta^{13}C$ signatures of both ambient sea water and pore water, which in turn led to both planktic and benthic foraminiferal tests recording a depleted $\delta^{13}C$ signal. Their SEM images also indicated authigenic overgrowths on both planktic and benthic foraminifera. Using leaching experiments, they were able to constrain the foraminiferal $\delta^{13}C$ signal to 80%-90% primary calcite and 10%-20% authigenic overgrowth. Overgrowths on the Quinault Formation foraminifera are similar in extent to those of the Greenland Sea foraminifera; thus, the $\delta^{13}C$ signal is a combination of both primary and secondary mineralization. In order to achieve a highly depleted signal such as those found in several Quinault specimens, the primary signal would necessarily be strongly depleted, indicating the foraminifera utilized strongly depleted carbonate when mineralizing their tests. Although no

studies of modern seep foraminifera have yielded such strongly depleted values as those found in the Quinault foraminifera, Mackensen, et al. (2006) did find rose bengal-stained (living) foraminifera from the Håkon Mosby mud volcano in the Barents Sea that displayed $\delta^{13}C$ values significantly lower than those of unstained (dead) tests. Thus, these foraminifera were employing depleted carbon in the construction of their shells. Close correlation between oxygen isotopes of Quinault foraminifera, inorganic carbonates, and bivalve shells indicate that both sedimentary carbonate and shell carbonate have undergone the same shallow burial experience.

Comparison of $\delta^{13}C$ values from this study and carbon sources in the marine environment are shown in Figure. 2.9. The $\delta^{13}C$ values for the nodules and the foraminifera *Globobulimina pacifica* and *Nonionella stella* are all considerably more depleted than normal sea water and marine organic carbon, and fall within the range of methane $\delta^{13}C$ values. In particular, three individuals of *G. pacifica* have $\delta^{13}C$ values that are consistent with those of biogenic methane. In addition, the co-occurrence of the carbonate nodule highly enriched in ^{13}C ($\delta^{13}C$ = +8.7‰ PDB) with the most depleted *G. pacifica* and *N. stella,* strongly suggests a biogenic methane source was responsible for at least some of the seepage in the Quinault Formation (cf. Budai, 2000). Furthermore, the Garfield Gas Mound (Figure 2.1) leaks thermogenic methane at present, with a $\delta^{13}C$ of −34.65‰ (Campbell, 1992). Thus, the extreme variability in $\delta^{13}C$ values for both foraminifera and sedimentary seep-carbonates is explained by the heterogeneity of seepage. We infer that a mixture of methane-derived carbon sources, bicarbonate derived from marine organic carbon or sulfate reduction, and normal dissolved inorganic carbon (DIC), combined with the tortuosity of fluid migration pathways produced numerous microhabitats of differing local geochemical conditions resulting in the wide range in carbon isotope values observed in both organic and inorganic carbonates.

7. Conclusions

In using foraminifera to investigate modern seeps, Rathburn et al. (2003) emphasized the importance of conducting isotope analyses on individual tests of foraminifera, because the extreme variability of $\delta^{13}C$ values within a species is unique to the seep environment. Results of this study of fossil seep foraminifera are consistent with those reported from Recent seep sites. Stable carbon isotopes from seep-associated foraminifera are sensitive microenvironmental indicators of near-surface pore fluid composition and variability of fluid flow. Inorganic carbonates such as nodules and blebs can form in many locations, even in the zone of methanogenesis, and syn- or post-depositionally, therefore they cannot be used as reliable indicators of near-surface conditions. $\delta^{13}C$ values from bivalve shell carbonates are similarly unreliable; their carbon isotope signals may be derived from sea water, pore water, and even the metabolic by-products of their symbionts (Tanaka et al., 1986; Hein et al., 2006).

In modern seep sites, and such fossil seeps as the Miocene "calcari a *Lucina*" of Italy and the Cretaceous TeePee Buttes, recognition and analysis of seeps has depended on large-scale features such as carbonate chimneys and concentrations of distinctive macrofaunal assemblages. In comparison, the seeps of the Quinault Formation are not "typical" cold methane seeps. In the Pacific Northwest and California, numerous diffuse seeps of Cretaceous and Cenozoic ages are being recognized using more subtle indicators (Campbell et al., 2006 and unpublished data). It is therefore probable that cold seeps were and are more numerous and diverse than has been previously recognized. Because of their ability to record, both during their lifetime and in early diagenesis, the isotopic signatures of the surrounding waters, foraminiferal tests are central to fine-scale identification and evaluation of biogeochemical conditions in pore fluids at, and just below, the sediment-water interface through geologic time. Because foraminifera are small, numerous, and distributed both epifaunally and infaunally, $\delta^{13}C$ values preserved in foraminiferal tests are uniquely capable of fingerprinting various carbon reservoirs as well as the ephemeral passage of methane through sediments. Their isotopic

heterogeneity in modern and fossil seeps, with $\Delta\delta^{13}C$ ranges as great as 22‰ PDB for a single species, reveals the fine-scale variability of pore-fluids near and at the sediment-water interface. Hence, foraminifera facilitate the construction of a more complete and accurate picture of the pore-fluid history in methane seepage areas. Their degree of $\delta^{13}C$ depletion, with infaunal species values as low as –55.3‰ PDB, helps characterize and identify carbon reservoirs in various settings. Thus, foraminiferal carbon isotopes, whether attributable to primary or secondary calcification, can be useful for inventories of global carbon and methane, and in the reconstruction of past tectonic activity and porewater fluid dynamics (Rathburn et al., 2003).

Acknowledgements

I appreciate the continued support of the Quinault Indian Nation for allowing access to the localities on their tribal land, and especially thank L. Workman for facilitation and field assistance. I thank D. Mucciaroni, Stanford University Stable Isotope Lab, for his guidance on isotope work and E. Hare for his expertise in SEM imaging. This chapter was greatly improved by constructive comments from K. Hoppe and R. Buick. Funding was provided by the Cushman Foundation for Foraminiferal Research, Geological Society of America, and the Barbara Chapple Fund of the Burke Musuem.

Table 2.4. Stable isotope values for foraminiferal tests.

Species name	Seep name	Burke Museum locality number	Number of individuals in analysis	$d^{13}C$ ‰ PDB	$d^{18}O$ ‰ PDB
Globobulimina auriculata	Camp Creek	B6858	16	-3.1	0.6
Globobulimina auriculata	Camp Creek	B6858	14	-3.0	-1.5
Globobulimina auriculata	Camp Creek	B6858	10	-2.7	-1.2
Globobulimina auriculata	Camp Creek	B6858	1	-3.308	-5.404
Globobulimina auriculata	Camp Creek	B6858	1	-2.068	1.632
Globobulimina auriculata	Camp Creek	B6858	1	-2.169	-8.143
Globobulimina pacifica	Camp Creek	B6858	1	-37.265	-2.120
Globobulimina pacifica	Camp Creek	B6858	1	-48.754	2.000
Globobulimina pacifica	Camp Creek	B6858	1	-38.804	-1.375
Globobulimina pacifica	Camp Creek	B6858	1	-54.857	2.159
Globobulimina pacifica	Camp Creek	B6858	1	-47.183	1.407
Globobulimina pacifica	Camp Creek	B6858	1	-55.261	2.005
Globobulimina pacifica	Camp Creek	B6858	1	-50.980	1.775
Nonionella stella	Camp Creek	B6858	1	-42.903	1.588
Uvigerina sp.	Camp Creek	B6858	1	-27.579	1.569
Nonionella basispinatum	Concretion Cove	B6877	1	-2.112	0.952
Nonionella basispinatum	Concretion Cove	B6877	1	-2.184	1.365
Nonionella basispinatum	Concretion Cove	B6877	1	-4.391	1.084
Nonionella stella	Concretion Cove	B6877	3	-2.134	0.217
Cassidulina reflexa	Main	B6849	1	0.564	0.951
Cassidulina reflexa	Main	B6849	1	0.214	1.009
Cassidulina reflexa	Main	B6849	1	-0.561	0.807
Cassidulina reflexa	Main	B6849	1	-2.907	1.147
Cassidulina reflexa	Main	B6849	1	0.435	1.060
Cassidulina reflexa	Main	B6849	1	0.794	0.922
Cassidulina reflexa	Main	B6850	1	-10.515	0.913
Cassidulina reflexa	Main	B6850	1	-11.549	0.852
Cassidulina reflexa	Main	B6850	2	0.993	0.832
Cassidulina reflexa	Main	B6851	1	-7.629	1.096

Table 2.4. (*continued)*

Species name	Seep name	Burke Museum locality number	Number of individuals in analysis	$d^{13}C$ ‰ PDB	$d^{18}O$ ‰ PDB
Cassidulina reflexa	Main	B6852	1	1.365	0.921
Cassidulina reflexa	Main	B6852	1	1.373	0.485
Cassidulina reflexa	Main	B6852	1	0.047	0.645
Cassidulina reflexa	Main	B6852	1	1.158	0.813
Cassidulina reflexa	Main	B6852	1	-1.631	0.658
Cibicides mckannai	Main	B6849	3	-3.103	0.550
Cibicides mckannai	Main	B6849	4	1.711	0.197
Cibicides mckannai	Main	B6849	6	0.794	0.549
Cibicides mckannai	Main	B6850	3	0.258	-0.559
Epistominella pacifica	Main	B6849	5	-4.352	0.977
Globobulimina pacifica	Main	B6850	1	-33.118	0.967
Nonionella stella	Main	B6849	3	-10.712	1.511
Nonionella stella	Main	B6850	3	-17.828	1.108
U. hootsi	Main	B6849	1	-10.760	1.528
U. hootsi	Main	B6849	2	-9.234	1.488
U. juncea	Main	B6849	3	-1.397	1.463
U. juncea	Main	B6849	3	-9.000	1.628
Globobulimina auriculata	South Camp Creek	B6875	1	-2.646	1.087
Globobulimina auriculata	South Camp Creek	B6875	2	-2.525	1.227
Nonionella basispinatum	South Camp Creek	B6875	1	-21.839	1.023
Nonionella basispinatum	South Camp Creek	B6875	1	-11.651	1.286
Nonionella basispinatum	South Camp Creek	B6875	1	-13.794	1.506
Cassidulina reflexa	Waterfall	B6872	1	-15.090	0.973
Cassidulina reflexa	Waterfall	B6872	1	-1.277	0.290
Cassidulina reflexa	Waterfall	B6872	2	-4.204	0.828
Globobulimina auriculata	Waterfall	B6856	1	-1.415	1.100
Globobulimina auriculata	Waterfall	B6856	1	-1.318	0.873
Globobulimina auriculata	Waterfall	B6856	1	-0.731	1.786
Globobulimina auriculata	Waterfall	B6856	1	-1.744	1.690
Globobulimina auriculata	Waterfall	B6856	1	-2.336	1.658
Globobulimina auriculata	Waterfall	B6856	1	-1.304	1.522
Globobulimina auriculata	Waterfall	B6856	1	-1.122	1.827
Globobulimina auriculata	Waterfall	B6856	1	-1.530	1.653
Cassidulina reflexa	Non	B6833	1	1.816	1.530
Cassidulina reflexa	Non	B6834	1	1.735	1.618
Cassidulina reflexa	Non	B6853	1	1.325	0.699
Cassidulina reflexa	Non	B6853	2	1.492	1.247

Table 2.4. (*continued)*

Species name	Seep name	Burke Museum locality number	Number of individuals in analysis	$d^{13}C$ ‰ PDB	$d^{18}O$ ‰ PDB
Cassidulina reflexa	Non	B6857	1	1.141	0.610
Cassidulina reflexa	Non	B6857	1	1.409	0.822
Cassidulina reflexa	Non	B6857	1	1.285	0.840
Cassidulina reflexa	Non	B6857	1	1.424	0.941
Cibicides mckannai	Non	B6831	3	1.732	0.539
Cibicides mckannai	Non	B6831	5	1.192	0.608
Cibicides mckannai	Non	B6831	5	1.833	1.018
Cibicides mckannai	Non	B6832	5	1.548	0.696
Cibicides mckannai	Non	B6832	4	1.667	0.681
Cibicides mckannai	Non	B6832	6	1.576	0.670
Cibicides mckannai	Non	B6832	4	1.288	0.731
Cibicides mckannai	Non	B6832	4	1.587	0.654
Cibicides mckannai	Non	B6833	4	1.650	0.095
Cibicides mckannai	Non	B6853	3	1.927	0.190
Cibicides mckannai	Non	B6853	43	1.124	0.476
Cibicides mckannai	Non	B6853	3	1.344	-0.343
Cibicides mckannai	Non	B6857	3	1.268	-0.107
Epistominella pacifica	Non	B6831	4	0.854	0.889
Epistominella pacifica	Non	B6832	5	0.886	1.302
Globobulimina auriculata	Non	B6834	2	-1.288	1.679
Globobulimina auriculata	Non	B6834	2	-1.290	1.887
Globobulimina auriculata	Non	B6834	2	-1.372	0.428
Globobulimina auriculata	Non	B6840	2	-0.511	1.348
Globobulimina auriculata	Non	B6840	2	-0.561	0.908
Globobulimina auriculata	Non	B6840	3	0.247	0.997
Globobulimina auriculata	Non	B6842	3	-0.716	1.671
Globobulimina auriculata	Non	B6842	1	-1.612	1.645
Globobulimina auriculata	Non	B6853	2	0.048	0.688
Globobulimina auriculata	Non	B6853	1	-0.940	0.617
Globobulimina auriculata	Non	B6857	1	-0.012	0.833
Globobulimina auriculata	Non	B6857	1	-0.213	-0.119
Globobulimina auriculata	Non	B6857	1	-1.769	0.781
Nonionella basispinatum	Non	B6842	3	-1.276	1.215
Nonionella basispinatum	Non	B6842	3	-0.459	1.087
Nonionella basispinatum	Non	B6842	4	-1.533	1.521
Nonionella basispinatum	Non	B6842	4	-1.075	1.489

Notes to Chapter 2

Aharon, P., 1994. Geology and biology of modern and ancient hydrocarbon seeps and vents: an introduction. Geo-Marine Letters, 14: 69-73.

Aharon, P. and Sen Gupta, B. K., 1994. Bathymetric reconstruction of the Miocene-age "calcari a *Lucina*" (Northern Appenines, Italy) from oxygen isotopes and benthic Foraminifera. Geo-Marine Letters, 14: 219-230.

Akimoto, K., Tanaka, T., Hattori, M. and Hotta, H., 1994. Recent benthic foraminiferal assemblages from the cold seep communities - a contribution to the methane gas indicator. In: R. Tsuchi (Editor), Pacific Neogene Events in Time and Space. University of Tokyo Press, Tokyo, pp. 11-25.

Alve, E. and Bernhard, J.M., 1995. Vertical migratory response of benthic foraminifera to controlled oxygen concentrations in an experimental mesocosm. Marine Ecology Progress Series, 116: 137-151.

Barbieri, R. and Panieri, G., 2004. How are benthic foraminiferal faunas influenced by cold seeps? Evidence from the Miocene of Italy. Palaeogeography, Palaeoclimatology, Palaeoecology, 204: 257-275.

Bernhard, J.M., 1992. Benthic foraminiferal distribution and biomass related to pore-water oxygen: central California continental slope and rise. Deep-Sea Research Part A, 39: 585-605.

Bernhard, J.M., 1996. Microaerophilic and facultative anaerobic benthic foraminifera: a review of experimental and ultrastructural evidence. Rev. Paleobiol. 15: 261-275.

Bernhard, J. M., 2003. Potential symbionts in bathyal foraminifera. Science, 299: 861.

Bernhard, J.M. and Bowser, S.S., 1999. Benthic foraminifera of dysoxic sediments: chloroplast sequestration and functional morphology. Earth-Science Reviews, 46(1-4): 149-165.

Bernhard, J.M., Sen Gupta, B.K., Borne, P.F., 1997. Benthic foraminiferal proxy to estimate dysoxic bottom-oxygen concentrations: Santa Barbara Basin, U.S. Pacific continental margin. Journal of Foraminiferal Research, 27: 301-310.

Bernhard, J.M., Buck, K.R. and Barry, J.P., 2001. Monterey Bay cold-seep biota: Assemblages, abundance, and ultrastructure of living foraminifera. Deep-Sea Research I, 48: 2233-2249.

Budai, J.M., Martin, A.M., Walter, L.M. and Ku, T.C.W., 2002. Fracture-fill calcite as a record of microbial methanogenesis and fluid migration: a case study from the Devonian Antrim Shale, Michigan Basin. Geofluids, 2: 163-183.

Buzas, M.A., 1979. The Measurement of Species Diversity. In: J.H. Lipps, W.H. Berger, M.A. Buzas, R.G. Douglas and C.A. Ross (Eds), Foraminiferal Ecology and Paleoecology. SEPM Short Course. p. 3-10.

Campbell, K.A., 1989. A Miocene-Pliocene methane seep fauna and associated authigenic carbonates in shelf sediments of the Quinault Formation, S.W. Washington. Geological Society of America Abstracts with Program 21, 290.

Campbell, K.A.,1992. Recognition of a Mio-Pliocene cold seep setting from the Northeast Pacific convergent margin, Washington, U.S.A. Palaios, 7: 422-433.

Campbell, K.A., 2006. Hydrocarbon seep and hydrothermal vent palaeoenvironments and palaeontology: Past developments and future research directions. Palaeogeography, Palaeoclimatology, Palaeoecology, 2: 362-407.

Campbell, K.A. and Bottjer, D.J., 1993. Fossil cold seeps. National Geographic Research & Exploration, 9: 326-242.

Campbell, K.A. and Nesbitt, E.A., 2000. High resolution architecture and paleoecology of an active margin, storm-flood influenced estuary, Quinault Formation (Pliocene), Washington. Palaios, 15: 553-579.

Campbell, K.A. and Nesbitt, E.A., 2004. Trace fossils and relative timing relationships of fluid-flow in hydrocarbon seep carbonates, 32nd International Geologic Congress, Abstracts. International Geological Congress, Florence, Italy, pp. 928.

Campbell, K.A., Farmer, J.D. and Des Marais, D., 2002. Ancient hydrocarbon seeps from the Mesozoic convergent margin of California: geochemistry, fluids and palaeoenvironments. Geofluids, 2: 63-94.

Campbell, K.A., Nesbitt, E.A. and Bourgeois, J., 2006. Signatures of storms, oceanic floods, and forearc tectonsim in marine shelf strata of the Quinault Formation (Pliocene), Washington, U.S.A. Sedimentology. doi: 10.1111/j.1365-3091.2006.00788.x.

Claypool, G.E. and Kaplan, I.R., 1974. The origin and distribution of methane in marine sediments. In: I.R. Kaplan, (Ed.), Natural Gases in Marine Sediments: Plenum, New York, p. 99-139.

Corliss, B.H., 1985. Microhabitats of benthic foraminifera within deep-sea sediments. Nature, 314: 435-438.

Corliss, B.H., 1991. Morphology and microhabitat preferences of benthic foraminifera from the northwest Atlantic Ocean. Marine Micropaleontology, 17: 195-235.

Distel, D.L., 1998. Evolution of chemoautotrophic endosymbioses in bivalves. Bioscience, 48(4): 277-286.

Erez, J., 2003. The source of ions for biomineralization in foraminifera and their implications for paleoceanographic proxies. Review in Mineralogy and Geochemistry, 54: 115-149.

Felbeck, H., 1983. Sulfide oxidation and carbon fixation by the gutless clam *Solemya reidi*: an animal-bacteria symbiosis. Journal of Comparative Physiology, 152: 3-11.

Geslin, E., Heinz, P., Jorissen, F., Hemleben, Ch., 2004. Migratory responses of deep-sea benthic foraminifera to variable oxygen conditions: laboratory investigations. Marine Micropaleontology, 53: 227-243.

Goedert, J. and Benham, S.R., 1999. A new species of *Depressigyra?* (Gastropoda: Peltospiridae) from cold-seep carbonates in Eocene and Oligocene Rocks of Western Washington. The Veliger, 42: 112-116.

Goedert, J. and Squires, R., 1990. Eocene deep-sea communities in localized limestones formed by subduction-related methane seeps, southwestern Washington. Geology, 18: 1182-1185.

Goedert, J., Peckmann, J. and Reitner, J., 2000. Worm tubes in an allochthonous cold-seep carbonate from lower Oligocene rocks of Western Washington. Journal of Paleontology, 74: 992-999.

Goedert, J.L., Thiel, V., Schmale, O., Rau, W.W., Michaelis, W., Peckmann, J., 2003. Late Eocene "Whiskey Creek" methane seep deposits (western Washington State) - Part I: Geology, paleontology and molecular geobiology. Facies, 48: 223-240.

Hallock, P., 1999. Symbiont-bearing foraminifera. In: B.K. Sen Gupta (Ed.), Modern Foraminifera. Kluwer Academic, Dordrecht, p. 123-140.

Hein, J.R., Normark, W.R., McIntyre, B.R., Lorenson, T.D., and Powell, C.L. 2006. Methanogenic calcite, ^{13}C-depleted bivalve shells, and gas hydrate from a mud volcano offshore southern California. Geology, 34: 109-112.

Heinz, P., Sommer, S., Pfannkuche, O., Hemleben, C., 2005. Living benthic foraminifera in sediments influenced by gas hydrates at the Cascadia convergent margin, NE Pacific. Marine Ecology Progress Series, 304: 77-89.

Hill, T.M., Kennett J.P. and Spero, H.J., 2003. Foraminifera as indicators of methane-rich environments: A study of modern methane seeps in Santa Barbara Channel, California. Marine Micropaleontology, 49: 123-138.

Hill, T.M., Kennett, J.P., Spero, H.J., 2004. High-resolution records of methane hydrate dissociation: ODP site 893, Santa Barbara Basin. Earth and Planetary Science Letters, 223: 127-140.

Ingle, J.C., Jr., 1980. Cenozoic paleobathymetry and depositional history of selected sequences withn the southern California continental borderland. Cushman Foundation Special Publication 19: 163-195.

Jones, R.W., 1993. Preliminary observations on benthonic foraminifera associated with a biogenic gas seep in the North Sea. In: D.G. Jenkins (Editor), Applied Micropaleontology. Kluwer Academic Publishers, Dordrecht, pp. 69-91.

Lee, J.J. and Anderson, O.R., 1991. Symbiosis in foraminifera. In: J.J. Lee and O.R. Anderson, (Eds.), Biology of Foraminifera. Academic Press, London, 157-220.

Levin, L.A., 2005. Ecology of cold seep sediments: Interactions of fauna with flow, chemistry, and microbes. Oceanography and Marine Biology, an Annual Review, 43: 1-46.

Levin, L.A. and Michener, R.H., 2002. Isotopic chemosynthesis-based nutrition of macrobenthos: the lightness of being at Pacific methane seeps. Limnology and Oceanography, 47: 1336 - 1345.

Linke, P. and Lutze, G.F., 1993. Microhabitat preferences of benthic foraminifera - a static concept or a dynamic adaptation to optimize food acquisition? Marine Micropaleontology, 20: 215-234.

Mackensen, A., Wollenburg, J., Licari, l., 2006. Low $\delta^{13}C$ in tests of live epibenthic and endobenthic foraminifera at a site of active methane seepage. Paleoceanography, 21: PA2022, doi:10.1029/2005PA001196,2006

Majima, R., Nobuhara, T. and Kitazaki, T., 2005. Review of fossil chemosynthetic assemblages in Japan. Palaeogeography, Palaeoclimatology, Palaeoecology, 277: 86 - 123.

Martin, J.B., Day S., Rathburn, A.E., Perez, M.E., Mahn, C., Gieskes, J., 2004. Relationships between the stable isotopic signatures of living and fossil foraminifera in Monterey Bay, California. Geochemistry Geophysics Geosystems, 5: Q04004, doi:10.1029/2003GC000629.

McCorkle, D.C., Corliss, B.H. and Farnham, C.A., 1997. Vertical distributions and stable isotopic compositions of live (stained) benthic foraminifera from the North Carolina and California continental margins. Deep-Sea Research I: Oceanographic, 44(6): 983-1024.

Millo, C., Sarnthein, M., Erlenkheuser, H., Grootes, P.M., Andersen, N., 2005. Methane-induced early diagenesis of foraminiferal tests in the southwestern Greenland Sea. Marine Micropaleontology, 58: 1-12.

Moodley, L., van der Zwaan, G.J., Rutten, G.M.W., Boom, R.C.E., Kempers, A.J., 1998. Subsurface activity of benthic foraminifera in relation to porewater oxygen content: laboratory experiments. Marine Micropaleontology, 34: 91-106.

Nesbitt, E.A. and Campbell, K.A., 2004a. Spatial and stratigraphic distribution of fossils from diffuse seeps in a Pliocene shelf setting, Cascadia convergent margin, Geological Society of America Abstracts with Programs vol.36, no.5, pp.314.

Nesbitt, E.A. and Campbell, K.A., 2004b. Trace fossil suite from diffuse seep carbonates in a storm and flood dominated mid-shelf setting, 32nd International Geological Congress Scientific Sessions: Abstracts. International Geological Congress, Florence, Italy, pp. 930.

Orange, D.L. and Campbell, K.A., 1997. Modern and ancient cold seeps on the Pacific Coast - Monterey Bay, California, and offshore Oregon as modern-day analogs to the Hoh accretionary complex and Quinault Formation, Washington. Washington Geology, 25(4): 1-13.

Panieri, G., 2005. Benthic foraminifera associated with a hydrocarbon seep in the Rockall Trough (NE Atlantic). Geobios, 38: 247-255.

Paull, C.K., Juli, A.J.T., Toolin, L.J. and Linick, T., 1984. Stable isotope evidence for chemosynthesis in an abyssal seep community. Nature, 317: 709-711.

Rathburn, A.E., and Corliss, B.H., 1994. The ecology of living (stained) deep-sea benthic foraminifera from the Sulu Sea. Paleoceanography, 9(1); 87-150

Rathburn, A.E., Levin, L.A., Held, Z. and Lohmann, K.C., 2000. Benthic foraminifera associated with cold methane seeps on the northern California margin: ecology and stable isotopic composition. Marine Micropaleontology, 38: 247-266.

Rathburn, A.E., Perez, M.E., Martin, J.B., Day, S.A., Mahn, C., Gieskes, J., Ziebis, W., Williams, D. and Bahls, A., 2003. Relationships between the distribution and stable isotopic composition of living benthic foraminifera and cold methane seep biogeochemistry in Monterey Bay, California. Geochemistry, Geophysics, Geosystems, 4(12) 1106, doi:10.1029/2003GC000595,2003.

Rau, W.W., 1970. Foraminifera, stratigraphy, and paleocology of the Quinault Formation, Point Grenville-Raft River coastal area, Washington. Washington Department of Natural Resources Division of Mines and Geology Bulletin, 62: 41 pp.

Rigby, J.K. and Goedert, J.L., 1996. Fossil sponges from a localized cold-seep limestone in Oligocene rocks of the Olympic Peninsula, Washington. Journal of Paleontology, 70(6): 900-908.

Roberts, H. and Whelan, T.W.I., 1975. Methane-derived carbonate cements in barrier and beach sands of a subtropical delta complex. Geochimica et Cosmochimica Acta, 19: 1085-1089.

Robinson, C.A., Bernhard, J.M., Levin, L.A., Mendoza, G.F. and Blanks, J., 2004. Surficial hydrocarbon seep infauna from the Blake Ridge (Atlantic Ocean, 2150 m) and the Gulf of Mexico (690-2240 m). Marine Ecology, 25(4): 313-336.

Sahling, H., Rickert, D., Lee, R.W., Linke, P. and Suess, E., 2002. Macrofaunal community structure and sulfide flux at gas hydrate deposits from the Cascadia convergent margin, NE Pacific. Marine Ecology Progress Series, 231: 121-138.

Sen Gupta, B.K. and Aharon, P., 1994. Benthic foraminifera of bathyal hydrocarbon vents of the Gulf of Mexico: initial report on communities and stable isotopes. Geo-Marine Letters, 14: 88-96.

Sen Gupta, B.K., Platon, E., Bernhard, J.M. and Aharon, P., 1997. Foraminiferal colonization of hydrocarbon-seep bacterial mats and underlying sediment, Gulf of Mexico slope. Journal of Foraminiferal Research, 27: 292-300.

Sibuet, M. and Olu, K., 1998. Biogeography, biodiversity and fluid dependence of deep-sea cold-seep communities at active and passive margins. Deep-Sea Research II, 45: 517-567.

Squires, R. and Goedert, J.L., 1991. New Late Eocene mollusks from localized limestone deposits formed by subduction-related methane seeps, Southwestern Washington. Journal of Paleontology, 65(3): 412-416.

Stewart, R.J., Brandon, M.T., Campbell, K.A., Nesbitt, E.A. and Pazzaglia, F.J., 2003. Tectonic Surfing: Evidence of Rapid Landward Transport in the Cascadia Subduction Wedge, NW Washington State. Eos Transactions, 84 Supplement 542.

Suess, E., Carson, B., Ritger, S.D., Moore, J.C., Jones, M.L., Kulm, L.D., Cochrane, G.R., 1985. Biological communities at vent sites along the subduction zone off Oregon. In: M.L. Jones, (Ed.), The hydrothermal vents of the eastern Pacific: An Overview. Biological Society of Washington Bulletin, 6: 475-484.

Tanaka, N., Monaghan, M.C., and Rye, D.M. 1986. Contributions of metabolic carbon to mollusc and barnacle shell carbonate. Nature , 320: 520-523.

Torres, M.E., Mix, A.C., Kinports, K., Haley, B., Klinkhammer, G.P., McManus, J., de Angelis, M.A., 2003. Is methane venting at the seafloor recorded by $\delta^{13}C$ of benthic foraminifera shells? Paleoceanography, 18(3): 13 pp,

Wefer, G., Heinz, P.M. and Berger, W.H., 1994. Clues to ancient methane release. Nature, 369: 282.

Whiticar, M.J., 1999. Carbon and hydrogen isotope systematics of bacterial formation and oxidation of methane. Chemical Geology, 161: 291-314.

Chapter 3. Tectonic Influence On Carbon Isotopes In Cenozoic Cold Methane Seeps From The Cascadia Accretionary Margin

1. Introduction

The Cascadia margin of the northeastern Pacific, extending from Vancouver Island to Northern California, (Figure 3.1) has been a zone of active subduction since the late Eocene. Since this time, voluminous siliciclastic sediments were deposited in the forearc basin and a substantial double-sided accretionary prism developed (Stewart and Brandon, 2004). Numerous Cenozoic and Recent cold methane seeps occur in both the onshore and offshore subduction wedge sedimentary packages. This study focused on fossil seeps from late Eocene through Pliocene sediments of the Keasey, Lincoln Creek, Blakeley, Pysht, and Quinault Formations of western Oregon and Washington State, USA, and the Sooke Formation of southern Vancouver Island, Canada (Figure 3.1). The goal of the study was to use integrated data from foraminiferal and authigenic carbonates to assess the hydrocarbon-rich fluid-flow regimes in these sediments during the Cenozoic and compare them with seepage systems operating on this margin today.

2. Background

Cold methane seeps are ubiquitous on continental margins, both passive and active. Passive margin seeps have been identified and studied in such places as Blake Ridge, Atlantic Ocean (Robinson et al., 2004) and the Gulf of Mexico (Aharon and Sen Gupta, 1994; Aharon et al., 1997; Sassen et al., 2004). Seeps on tectonically active margins have been investigated in locations including Hydrate Ridge (Torres et al., 2002; Treude et al., 2003), Heceta Bank (Torres et al., in press), off Vancouver Island (Hyndman et al., 1995; Torres and Kastner, 2009), and the Eel River Basin of California (Orphan et al., 2004) all on the Cascadia Margin; off Japan (Akimoto et al., 1994; Tomaru et al., 2007); and on the Hikurangi margin of New Zealand (Faure et al., 2006; Barnes et al., 2009).

Cold hydrocarbon seeps are seafloor sites of H_2S- and CH_4-rich fluid flow from depths within the sediment package, generally at ambient temperatures. Hydrocarbons result from the accumulation, burial and thermogenic or microbial diagenesis of organic matter. When sediment overpressuring, changes in sea level or tectonic regime, or altered deposition rates occur, accumulated hydrocarbons migrate through the sediments along faults, through permeable sediments, via diapirs, or other pathways to be released into the oceans and atmosphere. Before reaching the sediment/water interface, however, the majority of methane gas is oxidized by a consortium of methane-oxidizing archaea and sulfate-reducing bacteria. This process is extremely efficient; it is estimated that less than 5% of the methane generated in submarine sediments is discharged into the water column (Sommer et al., 2006).

Migration of hydrocarbons through sediment packages can leave behind robust geological signatures. Where temperature and pressure conditions are favorable, gas hydrates (clathrates) form in the sediments, trapping hydrocarbons within a lattice of ice. Estimates of the reserves of methane in these hydrates range from 210 Gt (Milkov et al., 2003) to 1500 Gt (Kvenvolden, 1999), with the estimate of Milkov et al. (2003) more generally accepted today. In addition, some localities such as Blake Ridge have vast amounts of free gas trapped beneath gas hydrates (Paull et al., 2000). Thus, marine reserves of methane are a potentially valuable source of commercial energy and possible agents of catastrophic climate change.

The oxidation of methane in pore water and at the sediment surface results in oversaturation of carbonate, leading to the precipitation of authigenic carbonates that are distinctive features in massive siliciclastic deposits. These carbonates range from massive chemoherms (Aharon, 1994) to plumbing features such as chimneys, fracture fills and burrow infillings, to crusts and pavements, and finally to small nodules and blebs characteristic of more diffuse seepage (e.g. Greinert et al., 2001; Campbell, 2006). Carbonates can form at many depths in the sediment, from the zone of methanogenesis up into the water column, and they display mineralogies

and morphologies characteristic of the zones in which they form (Greinert et al., 2001).

In addition to these inorganic features, cold seeps support a unique assemblage of chemosymbiotic organisms. For nutrition, these organisms rely on the oxidation of reduced sulfur and methane by their microbial symbionts. The most common invertebrate taxa in Recent seeps are characteristic genera of polychaetes (*Lamellibrachia, Escarpia, Alaysia)*, bathymodiolid mussels (*Bathymodiolus*), and vesicomyid clams (*Vesicomya, Calyptogena*). In addition, some seep sites include solemyid, thyasirid, and lucinid bivalves, pogonophoran worms, and abyssochrysid and provannid gastropods (Tunnicliffe, 1992; Sibuet and Olu, 1998; Levin, 2005). Indeed, seeps commonly display a zonation of biota that reflects sulfide concentrations and fluxes in the sediment. In areas of high sulfide flux at the sediment surface, cold seeps on the Cascadia margin sustain mats of the thiotrophic bacteria *Beggiatoa*. Surrounding this, with lower sulfide fluxes, is a zone occupied by the bivalves *Vesicomya* (*Calyptogena) pacifica* and *V. (C.) kulmeri*, and further away, with sulfide fluxes orders of magnitude lower than the *Calyptogena* zone, lie beds of the solemyid clam *Acharax johnsoni.* It is thus postulated that sulfide flux accounts for faunal distributions in these diverse geological settings (e.g. Sahling et al., 2002).

Unlike other biota, foraminifera have no endemic seep species; all species of foraminifera found in cold seeps also occur in normal marine sediments (Sen Gupta and Aharon, 1994; Rathburn et al., 2000; Bernhard et al., 2001). There are, however, a number of species found in cold seeps that preferentially inhabit dys- or anoxic sediments, for example, *Globobulimina affinis, G. pacifica, Uvigerina peregrina,*
Nonionella stella, Rutherfoidoides cornuta (Bernhard and Reimers, 1991; Akimoto et al., 1994; Bernhard and Bowser, 1999; Erbacher and Nelskamp, 2006). The mechanism for survival of foraminifera in the harsh seep environment is not fully understood. Possibilities include foraminifera employing symbionts (Bernhard and Bowser, 1999; Bernhard, 2003) dormancy during episodes of seepage (Sen Gupta

et al., 1997) and migration into and out of seep sites (Bernhard and Bowser, 1999). Ultrastructure studies in Monterey Bay seep foraminifera revealed no endosymbionts, however, an unusually large number of perixosomes was discovered in seep foraminifera, prompting speculation that the anaerobic metabolic pathways utilized in these may provide the survival mechanism (Bernhard et al., 2001).

More pertinent to the study of fossil seeps, sediments in areas of hydrocarbon seepage preserve geochemical signatures that not only indicate the passage of methane, but also the source of the methane involved. Microbial methanogenesis fractionates carbon isotopes strongly (28‰ to >100‰; Whiticar, 1999), resulting in ^{13}C values ranging between -50‰ and <-110 ‰ PDB (Paull et al., 1985; Whiticar, 1999). Microbial methanogenesis leaves residual CO_2 which becomes increasingly enriched in ^{13}C, and is available to be incorporated into the authigenic carbonates (Whiticar, 1999). Thermogenic methanogenesis fractionates carbon less strongly, with resulting $\delta^{13}C$ values between -30‰ and -50‰ PDB (Paull et al., 1985). Consumption of methane through anaerobic oxidation of methane (AOM) results in the production of HCO_3^- that contains carbon carrying the isotopic signal of the parent methane. Authigenic seep carbonates, having incorporated methane-influenced dissolved inorganic carbon (DIC), preserve $\delta^{13}C$ values as low as -76‰ PDB (K.A. Campbell, unpublished data), and as enriched as +30‰ PDB (Claypool and Kaplan, 1974; Greinert et al., 2001; Naehr et al., 2007).

Isotope values for foraminiferal carbonate in Recent seeps have been demonstrated to be in disequilibrium with surrounding pore water DIC by as much as 40% (Rathburn, 2003). The reason for this disequilibrium is unclear, but may be due to migration into and out of seep areas as seepage waxes and wanes (Bernhard and Bowser, 1999; Torres et al., 2003) and dormancy during adverse periods (Sen Gupta et al., 1997). On the other hand, studies of modern seeps show values of $\square^{13}C$ within foraminiferal species are considerably more variable in seep samples than those from non-seep sites. For example, in the Santa Barbara Channel, $\delta^{13}C$ values for seep individuals of *Cibicides mckannai* varied between -0.37‰ and -

2.28‰ PDB, and *Pyrgo* sp. recorded values between -0.01‰ and -25.23‰ PDB (Hill et al., 2003). Similarly, foraminiferal tests from fossil seeps show great heterogeneity of $\delta^{13}C$ values and have recorded values as low as -55‰ PDB (Martin et al., 2007). In modern and fossil non-seep sediments, the $\delta^{13}C$ value of foraminiferal tests varies within a narrow range: for example, the range of variation in non-seep specimens of *Uvigerina peregrina* is typically between 0.2‰ to 0.4‰ (Rathburn et al., 2003). In the homogeneous settings found with normal seawater, isotopic composition is influenced primarily by ambient seawater values, which vary only slightly from 0‰ PDB. In cold methane seeps, however, HCO_3^- in pore fluids may be derived from several sources, including highly enriched CO_2 from the zone of methanogenesis, or AOM of microbial or thermogenic methane. Addition of DIC carrying the isotopic signal of marine organic carbon and/or ambient sea water complicates the issue even further. Thus $\delta^{13}C$ values may reflect any one of these factors or a combination of two or more. This will be further complicated by the tortuosity of fluid-flow pathways through the sediments, which creates numerous micro-habitats. Thus the heterogeneity found in $\delta^{13}C$ values from seep foraminifera is not unexpected.

3. Geologic setting

The Cascadia subduction margin of the northeastern Pacific was initiated in the Late Eocene after the complete subduction of the oceanic Resurrection Plate, and change in motion of the Kula plate (Haussler et al., 2003, Figure 7; Madsen et al., 2006, Figure 9). This major tectonic change from a strike-slip regime of the Queen Charlotte-Fairweather coast-parallel transform fault to orthogonal subduction resulted in rapid uplift of a very active volcanic arc together with development of a deep forearc basin at the Middle-Late Eocene boundary (Irving et al. 1996; Hammond, 1998). Voluminous volcaniclastic sediments were deposited into the forearc basin and the Keasey and Lincoln Creek Formations record the rapid change from shallow neritic to bathyal depositional depths during the Late Eocene. All the formations that provided carbonates for this study were deposited as a

contiguous subduction wedge within the forearc basin that extended north to south. Although they are now defined as different formations, and are no longer contiguous, they were deposited as a single system. Biostratigraphic correlations indicate that the upper section of the Lincoln Creek Formation is the temporal equivalent to the Blakeley, Pysht and Sooke formations (Armentrout, 1981; Rau, 1981; Nesbitt, 2003; Nesbitt et al., in press).

In the middle Miocene the subduction wedge off northern Washington was uplifted to form the Olympic Mountains, exposing large sections of the forearc sediments as part of the landward displacement of the deformation front (Brandon et al., 1998; Stewart and Brandon, 2004). The Coastal unit of the Olympic Structural Complex (COSC) is an Eocene to Middle Miocene package of deep water (>2,000 m) sedimentary rocks that accreted beneath the frontal 50-100 km of the wedge (Stewart and Brandon, 2004). Fission track dating of detrital apatite from the COSC indicates exhumation began around 18 Ma. These rocks were originally accreted during late Oligocene to early Miocene time, when the central core of the Olympics was subjected to temperatures ranging from 240^{o} to 290^{o}C (Brandon et al., 1998). Along the present coastline and offshore, COSC rocks include mélange and broken formation of the Hoh complex that diapirically intrudes younger forearc sediments (Brandon et al., 1998, McNeill et al., 1997). Continued tectonic uplift and enhanced erosion of the topographic high has ensured a steady supply of sediment to the forearc basin. Today the subduction wedge is ~ 6,000 m thick and extends 100-150 km offshore (Goldfinger et al., 1997; Wells et al., 1998).

Large volumes of terrestrial organic matter incorporated into the sediments provide the source for hydrocarbons that are expelled when overpressuring caused by tectonic compression results in fluid migration to the surface via faults, fractures and diapirs with ensuing surface seepage. Exhumed fossil cold seeps outcrop in numerous localities along the coastal region. These include the sites used in this study: the late Eocene Rock Creek section of the Keasey Formation of northwest Oregon, the Oligocene Satsop/Canyon River section of the Lincoln Creek

Formation of southwest Washington, the Oligocene Blakeley and Pysht formations of northwest Washington, the Oligocene Sooke Formation of southern Vancouver Island, and the Pliocene Quinault Formation of western Washington (Figure 3.1). Recent seeps on this margin are best developed at Hydrate Ridge, off the Oregon coast where extensive deposits of gas hydrates are indicated by a well-developed bottom simulating reflector (BSR). Other evidence of gas seepage is provided by extensive carbonate deposits and communities of seep-specific organisms (Suess et al., 1985; Naehr et al., 1998; Greinert et al., 2001; Sahling et al., 2002; Torres et al., 2002; Teichert et al., 2005).

3.1 Stratigraphy and Sedimentology

Fossil cold seeps occur in Cenozoic formations along the Cascadia margin from the northwestern Oregon to the southwestern coast of Vancouver Island. For this study foraminifera and authigenic carbonates were sampled from six of these units (Figure 3.1).

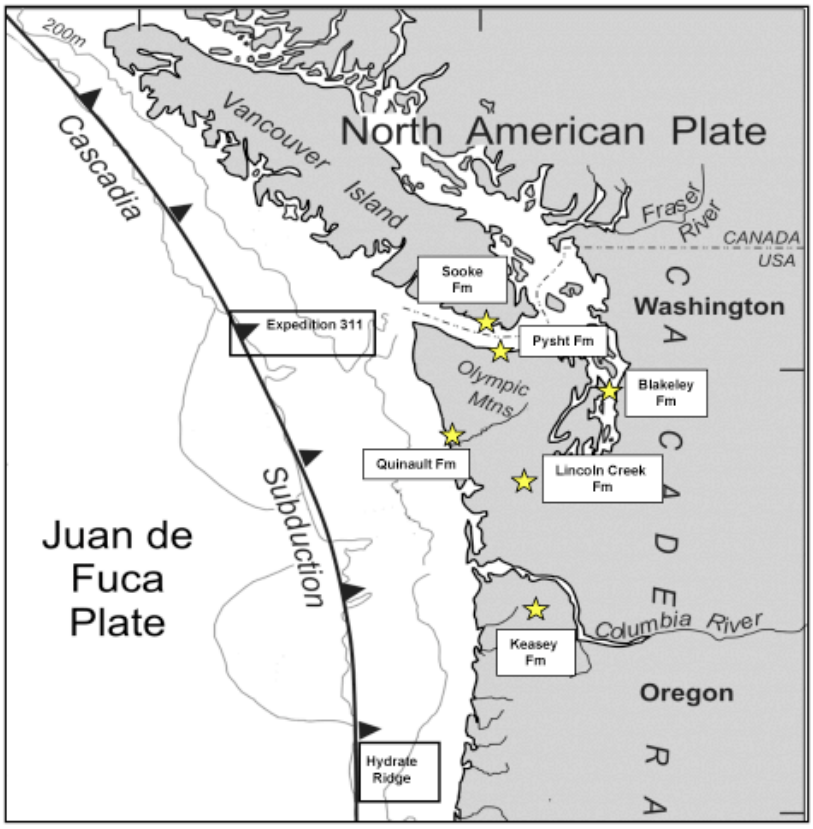

Figure 3.1. Location map of Cascadia Margin showing locations of cold seeps used in this study, as well as sites of modern seeps on the margin.

The late Eocene to early Oligocene Keasey Formation is exposed in the Nehalem River basin of northwestern Oregon. It consists of ~700 m of tuffaceous siltstones and clayey mudstones deposited in a shelf-slope and upper bathyal setting and is divided informally into three lithological members (Hickman, 1980). Foraminifera used in this study were collected from the outsides of a large chemoherm exposed along Rock Creek, within the middle member of the formation. Paleontologic and magnetostratigraphic evidence places the Eocene/Oligocene boundary near the top of the middle member (Hickman, 1980; Prothero and Hankins, 2000). The Keasey Formation overlies the Eocene Cowlitz Formation that is both the source of the hydrocarbons. Methane has been seeping from the Cowlitz sandstone reservoirs since the Late Eocene, and is presently supplying the Mist Gas Field (Armentrout and Suek, 1985; Burns et al., 2005).

Another fossil seep site in the Keasey formation is the large chemoherm on Vernonia-Timber road, and possibilities of methane seepage were documented at the Mist crinoid locality (Campbell and Bottjer, 1993; Nesbitt et al., 1994; Burns et al., 2005).

The Late Eocene to Early Miocene Lincoln Creek Formation extends from the southern slopes of the Olympic Mountains to the Chehalis River in southwestern Washington (Beikman et al., 1967; Rau, 1966; Prothero and Armentrout, 1985), with outcrops in river valleys and road cuts. The Lincoln Creek Formation is comprised of ~3,000 m of volcaniclastic sandstones, siltstones and mudstones deposited in the deepening forearc basin, from neritic depths at the base of the formation to bathyal depths through the Oligocene. The upper strata are lower Miocene in age, and reflect shallowing of the depositional basin (Beikman et al. 1967; Rau 1966). The lower units of the Lincoln Creek are equivalent to the Keasey Formation, and are now divided by the Miocene Columbia River flood basalt flows. Numerous cold seep sites have been identified along the Canyon River and Middle Fork of the Satsop River sections of the Lincoln Creek Formation, as well as in a temporally equivalent sedimentary unit at Menlo and Bear River, south of the Chehalis River (e.g. Goedert and Squires, 1990; Nesbitt et al., 1994; Goedert et al., 2000; Peckmann et al., 2002).

In the Puget Sound lowlands the Blakeley Formation crops out in a narrow band from Bainbridge Island to the foot of the Cascade mountains and consists of marine turbidites in its eastern exposures grading into shallow marine and marginal marine embayment deposits in its western outcrops (Weaver 1937; Fulmer , 1975). The eastern outcrops of the Blakeley Formation have been tilted to vertical in places by movement on the Seattle Fault. Biostratigraphy and paleomagnetic signatures show that the Blakeley is temporally equivalent to the upper Lincoln Creek, Pysht and Sooke formations (Prothero and Nesbitt, 2008)

The Oligocene Pysht Formation crops out on the northern Olympic Peninsula margin along the Straits of Juan de Fuca, and in river beds for ~ 10 km inland. The Pysht is the uppermost member of the Twin River Group, conformably

overlying the Makah Formation, and grading into the overlying Clallam Formation. The Pysht consists of ~1,000 m of grey tuffaceous mudstone and sandy siltstone turbidites that were deposited on the distal submarine fan, shallowing upwards to neritic sandstone units near the top (Brown and Gower, 1958). On the north side of the Strait of Juan de Fuca, the type section of the Sooke Formation is ~45m thick, consisting primarily of inner neritic to supratidal cross-stratified sandstone and conglomerate. Sooke rocks also are exposed in isolated bays from the type section west to Port Renfrew and further north in the Carmanah Point area, Vancouver Island. Molluscan and foraminiferal biostratigraphy place the Pysht and the Sooke formations in the regional Zemorrian Stage (Oligocene) The two are considered to be the same depositional units now separated by the Straits (Garver and Brandon 1994; Brandon et al. 1998) but complex folding and faulting from the uplift of the Olympic Mountains have made both stratigraphic thicknesses and refined biostratigraphic zonations unreliable (Nesbitt et al. in press). Cold seep faunas have also been described from localities at the mouth of both Murdock and Whiskey creeks in the easternmost (and presumably the stratigraphically lowest) section of the Pysht Formation (Goedert et al., 2003; Peckmann et al., 2003).

The Pliocene Quinault Formation is exposed in seacliff sections along a 10 km stretch of coastline north of Point Grenville, Washington in outcrops that are accessible only at lowest low tide. With a total thickness of 3000 m, the Quinault Formation outcrops in four sections which, though internally contiguous, are not preserved in stratigraphic sequence. Ancient methane seep-carbonate deposits (cf. Campbell, 1992) occur in the marine shelf section exposed north and south of Pratt Cliff (Campbell, 1992; Martin et al., 2007). Paleontological and sedimentological evidence imply that this section was deposited in mid-to-outer shelf depths (Rau, 1970; Campbell et al., 2006). The Pliocene age of the formation is based on benthic foraminifera (Rau, 1970; Campbell and Nesbitt, 2000).

4. Methods

Samples for this study were collected from outcrops during parts of four field seasons. In the Pysht, Sooke and Quinault Formations outcrops were generally accessible only at lowest tides. In the Canyon and Satsop River sections of the Lincoln Creek Formation and the Rock Creek section of the Keasey Formation outcrops were accessible during the dry season when rivers were low. Unweathered samples were collected from outcrops that contained macroscopic evidence of methane seepage (Figure 3.2a-f). Such evidence included fossils of chemosymbiotic invertebrates including the bivalves *Vesicomya (Calyptogena) pacifica* (Figure 3.2a), *Acharax ventricosa*, *Lucinoma annulata* (Figure 3.2b) and *Conchocele bisecta*, patches of carbonate nodules (physically distinct from surrounding sediments, having discrete boundaries) and carbonate blebs (small, with indistinct, wispy, diffuse boundaries) (Campbell, 1992) (Figure 3.2c), carbonate fracture fill (Figure 3.2d,e) and a chemoherm (Figure 3.2e). In addition, crystals of glendonite, a calcite pseudomorph of the low-temperature hydrated $CaCO_3$ mineral ikaite, were common in seep localities but were not found in non-seep sites, thus they were used in conjunction with the other seep indicators. Locality data and ages of seeps used in this study are listed in Table 3.1.

Figure 3.2. Examples of field indicators used to identify fossil seeps. a and b – representative seep bivalve taxa: a. Vesicomya (*Calyptogena) pacifica;* b. *Lucinoma annulata*. c. Nodules and blebs in the Twin Rivers locality of the Pysht Formation. d through f – carbonate fracture fills: d. Sooke Formation; e. Pysht Twin Rivers locality; f. Pysht Tree Farm locality. g. Keasey chemoherm.

Carbon and oxygen isotope analyses were conducted on foraminiferal tests and authigenic carbonates. Field and laboratory procedures for obtaining stable carbon isotope values from foraminifera are described in detail in Martin et al. (2007). Analyses were performed on individual foraminifera or on several individuals if they were very small. Isotope analyses were carried out at the Stanford University Stable Isotope Laboratory on a Finnegan Kiel III carbonate device interfaced with a MAT 252 IRMS and at the University of Washington Department of Earth and Space Sciences Isotope Laboratory on a ThermoScientific Kiel III carbonate device attached to a ThermoFinnigan DeltaPlus IRMS. Based on multiple analyses of the NBS 19 standard, precision was <0.05‰ for $\delta^{18}O$ and <0.03‰ for $\delta^{13}C$ in the Stanford laboratory and 0.06‰ for $\square^{18}O$ and 0.03‰ for $\square^{13}C$ in the University of Washington laboratory. Results are reported in delta notation ($\delta^{18}O$ and $\delta^{13}C$) relative to the PDB standard, where $\delta = (R_{sample}/R_{standard} - 1)\ 1000$. The difference between maximum and minimum isotopic values ($\delta^{13}C_{max} - \delta^{13}C_{min}$) is designated by $\square^{1\square}C$.

Foraminiferal taxa used for comparison in this study are *Globobulimina auriculata*, *G. pacifica*, *Nonionella applini*, *N. basispinatum, N. stella*, *Uvigerina cocoaensis*, *U. hootsi*, U. *juncea,* and *U.* cf *peregrina*. These species were chosen because they, or closely related species, have been found in modern seeps, and they were most numerous in these fossil seeps.

Table 3.1. Locations of sample sites for this study.

Burke locality number	Formation	Latitude	Longitude	Age	Seep indicators
B6858	Quinault	47.384 °N	124.324° W	Pliocene	Numerous. *Calyptogena*, *Acharax, Lucinoma,* blebs, nodules, glendonites
B7219	Sooke	48.100 °N	124.304° W	Oligocene/ Miocene	Carbonate pavement, nodules
B7218	Pysht - Tree Farm	48.220 °N	124.121° W	Oligocene	*Acharax, Calyptogena*, blebs, carbonate slab
B7217	Pysht - Twin Rivers	48.161 °N	123.888° W	Oligocene	*Acharax, Lucinoma,* blebs, glendonites, carbonate pavement
B7216	Pysht - Quarry	48.165 °N	123.964° W	Oligocene	*Acharax, Lucinoma*, blebs
B7272	Keasey - Rock Creek	45.896 °N	124.388° W	Eocene/ Oligocene	Large chemoherm with *Calyptogena*
B6895	Lincoln Creek - Canyon & Satsop Rivers	45.261 °N	123.367° W	Oligocene	Carbonate bodies, seep fauna (Peckmann et al., 2002; blebs (this study)

5. Results

Foraminiferal and authigenic carbonate isotope values are summarized in Tables 3.2 and 3.3, and Figures 3.3 and 3.4. Of note in both types of carbonates are the degree of depletion and variability in both $\delta^{13}C$ and $\delta^{18}O$, as well as the differences in values between seep locations. All formations investigated displayed foraminiferal $\delta^{13}C$ values that were more variable than the 0.2 to 0.4‰ PDB (Figure 3.3a-e) expected in ambient sea water (Rathburn et al., 2003). In addition, wide variability and strong depletion are apparent in different species from the Keasey, Lincoln Creek and Quinault formations, again a phenomenon recorded in modern and ancient seeps (e.g. Rathburn et al., 2003; Martin et al., 2007) With δ^{13}Ç values <-50‰ PDB, foraminifera from the Lincoln Creek and Quinault formations (Figure 3.3b,e) clearly documented the influence of AOM of microbial CH_4. This interpretation supports that of Peckmann et al. (2002), who analyzed small carbonate bodies in the Lincoln Creek Formation and found biomarkers that

confirmed the presence of archaeal methanogens and of AOM. Foraminifera from the Keasey Formation (Figure 3.3a) showed the greatest $\delta^{13}C$ variability ($D^{13}C$ = 41.6‰ PDB for *Globobulimina pupoides*), however the -30 to -50‰ PDB values of $\delta^{13}C$ indicated derivation from thermogenic CH_4 (Claypool & Kaplan, 1974). In contrast, foraminiferal carbonates from the Pysht and Sooke formations are more enriched in ^{13}C and more depleted in ^{18}O than the other formations and do not show the separation of species that is present in the Keasey, Lincoln Creek and Quinault formations (Figure 3.3c,d).

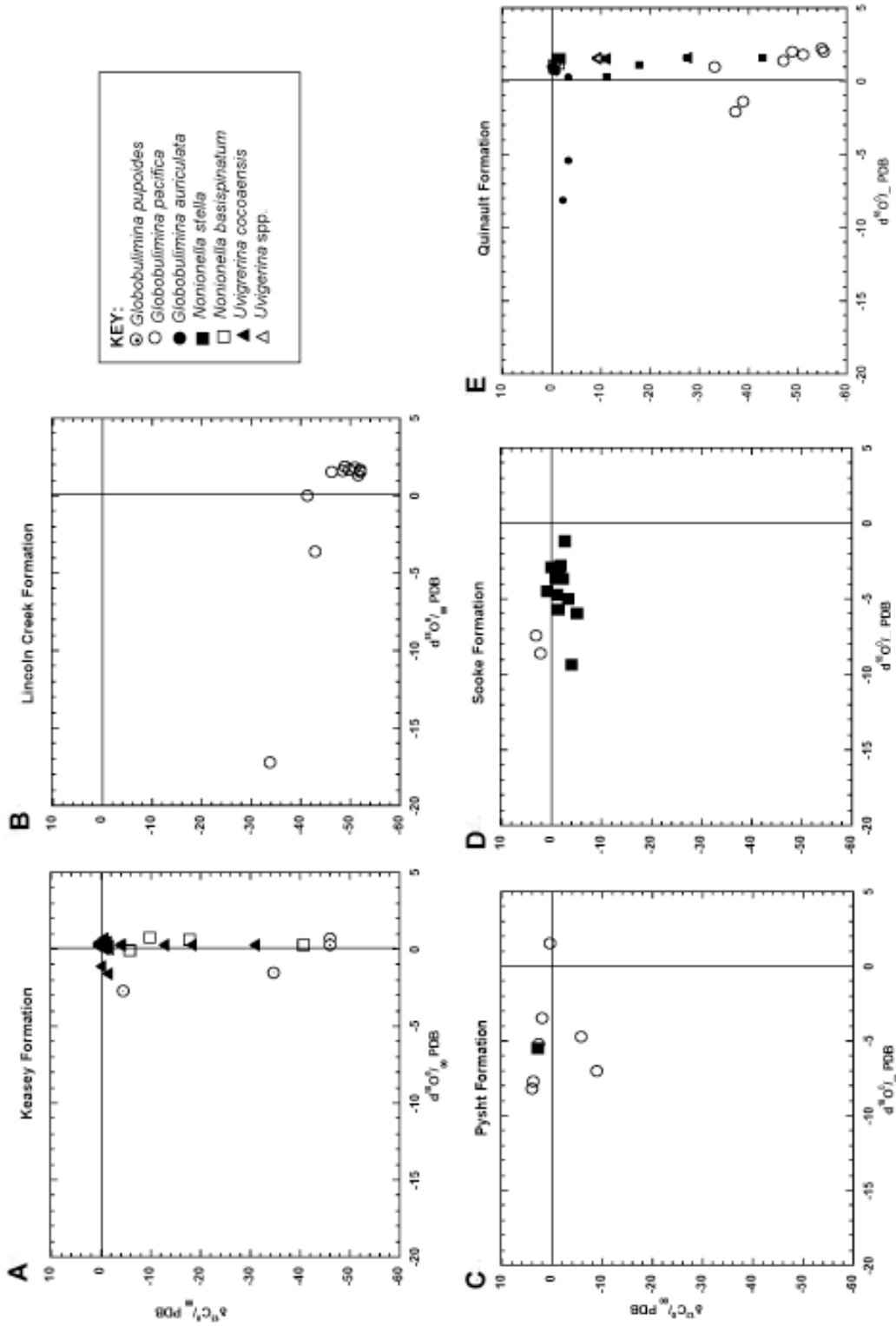

Figure 3.3. Isotope values for foraminiferal carbonates from each formation studied.

Similar to the foraminiferal carbonates, $\delta^{13}C$ values from authigenic carbonates in the Quinault and Lincoln Creek formations (Figure 3.4a, c) carried values indicative of microbial methanogenesis: a nodule from the Lincoln Creek registered -50.6‰ PDB, while a bleb from the Quinault recorded +8.7‰ PDB. Formation of this bleb utilized residual CO_2 from microbial methanogenesis (e.g. Whiticar, 1999; Budai et al., 2002). The majority of foraminiferal and authigenic carbonates in the Keasey, Lincoln Creek and Quinault formations displayed $\delta^{13}C$ values that undoubtedly resulted from DIC mixtures from different methane sources as well as the normal degradation of organic matter (e.g. Claypool et al., 2006; Torres & Kastner, 2009).

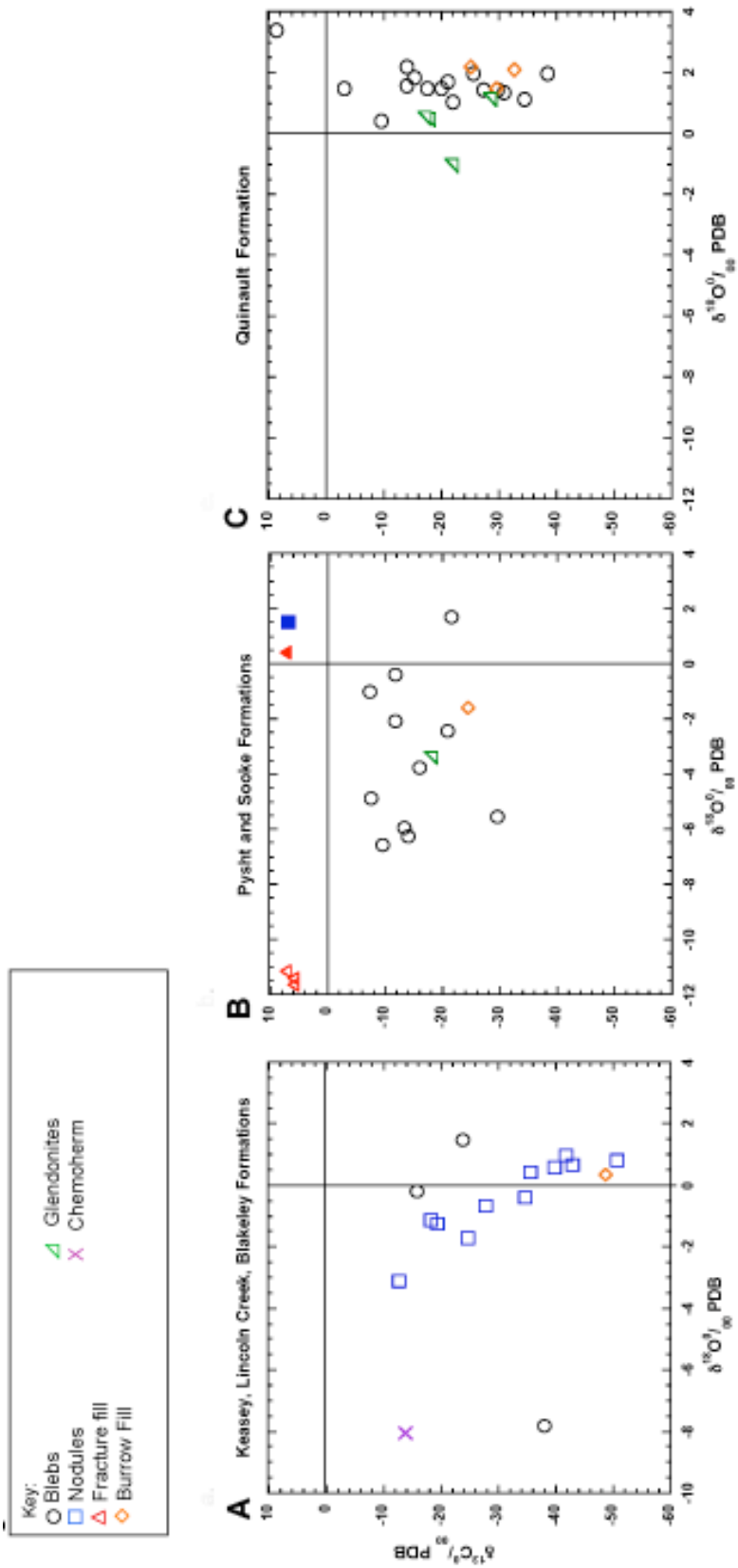

Figure 3.4. Authigenic carbonate isotope values. Note: in b, open symbols are Pysht Formation, closed symbols are Sooke Formation.

Oxygen isotope values in the Keasey, Lincoln Creek and Quinault formations displayed slightly less similarity than the carbon isotopes. Among all types of authigenic carbonates in the Quinault Formation $\delta^{18}O$ equaled 4.3‰ PDB, with values remaining close to 0‰ PDB. During the Pliocene, deep sea $\delta^{18}O$ values ranged between 2.8 and 3.6‰ PDB (Zachos et al., 2001), thus the values in the Quinault foraminiferal and authigenic carbonates are consistent with outer-shelf/upper slope ambient seawater of the time. Values of $d^{18}O$ for the Lincoln Creek Formation were slightly more variable (Figure 3.4a), however the majority were still within a range that would be expected for sea water in the early Oligocene (Zachos et al., 2001). The two exceptions were the Keasey chemoherm and a bleb from the Lincoln Creek. Both of these displayed considerable depletion in $\delta^{18}O$, indicating the influence of higher temperature fluids.

A comparison of foraminiferal carbonates from all seeps studied is shown in Figure 3.5. The foraminiferal carbonates are easily divided into two groups – the Pysht/Sooke foraminifera, and all others. The Pysht/Sooke foraminiferal carbonates are characterized by enriched $\delta^{13}C$ and depleted $d^{18}O$, the latter suggesting the original carbonate was overprinted by later, warmer fluids. The second group contains foraminifera of the Keasey, Lincoln Creek and Quinault formations. Because of the geographic and age differences in these formations, this grouping signifies similar fluid-flow histories for seepage, not temporal or spatial clustering.

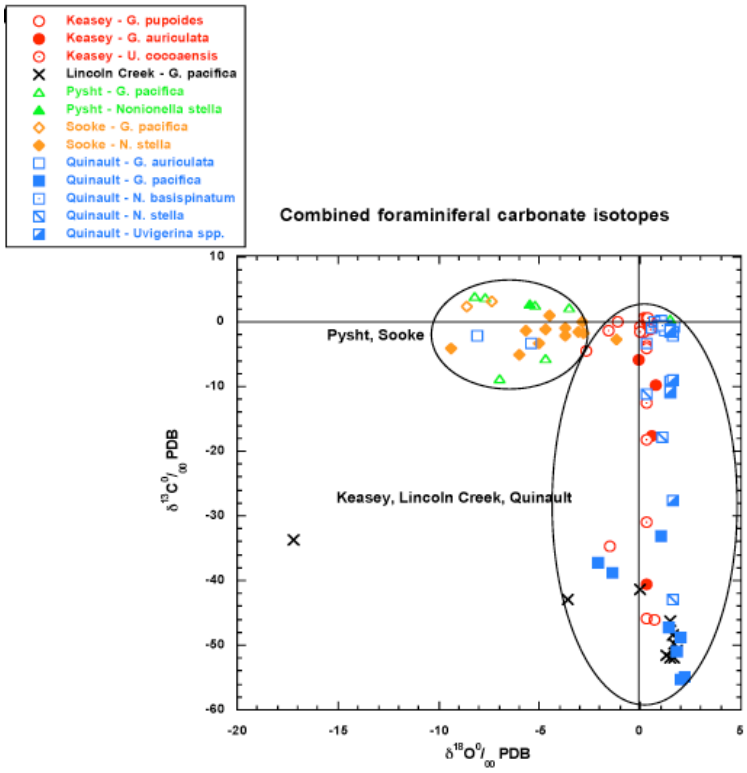

Figure 3.5. Combined foraminiferal isotope values for all formations. Foraminifera from the Pysht and Sooke formations are noticeably separated from all others by their enriched $\delta^{13}C$ and depleted $\delta^{18}O$ values.

In the authigenic carbonates also, three distinctive groups are readily discerned (Figure 3.6). Group I comprises the Pysht and Sooke formation fracture fills and nodule, Group II consists of the Pysht blebs and glendonite, and Group III includes all types of authigenic carbonates from the other four formations. Group III is characterized by depleted $\delta^{13}C$ with □ ^{18}O indicating temperatures close to ambient sea water. Thus, sediments were bathed in low temperature water or pore fluids influenced by AOM of either microbial or thermogenic CH_4, or both. These fluids were responsible for the precipitation of the authigenic carbonates in this group.

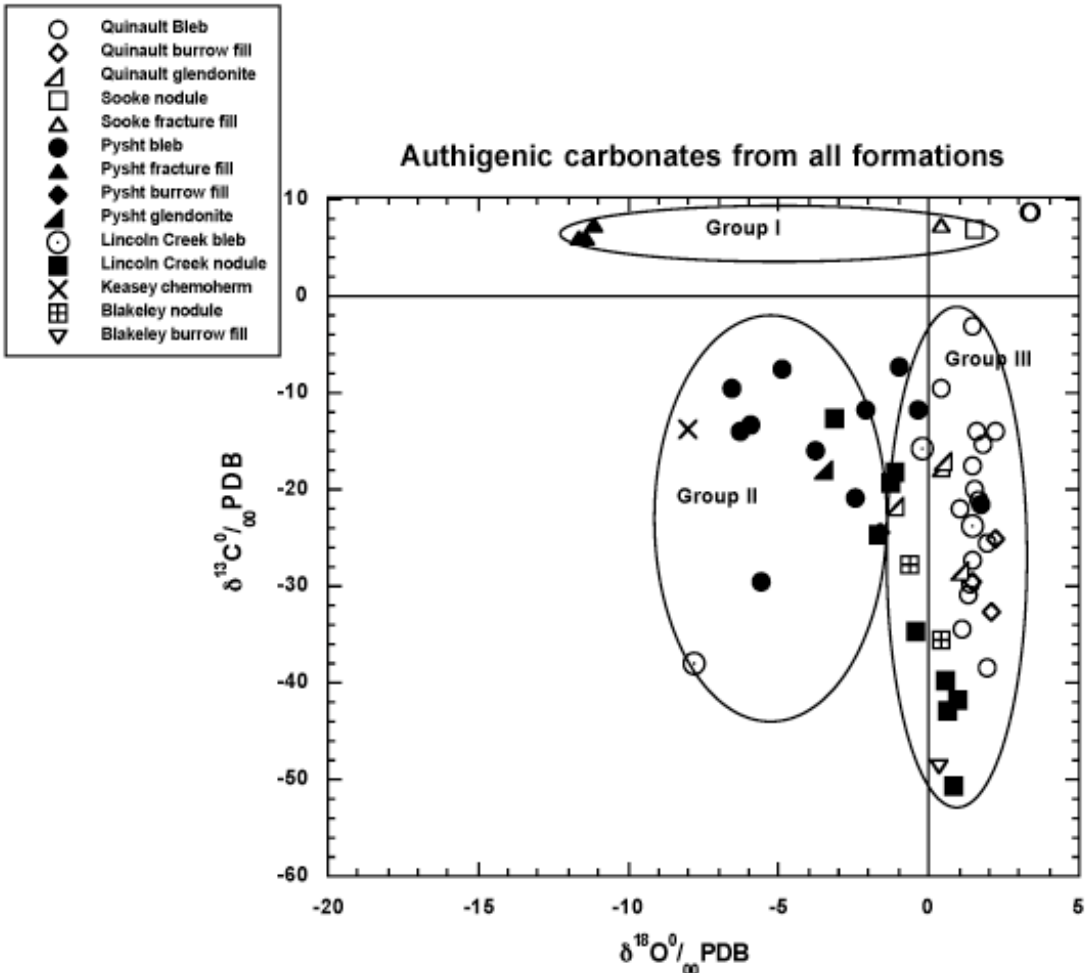

Figure 3.6. Combined authigenic carbonate isotope values showing three clearly distinguished groups. Group I is Pysht/Sooke fracture fills and nodule; Group II contains Pysht blebs, burrow fill, and glendonite along with the Keasey chemoherm. Group III comprises all Quinault, Blakely and Lincoln Creek authigenic carbonates.

In Groups I and II, carbonates from the Pysht and Sooke formations have been generated by distinctly different fluid flows. A closer examination of these carbonates is shown in Figure 3.7, which clearly shows the Pysht/Sooke carbonates arranged in several groups. The Pysht fracture fill is distinctive because of its combination of enriched $\delta^{13}C$ and depleted $d^{18}O$. This isotopic combination suggests precipitation from warm fluids containing HCO_3^- derived from CO_2 residual from microbial methanogenesis. The Pysht and Sooke foraminiferal isotopes reflect enriched $\delta^{13}C$ and slightly depleted $d^{18}O$. This contrasts markedly with foraminifera from the other three formations studied (Figs. 3.3c, 3.5). These

results are also markedly different from both fossil and Recent foraminiferal carbonates analyzed in other seep studies, which show conspicuous $\delta^{13}C$ depletions with $d^{18}O$ values close to 0‰ PDB (e.g Rathburn et al., 2003; Martin and Nesbitt, 2004; Mackensen et al., 2006; Martin et al., 2007). The likelihood here is that the foraminifera have been overprinted by the same warm, $\delta^{13}C$-enriched fluids that produced the Pysht fracture fill.

The remaining authigenic carbonates from the Pysht and Sooke formations (blebs, glendonite, and burrow fill) cluster into yet another distinctive group, characterized by more depleted $\delta^{13}C$, slightly less depleted $d^{18}O$ and greater variability. Here again, the $d^{18}O$ depletion suggests overprinting by later fluids, but these carbonates apparently retain more of the characteristics of the original material. The enigma in these two formations lies with the Sooke fracture fill and nodule, which do not fit into any other group. With their $\delta^{13}C$ almost identical to that of the Pysht fracture fill, they are conspicuous for their much more enriched $d^{18}O$ values. The simplest explanation for this is microbial methanogenesis operating near the sediment/water interface (e.g. Greinert et al., 2001; Teichert et al., 2005; Claypool et al., 2006) resulting in fluids containing enriched residual $\delta^{13}C$ at ambient temperatures.

Clearly, the Pysht and Sooke formations have undergone a different fluid-flow history from the other three formations, and were subjected to at least two distinct regimes of fluid flow. One was mineralization influenced by AOM of thermogenic and microbial methane, while the second consisted of one or more events of advecting warmer fluids containing ^{13}C from residual CO_2 from microbial methanogenesis. This data is consistent with other studies of the Tofino Basin that demonstrate the presence of later stage carbonates that precipitated at elevated temperatures (e.g. Brandon et al., 1998, von der Ahe, unpublished data).

6. Discussion and Conclusion

Isotopic compositions of carbonates are indicative of the diagenetic conditions present as the carbonates formed, and samples from fossil cold seeps

provide a snapshot of that area in ancient times. Unlike an actual photograph, however, fossil samples are temporally and spatially averaged, providing a less-than-precise look at the prevailing conditions. The Cascadia accretionary margin has been evolving since the Eocene in response to the subduction of the Juan de Fuca plate beneath the North American plate, thus comparison with present-day conditions in the well-studied cold seeps of this margin helps make sense of the data from ancient seeps. The three most notable elements observed in the fossil seeps, i.e. indications of several sources of DIC, unevenness in $d^{18}O$ values, and variability within and among sample sites, are all found in the modern seep environments of the Cascadia Margin.

In their study of the southern summit and surrounding basins of Hydrate Ridge (Figure 3.1), Claypool et al., (2006) differentiated three CH_4 types in the sediments: previously buried microbial CH_4; deep, thermogenic CH_4; and microbial CH_4 currently being generated in situ in shallow sediments. Although the gas geochemistry was complicated by the migration and mixing of these gases, the authors estimated that on the southern summit of Hydrate Ridge, 65% of the CH_4 was from older, deeper microbial sources, 15% was thermogenic, and 20% was surface CH_4 currently being microbially generated in situ. Thus, seepage at the summit is dominated by both microbial and thermogenic CH_4 that has been transported from depth (estimated to be 2.2 km; Claypool et al., 2006) along tectonically generated faults and fractures. On the other hand, the surrounding basins are dominated by in-situ-generated microbial CH_4 with little or no AOM operating. Similarly to the north, Torres and Kastner, (2009) investigated seep sites off Vancouver Island during IODP Expedition 311 (Figure 1) and found the majority of the CH_4 in the gas hydrates studied to be comprised of microbial CH_4. At some sites however, residual CO_2 rather than AOM was the more significant contributor to the total DIC. In addition, Torres and Kastner (2009) found a progressive enrichment of $\delta^{13}C$ along a transect from the western to the eastern limits of gas hydrate occurrence, reflecting the preferential consumption of ^{12}C during methanogenesis as sediments aged. This information yields a more

organized picture of CH_4 seepage here, with migration pathways channeling fluids from deep sources near the anticlinal summits, surface processes dominating in the surrounding basins, and sediments maturing with distance from the deformation front of the accretionary prism.

The unevenness in $\delta^{18}O$ values observed in the fossil seeps, particularly in the Pysht and Sooke formations, is also evident in modern Cascadia. For example, Kulm and Suess (1990) identified four subgroups of methane-derived carbonates that were the products of different fluid-flow regimes. Among these were $\delta^{18}O$ values suggesting deposition in the shallow subsurface, close to ambient sea water temperatures, as well as extremely depleted $\delta^{18}O$ that apparently originated from upward migration of warm hydrothermal fluids that tapped the subducting slab. Meteoric water as a source for these $\delta^{18}O$ values was ruled out on the basis of foraminiferal evidence of a depositional water depth of 3000 m, making the migration of meteoric water highly unlikely. Bohrmann et al. (1998) also found significantly depleted $\delta^{18}O$ values and interpreted them as the result of fluid migration from depths of 1 to 4 km. In contrast, these authors also observed enriched $\delta^{18}O$ values in near-surface carbonates, noting that these indicated gas hydrate dissociation. However, Tryon et al. (2002) observed that the Hydrate Ridge fluid source has been augmented by clay mineral dehydration within the accretionary wedge, and this would also enrich the $d^{18}O$ signature in the DIC.

The third striking feature of isotope signatures in the fossil seeps is their heterogeneity, even within a single sample. In modern Cascadia seeps, heterogeneity is well documented; the present Cascadia Margin is a complex hydrogeologic system characterized by extreme heterogeneity both spatially and temporally. In their investigation of Hydrate Ridge, Torres et al. (2002) documented three distinct fluid-flow regimes. The first were discrete sites of CH_4 ebullition at the northern summit, with flow through direct channels and velocities measured at ~1 m sec^{-1}. Second were extensive bacterial mats developed over sediments capped by gas hydrates; here, flow rates were 30 to 100 cm yr^{-1}. Finally, colonies of vesicomyid clams developed in areas where there was seawater inflow

part of the time, and the hydrocarbon flux was <1mmol m^{-2} day^{-1}. Additionally, areas of extensive pavement formed where seepage was more extensive and mature. Aside from spatial heterogeneity, these authors also recorded extreme temporal variability. On the northern summit, vents went from dormant to active in a few hours, with a periodicity linked to tidal pressure changes. Also, fluxes varied by orders of magnitude over small areas, making it difficult to generalize flux rates. Tryon et al. (2002) also observed the extreme heterogeneity of flow in time and space. While noting that tectonics is the driving force behind fluid flow in the area, they attributed the heterogeneity to the contributions of other factors, including gas-expulsion-driven pumping, aqueous entrainment in migrating gas, buoyancy driven fracturing of overlying sediments, changes in permeability due to gas injection, gas hydrate formation and dissociation, and tidal oscillations. With regard to the latter, some vents observed went from dormancy to vigorous flow in 30 minutes, then remained active for ~two hours.

Working on Hydrate Ridge, Tryon and Brown (2001) also documented widespread spatial and temporal variability in fluid flux. They observed high frequency fluid flow transience operating with the periodicity of tidal forcing and with amplitudes controlled by the amplitude of tidal levels and sediment permeability. The hydrologic regime was observed to have a profound impact on the seep ecology. Microbial mats and vesicomyid clam beds were mutually exclusive. Microbial mats were present in areas with high rates of fluid outflow ranging between 20 and >100 cm/yr on northern Hydrate Ridge, and up to 1000 cm/yr on southern Hydrate Ridge. Clam beds, on the other hand, were associated with low net flow (<10 cm yr^{-1}) and complex short period variability and flow reversals. Downflow in clam bed areas often resulted in seawater-like fluids in the sediments.

With the understanding that even the most carefully devised sampling in ancient seeps yields a comparatively random sample set, the results from this study can be re-evaluated in light of findings from the modern Cascadia Margin. The following conclusions can thus be made.

1. There were several fluid sources influencing sediments in Cenozoic methane seeps. Areas showing extensive influence of AOM where sources were mixed may have been located in regions of deeper-seated fluid flow. Samples showing more enriched $\delta^{13}C$ values (Pysht/Sooke fracture fills; Pysht foraminifera; Quinault bleb) may have been located in basins away from the deformation front, but most certainly in areas influenced by microbial methanogenesis where AOM was not the driving factor in DIC formation.

2. Extreme depletion in $\delta^{18}O$ (Pysht Formation fracture fills; Keasey chemoherm; Lincoln Creek foraminifera) was due to the influence of warm, deep-seated fluids migrating upward along tectonically-generated conduits. In modern Cascadia these are known to occur near anticlinal summits; it is reasonable to assume the same was true in the Cenozoic.

3. The extreme heterogeneity of isotopic values is the product not simply of the microhabitats of foraminifera (e.g. Martin et al., 2007), but of the macroenvironment as well. Heterogeneity is characteristic of seep provinces (e.g. Torres et al., 2002; Tryon & Brown, 2001; Formolo et al., 2004), thus it would be surprising, indeed, if such were not the case in fossil seeps. Therefore the following inferences are made regarding the Cascadia seeps.

First, with its lack of well-developed carbonate structures, the Quinault Formation was probably the least mature seepage area, characterized by diffuse seepage. The presence of *Vesicomya* (*Calyptogena) pacifica* suggests a lower fluid flux with a component of seawater inflow (e.g. Sahling et al., 2002), and depleted $\delta^{13}C$ values in both authigenic and foraminiferal carbonates signify active AOM of both microbial and thermogenic CH_4. Foraminiferal and sedimentologic evidence points to a neritic environment for this section of the Quinault Formation (Rau, 1966; Campbell, 1992). The source of the CH_4 for these seeps was the underlying Eocene-Miocene Hoh mélange, which intrudes diapirically into the Quinault Formation, causing the faulting and fracturing that became fluid-flow conduits (Orange, 1993).This is consistent with the findings of Torres et al. (in press) working on Heceta Bank south of Hydrate Ridge who observed two CH_4 source

regions that respond to different forcing mechanisms – a young prism characterized by the generation of microbial CH_4, and an older sequence that is the source for thermogenic CH_4 that vents on the shelf.

Second, with their better developed carbonate structures, the Keasey and Lincoln Creek Formations show evidence of more mature seepage and robust fluid flow. The Keasey chemoherm, which contains *in situ* specimens of *Acharax dalli* and *Conchocele bisecta*, may have developed along the model of Teichert et al. (2005) in which the carbonate chemoherm was deposited several meters into the water column, with the AOM consortium operating on the carbonate surface underneath bacterial mats. The clams would have lived in the oxic waters on the surface of the chemoherm and tapped the sulfide reservoirs in the less active fluid conduits.

Finally, the seeps of the Pysht and Sooke formations are more problematic. Certainly the biota present (vesicomyids, solemyids) indicate areas of less robust fluid flow, as do the less developed carbonates such as blebs and nodules. On the other hand, the fracture fill structures in both formations (Figure 2) are indicative of more vigorous, longer-lived fluid flow. Carbon isotope values for these ($\delta^{13}C$ between +5.93 and +7.37‰ PDB) are clearly indicative of DIC derived from CO_2 residual from microbial methanogenesis. Oxygen isotopic values, however, indicate different fluid sources for the two areas. The Pysht fracture fills, with $\delta^{18}O$ of -11.17 to -11.63‰ PDB suggest derivation from warm, deep-seated fluids, which would be consistent with the transport-dominated fluids observed by Claypool et al. (2006) at the northern summit of Hydrate Ridge. On the other hand, given the tectonic history of this particular area, with the massive uplift of the Olympic Mountains, these carbonates could well be post-depositional, thus unrelated to original seep activity. Brandon et al., 1998 demonstrated that the COSC rocks had been subjected to elevated temperatures that could have been the source of the diagenetic overprint in the Pysht/Sooke rocks.

This interpretation is further supported by the foraminiferal carbonates, which have isotopic values that are distinctive from those in other seeps in this

study and in other studies (e.g. Rathburn et al., 2003; Hill et al., 2004; Martin et al., 2007, 2009). The more depleted $\delta^{18}O$ values of the foraminifera suggest the presence of warm waters, and although foraminifera often display great adaptability, they are generally found in zones well-defined by temperature (e.g. Ingle, 1967). It is thus probable that the fluid flow that produced the Pysht fracture fills was secondary, and the original isotopic signatures of the foraminifera were overprinted at this time. The blebs, burrow fills and glendonites were less impacted, and still carry much of the original isotopic signature.

The Sooke fracture fill and nodule are distinct from those of the Pysht Formation. Although their $\delta^{13}C$ signatures are similar, the Sooke $\delta^{18}O$ values are indicative of ambient temperatures, thus equating them with carbonates forming in basins and influenced by shallow, in situ microbial methanogenesis. Therefore fluid flow in the basin where these formed was robust and prolonged enough for extensive fracture fill formation, but did not tap the deep, warm fluids utilized in the Pysht fracture fills.

In contrast to the Pysht Formation, authigenic carbonates from the severely deformed Blakeley indicate this formation was not subjected to high heat. Its isotope values cluster with those of the Lincoln Creek, Keasey, and Quinault formations, thus it has undergone similar fluid-flow regime.

It is clear, then, that fluid flow regimes on the Cascadia margin have been complex throughout their history. Stable isotope studies indicate most of the mechanisms operating today have been active throughout the history of the margin. Integration of data from foraminiferal carbonate and authigenic carbonates provides greater detail and also supplies data where authigenic carbonates are absent, for example, at the edge of the Keasey chemoherm. Thus a more complete picture of the fluid-flow history of this margin is emerging, dating nearly to the inception of subduction and continuing to the present.

Acknowledgements

James Goedert generously supplied sediment samples from Lincoln Creek Formation locality SR4 for foraminiferal analysis. Joern Peckmann kindly shared isotope analyses of authigenic carbonates from Satsop and Canyon River localities. Access to seep sites on Quinault Tribal Land was granted by the Quinault Tribe and facilitated by Larry Workman. The Pysht Tree Farm provided access to sites on their land, facilitated by Joe Murray. David Mucciarone of Stanford University and Andy Schauer of the University of Washington are thanked for their expertise in isotope analysis. Funding for isotope analyses was provided by a Research Award from the Department of Earth and Space Sciences at the University of Washington.

Table 3.2. Foraminiferal carbonate isotope values for all formations.

Formation	Species	$d^{13}C$ $^{0}/_{00}$ PDB	$d^{18}O^{0}/_{00}$ PDB
Keasey	*Globobulimina auriculata*	-2.6	-2.8
	Globobulimina auriculata	-17.7	0.6
	Globobulimina auriculata	-5.8	-0.1
	Globobulimina auriculata	-40.6	0.3
	Globobulimina auriculata	-9.7	0.8
	Globobulimina pacifica	-34.6	-1.5
	Globobulimina pacifica	-46.0	0.7
	Globobulimina pacifica	-45.9	0.3
	Globobulimina pacifica	-4.4	-2.7
	Uvigeria cocoaensis	0.2	0.4
	Uvigeria cocoaensis	0.6	0.3
	Uvigeria cocoaensis	0.3	0.4
	Uvigeria cocoaensis	0.3	0.4
	Uvigeria cocoaensis	-0.3	0.5
	Uvigeria cocoaensis	-0.4	0.7
	Uvigeria cocoaensis	-30.9	0.3
	Uvigeria cocoaensis	-4.1	0.3
	Uvigeria cocoaensis	-0.4	0.5
	Uvigeria cocoaensis	-1.2	0.5
	Uvigeria cocoaensis	0.6	0.4
	Uvigeria cocoaensis	-0.7	0.2
	Uvigeria cocoaensis	0.1	0.3
	Uvigeria cocoaensis	-0.7	0.0
	Uvigeria cocoaensis	0.0	0.3
	Uvigeria cocoaensis	-12.6	0.3
	Uvigeria cocoaensis	-1.4	-1.6
	Uvigeria cocoaensis	0.0	-1.1
	Uvigeria cocoaensis	-0.1	0.2
	Uvigeria cocoaensis	0.0	0.3
	Uvigeria cocoaensis	-1.5	0.2
	Uvigeria cocoaensis	-1.5	0.0
Lincoln Creek	*Globobulimina pacifica*	-36.4	0.2
	Nonionella applini	-26.5	-1.5
Pysht	*Globobulimina pacifica*	-5.7	-4.7
	Globobulimina pacifica	4.0	-8.2
	Globobulimina pacifica	3.8	-7.7
	Globobulimina	-8.9	-7.0

	pacifica		
	Globobulimina pacifica	0.4	1.5
	Globobulimina pacifica	2.1	-3.5
	Globobulimina pacifica	2.6	-5.2
	Nonionella stella	2.8	-5.5
Sooke	*Globobulimina pacifica*	3.2	-7.4
	Globobulimina pacifica	2.3	-8.6
	Nonionella stella	-5.1	-6.0
	Nonionella stella	-1.7	-2.8
	Nonionella stella	-1.5	-3.1
	Nonionella stella	-2.7	-1.2
	Nonionella stella	1.0	-4.5
	Nonionella stella	-3.3	-5.0
	Nonionella stella	-0.9	-3.7
	Nonionella stella	-1.4	-5.7
	Nonionella stella	-1.2	-4.7
	Nonionella stella	0.0	-2.9
	Nonionella stella	-4.1	-9.4
	Nonionella stella	-2.2	-3.7
Quinault	*Globobulimina auriculata*	-2.6	1.1
	Globobulimina auriculata	-2.5	1.2
	Globobulimina auriculata	-1.4	1.1
	Globobulimina auriculata	-1.3	0.9
	Globobulimina auriculata	-0.7	1.8
	Globobulimina auriculata	-1.7	1.7
	Globobulimina auriculata	-2.3	1.7
	Globobulimina auriculata	-1.3	1.5
	Globobulimina auriculata	-1.1	1.8
	Globobulimina auriculata	-1.5	1.7
	Globobulimina auriculata	-3.1	0.6
	Globobulimina auriculata	-3.0	-1.5
	Globobulimina auriculata	-2.7	-1.2
	Globobulimina auriculata	-3.3	-5.4

Table 3.2 (*continued)*

Formation	Species	$d^{13}C$ $^{0}/_{00}$ PDB	$d^{18}O^{0}/_{00}$ PDB
	Globobulimina auriculata	-2.1	1.6
	Globobulimina auriculata	-2.2	-8.1
	Globobulimina pacifica	-37.3	-2.1
	Globobulimina pacifica	-48.8	2.0
	Globobulimina pacifica	-38.8	-1.4
	Globobulimina pacifica	-54.9	2.2
	Globobulimina pacifica	-47.2	1.4
	Globobulimina pacifica	-55.3	2.0
	Globobulimina pacifica	-51.0	1.8
	Globobulimina pacifica	-33.1	1.0
	Nonionella stella	-42.9	1.6
	Nonionella stella	-2.1	0.2
	Nonionella stella	-10.7	1.5
	Nonionella stella	-17.8	1.1
	Uvigerina cf peregrina	-27.6	1.6
	Uvigerina hootsi	-10.8	1.5
	Uvigerina hootsi	-9.2	1.5
	Uvigerina juncea	-1.4	1.5
	Uvigerina juncea	-9.0	1.6

Table 3.3. Authigenic carbonate isotope values for all formations

Formation	**Type**	**$d^{13}C$ $^{0}/_{00}$ PDB**	**$d^{18}O^{0}/_{00}$ PDB**
Keasey	Chemoherm	-13.7	-8
Pysht	Carbonate pavement	6.0	-11.6
	Carbonate pavement	5.9	-11.4
	Carbonate pavement	7.4	0.4
	Bleb	-13.9	-6.3
	Bleb	-13.2	-6.0
	Bleb	-9.4	-6.6
	Bleb	-29.6	-5.6
	Bleb	-16.0	-3.8
Sooke	Carbonate pavement	7.4	0.4
	Zoned nodule	7.0	1.5
Quinault	Bleb	-22.0	1.0
	Bleb	8.7	3.3
	Bleb	-29.8	1.4
	Bleb	-21.0	1.7
	Bleb	-14.0	1.6
	Bleb	-34.5	1.1
	Bleb	-9.6	0.4
	Bleb	-3.0	1.5
	Bleb	-27.3	1.4
	Bleb	-19.9	1.5
	Bleb	-30.9	1.3
	Bleb	-15.4	1.8
	Bleb	-14.0	2.2
	Bleb	-17.4	1.5
	Bleb	-38.4	-1.9
	Burrow fill	-25.0	2.2
	Burrow fill	-29.5	1.5
	Burrow fill	-32.6	2.1
	Glendonite	-28.5	1.0
	Glendonite	-17.1	0.6
	Glendonite	-21.7	-1.0

Notes to Chapter 3

Aharon, P., 1994. Geology and biology of modern and ancient hydrocarbon seep vents: An introduction. Geo-Marine Letters, 14: 69-73.

Aharon, P., Schwarz, H.P. and Roberts, H., 1997. Radiometric dating of submarine hydrocarbon seeps in the Gulf of Mexico. GSA Bulletin, 109(5): 568-579.

Aharon, P. and Sen Gupta, B.K., 1994. Bathymetric reconstructions of the Miocene-age "calcari a Lucina" (Northern Apennines, Italy) from oxygen isotopes and benthic foraminifera. Geo-Marine Letters, 14: 219-230.

Akimoto, K., Tanaka, T., Hattori, M. and Hotta, H., 1994. Recent benthic foraminiferal assemblages from the cold seep communities - A contribution to the methane gas indicator. In: R. Tsuchi (Editor), Pacific Neogene Events in Time and Space. University of Tokyo Press, Tokyo, pp. 11 - 25.

Armentrout, J.M., 1981. Correlation and ages of Cenozoic chronostratigraphic units in Oregon and Washington. Geological Society of America Special Paper, 184: 137-148.

Armentrout, J.M. and Suek, D.H., 1985. Hydrocarbon exploration in western Oregon and Washington. American Association of Petroleum Geologists Bulletin, 69: 627-643.

Barnes, P.M. et al., 2009 online. Tectonic and Geological Framework for Gas Hydrates and Cold Seeps on the Hikurangi Subduction Margin, New Zealand. Marine Geology.

Beikman, H.M., Rau, W.W., Wagner, H.C., 1967. The Lincoln Creek Formation, Grays Harbor Basin, southwestern Washington. United States Geological Survey Bulletin, 1244-1: 11-114.

Bernhard, J.M., 2003. Potential symbionts in bathyal foraminifera. Science, 299: 861.

Bernhard, J.M. and Bowser, S.S., 1999. Benthic foraminifera of dysoxic sediments: chloroplast sequestration and functional morphology. Earth-Science Reviews, 46(1-4): 149-165.

Bernhard, J.M. and Bowser, S.S., 2008. Peroxisome proliferation in foraminifera inhabiting the chemocline:An adaptation to reactive oxygen species exposure? Journal of Eukaryotic Microbiology, 55: 135-144.

Bernhard, J.M., Buck, K.R. and Barry, J.P., 2001. Monterey Bay cold-seep biota: Assemblages, abundance, and ultrastructure of living foraminifera. Deep-Sea Research Part I-Oceanographic Research Papers, 48: 2233-2249.

Bernhard, J.M. and Reimers, C.E., 1991. Benthic foraminiferal population fluctuations related to anoxia: Santa Barbara Basin. Biogeochemistry: 127-149.

Bohrmann, G., Greinert, J., Suess, E. and Torres, M., 1998. Authigenic carbonates from the Cascadia subduction zone and their relation to gas hydrate stability. Geology, 26(7): 647-650.

Brandon, M., Roden-Tice, M. and Garver, J., 1998. Late Cenozoic exhumation of the Cascadia accretionary wedge in the Olympic Mountains, northwest Washington State. GSA Bulletin, 110(8): 985-1009.

Brown, R.D., Gower, H.D., 1958. Twin River Formation (Redefinition), Northern Olympic Peninsula, Washington. American Association of Petroleum Geologists Bulletin, 42: 2491-2512.

Budai, J.M., Martin, A.M., Walter, L.M. and Ku, T.C.W., 2002. Fracture-fill calcite as a record of microbial methanogenesis and fluid migration: a case study from the Devonian Antrim Shale, Michigan Basin. Geofluids, 2: 163-183.

Burns, C., Campbell, K.A. and Mooi, R., 2005. Exceptional crinoid occurrences and associated cargonates of the Keasey Formation (lower Oligocene) at Mist, Oregon.

Campbell, 1992. Recognition of a Mio-Pliocene cold seep setting from the Northeast Pacific convergent margin, Washington, U.S.A. Palaios, 7: 422-433.

Campbell, K.A., 2006. Hydrocarbon seep and hydrothermal vent palaeoenvironments and palaeontology: Past developments and future research directions . Palaeogeography, Palaeoclimatology, Palaeoecology, 232(2-4): 362-407.

Campbell, K.A., Bottjer, D.J., 1993. Fossil cold seeps (Jurassic–Pliocene) along the convergent margin of western North America. National Geographic Research and Exploration 9, 326–343.

Campbell, K.A. and Nesbitt, E.A., 2000. High resolution architecture and paleoecoloty of an active margin, storm-flood influenced estuary, Quinault Formation (Pliocene), Washington. Palaios, 15: 553-579.

Claypool, G.E. and Kaplan, I.R., 1974. The origin and distribution of methane in marine sediments. In: I.R.c. Kaplan (Editor), Natural Gases in Marine Sediments. Plenum, New York, pp. 99-139.

Claypool, G.E. et al., 2006. Microbial methane generation and gas transport in shallow sediments of an accretionary complex, southern Hydrate Ridge (ODP Leg 204), offshore Oregon, U.S.A. In: A.M. Trehu, G. Bohrmann, M. Torres and F.S. Colwell (Editors), Proceedings of the Ocean Drilling Program, Scientific Results, pp. 1-52.

Erbacher, J. and Nelskamp, S., 2006. Comparison of benthic foraminifera inside and outside a sulphur-oxidizing bacterial mat from the oxygen-minimum zone off Pakistan (NE Arabian Sea). Deep-Sea Research I, 53: 751-775.

Faure, K. et al., 2006. Methane seepage and its relation to slumping and gas hydrate at the Hikurangi margin, New Zealand. New Zealand Journal of Geology and Geophysics, 49: 503-516.

Formolo, M.J., Lyons, T.W., Zhang, C., Kelley, C., Sassen, R., Horita, J., Cole, D., 2004. Quantifying carbon sources in the formation of authigenic carbonates at gas hydrate sites in the Gulf of Mexico. Chemical Geology, 205: 2530264.

Fulmer, C.V. 1975. Stratigraphy and paleontology of the type Blakeley and Blakely Harbor formations. In Weaver, D.V. (ed.) Future Energy horizons of the Pacific Coast. Association of American Petroleum Geologists, Pacific Section, Bakersfield California pp. 210-271.

Garver, J.I. and Brandon, M.T. 1994. Erosional denudation of the British Columbia Coast Ranges as determined by fission–track ages of the detrital zircon from the Tofino basin , Olympic Peninsula, Washington. Geological Society of America Bulletin 106: 1398-1412.

Goedert, J.L., Squires, R., 1990. Eocene deep-sea communities in localized limestones formed by subduction-related methane seeps, southwestern Washington. Geology, 18: 1182-1185

Goedert, J.L., Peckmann, J., Reitner, J., 2000. Worm tubes in an allocthonous cold-seep carbonate from lower Oligocene rocks of Western Washington. Journal of Paleontology, 74: 992-999.

Goedert, J.L., Thiel, V., Schmale, O., Rau, W.W., Michaelis, W., Peckmann, J., 2003 Late Eocene "Whiskey Creek" methane seep deposits (western Washington State) – Part I: Geology, Paleontology, and Molecular Geobiology. Facies, 48: 223-240.

Goldfinger, C., Kulm, L.D., Yeats, R.S., McNeill, L. and Hummon, C., 1997. Oblique strike-slip faulting of the central Cascadia submarine forearc. Journal of Geophysical Research, 102(B4): 8217-8243.

Greinert, J., Bohrmann, G. and Suess, E., 2001. Gas hydrate-associated carbonates and methane-venting at Hydrate Ridge: classification, distribution, and origin of authigenic lithologies. In: C.K. Paull and W. Dillon (Editors), Natural Gas Hydrates: Occurrence, Distribution, and Detection. American Geophysical Union, Washington, D.C., pp. 99-113.

Hammond, P.E., 1998. Tertiary andesitic lava-flow complexes (stratovolcanoes) in the southern Cascade range of Washington - observations on tectonic processes within the Cascade arc. Washington Geology, 26(1): 20-30.

Haeussler, P.J., Bradley, D.C., Wells, R.E. and Miller, M.L., 2003. Life and death of the Resurrection plate: Evidence for its existence and subduction in the northeastern Pacific in Paleocene-Eocene time. GSA Bulletin, 115(7): 867-880.

Hickman, C.S., 1980. Paleogene marine gastropods of the Keasey Formation in Oregon. Bulletins of American Paleontology, 78: 1-112.

Hill, T.M., Kennett J.P. and Spero, H.J., 2003. Foraminifera as indicators of methane-rich environments: A study of modern methane seeps in Santa Barbara Channel, California. Marine Micropaleontology, 49: 123-138.

Hill, T.M., Kennett, J.P., Valentine, D.L., 2004. Isotopic evidence for the incorporation of methane-derived carbon into foraminifera from modern methane seeps, Hydrate Ridge. Geochimica et Cosmochimica Acta, 68: 4619-4627.

Hyndman, R.D., Spence, G.D., Yuan, T. and Davis, E.E., 1994. Regional geophysics and structural framework of the Vancouver Island margin accretionary prism. Proceedings of the Ocean Drilling Program, Initial Reports 146, 399-419.

Ingle, J.C., Jr., 1967. Foraminiferal biofacies of Mio-Plio of Southern California. Bull. Am. Paleo 52, 52(236).

Irving, A.J., Nesbitt, E.A., Renne, P.R., 1996. Age constraints on earliest Cascade volcanism and Eocene marine biozones from a feldspar-rich tuff in the Cowlitz Formation southwestern Washington. EOS Transactions American Geophysical Union, 77: F814.

Kulm, L.D. and Suess, E., 1990. Relationship between carbonate deposits and fluid venting: Oregon accretionary prism. Journal of Geophysical Research, 95(B6): 8899-8915.

Kvenvolden, K.A., 1999. Potential effects of gas hydrate on human welfare. National Academy of Science Proceedings, 96: 3420-3426.

Levin, L.A., 2005. Ecology of cold seep sediments: Interactions of fauna with flow, chemistry, and microbes. Oceanography and Marine Biology, an Annual Review, 43: 1-46.

Mackensen, A., Wollenburg, J. and Licari, l., 2006. Low δ13C in tests of live epibenthic and endobenthic foraminifera at a site of active methane seepage. Paleoceanography, 21: PA2022, doi:10.1029/2005PA001196,2006.

Madsen, J.K., Thorkelson, D.J. and Marshall, D.D., 2006. Cenozoic to Recent plate configuration on the Pacific Basin: ridge subduction and fracture fill window magnetism in western North America. Geosphere, 2: 11-34.

Martin, R.A. and Nesbitt, E.A., 2004. Benthic foraminiferal characteristics of a diffuse Pliocene mid-shelf hydrocarbon seep, Cascadia convergent margin, Geological Society of America, Denver, pp. 59.

Martin, R.A., Nesbitt, E.A. and Campbell, K.A., 2007. Carbon stable isotopic composition of benthic foraminifera from Pliocene cold methane seeps, Cascadia accretionary margin. Palaeogeography, Palaeoclimatology, Palaeoecology, 246: 260-277.

Milkov, A.V. et al., 2003. In situ methane concentrations at Hydrate Ridge, offshore Oregon: New constraints on the global gas hydrate inventory from an active margin. Geological Society of America Bulletin, 31(10): 833-836.

Naehr, T.H. et al., 2007. Authigenic carbonate formation at hydrocarbon seeps in continental margins. Deep-Sea Research II, 54: 1268-1291.

Naehr, T.H. et al., 1998. Authigenic carbonates from the Cascadia subduction zone and their relation to gas hydrate stability. Geology, 26(7): 647 - 650.

Nesbitt, E. A., 2003, Changes in shallow-marine faunas from the northeastern Pacific margin across the Eocene/Oligocene boundary, *in* Prothero, D.R. et al., eds., From Greenhouse to Icehouse: the Eocene- Oligocene transition: Columbia University Press, p. 57–70.

Nesbitt, E.A., Campbell, K.A., Goedert, J.L. , 1994. Paleogene cold seeps and macroinvertebrate fauna in a forearc sequence of Oregon and Washington. In: Swanson, D.A. and Haugerud, R.A. (eds.), Geological Field Trips in the Pacific Northwest. Geological Society of America Field Guides.

Nesbitt, E.A., Martin, R.A., Carroll, N. and Grieff, J., in revision. Reassessment of the Zemorrian foraminiferal Stage and Juanian molluscan Stage north of the Olympic Mountains, Washington State and Vancouver Island. Canadian Journal of Earth Sciences.

Orange, D.L., Geddes, D.S. and Moore, J.C., 1993. Structural and fluid evolution of a young accretionary complex: The Hoh rock assemblage of the western Olympic Peninsula, Washington. Geological Society of America Bulletin, 105: 1053-1075.

Orphan, V.J. et al., 2004. Geological, geochemical, and microbiological heterogeneity of the seafloor around methane vents in the Eel River Basin, offshore California. Chemical Geology, 205: 265-289.

Paull, C.K., Juli, A.J.T., Toolin, L.J. and Linick, T., 1985. Stable isotope evidence for chemosynthesis in an abyssal seep community. Nature, 317: 709-711.

Paull, C.K. et al., 2000. Isotopic composition of CH4, CO2 species, and sedimentary organic matter within samples from the Blake Ridge: Gas source implications. In: C.K. Paull, R.

Matsumoto, P.J. Wallace and W.P. Dillon (Editors), Proceedings of the Ocean Drilling Program, pp. 67-78.

Peckmann, J., Goedert, J.L., Thiel, V., Michaelis, W. and Reitners, J., 2002. A comprehensive approach to the study of methane-seep deposits from the Lincoln Creek Formation, western Washington State, U.S.A. Sedimentology, 49: 855-873.

Prothero, D.R. and Armentrout, J.M., 1985. Magnetostratigraphic sorrelation of the Lincoln Creek Formation, Washington: Implications for the age of the Eocene/Oligocene boundary. Geology, 13(3): 208-211.

Prothero, D.R. and Hankins, K.G., 2000. Magnetic stratigraphy and tectonic rotation of the Eocene-Oligocene Keasey Formation, northwest Oregon. Journal of Geophysical Research, 105(87): 16,473-16,480.

Prothero, D.R. and Nesbitt, E.A, 2008. Paleomagnetism and tectonic rotation of the Restoration Point Member of the Blakeley Formation (Type Blakeley Stage), Bainbridge Island Washington and the Pacific Coast Oligocene-Miocene boundary. In Lucas, S. (ed.) Neogene mammals. New Mexico Museum of Natural History and Science Bulletin, 44: 315-322.

Rathburn, A.E., Levin, L.A., Held, Z. and Lohmann, K.C., 2000. Benthic foraminifera associated with cold methane seeps on the northern California margin: Ecology and stable isotopic composition. Marine Micropaleontology, 38: 247-266.

Rathburn, A.E. et al., 2003. Relationships between the distribution and stable isotopic composition of living benthic foraminifera and cold methane seep biogeochemistry in Monterey Bay, California. Geochemistry, Geophysics, Geosystems, 4(12): 1106, doi:10.1029/2003GC000595, 2003.

Rau, W.W., 1966. Stratigraphy and Foraminifera of the Satsop River Area, southern Olympic Peninsula, Washington. State of Washington Division of Mines Geological Bulletin, 53: 66 pp.

Rau, W.W., 1970. Foraminifera, stratigraphy, and paleocology of the Quinault Formation, Point Grenville-Raft River coastal area, Washington. Washington Department of Natural Resources Division of Mines and Geology Bulletin, 62: 41.

Rau, W.W., 1981. Pacific Northwest Tertiary benthic foraminiferal biostratigraphic framework, an overview. Geological Society of America Special Paper 184: 67 – 84.

Robinson, C.A., Bernhard, J.M., Levin, L.A., Mendoza, G.F. and Blanks, J., 2004. Surficial hydrocarbon seep infauna from the Blake Ridge (Atlantic Ocean, 2150 m) and the Gulf of Mexico (690-2240 m). P.S.N.Z.: Marine Ecology, 25(4): 313-336.

Sahling, H., Rickert, D., Lee, R.W., Linke, P. and Suess, E., 2002. Macrofaunal community structure and sulfide flux at gas hydrate deposits from the Cascadia convergent margin, NE Pacific. Marine Ecology Progress Series, 231: 121-138.

Sassen, R. et al., 2004. Free hydrocarbon gas, gas hydrate, and authigenic minerals in chemosynthetic communities of the northern Gulf of Mexico continental slope: relation to microbial processes. Chemical Geology, 205: 195-17.

Sen Gupta, B.K. and Aharon, P., 1994. Benthic foraminifera of bathyal hydrocarbon vents of the Gulf of Mexico: Initial report on communities and stable isotopes. Geo-Marine Letters, 14: 88-96.

Sen Gupta, B.K., Platon, E., Bernhard, J.M. and Aharon, P., 1997. Foraminiferal colonization of hydrocarbon-seep bacterial mats and underlying sediment, Gulf of Mexico slope. Journal of Foraminiferal Research, 27(4): 292-300.

Sibuet, M. and Olu, K., 1998. Biogeography, biodiversity and fluid dependence of deep-sea cold-seep communities at active and passive margins. Deep-Sea Research II, 45: 517-567.

Sommer, S. et al., 2006. Efficiency of the benthic filter: Biological control of the emission of dissolved methane from sediments containing shallow gas hydrates at Hydrate Ridge. Global Biogeochemical Cycles, 20(GB2019): doi:10.1029/2004GB002389.2006.

Stewart, R.L. and Brandon, M.T., 2004. Detrital fission track ages for the "Hoh Formation": implications for late Cenozoic evolution of the Cascadia subduction wedge. Geological Society of America Bulletin, 116: 60-75.

Suess, E. et al., 1985. Biological communities at vent sites along the subduction zone off Oregon. In: M.L. Jones (Editor), The hydrothermal vents of the eastern Pacific: An Overview. Biological Society of Washington Bulletin, pp. 475-484.

Teichert, B.M.A., Bohrmann, G. and Suess, E., 2005. Chemoherms on Hydrate Ridge - Unique microbially-mediated carbonate build-ups growing into the water column. Paleogeography, Paleoclimatology, Paleoecology, 227: 67-85.

Tomaru, H., Lu, Z., Fehn, U., Muramatsu, Y. and Matsumoto, R., 2007. Age variation of pore water iodine in the eastern Nankai Trough, Japan: Evidence for different methane sources in a large gas hydrate field. Geology, 35: 1015-1018.

Torres, M. et al., Submitted. Methane feeding cold seeps on the shelf and upper continental slope off Central Oregon, USA.

Torres, M.E. and Kastner, M., 2009. Data report: clues about carbon cycling in methane-bearing sediments using stable isotopes of the dissolved inorganic carbon. Proceedings of the Integrated Ocean Drilling Program, 311.

Torres, M.E., McManus, J., Hammond, D.E., deAngelis, M.A., Heeschen, K.U., Colbert, S.L., Tryon, M.D., Brown, K.M., Suess, E., 2002. Fluid and chemical fluxes in and out of sediments hosting methane hydrate deposits on Hydrate ridge, OR, I: Hydrological provinces. Earth and Planetary Science Letters, 201: 525-540.

Treude, T., Boetius, A., Knittel, K., Wallmann, K. and Jorgensen, B.B., 2003. Anaerobic oxidation of methane above gas hydrates at Hydrate Ridge, N.E. Pacific Ocean. Marine Ecology Progress Series, 264: 1-14.

Tryon, M.D. and Brown, K., 2001. Complex flow patterns through Hydrate Ridge and their impact on seep biota. Geophysical Research Letters, 28(14): 2863-2866.

Tryon, M.D., Brown, K.M. and Torres, M.E., 2002. Fluid and chemical flux in and out of sediments hosting methane hydrate deposits on Hydrate Ridge, OR, II: Hydrological processes. Earth and Planetary Science Letters, 201: 541-557.

Tunnicliffe, V., 1992. The nature and origin of the modern hydrothermal vent fauna. Palaios, 7: 338-350.

Weaver, C.E. 1937. Tertiary stratigraphy of western Washington and northwestern Oregon. University of Washington Publication in Geology 4:1-266

Wells, R.E., Weaver, C.S. and Blakely, R.J., 1998. Fore-arc migration in Cascadia and its neotectonic significance. Geology, 26(8): 759-762.

Whiticar, M.J., 1999. Carbon and hydrogen isotope systematics of bacterial formation and oxidation of methane. Chemical Geology, 161: 291-314.

Zachos, J., Pagani, M., Sloan, L., Thomas, E. and Billups, K., 2001. Trends, rhythms, and aberrations in global climate 65 ma to present. Science, 292: 686-693.

Chapter 4. The Effects Of Anaerobic Methane Oxidation On Benthic Foraminiferal Assemblages And Stable Isotopes On The Hikurangi Margin Of Eastern New Zealand.

Summary

A study of benthic foraminiferal assemblages from cold hydrocarbon seeps of the Hikurangi Margin, New Zealand, was undertaken during RV SONNE cruise SO191-3 to establish what effects, if any, methane-influenced porewaters had on the foraminiferal assemblages and the carbon isotopes of their tests. The results of this study indicate that Hikurangi Margin foraminiferal assemblages are consistent with modern and fossil seeps worldwide. Foraminiferal distribution, species richness, density and diversity were little different between seep and non-seep sites, though there were noteworthy exceptions. The non-seep reference core samples were greatly enriched in agglutinate species, which constituted 45% of the total assemblage of that core. By contrast, seep sites contained a maximum of 11% agglutinate foraminifera. Seep and non-seep sites were not separated by density or diversity, except for the single site beneath a bacterial mat that exhibited the lowest density and diversity of all sites. Assemblages at all sites were dominated by *Uvigerina peregrina*, a species known to inhabit fossil and modern seeps elsewhere, but that also is well documented from normal marine environments. Carbon isotope data significantly differentiates seep and non-seep sites through the greater ^{13}C depletion and heterogeneity of $\delta^{13}C$ values in seep foraminifera. $\delta^{13}C$ values for *U. peregrina* were as low as –15.2‰ PDB. In addition, specimens of *Pyrgo depressa* and *Hoeglundina elegans* exhibited minimum $\delta^{13}C$ values of –29.8‰ and –35.7‰ PDB respectively, showing the influence of carbon that was derived from sulphate dependent anaerobic oxidation of methane. Authigenic carbonates and vesicomyid bivalve shells from seep Station 198 also recorded depleted $\delta^{13}C$ values, with the lightest values (–55.4‰ PDB) clearly within the range of biogenic methane sources.

1. Introduction

Cold hydrocarbon seeps are receiving a great deal of international attention for a number of reasons. The extreme high sulphide, low oxygen environments of cold seeps support luxurious and unique ecosystems that yield valuable insights into physiological adaptations in these environments and possibly the beginnings of life on Earth (Sassen and MacDonald, 1998; Levin, 2005). The gas hydrates that commonly underlie cold seeps are implicated as initiating submarine slope instability as they form and dissociate, resulting in slumping, landslides, or frost-heave effects (Paull et al., 1996; Maslin et al., 1998). In addition, dissociation of methane hydrates on a global scale has been suggested as a possible cause of sudden climate change (Kennett et al., 2003; Hill et al., 2004). Finally, cold hydrocarbon seeps are of interest in the search for commercially viable and environmentally sustainable energy sources.

The study reported investigated the effects of methane influenced pore waters on benthic foraminifera of the Hikurangi Margin, offshore eastern North Island, New Zealand. Specifically, the study tested for discernible imprints on the foraminiferal assemblage and on mineralization of foraminiferal tests.

1.1 Geologic setting

The Hikurangi Margin is the southernmost section of the 3000 km long Tonga-Kermadec-Hikurangi subduction system where the Pacific plate is subducting beneath the Australian plate (Figure 4.1). A plate boundary has existed here from ~40 Ma; however subduction only began ~21 Ma with a change from transtensional motion to convergence (Lewis and Pettinga, 1993; Faure et al., 2006). Convergence on this margin is strongly oblique, with anti-clockwise rotation up to 60°. At its southern end, the system ends with the intracontinental Alpine Fault and a mirror-image, west-facing subduction system in southern New Zealand (Lewis and Pettinga, 1993). Motion on this system varies greatly, from 100 mm/y in the Tonga-Kermadec section, to 40 mm/y in the northern part of the Hikurangi

Margin, and 20 mm/y at the southern end. Large volumes of sediment derived from high mountains to the south and transported by channeled density currents have resulted in an anomalously thick (~3 km) accretionary wedge that is intricately deformed.

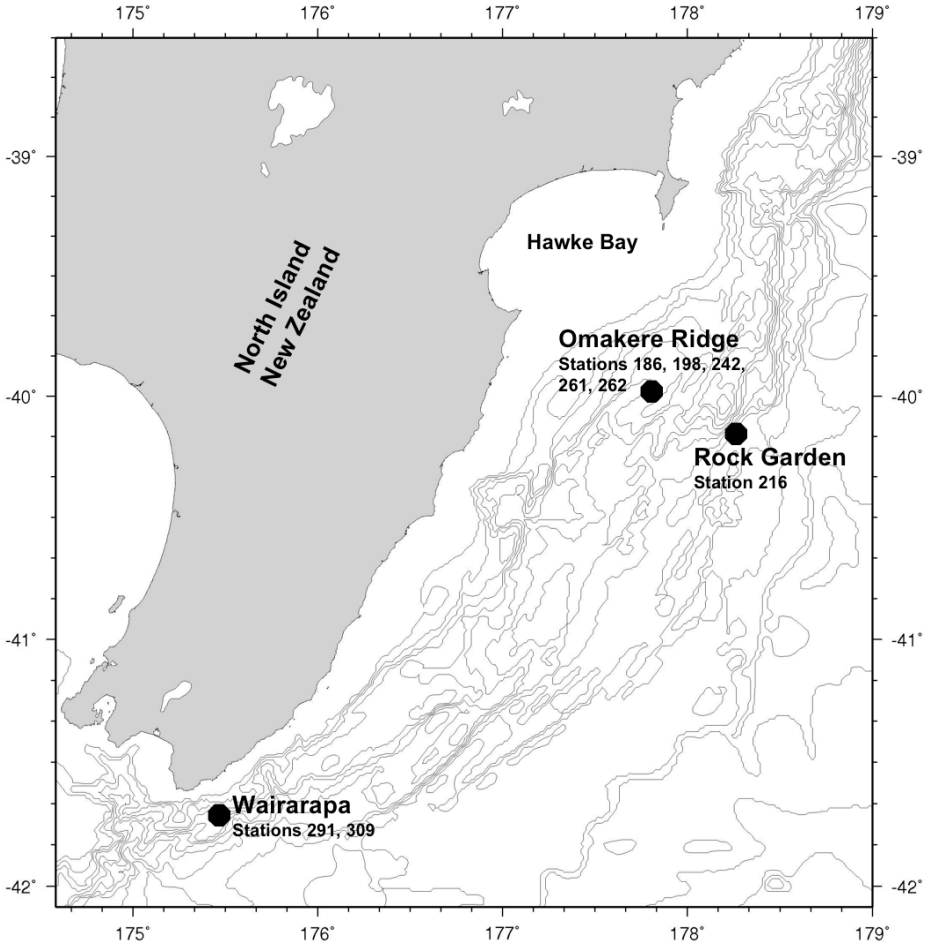

Figure 4.1. Location of sampling areas used in this study.

Methane seepage on the Hikurangi Margin was first recognized in 1994 when fishermen dredged a *Bathymodiolus*–like mussel associated with a piece of carbonate chimney and observed a sonar plume in the water column (Lewis and Marshall, 1996). Subsequently, dredging recovered carbonates with attached chemoautotrophic fauna, including the bivalve *Calyptogena.* In addition, a prominent Bottom Simulating Reflector (BSR) implied the presence of gas

hydrates in the sediments (Faure et al., 2006). All seep sites so far identified on the Hikurangi Margin are developed on the crests of thrust ridges, and are underlain by thrust faults that act as conduits for fluids (Barnes et al., this volume). In addition, beneath each site lie conspicuous breaks in the BSR, indicating discontinuous gas hydrate formation with accompanying fault/fracture development allowing migration of fluids (Barnes et al., this volume). The Rock Garden site (40º01.98'S, 178º09.65'E) differs from the other sites because it occurs directly above a subducting seamount, resulting in anomalous bathymetric elevation (Barnes, et al., this volume).

1.2 Foraminifera in methane seeps

Foraminifera in modern cold seeps have been studied at locations on tectonically active and passive margins, including Blake Ridge, Atlantic Ocean (Robinson et al., 2004; Panieri and Sen Gupta, 2008); Gulf of Mexico (Sen Gupta and Aharon, 1994; Sen Gupta et al., 1997; Robinson et al., 2004); the North Sea (Jones, 1993); coastal California (Bernhard et al., 2001); Hydrate Ridge, eastern Pacific (Torres et al., 2003; Heinz et al., 2005); the Rockall Trough, the Irish Sea (Panieri, 2005); Japan (Akimoto et al., 1994); and the Barents Sea (Mackensen et al., 2006). Foraminfera from Cenozoic seeps have been investigated from the Miocene of Italy (Barbieri and Panieri, 2004) and the Eocene through Pliocene of the Cascadia Margin of the eastern Pacific (Martin and Nesbitt, 2005; Martin et al., 2007). All of these studies found that, unlike seep invertebrate fauna, there are no foraminiferal species that are endemic to seeps. In addition, foraminiferal densities and diversity in modern seeps do not show consistent trends. In some cases, density was low relative to comparable non-seep sites (Sen Gupta et al., 1997; Bernhard et al., 2001). In others densities were similar in seep and non-seep samples (Rathburn et al., 2003); whereas Wiedicke and Weiss (2006) found densities enhanced in seepage areas. In two studies, statistical analyses resulted in the identification of diagnostic seep assemblages (Akimoto et al., 1994; Panieri, 2005).

Seep foraminifera respond to the presence of methane in pore waters by recording a depleted and variable $\delta^{13}C$ signal in their calcite tests (Hill et al., 2003;

Rathburn et al., 2003; Hill et al., 2004). In non-seep sediments, the $\delta^{13}C$ value of foraminiferal tests varies within a narrow range: for example, in non-seep specimens of *Uvigerina peregrina,* $\delta^{13}C$ is typically between 0.2‰ to 0.4‰ PDB (Rathburn et al., 2003). In foraminifera from modern seeps, however, $\delta^{13}C$ values are considerably more variable. Single species bulk samples from Santa Barbara Channel seeps recorded $\Delta^{13}C$ ($= \delta^{13}C_{max} - \delta^{13}C_{min}$) between species ranging from –0.9‰ to –20.1‰ PDB (Hill et al., 2003). Single–individual analyses of foraminifera indicate that the isotopic variation is large even within a single species. For instance, from seeps in the Santa Barbara Channel, *Cibicides mckannai* varied between –0.37‰ and –2.28‰ PDB, and *Pyrgo* sp. recorded values between –0.01‰ and –25.23‰ PDB (Hill et al., 2003). Thus, foraminiferal carbonate is capable of recording excursions of depleted ^{13}C in ambient seawater and interstitial waters.

Complicating the interpretation of data from cold seep foraminifera is the mobility of these organisms. Most foraminifera are motile, capable of moving to new microhabitats within the sediment in response to environmental changes. The stimulus for foraminiferal migration is not clear. Linke and Lutze (1993) attributed it to food acquisition, while others (Moodley et al., 1998; Geslin et al., 2004) concluded movement was due to varying oxygen availability. Despite their mobility, foraminifera are generally categorized as epifaunal or infaunal based on the depth within the sediment at which they are most often reported alive (Corliss, 1985; Rathburn and Corliss, 1994; McCorkle et al., 1997). Analysis of data from cold seeps must, however, include cognizance of environmental factors other than methane seepage that might influence the isotopic results.

2. Methods

Sediment samples used in this study were retrieved during Leg 3 of RV *SONNE* cruise 191 (SO191-3) in February and March, 2007 using a TV-guided multicorer. Sample sites (Figure 4.1) were identified by the presence of the vesicomyid bivalve *Calyptogena* spp, “raindrop” texture due to ampharetid worm

burrows (Sommer et al., this volume) or active bubbles (Table 1). The samples represent the northern and southern ends of the Hikurangi Margin. From the northern end of the margin, one sample was taken from the LM3 seep (Station 216) in the Rock Garden area. From Omakere Ridge, two samples were recovered from the Kaka seep (Stations 242 and 261), and two from the Bear's Paw seep (Stations 186 and 198). Two additional samples were obtained from the southern Wairarapa area, one from the North Tower seep (Station 291) and one from Takahae (Station 309). A non-seep reference core was collected from near the Kaka 2 seep (Station 262) and was identified using surficial features, particularly bioturbation and lack of seep-specific biota and bubbles. All cores were sub-sampled at 0.5 cm intervals in the top five centimetres. Samples were preserved in 10% formalin with 1g/L Rose Bengal added to stain living or recently dead individuals. Subsequently, samples were washed through a 63mm sieve, air-dried and picked. Specimens used for isotope analyses were cleaned of organic material by soaking in a 15% hydrogen peroxide solution for 20 minutes, then rinsing and sonicating with methanol, and finally rinsing and sonicating in DI water. In addition to foraminifera, a number of small pieces of carbonate slab, one carbonate nodule, and some *Calyptogena* sp. shells were recovered from Station 198 (Bear's Paw). One of these shells stained brightly in Rose Bengal, indicating it still contained cytoplasm when collected. The inorganic carbonates and stained and unstained shells also were analyzed for isotopes. Prior to analysis, shells were cleaned to eliminate organic material.

Table 4.1. Station numbers, names, depths and locations of samples used in this study, with visual indicators of methane seepage noted for each core site. Note: "raindrop texture" refers to dense beds of ampharetid polychaetes as described in Sommer et al., this volume.

Station number	Multicore number	Seep name	Region	Depth (m)	Latitude (S)	Longitude (E)	Seep identifiers	Core characteristics
186	19	Bear's Paw 1	Omakere Ridge	1078	40:3.18	177:49.20	Shell debris, carbonates, tube worm, patches of bacterial mat	Top 0.5 cm white, frothy mixed with black sulphidic layer. Black lenses throughout core. Sulphide odor.
198	22	Bear's Paw 2	Omakere Ridge	1105	40:03.19	177:49.17	Shell bed at edge of carbonates, tube worms, bubbling	Lengthy outgassing when cores on deck. Many polychaetes, black sulphidic layer at top of core. Strong sulphide odor.
216	28	LM3	Rock Garden	662	40:01.98	178:09.65	Shell debris, carbonate hardground	Core homogeneous. Few very small black lenses.
242	34	Kaka 1	Omakere Ridge	1175	40:02.14	177:47.91	Raindrop texture	Top 0.5 cm dark, sulphidic. Then at 5 cm, ~4 cm thick black sulphidic layer. Sulphide odor.
261	38	Kaka 2	Omakere Ridge	1171	40:02.12	177:47.96	Pogonophorans, shell debris, bubbles, raindrop texture	Top 0.5 cm dark, sulphidic. Outgassing at surface. Sulphide odor.
262	39	Reference	Omkere Ridge	1167	40:02.15	177:47.95	Bioturbated, no seep biota, carbonates	Core homogeneous throughout.
291	44	North Tower	Wairarapa	1061	41:46.93	175:24.16	Bubbles, sulphidic	Small, "fluffy" white patches – bacteria? Occasional black sulphidic lenses. Sulphide odor.
309	46	Takahae	Wairarapa	1054	41:46.35	175:25.69	Extensive bacterial mat, raindrop texture, bubbles	Core nearly black. Many fluffy white patches – bacteria? Strong sulphidic odor.

Isotope analyses were conducted at the Stanford University Stable Isotope Laboratory on a Finnegan Kiel III carbonate device interfaced with an MAT 252 IRMS, and at the University of Washington Department of Earth and Space Sciences Isotope Laboratory on a ThermoScientific Kiel III carbonate device attached to a ThermoFinnigan DeltaPlus IRMS. At the Stanford Isotope Lab, precision, based on multiple analyses of the NBS 19 standard was 0.05‰ for $\delta^{18}O$ and 0.03‰ for $\delta^{13}C$. At the University of Washington Isotope Lab, also based on multiple analyses of standards, precison is 0.06‰ for $\Box^{18}O$ and 0.03‰ for $\Box^{13}C$. Results are reported in delta notation ($\delta^{18}O$ and $\delta^{13}C$) relative to the PDB standard, where $\delta = (R_{sample}/R_{standard} - 1)\ 1000$. The difference between maximum and minimum isotopic values ($\delta^{13}C_{max} - \delta^{13}C_{min}$) is designated by $\Box^{13}C$. To test for post–depositional alteration, representative individual specimens from each sample were examined using SEM imaging.

The Shannon diversity index (H') and Simpson's index (λ) were used as measures of the diversity of seep and non-seep foraminiferal assemblages (see Buzas, 1979). Both of these indices take into account the richness and evenness of the species assemblage. The Simpson index, however, is more sensitive to evenness in the assemblage while the Shannon index is more influenced by richness; thus, the two complement each other (DeJong, 1975). In addition to diversity indices, foraminiferal density was calculated by dividing the number of foraminifera per sample by the volume of sediment picked, providing a measure of abundance.

3. Results

3.1 Foraminiferal assemblage

Eighty-two species of benthic foraminifera (stained and unstained) were recovered from the material studied. The distribution of species in the samples is shown in Table 4.2. Sixteen species occurred at all sites, and all assemblages were dominated by *Uvigerina peregrina,* which constituted between 8% and 36% of the assemblage in each core (Figure 4.2).

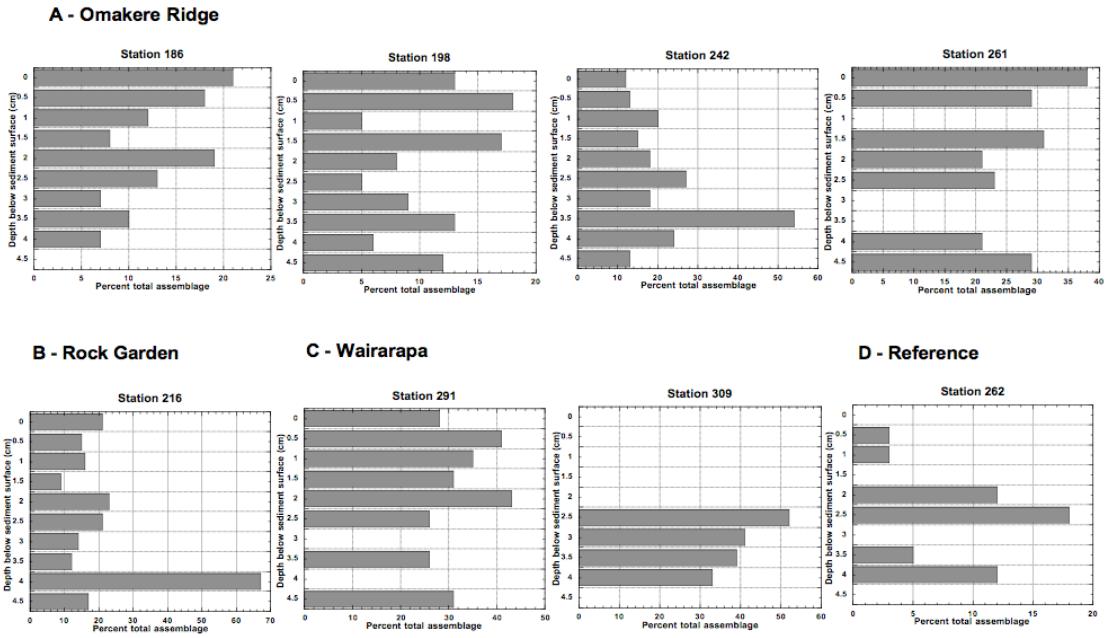

Figure 4.2. The abundance distribution of *Uvigerina peregrina* expressed as the percent of the assemblage in each core depth interval. This species is infaunal and typically reaches peak abundance from 2 to 4 cm below the sediment surface.

Bolivina quadrilatera comprised 24% and 31% of the assemblages in the two Wairarapa cores, but was a minor constituent of the assemblages in the cores from Rock Garden and Omakere Ridge. *Cassidulina carinata*, although absent from Station 309 (Takahae), made up as much as 16% of the assemblages in the other sites. Two species, *Cibicides lobatulus* and *Laevidentalina subemaciata*, occurred only in the northern seeps; two others, *Cuneata arctica* and *Laticarinina altocamerata*, appeared only in the Omakere Ridge seeps. *Notorotalia zealandica* was present only at Station 291 (North Tower). All other species were distributed throughout the studied area.

Table 4.2. Taxonomic list of all benthic foraminifera from the Hikurangi Margin sampling stations and species density in each core, expressed as percent of total assemblage of each core.

Station	186	198	216	242	261	262	291	309
MUC number	19	22	28	34	38	39	44	46
Seep Name	Bear's Paw 1	Bear's Paw 2	LM3	Kaka 1	Kaka 2	Reference	North Tower	Takahae
Water depth (m)	1078	1105	662	1175	1171	1167	1061	1054
Total foraminifera picked	2078	1962	3154	2770	770	870	2154	134
Species								
Abditodendrix pseudothalmanni (Boltovskoy & Guissani de Kahn)	0.77	0.37	0.00	5.34	2.86	2.30	2.27	1.42
Ammobaculites sp.	0.00	0.00	0.00	0.00	0.00	2.76	0.00	0.00
Ammodiscus incertus d'Orbigny	0.39	0.00	0.00	0.14	0.00	7.36	0.09	0.00
Anomalinoides globulosus (Chapman & Parr)	0.00	0.18	0.13	0.00	0.00	0.00	0.00	0.00
Anomalinoides tasmanica (Parr)	0.87	1.01	2.22	0.94	1.04	2.99	0.38	0.00
Astrononion novozealandicum Cushman & Edwards	0.96	4.66	1.20	0.00	0.78	0.00	0.00	0.00
Bathysiphon filiformis M. Sars	0.10	0.00	0.00	0.29	0.52	4.14	0.00	0.00
Bathysiphon sp.	0.00	0.00	0.00	0.07	0.00	3.22	0.00	1.06
Bolivina cacozela Vella	0.19	0.18	0.00	0.00	0.00	0.00	0.09	0.00
Bolivina seminuda Cushman	0.67	0.91	0.13	0.36	1.04	0.23	5.58	0.00
Bolivina spathula (Williamson)	0.87	0.46	0.38	1.23	0.52	0.23	1.23	1.42
Bolivina subexcavata Cushman & Wickenden	0.10	0.09	0.06	0.00	0.00	0.00	0.00	0.00
Bolivinita quadrilatera (Schwager)	1.83	3.47	2.22	0.51	0.26	0.69	24.39	30.85
Bulimina aculeata d'Orbigny	0.39	1.46	9.83	5.27	10.13	2.53	3.50	2.48
Bulimina gibba Fornasini	2.31	2.10	1.27	2.31	2.86	1.84	0.47	0.00
Bulimina marginata d'Orbigny	1.64	3.20	12.81	1.44	2.34	2.07	0.95	1.06
Bulimina truncana Gumbel	1.73	2.38	0.32	2.45	3.12	1.61	0.57	0.71
Cassidulina carinata Silvestri	16.96	14.17	2.09	9.60	9.09	6.67	6.62	0.00

Table 4.2. (*continued)*

Station	186	198	216	242	261	262	291	309
Chilostomella cf *czizecki* Reuss	3.28	1.83	0.13	1.08	1.56	0.00	0.47	0.00
Cibicides dispars (d'Orbigny)	1.25	2.10	3.42	1.81	1.82	0.46	0.95	0.71
Cibicides lobatuus (Walker & Jacob)	0.00	0.27	0.25	0.22	0.26	0.69	0.00	0.00
Cibicides wuellerstorfi (Schwager)	0.29	0.09	3.68	0.00	0.00	0.23	0.00	0.00
Cribrostomoides jeffriesi (Williamson)	1.16	0.18	0.00	0.94	0.78	2.76	0.00	2.13
Cribrostomoides subglobosus (Cushman)	0.87	0.00	0.13	0.43	0.78	5.75	0.19	0.71
Cuneata arctica (Brady)	0.00	0.00	0.00	0.07	0.52	0.23	0.00	0.00
Discorbinella bertheloti (d'Orbigny)	0.39	0.00	0.38	0.29	0.52	0.23	0.09	0.00
Elphidium advenum cf limbatum (Chapman)	0.00	0.00	0.00	0.14	0.26	0.00	0.00	0.35
Fissurina claricurta McCulloch	0.39	0.27	0.25	0.14	0.78	0.23	0.66	0.00
Fissurina clathrata (Brady)	0.00	0.00	0.00	0.00	0.00	0.00	0.66	0.00
Fissurina marginata (Montagu)	1.16	1.55	0.51	1.08	1.30	0.23	0.38	1.06
Fissurina orbignyana Seguenza	0.00	0.09	0.06	0.22	1.56	0.00	0.19	0.00
Frondiculari sp.	0.39	0.09	0.06	0.07	0.26	0.00	0.09	0.00
Furssenkoina complanata (Egger)	2.50	2.74	0.13	1.01	1.56	0.69	4.63	1.77
Gavelinopsis praegeri (Heron-Allen & Earland)	3.47	7.13	0.76	4.40	3.38	1.38	1.51	1.42
Glandulina sp.	0.10	0.46	0.13	0.00	0.52	0.00	0.00	0.00
Globobulimina pacifica Cushman	2.70	0.91	1.27	2.38	6.49	1.38	0.38	0.71
Globocassidulina crassa (d'Orbigny)	1.16	0.91	1.71	1.37	0.00	0.69	0.47	1.06
Globocassidulina minuta (Cushman)	1.83	2.93	0.25	2.31	4.68	0.69	0.28	0.00

Table 4.2. (*continued)*

Station	186	198	216	242	261	262	291	309
Grigelis orectus Loeblich & Tappan	0.00	0.37	0.00	0.36	0.52	0.00	0.00	0.00
Gyroidinoides kawagatai Ujiie	3.66	3.47	1.20	2.02	4.68	0.00	0.00	0.00
Gyroidinoides soldanii *(d'Orbigny)*	1.45	3.93	2.79	1.01	3.12	1.84	0.00	1.06
Haplophragmoides canariensis (d'Orbigny)	1.25	0.18	0.00	0.14	0.52	1.61	0.09	0.35
Hoeglundina elegans (d'Orbigny)	1.16	2.93	0.89	0.72	1.30	0.69	0.09	0.00
Hormosina globulifera Brady	0.19	0.00	0.00	0.00	0.00	0.00	0.00	0.00
Laevidentalina bradyensis (Dervieux)	0.00	0.00	0.00	0.07	0.00	0.00	0.00	0.00
Laevidentalina subemaciata (Parr)	0.48	0.37	0.51	0.29	1.56	0.23	0.00	0.00
Lagena hispida Reuss	0.58	0.18	0.51	0.79	1.30	0.69	0.57	0.00
Lagena laevicostatiformis McCulloch	1.64	0.91	0.19	0.65	0.26	0.69	0.76	0.71
Lagena meridonalis (Wiesner)	0.10	0.09	0.00	0.00	0.26	0.00	0.00	0.00
Lagenosolenia cf *confossa* McCulloch	0.19	0.09	0.32	0.00	0.00	0.00	0.00	0.00
Laticarinina altocamerata (Heron-Allen & Earland)	0.29	0.46	0.00	0.22	0.78	0.69	0.00	0.00
Lenticulina australis Parr	0.67	2.01	3.42	0.58	3.12	0.46	0.19	0.00
Lenticulina erratica Hornibrook	0.29	0.37	0.63	0.65	0.52	0.46	0.38	0.00
Lenticulina subgibba Parr	0.19	0.09	0.00	0.00	0.00	0.00	0.00	0.35
Martinotiella communis (d'Orbigny)	0.00	0.00	0.44	0.00	0.00	0.00	0.00	0.00
Multifidella nodulosa Cushman	0.10	0.09	0.00	0.22	0.26	0.69	0.00	0.35
Neouvigerina proboscidea (Schwager)	1.54	0.82	2.73	1.88	1.30	0.92	2.65	0.00

Table 4.2. (*continued)*

Station	186	198	216	242	261	262	291	309
Nonionella auris (d'Orbigny)	2.02	1.10	0.19	1.81	0.52	0.23	0.28	0.71
Nonionella magnalingua Finlay	0.48	0.73	0.00	0.00	1.82	0.00	0.00	0.00
Notorotalia zelandica (Finlay)	0.00	0.00	0.00	0.00	0.00	0.00	1.80	0.00
Nouria polymorphinoides Heron-Allen & Earland	0.39	0.00	0.00	0.00	0.00	5.06	0.00	0.35
Oridorsalis umbonatus (Reuss)	2.60	3.38	2.54	4.48	3.90	4.83	2.84	4.26
Paratrochaminna challengeri Bronniman & Whitaker	1.64	0.09	0.00	0.43	0.26	5.52	0.00	0.35
Planulinoides cf. *norcotti* Hedley, Hurdle & Burdett	0.10	0.00	0.13	0.00	0.00	0.00	0.00	0.00
Pullenia bulloides (d'Orbigny)	2.70	2.83	5.96	2.67	8.05	1.84	0.09	0.00
Pullenia quinqueloba Reuss	3.28	2.93	1.46	3.68	7.01	2.53	0.00	0.35
Pullenia salisburyi Stewart & Stewart	1.93	1.55	0.82	0.00	1.04	0.00	0.00	0.00
Pyrgo anomala (Schlumberger)	0.00	0.18	0.00	0.00	0.00	0.00	0.00	0.00
Pyrgo depressa (d'Orbigny)	1.35	1.92	0.38	0.29	1.82	0.00	0.00	0.00
Quinqueloculina incisa Vella	0.58	0.82	0.19	0.07	0.00	0.00	0.00	1.06
Quinqueloculina suborbicularis d'Orbigny	0.00	0.18	0.00	0.00	0.00	0.00	0.00	0.00
Rhabdammina linearis Brady	0.19	0.00	0.00	0.22	0.00	1.38	0.00	0.00
Sigmoilopsis schlumbergeri Silvestri	0.39	0.18	1.65	0.94	0.52	1.84	0.19	1.06
Sigmoilopsis wanganuiensis Vella	0.87	0.09	9.96	1.30	0.78	1.15	0.66	0.00
Sphaeroidina bulloides d'Orbigny	0.58	0.27	0.25	1.81	1.30	1.38	0.38	0.71
Textularia earlandi Parker	0.19	0.18	0.13	0.14	0.26	0.69	0.00	0.71

Table 4.2. (*continued)*

Station	186	198	216	242	261	262	291	309
Trifarina occidentalis (Cushman)	0.29	0.37	0.13	0.14	1.30	0.92	0.00	0.71
Trochammina sp.	0.19	0.00	0.00	0.14	0.26	0.23	0.00	0.00
Usbekistania charoides (Jones & Parker)	0.00	0.00	0.00	0.14	0.00	1.38	0.00	0.00
Uvigerina bradyana Fornasini	4.43	0.09	0.00	0.00	1.30	0.00	0.00	0.00
Uvigerina peregrina Cushman	10.98	10.51	16.49	24.04	30.65	7.82	33.65	36.17
Vaginulinopsis sp.	0.39	0.00	0.32	0.14	0.26	0.00	0.09	1.77

One striking feature of the foraminiferal assemblage was the distribution of agglutinate species (Table 4.3). A total of 15 agglutinate species occured in the study area; however, except for Station 186 (Bear's Paw 1) and the reference sample (Station 242), fewer than 10 species occurred at any one station. The percentage of the assemblage that constituted agglutinate specimens differed significantly. In the northern seeps, the percent of agglutinate individuals varied between 0.7% at LM3 and 6.4% at Bear's Paw 1. The latter also had the highest number of agglutinate species (12) of all the seep stations. The Wairarapa seeps contained fewer agglutinate species, two at North Tower and eight at Takahae, but these comprised 11.2% and 6.4% of the assemblages at those stations. In contrast, the assemblage in the reference core included 12 agglutinate species constituting 42% of the total assemblage, making this the single factor in the assemblage data that distinguished the reference core from the seep cores.

Table 4.3. Benthic foraminiferal species richness, density and diversity indices.

Station	Seep name	Depth	Number of agglutinate species	% agglutinate species	Number of stained species	% stained individuals
186	Bear's Paw	1078	12	6.4	17	3.4
198	Bear's Paw	1107	4	4	12	2.1
216	LM3	664	3	0.7	6	2.6
242	Kaka 1	1175	9	2.5	6	1.8
261	Kaka 2	1171	7	3.6	1	0.2
262	Reference	1167	12	42.1	1	1.4
291	North Tower	1061	2	11.2	9	1.2
309	Takahae	1054	8	6.4	4	2.8

3.1.1 Stained specimens

Staining of foraminifera was undertaken in order to compare living or recently dead assemblages with the total foraminiferal assemblages that have been affected by methane–influenced pore waters. Because the study of living specimens was not a primary objective of this study, Rose Bengal, which has limitations for the identification of living foraminifera (Bernhard et al., 2006), was chosen for its ease of use. Unfortunately, stained specimens were generally rare, although all stations contained stained foraminifera (Table 4.4). The numbers were small, usually one to three specimens per sample, and ranged between 0.2% (Station 261, Kaka) and 3% (Station 186, Bear's Paw) of the assemblages in each core. Due to the paucity of stained specimens, it was not possible to do analyses separately on stained and unstained assemblages, thus the assemblages were treated as total foraminiferal assemblages and include both stained and unstained specimens.

Table 4.4. Abundances of agglutinated and stained individual foraminifera from Hikurangi Margin seep samples expressed as percent of total assemblage of each core.

Station	**186**	**198**	**216**	**242**	**261**	**262**	**291**	**309**
Seep	Bear's Paw	Bear's Paw	LM3	Kaka 1	Kaka 2	Reference	North Tower	Takahae
Depth (m)	1078	1102	662	1175	1171	1167	1061	1054
Average species richness (number of species per sample)	34	32	27	32	18	16	16	7
Average density (individuals/cm^3 sediment)	48	59	645	46	8	17	38	2
Average Simpson Index	0.06	0.06	0.14	0.09	0.14	0.13	0.36	0.32
Average Shannon Index	4.37	4.45	3.77	3.72	3.34	3.41	2.44	1.87

3.1.2 Density and diversity

The foraminiferal density, measured as the number of individuals/cm^3 of sediment, varied dramatically between samples (Table 4.4, Figure 4.3A-D, Figure 4.4). Station 216 (LM3), with densities ranging between 27 and 1050 foraminifera/cm^3 (average 645 foraminifera/cm^3 of sediment) had considerably higher densities than any other station (Figure 4.3A). All other stations averaged less than 100 individuals/cm^3), with a low of two individuals/cm^3 at Station 309 (Takahae), followed by Station 261 (Kaka 2) with eight individuals and Station 262 (Reference) with 17 individuals. The greatest densities always occurred below the sample taken at the sediment surface (0.0 to 0.5 cm) and were generally found in the intervals between 1.0 and 4.5 cm below the sediment surface. There was, however, no consistency amongst cores. For example, at Station 198 (Bear's Paw), the greatest density (102 individuals/cm^3 sediment) was in the interval between 3.0 and 3.5 cm below the sediment surface; whereas, Station 186 (Bear's Paw) achieved its greatest density (95 individuals/cm^3) in the interval 4.0 to 4.5 cm (Figure 4.3A).

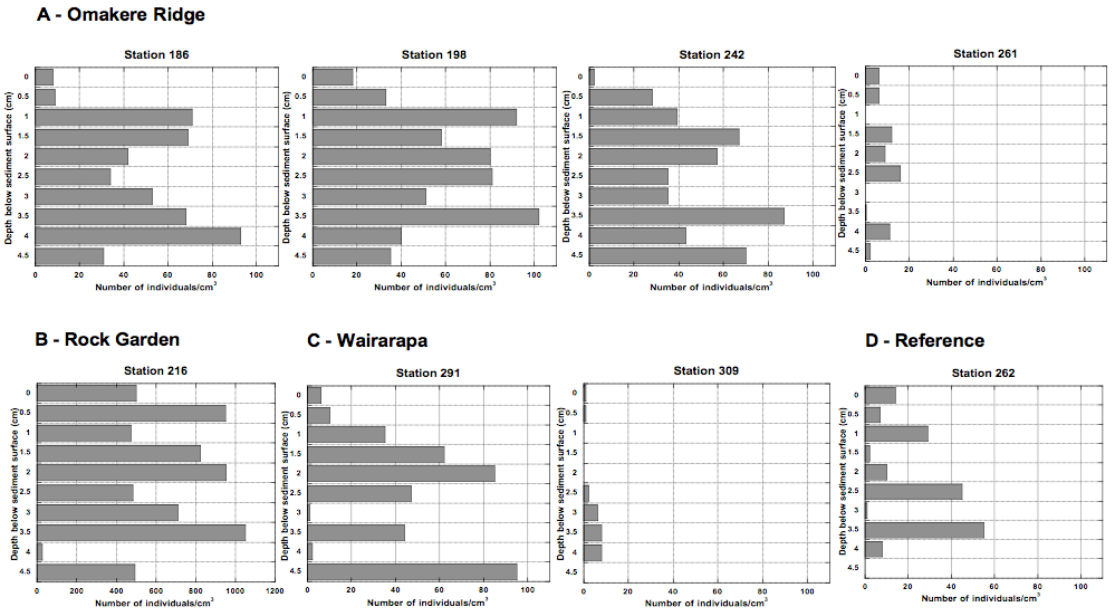

Figure 4.3. Foraminiferal density at depth intervals in each core measured as number of individuals/cm^3. A. Omakere Ridge samples. B. Rock Garden samples. Note the change of scale on the x–axis. C. Wairarapa samples. D. Reference sample.

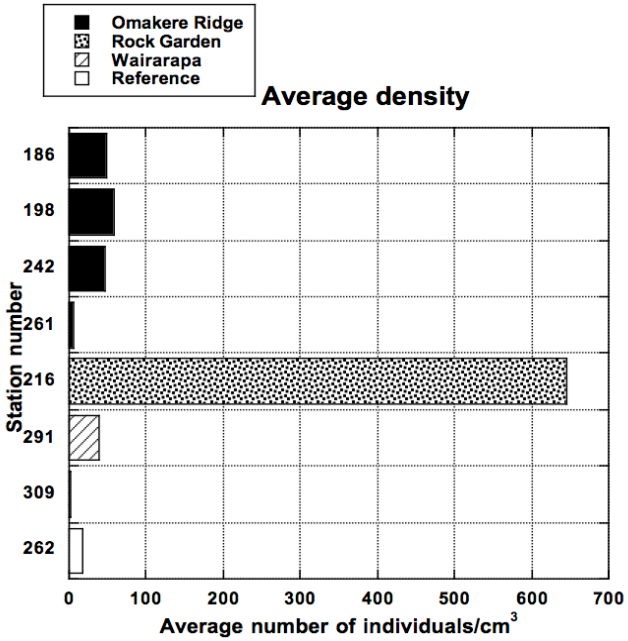

Figure 4.4. Average foraminiferal density at each station, grouped by geographic area.

The species richness, measured as the number of species per sample at each depth, is shown in Figure 4.5 and Table 4.4. The Bear's Paw seeps (Stations 186 and 198) yielded the greatest species richness, averaging 34 species per sample at Station 186 and 32 species per sample at Station 198. Station 242 (Kaka) was comparable, also averaging 32 species per sample. The lowest species richness occurred at Station 309 (Takahae) with an average of seven species per sample. The reference station, 262, contained an average of 16 species per sample, as did Station 291 (North Tower).

Sample diversity, measured using the Simpson (l) and Shannon (H') indices is shown in Table 4.4 and Figure 4.6. Overall, the greatest diversity occurs in the two Bear's Paw seeps (Stations 186, 198) and at Kaka 1 (Station 242). Diversity is considerably lower in the two southern seeps at Wairarapa. The reference seep (Station 262) is indistinguishable in diversity from the seeps at LM3 (Station 216) and one Kaka seep (Station 261).

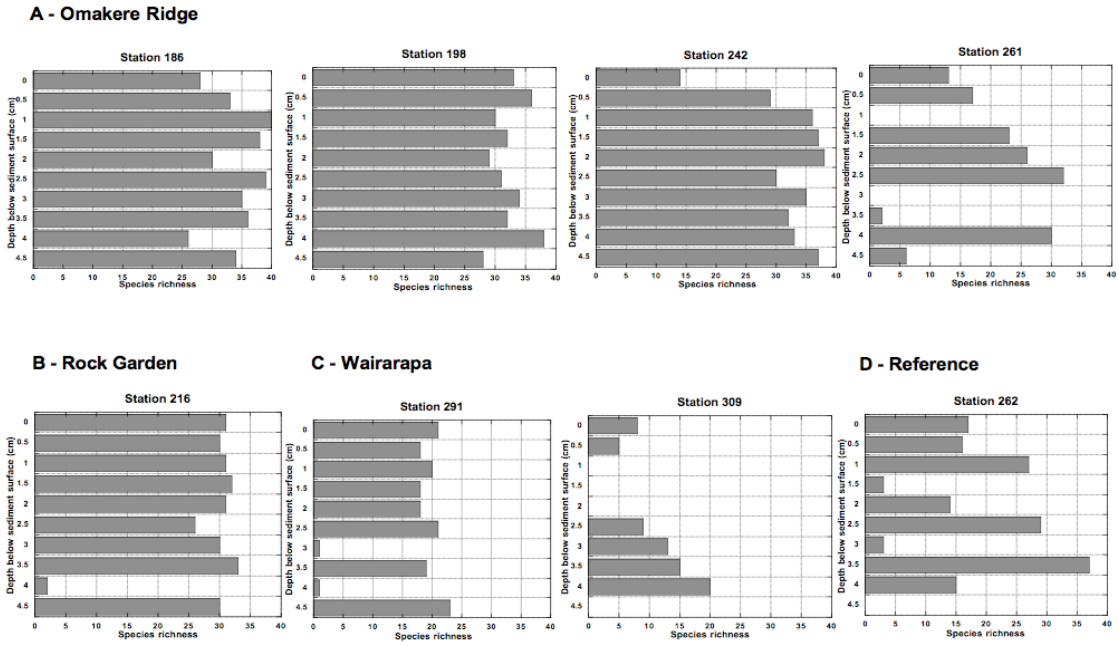

Figure 4.5. Foraminiferal species richness measured as the number of species in each sample. Species richness is generally greater in the Rock Garden (station 216) and Omakere Ridge (stations 186 and 198) seeps than in the reference core (Station 262) and Wairarapa seeps (stations 291 and 309).

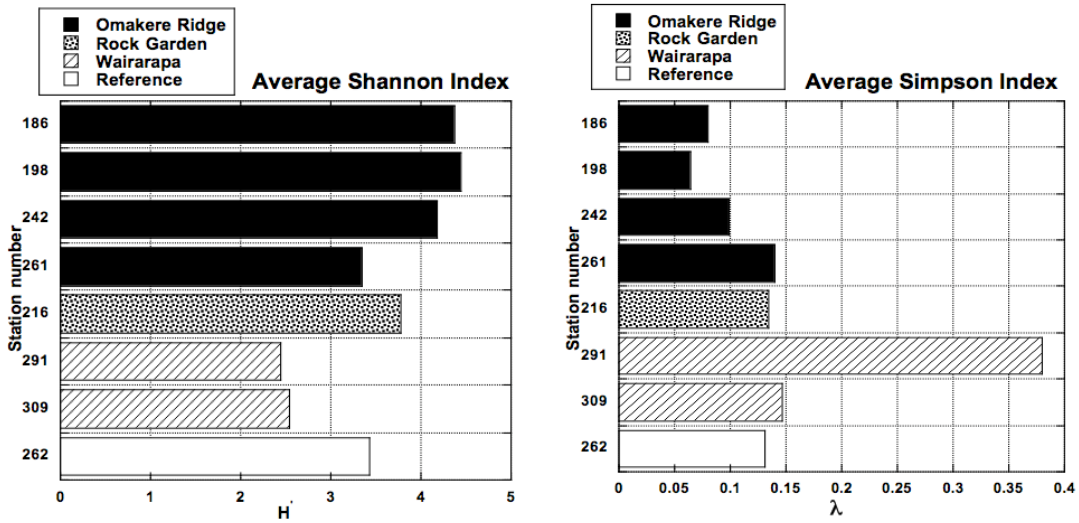

Figure 4.6. Average diversity indices for foraminiferal assemblages at each station. A. Shannon index. B. Simpson index.

3.2 Stable isotopes

3.2.1 Foraminiferal carbonate

Results of stable isotope analyses on foraminiferal carbonate from all cores are summarized in Table 4.5 and Figure 4.7. Most samples showed little variability (<0.5‰ PDB) in isotope values of all measured species near the tops of the cores. Due to low foraminiferal density and the preponderance of agglutinate species, the reference site (Station 262) yielded few specimens suitable for isotope analyses. The isotope values at this station, however, demonstrated little depletion and variability throughout the length of the core (Figure 4.6D). The largest $D^{13}C$ value for *Uvigerina peregrina* in this sample was 0.58‰ (3.5 to 4.0 cm below the sediment surface), very close to the 0.35‰ to 0.52‰ range for non-seep members of that species (McCorkle et al., 1997). Among the seep cores, Station 242 (Kaka 1) and Station 309 (Takahae) showed the least depletion and variability in foraminiferal carbonate values. *U. peregrina* at Station 242 yielded $\delta^{13}C$ values that ranged from –1.96 to +0.45‰ PDB, for a $\Delta^{13}C$ of 2.41‰. In the same core, *Bulimina aculeata* varied between –0.32 and +0.57‰ PDB, a $\Delta^{13}C$ of 0.89‰.

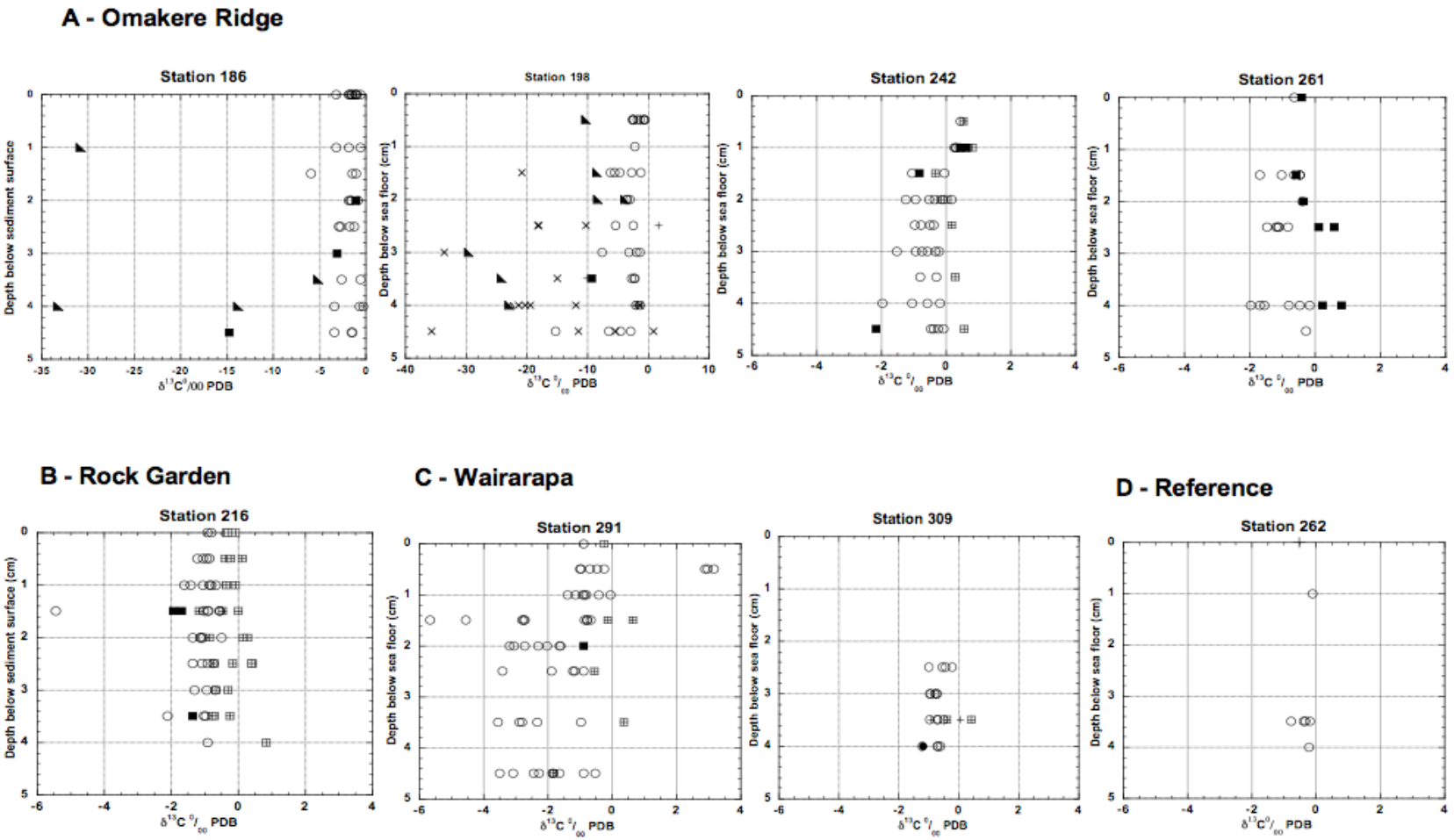

Figure 4.7. Foraminiferal carbonate $\delta^{13}C$ from the six species analyzed. A. Omakere Ridge sites. Note changes of scale on x–axis for Stations 186 and 198. B. Rock Garden.
C.Wairarapa sites. D. Reference site. Key: ○ *Uvigerina peregrina;* ▩ *Globobulimina pacifica;* ▲ *Pyrgo depressa;* × *Hoeglundina elegans;* + *Oridorsalis umbonatus;* △ *Pyrgo anomala.*

The other Kaka seep (Station 261), however, shows greater depletion and variability, although the most depleted species is again *U. peregrina.* Foraminiferal carbonate at Station 309 (Takahae) displayed somewhat more variation in $\delta^{13}C$ values. The most depleted values for this station occurred in the 3.0 to 3.5 cm depth interval in which *U. peregrina* varied between –0.73‰ and –2.69‰ PDB, for a $D^{13}C$ of 1.64‰. Displaying greater variability and depletion were the samples from Station 216 (LM3) and Station 291 (North Tower). In the former sample *U. peregrina* had a low $\delta^{13}C$ value of –5.45‰ PDB at a depth of 1.5 to 2.0 cm with a $\Delta^{13}C$ of 4.89‰. At North Tower (Station 291), the same species, also at 1.5 to 2.0 cm below the sediment surface, had a low $\delta^{13}C$ value of –5.68‰ PDB, with a $\Delta^{13}C$ of 4.77‰. As with density and diversity, the two Bear's Paw seeps (Stations 186 and 198) were conspicuous in the isotopic values of their foraminiferal shells. First, *U. peregrina* exhibited greater depletion and variability than at all other stations. At Station 186, the most depleted value was in the 1.5 to 2.0 cm interval, at –5.98‰ PDB with a $\Delta^{13}C$ of 5.44‰. At Station 198, on the other hand, the lowest $\delta^{13}C$ value for the same species was –15.32‰ PDB in the 4.5 to 5.0 cm interval, with a $\Delta^{13}C$ of 12.44‰. Two other species, however, demonstrated considerably more depleted and variable signals than did *U. peregrina.* At Station 186, *Pyrgo depressa*, represented by one or two individuals per depth interval, displayed $\delta^{13}C$ values for the entire core ranging between –5.31‰ and –33.46‰ PDB, with $\Delta^{13}C$ in the 4.0 to 4.5 cm interval of 19.43‰. At Station 198, the same species had $\delta^{13}C$ values from –4.21 to –29.79‰ PDB, and a single specimen of *Pyrgo anomala* returned a value of –22.69‰ PDB. Also at this station, *Hoeglundina elegans* yielded $\delta^{13}C$ values ranging between +0.82 and –35.70‰ PDB. In the 4.0 to 4.5 cm interval, the $\Delta^{13}C$ for this species was 20.09‰ and in the 4.5 to 5.0 interval, the $\Delta^{13}C$ value was 36.52‰.

Comparison of $\delta^{13}C$ and $\delta^{18}O$ values for foraminiferal carbonate yields a clear distinction between the three geographic areas (Figure 4.8). Based on $\delta^{18}O$ values, Rock Garden and Wairarapa fall into separate groups, with Rock Garden having an average $\delta^{18}O$ of 4.25‰ PDB and Wairarapa an average of 2.69‰ PDB.

Variability in the two is also dissimilar; at Rock Garden □Ĩ O is 3.59‰ PDB and at Wairarapa it is 4.24‰ PDB. Omakere Ridge straddles the two, with an average $\delta^{18}O$ of 3.72‰ PDB, and $\delta^{18}O$ values are more variable than either of the other two with a □[1□]O of 5.21‰ PDB.

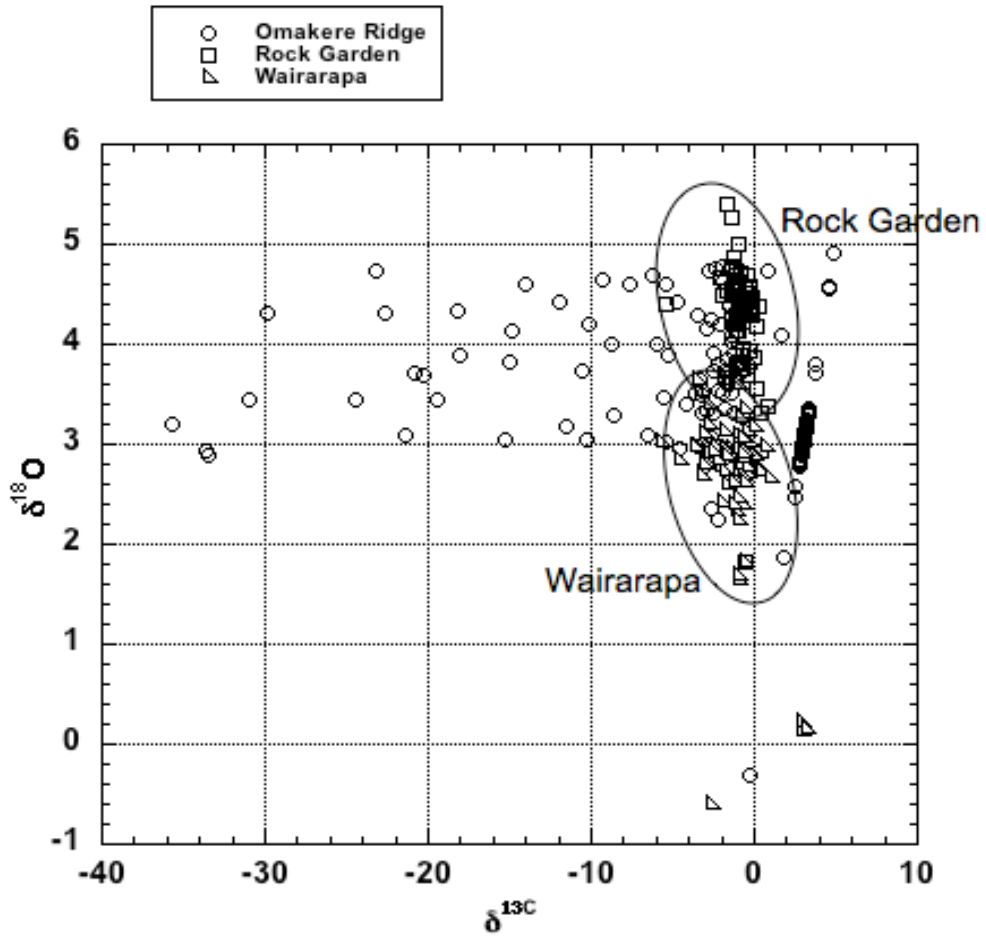

Figure 8. Comparison of carbon and oxygen isotopes for all foraminiferal carbonates showing clear distinction between Rock Garden and Wairarapa.

Table 4.5. Stable isotope values for foraminifera.

Station	Depth below sediment surface (cm)	Species	$d^{13}C$	$d^{18}O$
186	0.0-0.5	*Uvigerina peregrina*	-1.59	3.66
186	0.0-0.5	*Uvigerina peregrina*	-1.50	3.63
186	0.0-0.5	*Uvigerina peregrina*	-1.15	3.76
186	0.0-0.5	*Uvigerina peregrina*	-0.96	2.64
186	0.5-1.0	*Uvigerina peregrina*	-1.06	3.67
186	0.5-1.0	*Uvigerina peregrina*	-1.87	3.51
186	0.5-1.0	*Uvigerina peregrina*	-3.22	3.48
186	0.5-1.0	*Uvigerina peregrina*	-1.73	3.63
186	0.5-1.0	*Uvigerina peregrina*	-0.62	3.31
186	1.0-1.5	*Pyrgo depressa*	-31.01	3.44
186	1.0-1.5	*Uvigerina peregrina*	-0.54	3.24
186	1.0-1.5	*Uvigerina peregrina*	-3.21	2.99
186	1.0-1.5	*Uvigerina peregrina*	-1.86	3.67
186	1.5-2.0	*Uvigerina peregrina*	-1.42	3.51
186	1.5-2.0	*Uvigerina peregrina*	-5.94	4.00
186	1.5-2.0	*Uvigerina peregrina*	-1.03	3.77
186	2.0-2.5	*Globobulimina pacifica*	-1.06	4.56
186	2.0-2.5	*Uvigerina peregrina*	-1.54	4.39
186	2.0-2.5	*Uvigerina peregrina*	-0.91	2.86
186	2.0-2.5	*Uvigerina peregrina*	-1.81	3.36
186	2.0-2.5	*Uvigerina peregrina*	-1.64	3.85
186	2.5-3.5	*Uvigerina peregrina*	-1.78	3.73

Table 4.5 (*continued)*

Station	Depth below sediment surface (cm)	Species	$d^{13}C$	$d^{18}O$
186	2.5-3.5	*Uvigerina peregrina*	-2.70	4.24
186	2.5-3.5	*Uvigerina peregrina*	-1.28	3.32
186	2.5-3.5	*Uvigerina peregrina*	-2.94	4.16
186	3.0-3.5	*Globobulimina pacifica*	-3.15	3.32
186	3.5-4.0	*Pyrgo depressa*	-5.31	3.88
186	3.5-4.0	*Uvigerina peregrina*	-0.54	4.58
186	3.5-4.0	*Uvigerina peregrina*	-2.59	3.07
186	4.0-4.5	*Pyrgo depressa*	-33.46	2.89
186	4.0-4.5	*Pyrgo depressa*	-14.03	4.59
186	4.0-4.5	*Uvigerina peregrina*	-0.27	3.78
186	4.0-4.5	*Uvigerina peregrina*	-0.66	4.21
186	4.0-4.5	*Uvigerina peregrina*	-3.39	3.64
186	4.5-5.0	*Globobulimina pacifica*	-14.79	4.14
186	4.5-5.0	*Uvigerina peregrina*	-3.43	4.28
186	4.5-5.0	*Uvigerina peregrina*	-1.47	3.59
186	4.5-5.0	*Uvigerina peregrina*	-1.58	4.38
198	0.5-1.0	*Pyrgo depressa*	-10.54	3.74
198	0.5-1.0	*Uvigerina peregrina*	-2.56	3.74
198	0.5-1.0	*Uvigerina peregrina*	-0.54	2.78
198	0.5-1.0	*Uvigerina peregrina*	-1.86	3.63
198	0.5-1.0	*Uvigerina peregrina*	-0.85	3.80
198	0.5-1.0	*Uvigerina peregrina*	-2.51	3.31
198	0.5-1.0	*Uvigerina peregrina*	-2.69	2.35
198	0.5-1.0	*Uvigerina peregrina*	-1.41	2.88

Table 4.5 (*continued)*

Station	Depth below sediment surface (cm)	Species	$d^{13}C$	$d^{18}O$
198	0.5-1.0	*Uvigerina peregrina*	-1.45	4.02
198	0.5-1.0	*Uvigerina peregrina*	-0.74	3.73
198	1.0-1.5	*Calyptogena shell*	-2.53	3.11
198	1.0-1.5	*Uvigerina peregrina*	-2.20	3.80
198	1.5-2.0	*Hoeglundina elegans*	-20.83	3.71
198	1.5-2.0	*Pyrgo depressa*	-14.29	3.99
198	1.5-2.0	*Uvigerina peregrina*	-5.52	3.47
198	1.5-2.0	*Uvigerina peregrina*	-6.25	4.68
198	1.5-2.0	*Uvigerina peregrina*	-4.69	4.42
198	1.5-2.0	*Uvigerina peregrina*	-2.77	4.73
198	1.5-2.0	*Uvigerina peregrina*	-1.28	3.91
198	2.0-2.5	*Pyrgo depressa*	-8.57	3.29
198	2.0-2.5	*Pyrgo depressa*	-4.21	3.39
198	2.0-2.5	*Uvigerina peregrina*	-3.63	3.52
198	2.0-2.5	*Uvigerina peregrina*	-3.47	2.97
198	2.0-2.5	*Uvigerina peregrina*	-3.02	2.78
198	2.5-3.0	*Hoeglundina elegans*	-18.20	4.34
198	2.5-3.0	*Hoeglundina elegans*	-10.23	3.04
198	2.5-3.0	*Hoeglundina elegans*	-18.05	3.90
198	2.5-3.0	*Oridorsalis umbonatus*	1.70	4.08
198	2.5-3.0	*Uvigerina peregrina*	-2.52	3.92
198	2.5-3.0	*Uvigerina peregrina*	-5.37	4.60
198	3.0-3.5	*Hoeglundina elegans*	-33.57	2.94
198	3.0-3.5	*Pyrgo depressa*	-29.79	4.32

Table 4.5 (*continued)*

Station	Depth below sediment surface (cm)	Species	$d^{13}C$	$d^{18}O$
198	3.0-3.5	*Uvigerina peregrina*	-3.12	3.53
198	3.0-3.5	*Uvigerina peregrina*	-7.70	4.60
198	3.0-3.5	*Uvigerina peregrina*	-1.89	4.62
198	3.0-3.5	*Uvigerina peregrina*	-1.38	4.09
198	3.5-4.0	*Globogulimina pacificus*	-9.26	4.64
198	3.5-4.0	*Hoeglundina elegans*	-15.02	3.82
198	3.5-4.0	*Oridorsalis umbonatus*	-10.16	4.21
198	3.5-4.0	*Pyrgo depressa*	-24.38	3.45
198	3.5-4.0	*Uvigerina peregrina*	-2.75	3.01
198	3.5-4.0	*Uvigerina peregrina*	-2.32	4.76
198	3.5-4.0	*Uvigerina peregrina*	-2.25	3.54
198	4.0-4.5	*Hoeglundina elegans*	-1.32	4.58
198	4.0-4.5	*Hoeglundina elegans*	-21.41	3.10
198	4.0-4.5	*Hoeglundina elegans*	-19.45	3.45
198	4.0-4.5	*Hoeglundina elegans*	-20.21	3.69
198	4.0-4.5	*Hoeglundina elegans*	-11.87	4.43
198	4.0-4.5	*Oridorsalis umbonatus*	-2.16	2.25
198	4.0-4.5	*Oridorsalis umbonatus*	-1.90	4.78
198	4.0-4.5	*Oridorsalis umbonatus*	-1.10	4.76
198	4.0-4.5	*Pyrgo anomala*	-22.69	4.32
198	4.0-4.5	*Pyrgo depressa*	-23.15	4.73
198	4.0-4.5	*Uvigerina peregrina*	-1.43	4.21
198	4.0-4.5	*Uvigerina peregrina*	-2.01	4.20

Table 4.5 (*continued)*

Station	Depth below sediment surface (cm)	Species	$d^{13}C$	$d^{18}O$
198	4.5-5.0	*Hoeglundina elegans*	0.82	4.74
198	4.5-5.0	*Hoeglundina elegans*	-5.38	3.03
198	4.5-5.0	*Hoeglundina elegans*	-11.54	3.18
198	4.5-5.0	*Hoeglundina elegans*	-35.70	3.19
198	4.5-5.0	*Uvigerina peregrina*	-2.88	3.33
198	4.5-5.0	*Uvigerina peregrina*	-6.56	3.09
198	4.5-5.0	*Uvigerina peregrina*	-4.60	2.95
198	4.5-5.0	*Uvigerina peregrina*	-15.32	3.05
216	0.0-0.5	*Bulimina aculeata*	-0.37	4.45
216	0.0-0.5	*Bulimina aculeata*	-0.09	4.36
216	0.0-0.5	*Bulimina aculeata*	-0.30	3.93
216	0.0-0.5	*Uvigerina peregrina*	-0.80	3.76
216	0.0-0.5	*Uvigerina peregrina*	-0.92	4.14
216	0.5-1	*Bulimina aculeata*	0.10	3.56
216	0.5-1	*Bulimina aculeata*	-0.38	3.69
216	0.5-1	*Bulimina aculeata*	-0.23	4.42
216	0.5-1	*Uvigerina peregrina*	-1.05	4.25
216	0.5-1	*Uvigerina peregrina*	-0.85	3.81
216	0.5-1	*Uvigerina peregrina*	-0.94	4.40
216	0.5-1	*Uvigerina peregrina*	-1.21	4.57
216	1.0-1.5	*Bulimina aculeata*	-0.08	4.28
216	1.0-1.5	*Bulimina aculeata*	-0.37	4.52

Table 4.5 (*continued)*

Station	Depth below sediment surface (cm)	Species	$d^{13}C$	$d^{18}O$
216	1.0-1.5	*Uvigerina peregrina*	-0.66	3.76
216	1.0-1.5	*Uvigerina peregrina*	-0.85	4.31
216	1.0-1.5	*Uvigerina peregrina*	-1.42	4.56
216	1.0-1.5	*Uvigerina peregrina*	-0.79	4.28
216	1.0-1.5	*Uvigerina peregrina*	-1.05	4.30
216	1.0-1.5	*Uvigerina peregrina*	-1.61	4.53
216	1.5-2	*Bulimina aculeata*	-1.17	3.81
216	1.5-2	*Bulimina aculeata*	-0.47	4.68
216	1.5-2	*Bulimina aculeata*	0.01	3.86
216	1.5-2	*Globobulimina pacifica*	-1.71	5.41
216	1.5-2	*Globobulimina pacifica*	-1.95	4.50
216	1.5-2	*Uvigerina peregrina*	-0.56	4.34
216	1.5-2	*Uvigerina peregrina*	-0.92	3.79
216	1.5-2	*Uvigerina peregrina*	-0.89	4.35
216	1.5-2	*Uvigerina peregrina*	-5.45	4.39
216	1.5-2	*Uvigerina peregrina*	-1.03	5.01
216	1.5-2	*Uvigerina peregrina*	-0.56	4.41
216	2.0-2.5	*Bulimina aculeata*	0.27	4.37
216	2.0-2.5	*Bulimina aculeata*	0.14	4.17
216	2.0-2.5	*Bulimina aculeata*	-0.85	4.38
216	2.0-2.5	*Uvigerina peregrina*	-1.06	4.49
216	2.0-2.5	*Uvigerina peregrina*	-1.10	4.74

Table 4.5 (*continued)*

Station	Depth below sediment surface (cm)	Species	$d^{13}C$	$d^{18}O$
216	2.0-2.5	*Uvigerina peregrina*	-1.13	4.56
216	2.0-2.5	*Uvigerina peregrina*	-0.49	1.82
216	2.0-2.5	*Uvigerina peregrina*	-1.35	4.27
216	2.5-3	*Bulimina aculeata*	-0.73	3.95
216	2.5-3	*Bulimina aculeata*	-0.18	4.46
216	2.5-3	*Bulimina aculeata*	0.41	3.31
216	2.5-3	*Bulimina aculeata*	0.40	2.93
216	2.5-3	*Uvigerina peregrina*	-0.73	3.76
216	2.5-3	*Uvigerina peregrina*	-1.36	4.76
216	2.5-3	*Uvigerina peregrina*	-1.08	4.13
216	2.5-3	*Uvigerina peregrina*	-0.92	4.62
216	3.0-3.5	*Bulimina aculeata*	-0.30	4.30
216	3.0-3.5	*Bulimina aculeata*	-0.67	4.30
216	3.0-3.5	*Uvigerina peregrina*	-0.69	3.90
216	3.0-3.5	*Uvigerina peregrina*	-1.30	4.86
216	3.0-3.5	*Uvigerina peregrina*	-0.94	3.82
216	3.5-4	*Bulimina aculeata*	-0.25	4.58
216	3.5-4	*Bulimina aculeata*	-0.71	4.23
216	3.5-4	*Bulimina aculeata*	-0.78	4.71
216	3.5-4	*Globobulimina pacifica*	-1.36	5.27
216	3.5-4	*Uvigerina peregrina*	-1.03	4.25
216	3.5-4	*Uvigerina peregrina*	-2.11	4.66

Table 4.5 (*continued)*

Station	Depth below sediment surface (cm)	Species	$d^{13}C$	$d^{18}O$
216	3.5-4	*Uvigerina peregrina*	-0.98	4.53
216	4.0-4.5	*Bulimina aculeata*	0.84	3.37
216	4.0-4.5	*Uvigerina peregrina*	-0.91	4.20
216	4.0-4.5	*Uvigerina peregrina*	-1.06	4.70
216	4.0-4.5	*Uvigerina peregrina*	-1.45	4.78
242	0.5-1	*Bulimina aculeata*	0.11	2.99
242	0.5-1	*Uvigerina peregrina*	0.25	3.22
242	0.5-1	*Uvigerina peregrina*	-0.83	2.92
242	1.0-1.5	*Bulimina aculeata*	0.40	2.89
242	1.0-1.5	*Bulimina aculeata*	0.27	2.91
242	1.0-1.5	*Globobulimina pacifica*	-1.48	3.15
242	1.0-1.5	*Globobulimina pacifica*	-1.39	3.25
242	1.0-1.5	*Uvigerina peregrina*	-0.18	3.21
242	1.0-1.5	*Uvigerina peregrina*	0.21	2.96
242	1.0-1.5	*Uvigerina peregrina*	0.00	3.23
242	1.0-1.5	*Uvigerina peregrina*	-0.17	1.87
242	1.5-2	*Bulimina aculeata*	-0.32	2.57
242	1.5-2	*Globobulimina pacifica*	-0.83	3.12
242	1.5-2	*Uvigerina peregrina*	-1.05	2.91
242	1.5-2	*Uvigerina peregrina*	-0.05	2.85
242	2.0-2.5	*Bulimina aculeata*	-0.18	2.47
242	2.0-2.5	*Uvigerina peregrina*	-0.11	3.00

Table 4.5 (*continued)*

Station	Depth below sediment surface (cm)	Species	$d^{13}C$	$d^{18}O$
242	2.0-2.5	*Uvigerina peregrina*	-1.26	2.81
242	2.0-2.5	*Uvigerina peregrina*	0.17	2.88
242	2.0-2.5	*Uvigerina peregrina*	-0.95	3.25
242	2.0-2.5	*Uvigerina peregrina*	-0.52	3.10
242	2.0-2.5	*Uvigerina peregrina*	-0.37	3.17
242	2.5-3	*Bulimina aculeata*	0.17	2.88
242	2.5-3	*Uvigerina peregrina*	-0.49	3.18
242	2.5-3	*Uvigerina peregrina*	-0.38	3.22
242	2.5-3	*Uvigerina peregrina*	-0.96	3.22
242	2.5-3	*Uvigerina peregrina*	-0.77	2.77
242	3.0-3.5	*Uvigerina peregrina*	-0.96	2.91
242	3.0-3.5	*Uvigerina peregrina*	-0.34	3.07
242	3.0-3.5	*Uvigerina peregrina*	-0.22	3.24
242	3.0-3.5	*Uvigerina peregrina*	-0.58	2.99
242	3.0-3.5	*Uvigerina peregrina*	-1.54	2.88
242	3.0-3.5	*Uvigerina peregrina*	-0.75	2.98
242	3.5-4	*Bulimina aculeata*	0.28	2.90
242	3.5-4	*Uvigerina peregrina*	-0.82	2.99
242	3.5-4	*Uvigerina peregrina*	-0.32	3.14
242	4.0-4.5	*Uvigerina peregrina*	-1.06	2.82
242	4.0-4.5	*Uvigerina peregrina*	-0.19	3.35
242	4.0-4.5	*Uvigerina peregrina*	-1.96	3.04

Table 4.5 (*continued)*

Station	Depth below sediment surface (cm)	Species	$d^{13}C$	$d^{18}O$
242	4.0-4.5	*Uvigerina peregrina*	-0.57	3.81
242	4.5-5	*Bulimina aculeata*	0.57	3.06
242	4.5-5	*Globobulimina pacifica*	-2.17	3.30
242	4.5-5	*Uvigerina peregrina*	-0.09	3.06
242	4.5-5	*Uvigerina peregrina*	-0.39	3.02
242	4.5-5	*Uvigerina peregrina*	-0.24	2.97
242	4.5-5	*Uvigerina peregrina*	-0.47	3.00
242	2.0-2.5	*Bulimina aculeata*	0.04	3.33
261	0.0-0.5	*Bulimina aculeata*	-0.41	3.16
261	0.0-0.5	*Uvigerina peregrina*	-0.65	2.93
261	1.5-2.0	*Bulimina aculeata*	-0.57	3.03
261	1.5-2.0	*Uvigerina peregrina*	-0.64	3.32
261	1.5-2.0	*Uvigerina peregrina*	-0.48	3.09
261	1.5-2.0	*Uvigerina peregrina*	-1.70	2.91
261	1.5-2.0	*Uvigerina peregrina*	-1.02	3.01
261	1.5-2.0	*Uvigerina peregrina*	-0.46	2.80
261	2.0-2.5	*Bulimina aculeata*	-0.35	3.06
261	2.0-2.5	*Uvigerina peregrina*	-0.39	3.13
261	2.5-3.0	*Bulimina aculeata*	0.59	3.06
261	2.5-3.0	*Bulimina aculeata*	0.11	4.91
261	2.5-3.0	*Uvigerina peregrina*	-0.82	2.98
261	2.5-3.0	*Uvigerina peregrina*	-1.18	4.58

Table 4.5 (*continued)*

Station	Depth below sediment surface (cm)	Species	$d^{13}C$	$d^{18}O$
261	2.5-3.0	*Uvigerina peregrina*	-1.48	3.03
261	2.5-3.0	*Uvigerina peregrina*	-1.11	2.96
261	2.5-3.0	*Uvigerina peregrina*	-1.14	3.02
261	4.0-4.5	*Bulimina aculeata*	0.81	3.05
261	4.0-4.5	*Bulimina aculeata*	0.22	3.07
261	4.0-4.5	*Uvigerina peregrina*	-0.47	-0.30
261	4.0-4.5	*Uvigerina peregrina*	-1.55	3.11
261	4.0-4.5	*Uvigerina peregrina*	-0.81	3.20
261	4.0-4.5	*Uvigerina peregrina*	-0.17	3.09
261	4.0-4.5	*Uvigerina peregrina*	-1.69	3.19
261	4.0-4.5	*Uvigerina peregrina*	-1.98	4.55
261	4.5-5.0	*Uvigerina peregrina*	-0.28	3.72
262	0.0-0.5	*Oridorsalis umbonatus*	-0.54	3.01
262	1.0-1.5	*Uvigerina peregrina*	0.10	2.72
262	3.5-4.0	*Uvigerina peregrina*	-0.19	2.80
262	3.5-4.0	*Uvigerina peregrina*	-0.39	3.09
262	3.5-4.0	*Uvigerina peregrina*	-0.32	2.84
262	3.5-4.0	*Uvigerina peregrina*	-0.77	3.18
262	4.0-4.5	*Uvigerina peregrina*	-0.22	3.01
262	4.0-4.5	*Uvigerina peregrina*	-0.22	2.70
291	0.0-0.5	*Bulimina aculeata*	-0.24	2.86
291	0.0-0.5	*Uvigerina peregrina*	-0.90	2.78

Table 4.5 (*continued)*

Station	Depth below sediment surface (cm)	Species	$d^{13}C$	$d^{18}O$
291	0.5-1	*Uvigerina peregrina*	-0.26	2.74
291	0.5-1	*Uvigerina peregrina*	-0.68	2.78
291	0.5-1	*Uvigerina peregrina*	2.97	0.13
291	0.5-1	*Uvigerina peregrina*	2.88	0.22
291	0.5-1	*Uvigerina peregrina*	3.16	0.16
291	0.5-1	*Uvigerina peregrina*	-0.47	3.14
291	0.5-1	*Uvigerina peregrina*	-0.98	2.96
291	0.5-1	*Uvigerina peregrina*	-0.99	2.95
291	1.0-1.5	*Uvigerina peregrina*	-0.06	3.17
291	1.0-1.5	*Uvigerina peregrina*	-0.80	2.94
291	1.0-1.5	*Uvigerina peregrina*	-1.38	2.95
291	1.0-1.5	*Uvigerina peregrina*	-0.42	3.05
291	1.0-1.5	*Uvigerina peregrina*	-0.86	3.26
291	1.0-1.5	*Uvigerina peregrina*	-0.92	2.92
291	1.0-1.5	*Uvigerina peregrina*	-1.12	2.33
291	1.5-2	*Bulimina aculeata*	0.64	2.97
291	1.5-2	*Bulimina aculeata*	-0.15	2.93
291	1.5-2	*Uvigerina peregrina*	-0.79	2.82
291	1.5-2	*Uvigerina peregrina*	-2.81	2.91
291	1.5-2	*Uvigerina peregrina*	-0.85	2.87
291	1.5-2	*Uvigerina peregrina*	-2.71	2.92
291	1.5-2	*Uvigerina peregrina*	-0.68	2.86

Table 4.5 (*continued)*

Station	Depth below sediment surface (cm)	Species	$d^{13}C$	$d^{18}O$
291	1.5-2	*Uvigerina peregrina*	-5.68	3.02
291	1.5-2	*Uvigerina peregrina*	-4.56	2.85
291	1.5-2	*Uvigerina peregrina*	-2.74	3.19
291	1.5-2	*Uvigerina peregrina*	-0.79	2.66
291	2.0-2.5	*Globobulimina pacifica*	-0.87	2.96
291	2.0-2.5	*Uvigerina peregrina*	-2.04	2.77
291	2.0-2.5	*Uvigerina peregrina*	-2.72	3.40
291	2.0-2.5	*Uvigerina peregrina*	-0.92	1.64
291	2.0-2.5	*Uvigerina peregrina*	-0.62	1.79
291	2.0-2.5	*Uvigerina peregrina*	-3.20	2.69
291	2.0-2.5	*Uvigerina peregrina*	-2.31	2.91
291	2.0-2.5	*Uvigerina peregrina*	-3.06	3.12
291	2.0-2.5	*Uvigerina peregrina*	-1.63	2.96
291	2.0-2.5	*Uvigerina peregrina*	-1.61	2.60
291	2.5-3	*Bulimina aculeata*	-0.55	2.75
291	2.5-3	*Uvigerina peregrina*	-1.23	2.86
291	2.5-3	*Uvigerina peregrina*	-3.41	2.98
291	2.5-3	*Uvigerina peregrina*	-1.90	2.42
291	2.5-3	*Uvigerina peregrina*	-1.17	2.90
291	2.5-3	*Uvigerina peregrina*	-0.90	3.60
291	3.5-4	*Bulimina aculeata*	0.35	2.78
291	3.5-4	*Uvigerina peregrina*	-2.88	2.82

Table 4.5 (*continued)*

Station	Depth below sediment surface (cm)	Species	$d^{13}C$	$d^{18}O$
291	3.5-4	*Uvigerina peregrina*	-2.80	2.91
291	3.5-4	*Uvigerina peregrina*	-0.97	3.10
291	3.5-4	*Uvigerina peregrina*	-2.33	2.97
291	3.5-4	*Uvigerina peregrina*	-3.54	2.97
291	4.5-5	*Bulimina aculeata*	-1.84	2.74
291	4.5-5	*Uvigerina peregrina*	-3.08	2.80
291	4.5-5	*Uvigerina peregrina*	-1.85	2.96
291	4.5-5	*Uvigerina peregrina*	-1.65	2.90
291	4.5-5	*Uvigerina peregrina*	-2.28	2.85
291	4.5-5	*Uvigerina peregrina*	-0.52	3.36
291	4.5-5	*Uvigerina peregrina*	-0.90	3.00
291	4.5-5	*Uvigerina peregrina*	-3.50	3.65
291	4.5-5	*Uvigerina peregrina*	-1.83	3.14
291	4.5-5	*Uvigerina peregrina*	-2.43	2.93
309	2.5-3.0	*Uvigerina peregrina*	-0.22	3.02
309	2.5-3.0	*Uvigerina peregrina*	-0.43	2.71
309	2.5-3.0	*Uvigerina peregrina*	-0.55	1.82
309	2.5-3.0	*Uvigerina peregrina*	-1.01	2.73
309	3.0-3.5	*Uvigerina peregrina*	-0.73	2.68
309	3.0-3.5	*Uvigerina peregrina*	-0.94	2.25
309	3.0-3.5	*Uvigerina peregrina*	-0.75	2.40
309	3.0-3.5	*Uvigerina peregrina*	-0.97	2.62

Table 4.5 (*continued)*

Station	Depth below sediment surface (cm)	Species	$d^{13}C$	$d^{18}O$
309	3.0-3.5	*Uvigerina peregrina*	-0.81	2.79
309	3.0-3.5	*Uvigerina peregrina*	-2.69	-0.59
309	3.5-4.0	*Bulimina aculeata*	-0.38	2.78
309	3.5-4.0	*Bulimina aculeata*	0.42	2.73
309	3.5-4.0	*Globobulimina pacifica*	-1.03	1.70
309	3.5-4.0	*Oridorsalis umbonatus*	0.06	2.88
309	3.5-4.0	*Oridorsalis umbonatus*	-0.93	2.95
309	3.5-4.0	*Uvigerina peregrina*	-0.70	2.87
309	3.5-4.0	*Uvigerina peregrina*	-0.97	2.47
309	3.5-4.0	*Uvigerina peregrina*	-0.73	2.95
309	3.5-4.0	*Uvigerina peregrina*	-0.49	2.94
309	4.0-4.5	*Bulimina aculeata*	0.92	2.66
309	4.0-4.5	*Globobulimina pacifica*	-1.19	2.39
309	4.0-4.5	*Uvigerina peregrina*	-0.69	3.07
309	4.0-4.5	*Uvigerina peregrina*	-0.72	2.91
309	4.0-4.5	*Uvigerina peregrina*	-1.22	2.62
309	4.0-4.5	*Uvigerina peregrina*	-0.61	2.63

3.2.2 Non-foraminiferal carbonate

Results of isotope analyses on non-foraminiferal carbonates from Station 198 (Bear's Paw) are shown in Figure 4.9 and Table 4.6. The most depleted $\delta^{13}C$ signals in this study were recorded by the authigenic carbonates, with values ranging from –48.53‰ to –55.41‰ PDB. Two samples obtained from the same interval, 4.0 to 4.5 cm, were fairly close, at 51.93‰ and 52.96‰ PDB. This degree of depletion indicates a biogenic source for the methane at this site, and is comparable to results reported by Campbell et al. (this volume) for seep carbonates at various sites on the Hikurangi Margin.

Carbonate from the *Calyptogena* shells were considerably less depleted, with the single stained shell showing the greatest enrichment in $\delta^{13}C$ at –0.04‰ PDB, a value consistent with normal ambient seawater. On the other hand, the unstained *Calyptogena* shells were more depleted, returning values of –2.53‰ to –19.99‰ PDB.

3.3 SEM Imaging

SEM images of specimens of foraminifera used for isotope analyses were obtained for each sample site. Representative images are shown in Figure 4.10. The shells appear pristine and without overgrowths, and the pores are open, with distinct edges. It is therefore reasonable to assume that the foraminifera were unaltered, and their isotope signals result from primary calcification.

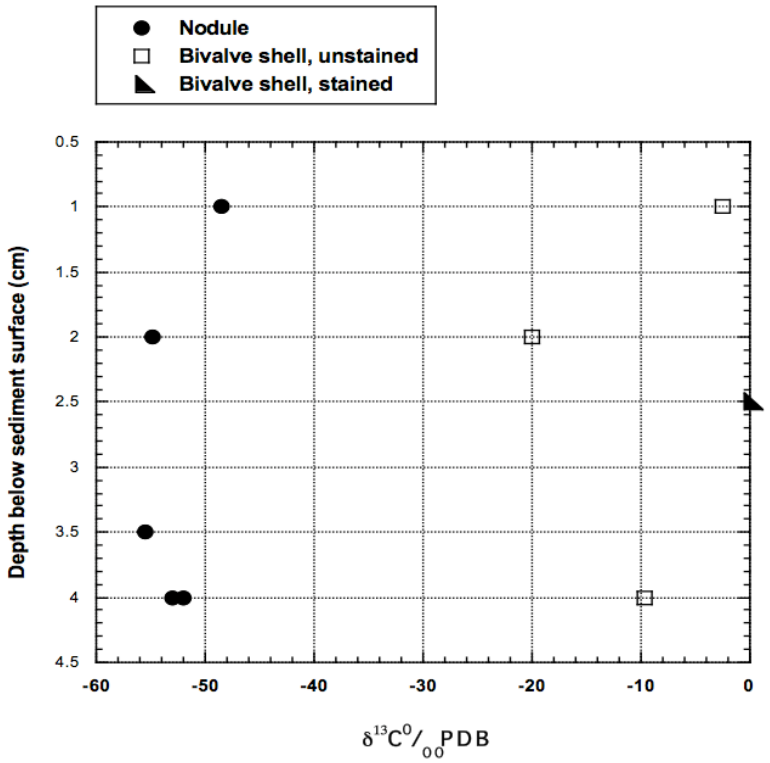

Figure 4.9. Non–foraminiferal carbonate isotope results from Rock Garden Station 198, Bear's Paw, showing extreme depletion of $\delta^{13}C$ in authigenic carbonates, and greater depletion in unstained bivalve shells than in the stained shell.

Table 4.6. Stable isotope values for non-foraminiferal carbonates from Rock Garden station 198, Bear's Paw 2.

Depth below sediment surface (cm)	**Type of carbonate**	**$d^{13}C^{0}/_{00}$ PDB**	**$d^{18}O^{0}/_{00}$ PDB**
1.0-1.5	Nodule	-48.53	2.91
1.0-1.5	*Calyptogena* sp. shell unstained	-2.53	3.11
2.0-2.5	*Calyptogena* sp. shell unstained	-19.99	3.20
2.0-2.5	Nodule	-54.85	4.90
2.5-3.0	*Calyptogena* sp. shell stained	-0.04	2.75
3.5-4.0	Nodule	-55.41	3.99
4.0-4.5	*Calyptogena* shell unstained	-9.68	3.99
4.0-4.5	Nodule	-51.93	4.62
4.0-4.5	Nodule	-52.96	3.38

4. Discussion

4.1 Foraminiferal assemblage

Results from the Hikurangi Margin are consistent with studies of foraminiferal assemblages from other modern cold seeps as well as fossil seeps from the Cascadia Margin. No endemic seep taxa were present in the Hikurangi Margin seeps, and all species found in this study have been documented in normal marine environments around New Zealand (Hayward et al., 1999; Hayward et al., 2001). The dominant species in these seeps, *Uvigerina peregrina*, is a major component of normal marine environments and seep assemblages worldwide, both modern and fossil (Jones, 1993; Rathburn et al., 2000; Rathburn et al., 2003; Torres et al., 2003; Heinz et al., 2005; Erbacher and Nelskamp, 2006; Wiedecke and Weiss, 2006; Martin et al., 2007). It has demonstrated an ability to survive in methane seeps and dysoxic environments (Sen Gupta and Aharon, 1994; Rathburn et al., 2000; Bernhard et al., 2001; Hill et al., 2004). Other taxa present on the Hikurangi Margin that have been found in seeps or dysoxic environments include *Bulimina aculeata, Bulimina marginata, Bolivina seminuda, Cassidulina carinata*, *Fursenkoina complanata*, *Globobulimina pacifica*, *Hoeglundina elegans*, *Oridorsalis umbonatus,* and *Sigmoilopsis schlumbergeri,* as well as species of *Gyroidinoides* and *Pyrgo*. (e.g. Rathburn et al., 2000: Rathburn et al., 2003; Martin et al., 2004; Heinz et al., 2005; Panieri and Sen Gupta, 2008). The foraminiferal assemblages of the Hikurangi Margin are thus taxonomically comparable to those in other modern cold seeps.

The single distinction between the seep and reference assemblages of this study is the proportion of agglutinate species. With 45% of its assemblage comprising agglutinate individuals, the reference core was unique among the cores sampled. Panieri and Sen Gupta (2008), working at Blake Ridge, and Heinz et al. (2005), working on Hydrate Ridge, noted similar results. The non-seep samples in their areas contained a considerably larger number of agglutinate foraminifers than did the seep samples. Conversely, Bernhard et al. (2001) observed an agglutinate foraminifer as the only species found strictly in seep samples. It has been suggested

that agglutinate species, in general, are less tolerant of seep gases and low oxygen conditions (Panieri and Sen Gupta, 2008) and that they are responding to a change in food supply in non-seep areas (Heinz et al., 2005). There is, however, no conclusive explanation for the presence or absence of agglutinate species in seep environments. The numbers of agglutinated foraminifera at Stations 186 (Bear's Paw), 291 (North Tower), and 309 (Takahae) suggest that the relationship between methane seepage and agglutinate foraminifera is complex.

Foraminiferal density also reveals dissimilarities among sites. The most significant difference is that between Station 216 (LM3) and all other stations. The average density at LM3 is more than an order of magnititude greater than the next highest density at Station 198 (Bear's Paw 2). It is probable that the greater number of foraminifera at Station 216 (LM3) is due to the much shallower depth (662 m) at this station, with its resulting increase in productivity yielding a better food supply than at the deeper stations. In addition, Rock Garden has the highest temperatures of the three sites (6.7°C to 7.2ºC) (Faure et al., this volume) which may provide a more equitable environment for foraminifera. Among the remaining stations, densities in the two Bear's Paw seeps (Stations 186 and 198) were relatively consistent, whereas those at the two Kaka seeps differed considerably, with Station 242 (Kaka 1) displaying 46 individuals/cm^3 while Station 261 (Kaka 2) had an average density of only 8 individuals/cm^3. The reference core (Station 262) had a density of 17 individuals/cm^3, which was at the lower end of the density spectrum for these samples. Nonetheless, this finding does not distinguish the reference core from seep cores on the basis of density, because two seep cores had lower densities. The lowest density, two individuals/cm^3, occurred at Station 309 (Takahae). The sediment surface at this station was covered by a white bacterial mat, and the top 2.0 cm of the sediment itself were extremely "fluffy" and contained few foraminifera. With regard to foraminiferal densities under bacterial mats, other modern seeps are inconsistent. Erbacher and Nelskamp (2006) reported finding density lower under bacterial mats, whereas Heinz et al. (2005) found densities slightly higher under bacterial mats than in other nearby stations. Thus the

significance of the lower density at Takahae is not clear. Density patterns from the Hikurangi Margin are comparable to those from Monterey Bay obtained by Rathburn et al. (2003) who concluded that foraminiferal densities are not impacted by cold seeps. This is also in agreement with the findings of Panieri and Sen Gupta (2008) who observed remarkable variability in the foraminiferal densities of the Blake Ridge mound. Given the heterogeneity in density distributions, it is likely the variable abundances are due to the normal patchiness of foraminiferal distribution in deep sea sediments (Robinson et al., 2004; Erbacher and Nelskamp, 2006), variable food availability (Heinz et al., 2005), or small–scale fluctuations in environmental conditions (Treude et al., 2003).

It is interesting to note that both density and species richness peaked downcore from the sediment surface (Figure 4.3,4.5). Both parameters rose markedly in the 1.0 to 1.5 cm interval, and from there to the bottom of the core remained higher than they were from 0 to 1.0 cm depth, although with fluctuations throughout the remaining length of the core. This is inconsistent with some other studies, such as results from the northeast Arabian Sea, where abundances are greatest in the "fluff" at the sediment surface and drop sharply downcore (Erbacher and Nelskamp, 2006). On the other hand, in Monterey Bay seeps, Rathburn et al. (2003) reported that maximum densities occurred between 2 and 4 cm below the sediment surface. The peak abundances of infaunal species such as *Globobulimina pacifica* and *Uvigerina peregrina* were found as deep as 4 cm below the sediment surface. It is therefore probable that the downcore patterns in the Hikurangi Margin samples are due to the dominance of *Uvigerina peregrina,* a shallow infaunal species that reaches its peak abundance below the sediment/water interface (Figure 4.2).

Diversity of the foraminiferal assemblages reveals a somewhat different picture (Figure 4.6). As measured by both the Simpson and Shannon indices, the highest diversity occurs in the two Bear's Paw seep samples (Stations 186 and 198), which displayed nearly identical Simpson indices, and very similar Shannon indices. The lowest diversity was found in the two Wairarapa seeps (Stations 291

and 309), with Station 309 yielding the lowest diversities in both indices. The two samples from the Kaka seeps (stations 242 and 261) differed in their diversities, as they did in density. Once again, the reference core (Station 262) is not differentiated. In their study of the Blake Ridge Mound, Panieri and Sen Gupta (2008) reported no appreciable difference between the diversities of foraminiferal assemblages under bacterial mats and other seep assemblages, but they did report the highest diversity in their control sample. In addition, lower foraminiferal diversities in seep samples were reported from the Adriatic Sea (Panieri, 2003), the Rockall Trough (Panieri, 2005), and the northeast Arabian Sea (Erbacher and Nelskamp, 2006). The diversity distribution of the Hikurangi Margin samples is therefore inconsistent with other modern cold seeps. Again, this could be explained by normal patchiness found in deep-sea sediments, or it could result from methane release that is intermittent or of short duration. It is clear, however, that the foraminiferal assemblages of the Hikurangi Margin do not reflect differences that can be attributed to methane seepage alone. The exception to this may be the extremely low density and diversity at Station 309 (Takahae). Four species in this seep, *Bulimina marginata, Gyroidinoides soldanii, Oridorsalis umbonatus,* and *Uvigerina peregrina,* all presented stained specimens, indicating some foraminifera were recently living. All of these species have been found living in other modern seeps (Sen Gupta and Aharon, 1994; Rathburn et al., 2003; Martin et al., 2004; Robinson et al., 2004). In their study of Hydrate Ridge on the Cascadia Margin, Sahling et al. (2002) noted a distinct zonation in which mat–forming bacteria directly overlie gas hydrates and maximum hydrogen sulphide venting. As sulphide concentrations decrease, bacterial mats give way to a zone of vesicomyid bivalves, then to a zone of solemyid bivalves. Similar zonation has been noted in the seeps of Monterey Bay (Rathburn et al., 2003). The presence of bacterial mats at Station 309 (Takahae) indicates the area is subject to high sulphide fluxes. It is thus possible that this sulphide concentration killed or drove away the majority of foraminifera, leaving only those species capable of tolerating the extreme conditions.

4.2 Stable isotopes

Carbon stable isotope data from foraminifera on the Hikurangi Margin display clear indication of the effects of methane-influenced pore waters. Even the least depleted $\delta^{13}C$ values from seep sites are more depleted and variable than those from the non-seep sites. Consistent with other studies of modern seeps, $\delta^{13}C$ values are not in equilibrium with present day pore water $\delta^{13}C$ values (c.f. Rathburn et al., 2003). For example, at Omakere Ridge stations 186 and 198, the stations with the most depleted foraminiferal carbonate in this study, $\delta^{13}C$ of tests goes as low as –33.46‰ PDB and –35.70‰ PDB respectively. Pore water $\delta^{13}C$ at this site ranges between –75.6 ‰ PDB and –66.5 ‰ PDB (Haeckel, unpublished data). The most depleted pore waters among the samples studied occurred at North Tower, with values ranging between –80.5‰ PDB and –64.5‰ PDB (Haeckel, unpublished data) whereas the foraminiferal carbonate at North Tower ranged between –5.68‰ PDB and +3.16‰ PDB, highly variable, but distinctly different from pore water values. The foraminiferal carbonate $\delta^{13}C$ values are undoubtedly the result of mixing of fluids from different sources including ambient seawater and methane-influenced fluids. Also consistent with results from studies of other modern seeps, $\delta^{13}C$ values of foraminiferal carbonate at all stations except the reference station (Station 262) are considerably more variable than values from normal seawater (Figure 4.7) (cf Rathburn et al., 2003; Torres et al. 2003). Interestingly, the least variable seep samples were those found in areas of "raindrop" texture (ampharetid polychaetes), stations 242, 261 (Kaka seeps), and 309 (Takahae). The reason for this is unclear. Sommer et al. (this volume), reported that these sites display exceptionally high oxygen uptake, with over 60% of the oxygen consumed by the ampharetids. It is possible that the intense biological activity in these dense beds of polychaetes resulted in more uniform irrigation of the sediments and less variable micro-habitats than are found in other seep sites. This would certainly reinforce the suggestion of Bernhard et al. (2001) that aerobic microhabitats in seeps may be

created through the action of other biota and that foraminifera may seek out these environments.

The striking differences in ^{13}C depletion of foraminifera and variability among these seeps may be due to differences in venting characteristics. Faure et al. (this volume) found seepage at the Rock Garden site LM3 is constant, but diffusive, and may be waning. In contrast, Omakere Ridge is actively venting, with activity particularly high at Bear's Paw. The most active area, however, is Wairarapa, although the greatest activity was not at North Tower or Takahae. Thus, the depletion and variability in foraminiferal $\delta^{13}C$ values is likely related to the strength of venting activity.

The separation of the geographic areas based on $\delta^{18}O$ values is distinctive and puzzling (Figure 4.8). Temperature would be the simplest explanation for this difference; however, Faure et al. (this volume) measured bottom water temperatures and reported that temperatures at Rock Garden (LM3, Station 216) ranged between 6.7°C and 7.2°C, those at Omakere Ridge (Bear's Paw, Stations 186, 198) between 4.4°C and 4.9°C, and at Wairarapa, the range was 4.9°C to 5.5°C. Thus, the isotopic differences are not explained by temperature because Wairarapa should display more enriched $\delta^{18}O$ values than Rock Garden. Another possibility is dissociation of methane hydrates with the resulting enrichment of ^{18}O in surrounding waters. However, pore water chloride data do not support this hypothesis (Haeckel, unpublished data). The oxygen isotopic anomaly between Rock Garden and Wairarapa is undergoing further investigation and will be reported in a later paper.

Depleted carbon isotopes in foraminiferal tests raise a number of questions. Primary among these is whether foraminifera actually live and mineralize in cold seeps. Numerous studies have concluded that various species of foraminifera live in seeps (e.g. Sen Gupta et al., 1997; Bernhard et al., 2001; Hill et al., 2003; Rathburn et al., 2003; Heinz et al., 2005; Mackensen et al., 2006). Most of these studies, however, relied on Rose Bengal to identify living foraminifera. This stain has been demonstrated to have significant limitations for this application, because it stains

cytoplasm regardless of whether the organism is living or dead, and foraminiferal cytoplasm has been shown to remain in the test for weeks after death (Bernhard, 1988). In Monterey Bay, Bernhard et al. (2001) used three methods to identify living foraminifera, including Rose Bengal (for comparison), adenosine triphosphate assay (ATP), and ultrastructural studies. The ATP data indicated that foraminifera did, indeed, inhabit methane seeps in Monterey Bay. The mechanism for survival of these aerobic organisms in seep environments is, as yet, unclear. Ultrastructural studies in the Monterey Bay seep foraminifera revealed no endosymbionts, although one specimen of *U. peregrina* had prokaryotes associated with its pore plugs, leading Bernhard et al. (2001) to suggest these may enable the foraminifera to survive in seeps. In addition, an unusually large number of perixosomes was discovered in the seep foraminifera, prompting speculation that the anaerobic metabolic pathways utilized in these may provide the survival mechanism. Peroxisomes, on the other hand, provide other cellular metabolic functions and their proliferation may be unrelated to anoxia in seeps. Bernhard and Bowser (2008) further investigated this idea and hypothesized that in some foraminifera, environmentally and metabolically produced H_2O_2 is converted to water and oxygen, and the latter is used in foraminiferal respiration. Clearly, the question of foraminiferal survival in cold seeps is as yet unanswered.

Foraminiferal test mineralization is based on seawater vacuolization, which renders them extremely valuable in paleoecologic reconstructions (Erez, 2003). Thus, it is expected that foraminiferal carbonate should faithfully record the isotopic signature of surrounding pore waters. Unfortunately, carbon isotopes from cold seep foraminifera have been demonstrated to be in marked disequilibrium with surrounding pore waters (Rathburn et al., 2003; Torres et al., 2003). Again, the reason for this is unclear, although a number of suggestions have been made. In their study of laminated sediments in the Santa Barbara Basin, Bernhard and Bowser (1999) suggested foraminifera may migrate into and out of seeps, which would result in isotopic disequilibrium of the foraminifera that only calcified in less toxic environments. Sen Gupta et al. (1997) observed a thickened organic lining in

Cassidulina neocarinata in Gulf of Mexico seeps, leading them to speculate that the foraminifer might become dormant during periods of environmental stress. Again, this would lead to isotopic disequilibrium if calcification only took place when seepage was less intense or absent. If foraminiferal pseudopodia do extend from anoxic to oxic microhabitats within seeps, it is conceivable they could incorporate a mixture of ^{13}C-depleted and undepleted seawater into their vacuoles during the mineralization process. Finally, the incorporation of depleted metabolic carbon resulting from the ingestion of methanotrophic prokaryotes is a possible explanation for at least some of the depletion observed in foraminiferal carbonate in cold seeps.

4.3 Diagenesis

Because cold seep sediments are inherently saturated in $CaCO_3$, precipitation of authigenic calcite is to be expected. The occurrence of small calcite nodules is consistent with this (see also Campbell et al., this volume), as are the carbon isotope values of the vesicomyid shells. The greater depletion of the unstained shells with respect to the stained shell suggests post-depositional alteration. In most studies of carbon isotopes in seep foraminifera, the greatest $\delta^{13}C$ depletion is found among unstained (dead) specimens (e.g. Rathburn et al., 2003), although Mackenson et al. (2006) noted lower $\delta^{13}C$ values in living foraminifera from the Hakon Mosby mud volcano in the Barents Sea. Although the SEM images from the Hikurangi Margin foraminifera reveal apparently pristine foraminiferal tests (Figure 4.10), the presence of authigenic carbonates and depleted unstained bivalve shells suggest the possibility of post-depositional alteration of foraminiferal tests. Clearly, this question warrants further exploration, which is presently being done using Mg/Ca ratios, and will be reported in a later publication.

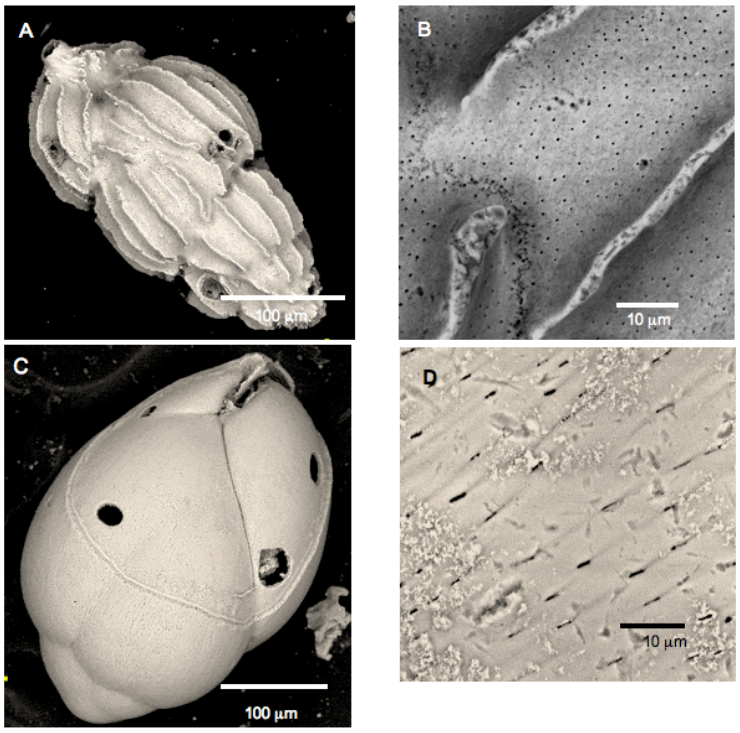

Figure 10. SEM images representative of foraminifera used in isotope analyses. A. *Uvigerina peregrina,* entire specimen. B. *U. peregrina* at high magnification, where the surface shows no apparent authigenic overgrowths, and pores are clean and sharp–edged. C. *Globobulimina pacifica*, entire specimen. D. *G. pacifica* at high magnification, showing no apparent authigenic overgrowths. This specimen was not cleaned before being imaged, thus there is dirt on the surface.

5. Conclusions

1. The foraminiferal assemblage data from Hikurangi Margin cold seeps do not provide a definitive mechanism for identifying or characterizing seep and non-seep sites. Although there are clear differences in some parameters, particularly the distribution of agglutinate species and assemblage diversity, these are generally inconclusive and could be attributable to the normal patchiness of deep-sea foraminiferal distribution.
2. Carbon isotope data, on the other hand, are clear in differentiating seep and non-seep cores. The reference core is distinct from the seep cores in containing carbon isotope signatures that are all near 0‰ PDB, and vary within narrow limits. Foraminiferal carbonates from seep sites, on the other

hand, show substantial depletion in $\delta^{13}C$, as well as considerable variability in these values. The heterogeneity of isotope values can be attributed to the mixing of pore waters and ambient seawater, possible multiple sources of hydrocarbons, and the tortuosity of fluid-flow pathways.

3. Differences in variability and depletion of $\delta^{13}C$ in foraminiferal carbonate are due largely to differences in fluid-flow regimes. Where CH_4 is actively venting, such as at Bear's Paw, $\delta^{13}C$ values are more variable and depleted than they are where seepage is diffusive and less active (LM3).
4. The $\delta^{18}O$ distinction between Rock Garden and Wairarapa is as yet unexplained.
5. Non-foraminiferal carbonates, particularly the inorganic nodules, provide substantial reinforcement to the oxidized methane origin of much of the carbonate in the pore waters.
6. The results of this study are consistent with findings in other modern seeps worldwide and in the fossil record. Heterogeneity of foraminiferal assemblages and carbon isotopes is a feature of cold hydrocarbon seeps that is recognized regularly in modern cores and in the rock record. Thus it is not an artifact of taphonomy and time averaging, but a typical aspect of foraminiferal assemblages in ancient seeps (Martin et al., 2007)
7. Although SEM imaging suggests the foraminifera analyzed were largely pristine, there is a possibility of at least a small amount of diagenetic alteration. This warrants further investigation using Mg/Ca analyses to verify the foraminiferal carbonate as primary. Regardless of whether the most depleted values of $\delta^{13}C$ are from primary or secondary calcite, it appears that foraminifera are a convenient repository for depleted carbon, and provide reliable records of the presence of oxidized methane in sediments, either while they mineralize or during the diagenetic process. They thus become archives documenting the passage of ^{13}C-depleted pore waters and the heterogeneity of fluid-flow pathways near the sediment-water interface.

Acknowledgements

I wish to thank the officers and crew of RV SONNE for their expertise and efficiency. The scientific community on board provided many stimulating discussions. The cruise was funded by BMBF (the German Federal Ministry for Education and Research). Funding for travel and for analyses was provided by the Marsden Fund Council for government funding, administered by the Royal Society of New Zealand, and a University of Washington Department of Earth and Space Sciences Graduate Research Award. I also thank David Mucciarone of Stanford University and Andrew Schauer of the University of Washington for their assistance with isotope analyses, and Ed Hare for SEM imaging. Thank you, also, to Bruce Hayward for providing materials for identification of foraminifera, and to Matthias Haeckel for pore water data.

Notes to Chapter 4

Akimoto, K., Tanaka, T., Hattori, M., Hotta., 1994. Recent foraminiferal assemblages from the cold seep communities - A contribution to the methane gas indicator. In Tuschi, R. (Editor), Pacific Neogene Events in Time and Space. University of Tokyo Press, Tokyo, pp. 11-25.

Barbieri, R., Panieri, G., 2004. How are benthic foraminiferal faunas influenced by cold seeps? Evidence from the Miocene of Italy. Palaeogeogr. palaeoclimatol. palaeoecol., 204: 257-275.

Barnes, P.M., Lamarche, G., Bialas, J., Henrys, S., Pecher, I., Netzeband, G.L., Greinert, J., Mountjoy, J.J., Pedley, K., Crutchley, G., this volume. Tectonic amd geological framework for gas hydrates and cold seeps on the Hikurangi subduction margin, New Zealand. Marine Geology.

Bernhard, J.M., 1988. Postmortem vital staining in benthic foraminifera: Duration and importance in population and distributional studies. J. foraminifer res., 18: 143-146.

Bernhard, J.M., Bowser, S.S., 1999. Benthic foraminifera of dysoxic sediments: chloroplast sequestration and functional morphology. Earth-sci. rev., 46(1-4): 149-165.

Bernhard, J.M., Bowser, S.S., 2008. Perixosome proliferation in foraminifera inhabiting the chemocline: An adaptation to reactive oxygen species exposure? Journal of eukaryotic microbiology, 55(3): 135-144.

Bernhard, J.M., Buck, K.R., Barry, J.P., 2001. Monterey Bay cold-seep biota: Assemblages, abundance, and ultrastructure of living foraminifera. Deep-sea res., Part 1, Oceanogr. res. pap., 48: 2233-2249.

Bernhard, J.M., Ostermann, D.R., Williams, D.S., Blanks, J.K., 2006. Comparisons of two methods to identify live benthic foraminifera: a test between Rose Bengal and Cell Tracker Green with implications for stable isotope paleoreconstructions. Paleoceanography, 21: doi: 10.1029/2006PA001290 (PA 4210).

Buzas, M.A., 1979. The Measurement of Species Diversity. In: J.H. Lipps, W.H. Berger, M.A. Buzas, R.G. Douglas and C.A. Ross (Editors), Foraminiferal Ecology and Paleoecology. SEPM Short Course: 3-10.

Campbell, K.A., Nelson, C.S., Alfaro, A.C., Boyd, S., Greinert, J., Nyman, S.L., Grosjean, E., Logan, G.A., Gregory, M.R., Cooke, S., Linke, P., Milloy, S., Wallis, I. Geological imprint of methane seepage on the seabed and biota of the convergent Hikurangi Margin, New Zealand: survey of core and grab carbonates. Mar. Geol., this volume.

Corliss, B.H., 1985. Microhabitats of benthic foraminifera within deep-sea sediments. Nature, 314: 435-438.

DeJong, T.M., 1975. A comparison of three diversity indices based on their components of richness and evenness. OIKOS, 26: 222-227

Erbacher, J., Nelskamp, S., 2006. Comparison of benthic foraminifera inside and outside a sulphur-oxidizing bacterial mat from the oxygen-minimum zone off Pakistan (NE Arabian Sea). Deep-sea res., Part 1, Oceanogr. res. pap., 53: 751-775.

Erez, J., 2003. The source of ions for biomineralization in Foraminifera and their implications for paleoceanographic proxies. Rev. mineral. geochem., 54: 115-149.

Faure, K., Greinert, J., Pecher, I., Graham, I.J., Massoth, G.J., De Ronde, C.E.J., Wright, I.C., Baker, E.T., Olson, E.J., 2006. Methane seepage and its relation to slumping and gas hydrate at the Hikurangi Margin, New Zealand. N.Z. J. Geol. Geophys., 49: 503-516.

Faure, K., Greinert, J., Schneider von Deimling, J., McGinnis, D.F., Kipfer, R, Linke, P., Methane seepage along the Hikuangi Margin of New Zealand: geochemical and physical evidence from the water column, sea surface and atmosphere. Mar. Geol. this volume.

Geslin, E., Heinz, P., Jorissen, F., Hemleben, C., 2004. Migratory responses of deep-sea benthic foraminifera to variable oxygen conditions: laboratory investigations. Marine Micropaleontology, 53: 227–243.

Hayward, B.W., Grenfell, H.R., Reid, C.M. and Hayward, K.A., 1999. Recent New Zealand shallow-water benthic foraminifera: Taxonomy, ecologic distribution, biogeography, and use in paleoenvironmental assessment. Institute of Geological and Nuclear Sciences Monograph 21 (New Zealand Geological Survey paleontological bulletin 75): 258 pp.

Hayward, B.W., Carter, R., Grenfell, H.R., Hayward, J.J., 2001. Depth distribution of Recent deep-sea benthic foraminifera east of New Zealand, and their potential for improving paleobathymetric assessments of Neogene microfaunas. N.Z. J. Geol. Geophys., 44: 555–587.

Heinz, P., Sommer, S., Pfannkuche, O., Hemleben, C., 2005. Living benthic foraminifera in sediments influenced by gas hydrates at the Cascadia convergent margin, NE Pacific. Mar. ecol., Prog. ser., 304: 77–89.

Hill, T.M., Kennett, J.P., Valentine, D.L., 2004. Isotopic evidence for the incorporation of methane-derived carbon into foraminifera from modern methane seeps, Hydrate Ridge, Northeast Pacific. Geochim. cosmochim. acta Acta, 68: 4619-4627.

Hill, T.M., Kennett J.P., Spero, H.J., 2003. Foraminifera as indicators of methane-rich environments: A study of modern methane seeps in Santa Barbara Channel, California. Marine Micropaleontology, 49: 123-138.

Jones, R.W., 1993. Preliminary observations on benthonic foraminifera associated with biogenic gas seep in the North Sea. In: D.G. Jenkins (Editor), Applied Micropaleontology. Kluwer Academic Publishers, Dordrecht, pp. 69-91.

Kennett, J.P., Cannariato, K.G., Hendy, I.L., Behl, R.J., 2003. Methane Hydrates in Quaternary Climate Change: The Clathrate Gun Hypothesis. AGU Special Publication, 54, 216 pp.

Levin, L.A., 2005. Ecology of cold seep sediments: Interactions of fauna with flow, chemistry, and microbes. Oceanogr. Mar. Biol. an annual review, 43: 1-46.

Lewis, K.B. and Marshall, B.A., 1996. Seep faunas and other indicators of methane-rich dewatering on New Zealand convergent margins. N.Z. J. Geol. Geophys., 39: 181-200.

Lewis, K.B., Pettinga, J.R., 1993. The emerging, imbricate frontal wedge of the Hikurangi Margin. In: P.F. Ballance (Editor), Sedimentary Basins of the World 2: Basins of the South West Pacific. Elsevier Science Publishers, Amsterdam, pp. 225-250.

Linke, P., Lutze, G.F., 1993. Microhabitat preferences of benthic foraminifera – a static concept or a dynamic adaptation to optimize food acquisition? Marine Micropaleontology, 20: 215-234.

Mackensen, A., Wollenburg, J., Licari, l., 2006. Low $\delta^{13}C$ in tests of live epibenthic and endobenthic foraminifera at a site of active methane seepage. Paleoceanography, 21: PA2022, doi:10.1029/2005PA001196,2006.

Martin, J.B., Day, S.A., Rathburn, A.E., Perez, M.E., Mahn, C., Gieskes, J., 2004. Relationships between the stable isotopic signatures of living and fossil foraminifera in Monterey Bay, California. Geochem. geophys. geosyst., 5: Q04004, doi:10.1029/2003GC000629.

Martin, R.A., Nesbitt, E.A., 2005. Benthic foraminiferal characteristics of Cenozoic cold seeps on the Northeast Pacific margin, Abstracts volume, AAPG Annual Convention, Calgary: p. A87.

Martin, R.A., Nesbitt, E.A., Campbell, K.A., 2007. Carbon stable isotopic composition of benthic foraminifera from Pliocene cold methane seeps, Cascadia accretionary margin. Palaeogeogr. palaeoclimatol. palaeoecol., 246: 260-277.

Maslin, M., Mikkelsen, N., Vilela, C., Haq, B., 1998. Sea-level- and gas-hydrate-controlled catastrophic sediment failures of the Amazon Fan. Geology, 26: 1107-1110.

McCorkle, D.C., Corliss, B.H., Farnham, C.A., 1997. Vertical distributions and stable isotopic compositions of live (stained) benthic foraminifera from the North Carolina and California continental margins. Deep-sea res., Part 1, Oceanogr., 44(6): 983-1024.

Moodley, L., van der Zwaan, G.J., Rutten, G.M.W., Boom, R.C.E., Kempers, A.J., 1998. Subsurface activity of benthic foraminifera in relation to porewater oxygen content: laboratory experiments. Marine Micropaleontology, 34: 91-106.

Panieri, G., 2003. Benthic foraminifera response to methane release in an Adriatic Sea pockmark. Riv. ital. paleontol. stratigr., 109(3).

Panieri, G., 2005. Benthic foraminifera associated with a hydrocarbon seep in the Rockall Trough (NE Atlantic). Geobios, 38: 247-255.

Panieri, G., Sen Gupta, B.K., 2008. Benthic foraminifera of the Blake Ridge hydrate mound, Western North Atlantic Ocean. Marine Micropaleontology, 66: 91-102.

Paull, C.K., Buelow, W.J., Ussler, W., III, Borowski, W.S., 1996. Increased continental-margin slumping frequency during sea-level lowstands above gas hydrate-bearing sediments. Geology, 24: 143-146.

Rathburn, A.E., Corliss, B.H., 1994. The ecology of living (stained) deep-sea benthic foraminifera from the Sulu Sea. Paleoceanography, 9: 87-150.

Rathburn, A.E., Levin, L.A., Held, Z. and Lohmann, K.C., 2000. Benthic foraminifera associated with cold methane seeps on the northern California margin: Ecology and stable isotopic composition. Marine Micropaleontology, 38: 247-266.

Rathburn, A.E., Perez, M.E., Martin, J.B., Day, S.A., Mahn, C., Gieskes, J., Ziebis, W., Williams, D., Bahls, A., 2003. Relationships between the distribution and stable isotopic composition of living benthic foraminifera and cold methane seep biogeochemistry in Monterey Bay, California. Geochem. geophys. geosyst., 4: 1106, doi:10.1029/2003GC000595, 2003.

Robinson, C.A., Bernhard, J.M., Levin, L.A., Mendoza, G.F., Blanks, J., 2004. Surficial hydrocarbon seep infauna from the Blake Ridge (Atlantic Ocean, 2150 m) and the Gulf of Mexico (690-2240 m). P.S.N.Z.: Marine Ecology, 25: 313-336.

Sahling, H., Rickert, D., Lee, R.W., Linke, P. and Suess, E., 2002. Macrofaunal community structure and sulphide flux at gas hydrate deposits from the Cascadia convergent margin, NE Pacific. Mar. ecol., Prog. ser., 231: 121-138.

Sassen, R., MacDonald, I., 1998. Bacterial methane oxidation in sea-floor gas hydrate: Significance to life in extreme environments. Geology, 26: 851-854.

Sen Gupta, B.K., Aharon, P., 1994. Benthic foraminifera of bathyal hydrocarbon vents of the Gulf of Mexico: Initial report on communities and stable isotopes. Geo–Marine Letters, 14: 88-96.

Sen Gupta, B.K., Platon, E., Bernhard, J.M., Aharon, P., 1997. Foraminiferal colonization of hydrocarbon-seep bacterial mats and underlying sediment, Gulf of Mexico slope. J. foraminifer. res., 27(4): 292-300.

Sommer, S., Linke, P., Pfannkuche, O., Niemann, H., Treude, T., Benthic respiration in a novel seep habitat dominated by dense beds of ampharetid polychaetes at the Hikurangi Margin (New Zealand). Mar. Geol., this volume.

Torres, M.E., Mix, A.C., Kinports, K., Haley, B., Klinkhammer, G., McManus, J., DeAngelis, M.A., 2003. Is methane venting at the seafloor recorded by $\delta^{13}C$ of benthic foraminifera shells? Paleoceanography, 18(3): doi:10.1029/2002PA000824.

Treude, T., Boetius, A., Knittel, K., Wallmann, K., Jorgensen, B.B., 2003. Anaerobic oxidation of methane above gas hydrates at Hydrate Ridge, N.E. Pacific Ocean. Mar. ecol., Prog. ser., 264: 1-14.

Wiedicke, M., Weiss, W., 2006. Stable carbon isotope records of carbonates tracing fossil seep activity off Indonesia. Geochem. geophys. Geosyst., 7(11): Q11009, doi:10.1029/2006GC001292.

Chapter 5. Assessing Post-Depositional Alteration of Foraminiferal Shells in Cold Seep Settings

1. Introduction

This chapter reports initial findings from a pilot investigation assessing diagenesis in foraminifera from Cenozoic cold seeps of the Cascadia margin. Undertaken in collaboration with Prof. Marta Torres and Prof. Gary Klinkhammer of the College of Atmospheric and Oceanic Sciences (COAS), Oregon State University, this study uses an innovative technique developed at the COAS to measure elemental ratios in both biogenic and authigenic carbonates.

Carbonate precipitation is ubiquitous in cold methane seeps, the result of methanogenesis and anaerobic oxidation of methane (AOM) performed by a consortium of methane-oxidizing archaea and sulfate-reducing bacteria (Hinrichs et al., 1999; Boetius et al., 2000). AOM results in increased alkalinity and super-saturation of HCO_3^-, with the carbon carrying the isotopic signature of the CH_4 from which it was derived. This carbon is available to be incorporated into $CaCO_3$ precipitated authigenically in the sediments, and can also be used by organisms performing biomineralization. These authigenic and biogenic carbonates then become a record of the passage of methane-derived fluids in the rock record. Results of investigations reported in earlier chapters of this volume demonstrate that because foraminifera are numerous, widely distributed even in areas of in methane seepage, and relatively easily extracted from marine sediments, the chemical signals in their calcareous shells should be ideal for characterizing methane-influenced fluid flow and sources of methane in cold seeps.

The use of foraminiferal carbonate as a proxy in paleoenvironmental reconstruction is well established in areas of marine sedimentation unaffected by hydrocarbon fluid-flow (e.g. Kennett and Stott, 1991; Lear et al., 2000; Pearson et al., 2001; Zachos et al., 2001; Billups and Schrag, 2002; Lear et al., 2003). A major difficulty with using foraminiferal shells in paleoenvironmental reconstructions lies in ascertaining whether the isotopic signal is primary or secondary, especially in

areas where climate models and data disagree (e.g. Veizer et al., 2000). Many carbon isotopic excursions noted in the geologic record have been observed in samples collected away from non-seep environments, where authigenic carbonate precipitation may be minimal (e.g. Kennett and Stott, 1991), In contrast, significant post-depositional isotopic overprinting is well established at sites of active seepage and intense carbonate formation (e.g. Millo et al., 2005; Torres et al., 2003). The origin and nature of any overprint on the original shell material is important because methane-influenced authigenic carbonate is typically highly depleted in ^{13}C (e.g., Gieskes et al., 2005), such that a small post-depositional inorganic deposit on the shells may obscure the original biogenic signal.

Various studies have approached the problem of diagenetic overprinting on foraminiferal tests in different ways. The most common approaches are microscopic examination, either by light microscope or scanning electron microscope (SEM) (Hill et al., 2003), or by utilizing only living or recently dead specimens as determined by Rose Bengal staining (Rathburn et al., 2003; Heinz et al., 2005). SEM images of Cenozoic seep foraminifera (Figure 5.1) reveal how ambiguous these images can be with regard to alteration. Images may show foraminifera with nearly pristine test walls, open pores and minor contamination that could be removed with judicious cleaning (Figure 5.1a). However a much higher magnification reveals obvious diagenetic overgrowths (Figure 5.1b). Torres et al. (2003) used Mg/Ca analyses of foraminiferal shells to demonstrate geochemically that visual inspection is not always a reliable indicator of carbonate overgrowths or replacements in foraminifera, even in modern specimens. Residual carbonate encrustation was observed in both planktonic and benthic foraminiferal tests from Miocene seeps of Italy (Barbieri and Panieri, 2004), and geochemical evidence of diagenetic alteration was found in Pliocene seeps of the Cascadia margin (Torres et al., in prep.). Therefore, although it can be accurate in cases of obvious alteration, the use of imaging to establish the condition of foraminifera for paleoenvironmental reconstruction must be approached judiciously.

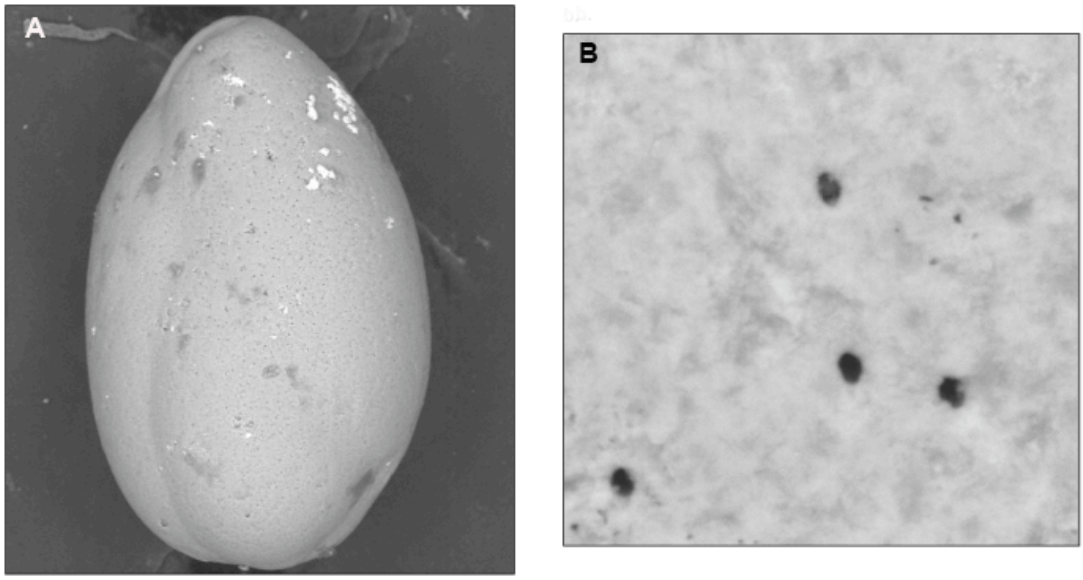

Figure 5.1. Representative scanning electron micrographs of foraminifera. A. Specimen of *Globobulimina pacifica* displaying minor surface contamination that can be removed with cleaning. Identical specimens were revealed to have undergone post-depositional alteration when analyzed for Mg/Ca ratio. B. Close-up micrograph of surface of another specimen of *G. pacifica*, clearly showing post-depositional deposits on the surface, but still preserving primary features such as pores.

One geochemical parameter in foraminiferal calcite that has been extensively used in paleoenvironmental reconstruction is the magnesium-to-calcium ratio (Mg/Ca) This has become an important proxy in paleothermometry and is widely used in assessing paleoclimate (Lear et al., 2000; Rosenthal et al., 2006; Ferguson et al., 2008). Use of Mg/Ca in paleotemperature analyses of biogenic calcite is based on experimental data that demonstrate the partition coefficient of Mg^{2+} in marine biogenic calcite strongly correlates with temperature (Lear et al., 2000 and references therein). On the other hand, the partition coefficient for Mg^{2+} in inorganically precipitated calcite is orders of magnitude higher than that of biogenic calcite (Nurnberg et al., 1996; Torres et al., 2003), thus in addition to its role in reconstructing paleotemperature, Mg/Ca can serve as a tracer for post-depositional contamination in foraminiferal shells.

Other geochemical proxies, though less well understood than Ma/Ca ratios,

are also extremely valuable in reconstructing past environments. Ba cycling for example, is closely coupled with methane fluxes and barite phases are known to occur at sites of fluid venting and at the methane-sulfate transition zone in methane-rich systems (Dickens, 2003). Thus, Ba/Ca ratios in foraminifera can be used to identify barite phases and serve as a proxy for methane venting episodes, as well as depth of fluid source.

Therefore, in order to better exploit the wealth of information in foraminiferal shells, I am involved in a collaborative study with Marta Torres and Gary Klinkhammer at the College of Oceanic and Atmospheric Sciences, Oregon State University, working to develop a systematic approach for reconstructing paleo-seepage information from the elemental and isotopic geochemical records of foraminifera.

2. Mg/Ca analysis of foraminiferal carbonate

2.1 Methods

Elemental ratios of recent foraminiferal tests and authigenic carbonates from Cenozoic methane seep sites using flow-through time-resolved analysis (FT-TRA) were preformed at the W.M. Keck Plasma Collaboratory, Oregon State University. FT-TRA is an online sequential leaching technique for cleaning and dissolving foraminiferal calcite. This is linked to an inductively-coupled-plasma-mass-spectrometer (ICP-MS). The system was developed by (Haley and Klinkhammer, 2002) using off-the-shelf-Dionex chromatographic components (Figure 5.2). The set-up uses an advanced gradient pump to push a continuous flow of eluants over the sample at constant flow rates.

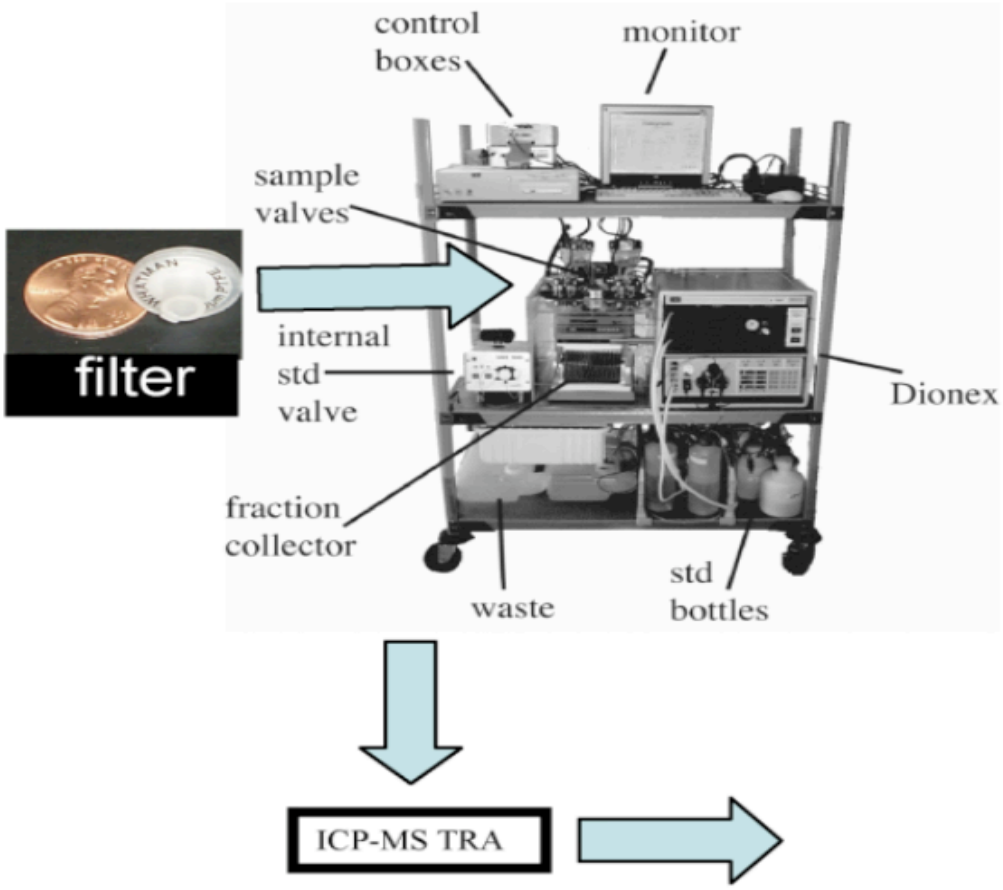

Figure 5.2. The flow through time-resolved-analysis system of the COAS at Oregon State University. See text for full explanation.

Together with a proportioning valve, the Dionex AGP module can control the composition, flow rate and pressure of the eluant that flows through the system. A heater maintains the eluant at a constant temperature, which in the case of foraminiferal analyses is set at 80 ± 2^{o}C. Different temperatures can be selected to optimize the reaction with the various leaching reagents. The eluate then passes from the sampling column into a mixing tee, where it mixes with a flow of 2M HNO_3 that has been spiked with internal standards (Be, Rh, In). It is split into two streams: one travels to the ICP-MS for real-time continuous analysis and the other goes to a fraction collector to gather discrete samples for post-run measurements as

needed. Additional valves in the system allow for the incorporation of rinsing steps within the analytical procedure, as well as for the injection of standard solutions to generate calibration curves. The incorporation of time-resolved analyses, using gradually increasing and highly regulated acid strengths, produces continuous records of elemental composition at various stages of digestion sorted by their dissolution susceptibility.

Data from FT-TRA are best displayed as chromatograms of dissolution curves with Ca concentration (ppm, left axis) and Mg/Ca ratio (mmol/mol, right axis) plotted *versus* time (Figure 5.3). The vertical dashed green lines can be adjusted as needed. In the case of foraminiferal analyses, they are used to denote the part of the plot that represents dissolution of the major part of the calcium carbonate shell. The area between the lines is used to generate the average elemental ratio for the run. The irregular Mg/Ca values at the beginning of the run are “noise” due to the low volume of Ca and Mg at that point in the run.

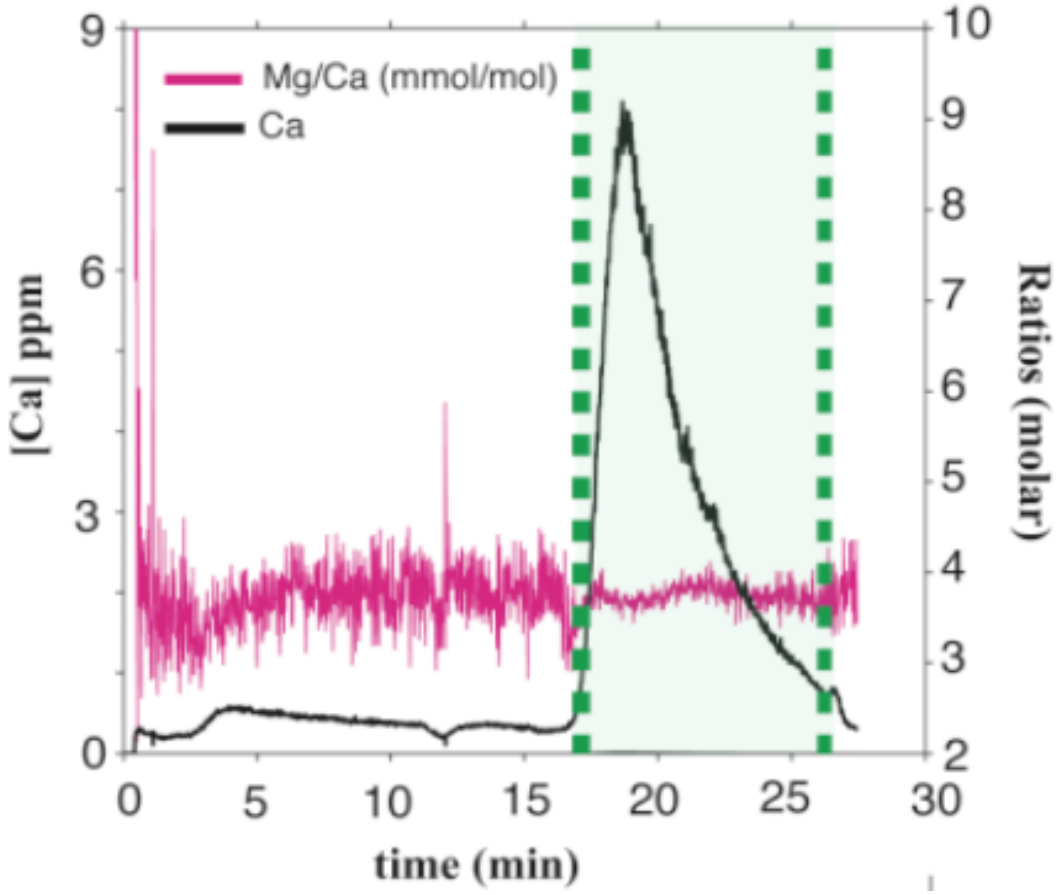

Figure 5.3. Typical chromatogram generated by FT-TRA. This example is from a calcite standard. Ca curve is black, Mg/Ca is magenta. Time given is the time of the analytical run. The area between the vertical dashed green lines is the part of the curve used to generate the average Mg/Ca and can be adjusted as necessary. The ragged section at the beginning of the magenta ratio curve results from "noise" due to low sample volume at the beginning of the run.

In addition to Mg/Ca, FT-TRA returns analyses of other minor or trace elements in the foraminiferal carbonate, including Ba, Sr, and Mn, thus yielding an enormous amount of data.

This innovative technique has been used successfully in various applications including identifying and characterizing diagenetic signals in foraminiferal carbonates from Recent sediments (Torres et al., 2003; Klinkhammer et al., 2004; Klinkhammer and Haley, 2006; Klinkhammer et al., 2009), but it has not previously been tested on fossil samples. For this initial test study, FT-TRA was

performed on selected specimens of fossil foraminiferal shells from the Eocene-Oligocene Keasey, Pysht and Sooke formations and Pliocene Quinault Formation of the Cascadia Margin. A duplicate set of foraminiferal shell calcite was previously analyzed for carbon and oxygen isotopes (this volume, chapters two and three). Prior to FT-TRA, foraminiferal shells were cleaned using techniques described in the aforementioned chapters.

Table 5.1. Samples used in FT-TRA analyses with summary of isotope and Mg/Ca values.

Burke Museum locality number	**ID**	**Species**	**Seep name**	**$d^{13}C$ ‰ PDB (average)**	**$d^{18}O$ ‰ PDB (average)**	**Mg/Ca (mmol/mol)**
B6858	Q1	*Globulimina auriculata*	Camp creek	-2.1	-6.7	2.52
B6849	Q2	*Cibicidoides mckannai*	Main	2.0	2.2	6.18
B6833	Q3	*Cibicidoides mckannai*	Non-Seep	1.7	0.1	2.37
B6849	Q4	*Cassidulina reflexa*	Main	0.8	0.1	16.20
B6849	Q5	*Nonionella stella*	Main	-10.7	1.5	34.00
B6858	Q6	*Nonionella stella*	Camp creek	-43.0	1.7	14.00
B6858	Q7	*Globulimina pacifica*	Camp creek	-37.0	0.2	31.00
B6875	Q8	*Nonionella basispinatum*	South camp creek	-12.0	1.3	9.50
B6850	Q9	*Globulimina pacifica*	Main	-33.0	1.0	69.00
B7219	PS1	*C. carinata*	Sooke			5.47
B7219	PS2	*G. praebulloides*	Sooke	0.0	-4.1	4.42
B7219	PS3	*G. praebulloides*	Sooke	0.0	-4.1	3.76
B7219	PS4	*G. praebulloides*	Sooke	0.0	-4.1	5.74
B7216	PS5	*G. pacifica*	Pysht Quarry	-0.4	-7.7	3.38
B7216	PS6	*C. carinata*	Pysht Quarry	3.4	-1.8	3.04
B7216	PS7	*C. carinata*	Pysht Quarry	3.4	-1.8	3.15
B7217	PS8	*C. carinata*	Pysht-Twin Rivers	1.1	-1.0	2.02
B7218	PS9	*C. carinata*	Pysht-Twin Rivers	1.1	-1.0	2.17
B7218	PS10	*G. pacifica*	Pysht-Tree Farm	-0.4	-7.7	13.70

3. Initial results

A list of specimens used in these analyses, along with their isotopic values and the average Mg/Ca value from this analysis, is given in Table 5.1. The average Mg/Ca values in Table 5.1 are derived from the continuum of values bracketed by the dashed vertical lines on each plot, however the results of these analyses are best displayed graphically as chromatograms (Figures 5.4-5.6). Several features are notable in these chromatograms.

1. There is clear indication of diagenetic alteration in most of the foraminifera analyzed. With the exception of *Uvigerina cocoaensis* from the Keasey Formation (Figure 5.4A) and *Cibicides mckannai* from a non-seep sample of the Quinault Formation (Figure 5.5A) all of the specimens analyzed display some degree of diagenetic alteration, as evidenced by their elevated Mg/Ca ratios. Unaltered foraminifera typically display Mg/Ca values < 4 mmol/mol. In all three areas, the highest ratios occur in the samples of the genus *Globobulimina.*
2. In chromatograms from all three seep areas studied, changes in the slopes of the ratio curves indicate there has been more than one episode of mineralization in these shells. For example, Figure 5.4B, *Globobulimina pupoides,* shows a clear slope break at ~15 minutes into the run, denoting a difference in solubility of the material; the same is true in *G. pacifica* from the Quinault Formation (Figure 5.5C,D) and to some extent in *Cibicides mckannai* (Figure 5.5A). In the Pysht Formation, clear breaks appear in chromatograms for *Cassidulina carinata* (Figure 5.6A-C) and *G. pacifica (*Figure 5.6D,E).
3. These results suggest a species-dependent susceptibility to diagenetic alteration of foraminifera, and in general species of *Globobulima* have tests with the most diagenetic alteration. In the Keasey Formation, for example, both species (*Globobulimina pupoides* and *Uvigerina cocoaensis)* were picked from the same sediment sample, and are thus presumed to have

undergone the same diagenetic history, however the results show that *U. cocoaensis* displays Mg/Ca values of a pristine shell that has undergone no alteration (Figure 5.4A) whereas *G. pupoides*, has been severely altered, retaining little or no original calcite (Figure 5.4B). In the Quinault Formation as well, two different species from the same seep site exhibit considerably different Mg/Ca values; in *Globobulima pacifica*, the shell has again been severely altered, while the shell of *Cibicides mckannai* is virtually unaltered. It is interesting to note, however, that *C. mckannai* shells were also analyzed from a non-seep site in the Quinault Formation, and that analysis also showed Mg/Ca values close to those of pristine foraminiferal shells. Similarly in the Pysht Formation, *Globobulimina pacifica* shows much higher Mg/Ca than *Cassidulina carinata* from the same site, indicating the two shells underwent different diagenesis presumably within the same fluid regime.

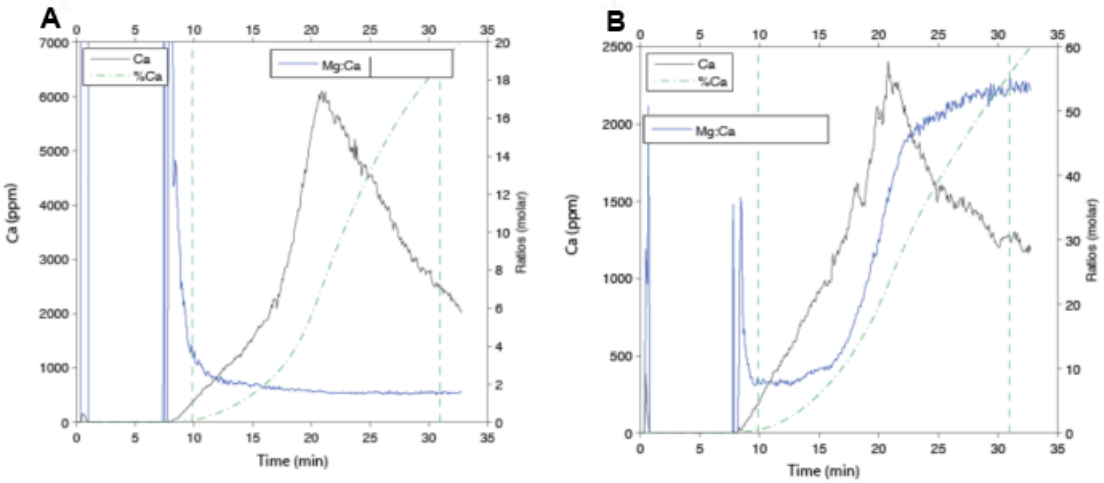

Figure 4. FT-TRA chromatograms of foraminiferal shells from the Rock Creek section of the Keasey Formation of northwestern Oregon. A. *Uvigerina cocoaensis*. B. *Globobulimina pupoides*. The -.-. indicates the percent carbonate dissolved. Note the considerable change of slope in the Mg:Ca curve, indicating different phases of mineralization.

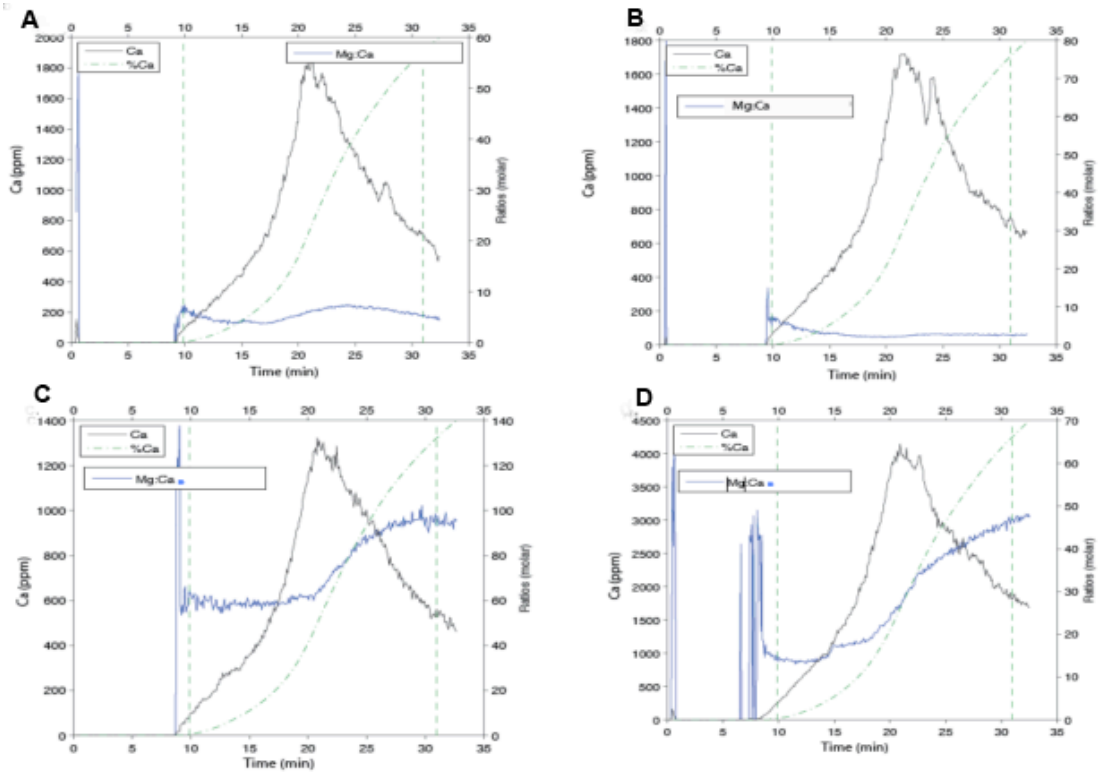

Figure 5.5 FT-TRA chromatograms of foraminiferal shells from the Quinault Formation, western Washington coast. Top row: A. *Cibicides mckannai*, Main seep site. B. *C. mckannai* from a non-seep site.
Bottom row: C. *Globobulimina pacifica*, Main seep site. D. *G. pacifica,* Camp Creek seep site. Note striking differences in the two species, even when from the same site. Note also the apparent lack of alteration in the non-seep sample.

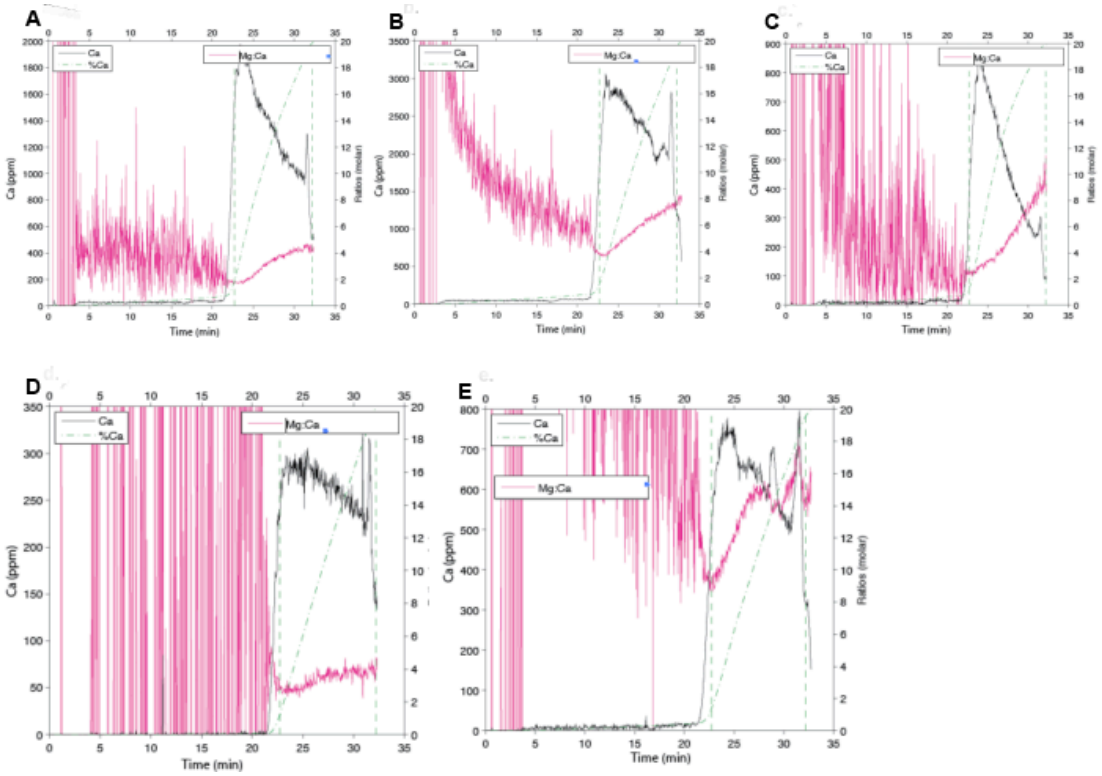

Figure 6. FT-TRA chromatograms of foraminiferal shells from the Pysht and Sooke formations, northern Washington, southern Vancouver Island. Top row, *Cassidulina carinata:* A. Pysht Quarry; B. Pysht Tree Farm; C. Sooke Formtion.
Bottom row, *Globobulimina pacifica* D. Pysht Quarry; E. Pysht Tree Farm.
Again, note differences in magnitude of Mg/Ca values between species, and among species from different sites.

From these results it is apparent that refinement of the FT-TRA technique will result in even more detailed information being obtained. The most obvious change would be to increase the run time. In the Pysht Formation particularly, the 35-minute run time is clearly too short, cutting off before completion of the analyses in all of the samples. Analyses of *G. pacifica* in the Quinault and *G. pupoides* in the Keasey would also have yielded better information had the runs been longer. Adjustments to the eluant strength and/or temperature may also produce more refinement in the data.

4. Discussion

In cold seeps, where deposition of authigenic carbonate is the rule rather than the exception, diagenesis of foraminiferal shells is a serious concern for

environmental reconstruction based on geochemical data of the biogenic calcite. On the other hand, the diagenetic products are potentially a rich source of additional information. Because overprinting occurs post-depositionally, such information is out of stratigraphic order, but the acquired data yields valuable insights into processes and mechanisms operating in cold seep provinces. Clearly, the majority of the Cenozoic foraminiferal shells examined in this study were influenced to some degree by post-depositional alteration due to the oversaturation of HCO_3^- resulting from methanogenesis and methanotrophy. Moreover, the post-depositional fluid flow regimes can be seen to differ in the various areas, and further refinement of the FT-TRA technique as well as addition of other elemental data, particularly Ba/Ca and Sr/Ca should help constrain fluid sources and depths even further.

To further exploit the wealth of information in foraminifera, a systematic approach to reconstructing paleo-seepage information from the geochemical and isotopic records of foraminifera needs to be developed. In future studies, I propose to analyze the chemical and isotopic composition of large sets of foraminiferal samples collected from zones of methane seepage from different cold seep settings as part of continuing studies aimed at understanding methane and gas hydrate dynamics. The critical questions to be resolved are:

- Can detailed analyses of foraminiferal shells allow quantification of the degree of alteration and can this information be used to better interpret the carbon isotopic record?
- Are some species more sensitive to alteration than others? If so, which ones?
- Other than hydrocarbon fluid flow, what environmental factors contribute to post-depositional alteration, and how is this manifested in the shell record?
- Are foraminifera nucleation sites for diagenetic products in methane-rich sediments?
- Can the chemistry of the alteration phases in foraminifera be used to obtain information on methane venting and geochemical cycling analogous to authigenic minerals?

There are three direct applications arising from these results:

1) they facilitate the determination of the degree of alteration in order to identify which samples can be used for traditional isotopic and paleoceanographic reconstructions based on the primary carbonate signal,

2) they allow the exploitation of the geochemical record stored in secondary carbonate, and

3) gaining a better understanding of Mg-rich overprinting in general is of broad interest because such overgrowths are thought to be first responders to increasing CO_2 during climate change (Morse et al., 2006) and references therein).

Authigenic carbonates are known to provide critical data on fluid sources and on microbial, hydrological and carbon cycling processes in methane-rich sediments and at seep sites e.g. (Bohrmann et al., 1998; Greinert et al., 2002; Teichert et al., 2005). These carbonates occur at sites of hydrocarbon fluid discharge, on the seafloor and within the sediments, but they are limited to discrete sites. Foraminifera, on the other hand, are widespread in the sediment record and may serve as nucleation sites for authigenic mineralization. These authigenic minerals on foraminiferal shells may therefore provide similar information as the massive authigenic carbonates, although at a more widely distributed and higher resolution scale. Thus, the results of future studies may lead to a sensitive proxy for methane flux through time.

Notes to Chapter 5

Barbieri, R. and Panieri, G., 2004. How are benthic foraminiferal faunas influenced by cold seeps? Evidence from the Miocene of Italy. Palaeogeography, Palaeoclimatology, Palaeoecology, 204: 257-275.

Billups, K. and Schrag, D.P., 2002. Paleotemperatures and ice volume of the past 27 Myr revisited with paired Mg/Ca and 18O/16O measurements on benthic foraminifera. Paleoceanography, 17(1).

Boetius, A. et al., 2000. A marine microbial consortium apparently mediating anaerobic oxidation of methane. Nature, 407: 623-626.

Bohrmann, G., Greinert, J., Suess, E. and Torres, M., 1998. Authigenic carbonates from the Cascadia subduction zone and their relation to gas hydrate stability. Geology, 26(7): 647-650.

Dickens, G.R., 2003. Rethinking the global carbon cycle with a large, dynamic and microbially mediated gas hydrate capacitor. Earth and Planetary Science Letters, 213(3-4): 169-183.

Ferguson, J.E., Henderson, G.M., Kucera, M. and Rickaby, R.E.M., 2008. Systematic change of foraminiferal Mg/Ca ratios across a strong salinity gradient. Earth and Planetary Science Letters, 265: 153-166.

Greinert, J., Bohrmann, G. and Elvert, M., 2002. Stromatolitic fabric of authigenic carbonate crusts: result of anaerobic methane ocidatin at cold seeps in 4,850 m water depth. International Journal of Earth Sciences, 91: 698-711.

Haley, B. and Klinkhammer, G.P., 2002. Development of a flow-through system for cleaning and dissolving foraminiferal tests. Chemical Geology, 185: 51-69.

Heinz, P., Sommer, S., Pfannkuche, O., Hemleben, C., 2005. Living benthic foraminifera in sediments influenced by gas hydrates at the Cascadia convergent margin, NE Pacific. Marine Ecology Press Series, 304: 77-89.

Hill, T.M., Kennett J.P. and Spero, H.J., 2003. Foraminifera as indicators of methane-rich environments: A study of modern methane seeps in Santa Barbara Channel, California. Marine Micropaleontology, 49: 123-138.

Hinrichs, K.-U., Hayes, J.M., Sylva, S.P., Brewer, P.G. and DeLong, E.F., 1999. Methane-consuming archaebacteria in marine sediments. Nature, 398: 802-805.

Kennedy, M.J., Christie-Blick, N. and Sohl, L., 2001. Are Proterozoic cap carbonates and isotopic excursions a record of gas hydrate destabilization following Earth's coldest intervals? Geology, 29(5): 443-446.

Kennett, J.P. and Stott, L.D., 1991. Abrupt deep-sea warming, palaeoceanographic changes and benthic extinctions at the end of the Palaeocene. Nature, 353: 225-229.

Klinkhammer, G.P. and Haley, B., 2006. Multi-proxy relationships in foraminiferal tests as delineated from element-element plots of time-resolved flo-thru data. Geochimica et Cosmochimica Acta, 70: A325-A325.

Klinkhammer, G.P., Haley, B., Mix, A.C., Benway, H.M. and Cheseby, M., 2004. Further evaluation of flow-through as a method for cleaning and dissolving

shells of planktonic foraminifera for Mg/Ca paleothermometry. Geochimica et Cosmochimica Acta, 68: A335-A335.

Klinkhammer, G.P., Mix, A.C. and Haley, B., 2009. Increased dissolved terestrial input to the coastal ocean during the last deglaciation. Geochemistry, Geophysics, Geosystems, 10(3).

Lear, C.H., Elderfield, H. and Wilson, P.A., 2000. Cenozoic deep-sea temperatures and global ice volumes from Mg/Ca in benthic foraminiferal calcite. Science, 287: 269-272.

Lear, C.H., Rosenthal, Y. and Wright, J.D., 2003. The closing of a seaway: ocean water masses and global climate change. Earth and Planetary Science Letters, 210: 425-436.

Millo, C., Sarnthein, M., Erlenkheuser, H., Grootes, P.M. and Andersen, N., 2005. Methane-induced early diagenesis of foraminiferal tests in the southwestern Greenland Sea. Marine Micropaleontology, 58: 1-12.

Morse, J.W., Andersson, A.J. and Mackenzie, F.T., 2006. Initial responses of caronate-rich shelf sediments to rising atmospheric pCO2 and "ocean adicification": Role of high Mg-calcites. Geochimica et Cosmochimica Acta, 70: 5814-5830.

Nurnberg, D., Bjima, J. and Hemleben, C., 1996. Assessing the reliability of magnesium in foraminiferal calsite as a proxy for water mass temperatures. Geochimica et Cosmochimica Acta, 60: 803-814.

Pearson, P.N. et al., 2001. Warm tropical sea surface temperatures in the Late Cretaceous and Eocene epochs. Nature, 413: 481-487.

Rathburn, A.E. et al., 2003. Relationships between the distribution and stable isotopic composition of living benthic foraminifera and cold methane seep biogeochemistry in Monterey Bay, California. Geochemistry, Geophysics, Geosystems, 4(12): 1106, doi:10.1029/2003GC000595, 2003.

Rosenthal, Y., Lear, C.H., Oppo, D.W. and Braddock, K.L., 2006. Temperature and carbonate ion effects on Mg/Ca and Sr/Ca ratios in benthic foraminifera: Aragonitic species *Hoeglundina elegans*. Paleoceanography, 21.

Teichert, B.M.A., Bohrmann, G. and Suess, E., 2005. Chemoherms on Hydrate Ridge - Unique microbially-mediated carbonate build-ups growing into the water column. Paleogeography, Paleoclimatology, Paleoecology, 227: 67-85.

Torres, M. et al., 2003. Is methane venting at the seafloor recorded by the d13C of benthic foraminifera shells? Paleoceanography, 18: 1062-1075.

Veizer, J., Godderis, Y. and Francois, L.M., 2000. Evidence for decoupling of atmospheric CO2 and global climate during the Phanerozoic eon. Nature, 408: 698-701.

Zachos, J., Pagani, M., Sloan, L., Thomas, E. and Billups, K., 2001. Trends, rhythms, and aberrations in global climate 65 ma to present. Science, 292: 686-693

.

Chapter 6. Conclusion

1. Introduction

Since cold methane seeps were first recognized in 1975 by Roberts and Whelan, their study has progressed to encompass detailed geological, geochemical, geophysical and biological investigations. Methane seeps play a key role in carbon cycling by providing major sources and sinks for carbon on continental margins worldwide (Valentine, 2002; Peckmann and Thiel, 2004; Thauer et al., 2008). Gas hydrates forming and dissociating at seeps sites have been implicated in submarine slope instability (Maslin et al., 1998; Faure et al., 2006; Krabbenhoeft et al., 2009) and global climate perturbations (Kennett et al., 2003). Biota associated with seeps display specialized adaptations enabling their survival in dysoxic and anoxic, high sulfide environments (Paull et al., 1985; Distel, 1998; Sibuet and Olu, 1998; Levin and Michener, 2002; Robinson et al., 2004). These chemoautotrophic communities share affinities with those found in whalefalls and hydrothermal vents, and have been suggested as analogs for early communities on Earth (Sassen and MacDonald, 1998; Smith and Baco, 1998; Levin, 2005).

The study documented in this dissertation utilized benthic foraminifera to develop a proxy for the recognition and characterization of cold methane seeps in the rock record, and for fine-scale understanding of fossil and modern methane-influenced regimes. Calcareous foraminifera were chosen because they are nearly ubiquitous in marine sediments and are thus available where authigenic carbonates are absent. Their shells, derived primarily from dissolved inorganic carbon (DIC) from the surrounding sea/pore water, should reflect the geochemical and isotopic composition of that DIC.

This study began with an investigation of methane seeps in the Pliocene Quinault Formation of western Washington (Chapter 2, this study) and progressed to investigations of late Eocene through late Oligocene seeps from northwest Oregon, western Washington and southern Vancouver Island (Chapter 3, this

study). An invitation to join a research cruise on the German research vessel *RV SONNE* on the Hikurangi margin off New Zealand added information from a modern analog (Chapter 4, this study). As it became apparent that post-depositional alteration was playing a significant role in the isotopic signatures of the foraminifera analyzed, additional data was necessary for assessing diagenesis. This resulted in an ongoing collaboration with investigators from the College of Oceanic and Atmospheric Sciences at Oregon State University, to develop a sensitive proxy for methane seepage using multi-element geochemical parameters to quantify post-depositional mineralization (Chapter 5, this volume).

2. Assessment of the proxy

Prior to this study there had been few investigations of foraminifera in fossil methane seeps, and those focused primarily on foraminiferal assemblages (Aharon and Sen Gupta, 1994; Barbieri and Panieri, 2004). Taxonomic assemblages, however, have limited use in seep studies. No seep-specific foraminiferal species have yet been identified in modern or fossil seeps, although some have been found to preferentially inhabit dysoxic environments (Bernhard and Bowser, 1999, 2008). Two studies identified foraminiferal assemblages that favor cold seeps (Akimoto et al., 1994; Panieri, 2006), but these results have not been duplicated. In addition, parameters such as taxonomic diversity, density and species richness are inconsistent in both fossil and modern seeps (Sen Gupta et al., 1997; Rathburn et al., 2003; Wiedicke and Weiss, 2006; Martin et al., 2007; Martin et al., 2009).

However, their persistence in cold seep environments makes benthic foraminifera attractive subjects for isotopic and geochemical studies. Ratios of the stable isotopes of carbon and oxygen have been analyzed in foraminiferal shells from numerous modern seeps worldwide (Hill et al., 2003; Rathburn et al., 2003; Wiedicke and Weiss, 2006; Martin et al., 2009 online) as well as a few ancient seeps (Martin and Nesbitt, 2005; Martin et al., 2005; Martin et al., 2007; Panieri et al., in press). All of these studies demonstrate that foraminifera do, indeed, record the presence of methane-influenced DIC in their carbon isotopes; foraminiferal

$\delta^{13}C$ from seeps is more depleted and considerably more variable than that from non-seep localities. This depletion and variability is recorded even in samples where macroscopic evidence of seepage is absent (Martin and Nesbitt, 2005; Martin et al., 2007; Chapter 3, this volume).

Studies in modern seeps reveal that foraminiferal $\delta^{13}C$ is not in equilibrium with pore water values, and this disequilibrium can be as much as 40% (Rathburn et al., 2003). Any proxy that utilizes foraminifera must contend with this biological effect. Thus, although the degree of depletion and variability in foraminiferal $\delta^{13}C$ is characteristic of methane seep environments and can be used to recognize such, furtherinterpretations must be approached with caution.

As a further complication, the potential for post-depositional alteration is extremely high in the cold seep environment, where authigenic carbonate precipitation is the rule, and foraminiferal shells provide convenient nucleation centers. It is highly probable, then, that extremely depleted $\delta^{13}C$ values recovered from both modern and fossil seeps are, at least in part, the result of overprinting by authigenic carbonate rather than primary mineralization (Hill et al., 2003; Martin et al., 2007; Martin et al., 2009; Panieri et al., in press). This is particularly important because carbonate overprints are commonly heavily depleted in ^{13}C and will skew any isotope analyses (Gieskes et al., 2008). Consequently, isotope effects in foraminiferal carbonate may be reliable indicators of environmental parameters, but this is most likely not preserved in stratigraphic context.

Diagenetic alteration may be recognized using SEM imaging or $\delta^{18}O$ values; SEM imaging, with its significantly higher magnifications, is often capable of showing authigenic layers that have grown on foraminiferal shells. In addition, $\delta^{18}O$ values that are significantly depleted signify that higher temperature fluids were present, thus suggesting the presence of diagenetic alteration. However even these techniques are not always dependable where overprinting of the biogenic carbonate is slight or where sediments are bathed in CH_4 – influenced fluids at ambient temperatures (Torres et al., 2003b). Conditions such as the latter (CH_4-rich fluids at ambient temperatures) are inherent in seeps (Claypool et al., 2006; Torres

and Kastner, 2009; Schwalenberg et al., 2009; Sommer et al., 2009) and impact any carbonates deposited therein. The identification of authigenic overprinting thus becomes more difficult, and other geochemical parameters are needed to detect post-depositional alterations. To date, the most useful of these parameters is analysis of Mg/Ca ratios of the foraminiferal carbonate. Inorganic carbonates demonstrate dramatically higher Mg/Ca ratios than biogenic carbonates due to the partition coefficient of Mg in authigenic calcite being orders of magnitude higher than that of biogenic calcite (Nurnberg et al., 1996). It is thus possible to distinguish overprinting in foraminiferal shells using this elemental analysis. For example, Mg/Ca analyses of dead foraminiferal shells from modern seeps on Hydrate Ridge revealed overprinting amounting to ~30% of the original carbonate (Torres et al., 2003b). Additionally, Mg/Ca analyses of foraminifera from Cenozoic seeps of the Cascadia margin indicate some individuals display nearly total replacement of their original carbonate despite retaining their morphologic features (Torres et al., submitted; Chapter 5, this volume). Thus, the interpretation of stable isotopic evidence from foraminifera should be coupled with careful examination and understanding of their environment, and, ideally, with other geochemical analyses.

The major strengths of the foraminiferal proxy survive despite the limitations discussed above. The ubiquitous distribution and small size of foraminifera enable them to measure environmental conditions on a fine scale. Consequently, even though $\delta^{13}C$ values may not be in equilibrium with pore waters, their heterogeneity repeats at very small scales the heterogeneity measured at macro-scale (Tryon et al., 2002; Formolo et al., 2004; Krabbenhoeft et al., 2009; Law et al., 2009). When measured in pristine shells, this yields an accurate reproduction of environmental heterogeneity in stratigraphic context. When measured in altered shells, isotopic values record diagenetic episodes. A clear example of this occurs in the foraminifera from the Pysht and Sooke formations (late Oligocene) of the Cascadia margin (Chapter 3, this volume). Their carbonate isotopic values are distinct from the smaller authigenic carbonates in these

formations (blebs, burrow fill, glendonites) and are more closely associated with the authigenic fracture fills and nodules from the Pysht Formation.; the foraminiferal carbonates clearly record the passage of a later, warmer fluid carrying carbonate formed from residual CO_2 from microbial methanogenesis (Chapter 3, this volume, fig. 7). Comparison with foraminiferal isotopic values from other fossil seeps in the Cascadia margin shows that foraminifera from the Pysht and Sooke formations record distinctly different environmental conditions; the most plausible explanation for this is that the episode of diagenetic fluid-flow documented by these resulted from deep, warm fluids migrating toward the surface along tectonically-generated pathways (Chapter 3, this volume, fig. 3; Claypool et al., 2006). Thus, although we cannot use foraminifera to date these episodes, we can confidently use foraminiferal carbonate to document and characterizepost-depositional episodes.

It is also possible to use foraminiferal $\delta^{13}C$ values to assess CH_4 source. In the above example, $\delta^{13}C$ and $\delta^{18}O$ isotopic values combine to indicate the microbial origin of the methane along with the warm, presumably deeper sourced, fluid. In another example, $\delta^{13}C$ measurements of shells of the foraminifera species *Globobulimina pacifica* and *G. pupoides* from the Cenozoic of the Cascadia margin were sufficiently depleted to unequivocally indicate the presence of microbial CH_4, whereas other species returned values within the range of thermogenic CH_4 (Martin et al., 2005; Martin et al., 2007). In modern seeps from the Hikurangi margin, $\delta^{13}C$ values of specimens of *Hoeglundina elegans* and *Pyrgo depressa* displayed values well within the range of thermogenic CH_4 (Martin et al., 2009). Both microbial and thermogenic CH_4 are present on the Cascadia and Hikurangi margins today, both onshore and offshore (Claypool et al., 2006; Faure et al., in press), making these data consistent with observed parameters in modern seeps. On the other hand, subsequent Mg/Ca analyses of the same species from the Cenozoic localities indicated that some of the shells had been altered significantly and, in at least one case, by more than one phase of fluid flow (Torres et al., submitted; Chapter 5, this volume). The altered shells certainly record the presence of DIC influenced by the

anaerobic oxidation of both thermogenic and microbial CH_4 (AOM), but not necessarily during the original deposition of the sediments.

3. Future Investigations

Clearly, the information that can be obtained from foraminifera in cold seeps has the potential to contribute substantially to our understanding of these systems and their global impacts. Equally clearly, further development will produce a more useful proxy, capable of returning a broader spectrum of quantifiable data. Potentially the most profitable course will be the pursuit of the wealth of geochemical information stored in both the primary and the secondary carbonates of the foraminiferal shells.

Elemental analyses

Apart from their usefulness in identifying diagenetic alteration, Mg/Ca analyses are already widely used in paleoecologic reconstructions due to the temperature sensitivity of this ratio (e.g. Lear et al., 2000; Lear et al., 2002). The same technique used to analyze Mg/Ca ratios returns other elemental data that can generate extremely useful information. One such parameter is barium, as measured by the Ba/Ca ratio. Ba cycling is closely coupled with CH_4 fluxes as Ba is remobilized in zones of sulfate reduction associated with cold seeps (Dickens, 2001; Torres et al., 2003a). Ba phases have been observed at fluid venting sites and at the methane-sulfate transition zone (Dickens, 2003; Snyder et al., 2007). To date there has been no systematic attempt to the use of this potentially powerful proxy, and this will be a focus of future work.

$^{87}Sr/^{86}Sr$ analysis

Another geochemical parameter capable of yielding useful information is $^{87}Sr/^{86}Sr$ analysis. Coupled with $\delta^{13}C$ and $\delta^{18}O$ measurements, this has been used to identify sources and depths of diagenetic fluids on the Cascadia margin (Sample and Reid, 1998). Utilizing foraminifera in such analyses will produce an extremely fine-scale, high resolution picture of fluid flow; again, this proxy has not been

pursued to date, but is planned as part of the further development of this foraminiferal proxy.

U/Th dating

U/Th dating by Thermal Ionization Mass Spectrometry (TIMS) has been utilized in a number of Recent seeps, for example at Hydrate Ridge, Oregon, and the Nanaki Trench off Japan, returning high precision ages extending back to 267 kyr (Teichert et al., 2003;Watanabe et al., 2008). The same aliquots of carbonate dissolved in HNO_3 utilized for $^{87}Sr/^{86}Sr$ can be used for U/Th analyses. Although this dating technique does not return dates far back into geologic time, it will allow correlation of events at least into the Pleistocene, and also help place these events in stratigraphic context.

4. Broader implications

Cold seeps and their associated features are a consequence of methanogenesis and methanotrophy, which result in the reduction of organic matter into CH_4, and its transformation by AOM into carbonate carbon and sulfide. This process is a significant carbon sink in both marine and terrestrial settings, and is plays a major role in the global carbon cycle and possibly in climate change. Authigenic carbonates formed at marine methane seep sites carry a wealth of information, but they are limited in extent and occur as discrete deposits on a macro-scale. Authigenic mineral overprints on foraminiferal shells may yield the same information, but at a higher resolution. On the other hand, utilizing foraminiferal shells with their wide distribution and availability enables the fine-scale mapping of the extent of environmental conditions. This yields a more detailed understanding of the mechanisms of methane flux as well as its interconnection with other factors such as hydrate dissociation, tectonic activity, and climate change.

As refined by further development of elemental and isotopic analyses, the proxy will be useful in other spheres. For example, the utilization of foraminifera in paleoclimate reconstructions is well documented. The proxy developed here will enable greater confidence in measurements made on foraminiferal carbonate by determining the degree of alteration in samples and identifying those most suitable for paleoclimate analysis. In addition, the use of $^{87}Sr/^{86}Sr$ analyses on foraminiferal carbonate will further refine the elucidation of fluid-flow regimes and origins in tectonic provinces.

As a proxy for CH_4 seepage, foraminifera were formerly considered to have limited efficacy due to their lack of seep-specific taxa and their disequilibrium with pore waters measured in seeps. Their usefulness was therefore limited to qualitative rather than quantitative applications. Investigations undertaken in this study established the effectiveness of foraminiferal carbonates in recording the presence of methane-influenced fluids. It has been demonstrated that isotopic measurements from foraminiferal shell can, indeed, be used to recognize and characterize seep environments. Additionally, analyses of conditions found in modern methane seep provinces allows us to infer conditions present when fossil methane seeps were formed.

One of the major limitations of the use of foraminifera in paleoenvironmental studies is the likelihood of diagenetic alteration. Initial Mg/Ca analyses of foraminiferal carbonate from fossil seeps indicated the foraminifera had undergone some degree of diagenetic alteration, thus isotopic measurements may not be in stratigraphic context. The proxy under development in this study recognizes the potential for post-depositional alteration of foraminiferal shells and builds on that. As nucleation centers for minerals carried in diagenetic fluids, foraminiferal shells become repositories of a wealth of geochemical information that can be utilized to reconstruct ancient environments and fluid-flow regimes. Further refinement of analytical techniques used on foraminiferal carbonate will yield a more sensitive proxy capable of returning high resolution information with widespread applications.

Notes to Chapter 6

Aharon, P. and Sen Gupta, B.K., 1994. Bathymetric reconstructions of the Miocene-age "calcari a Lucina" (Northern Apennines, Italy) from oxygen isotopes and benthic foraminifera. Geo-Marine Letters, 14: 219-230.

Akimoto, K., Tanaka, T., Hattori, M. and Hotta, H., 1994. Recent benthic foraminiferal assemblages from the cold seep communities - A contribution to the methane gas indicator. In: R. Tsuchi (Editor), Pacific Neogene Events in Time and Space. University of Tokyo Press, Tokyo, pp. 11 - 25.

Barbieri, R. and Panieri, G., 2004. How are benthic foraminiferal faunas influenced by cold seeps? Evidence from the Miocene of Italy. Palaeogeography, Palaeoclimatology, Palaeoecology, 204: 257-275.

Bernhard, J.M. and Bowser, S.S., 1999. Benthic foraminifera of dysoxic sediments: chloroplast sequestration and functional morphology. Earth-Science Reviews, 46(1-4): 149-165.

Bernhard, J.M. and Bowser, S.S., 2008. Peroxisome proliferation in foraminifera inhabiting the chemocline: An adaptation to reactive oxygen species exposure? Journa of Eukaryotic Microbioloby, 55(3): 135-144.

Claypool, G.E. et al., 2006. Microbial methane generation and gas transport in shallow sediments of an accretionary complex, southern Hydrate Ridge (ODP Leg 204), offshore Oregon, U.S.A. In: A.M. Trehu, G. Bohrmann, M. Torres and F.S. Colwell (Editors), Proceedings of the Ocean Drilling Program, Scientific Results, pp. 1-52.

Dickens, G.R., 2001. Sulfate profiles and barium fronts in sediment on the Blake Ridge: Present and past methane fluxes through a large hydrate reservoir. Geochimica et Cosmochimica Acta, 65(4): 529-543.

Dickens, G.R., 2003. A methane trigger for rapid warming? Science, 299: 1017.

Distel, D.L., 1998. Evolution of chemoautotrophic endosymbioses in bivalves. Bioscience, 48(4): 277-286.

Faure, K. et al., 2006. Methane seepage and its relation to slumping and gas hydrate at the Hikurangi margin, New Zealand. New Zealand Journal of Geology and Geophysics, 49: 503-516.

Faure, K. et al., 2009 online. Methane seepage along the Hikurangi Margin of New Zealand: geochemical and physical evidence from the water column, sea surface and atmosphere. Marine Geology

Formolo, M.J. et al., 2004. Quantifying carbon sources in the formation of authigenic carbonates at gas hydrate sites in the Gulf of Mexico. Chemical Geology, 205: 253-264.

Gieskes, J. et al., 2008. Systematic change of foraminiferal Mg/Ca ratios across a strong salinity gradient. Earth and Planetary Science Letters, 265(1-2): 153-166.

Hill, T.M., Kennett J.P. and Spero, H.J., 2003. Foraminifera as indicators of methane-rich environments: A study of modern methane seeps in Santa Barbara Channel, California. Marine Micropaleontology, 49: 123-138.

Kennett, J.P., Cannariato, K.G., Hendy, I.L. and Behl, R.J., 2003. Methane Hydrates in Quaternary Climate Change: The Clathrate Gun Hypothesis. AGU Special Publication, 54, 216 pp.

Krabbenhoeft, A., Netzeband, G.L., Bialas, J. and Papenberg, C., 2009 online. Methane concentrations from ocean bottom stations and their relation to seismic structures. Marine Geology.

Law, C.S. et al., 2009 online. Geological, hydrodynamic and biogeochemical characterisation of a New Zealand deep-water methane cold seep during a three-year time-series study. Marine Geology.

Lear, C.H., Elderfield, H. and Wilson, P.A., 2000. Cenozoic deep-sea temperatures and global ice volumes from Mg/Ca in benthic foraminiferal calcite. Science, 287: 269-272.

Lear, C.H., Rosenthal, Y. and Slowey, N., 2002. Benthic foraminiferal Mg/Ca-paleothermometry: A revised core-top calibration. Geochimica et Cosmochimica Acta, 66(19): 3375-3387.

Levin, L.A., 2005. Ecology of cold seep sediments: Interactions of fauna with flow, chemistry, and microbes. Oceanography and Marine Biology, an Annual Review, 43: 1-46.

Levin, L.A. and Michener, R.H., 2002. Isotopic chemosynthesis-based nutrition of macrobenthos: the lightness of being at Pacific methane seeps. Limnology and oceanography, 47: 1336 - 1345.

Martin, R.A. and Nesbitt, E.A., 2005. Benthic foraminiferal characteristics of Cenozoic cold seeps on the Northeast Pacific margin, American Association of Petroleum Geologists, Calgary.

Martin, R.A., Nesbitt, E.A. and Campbell, K.A., 2005. Benthic foraminiferal characterization of two Cenozoic cold seeps, Cascadia accretionary margin, Third International Symposium on Hydrothermal Vent and Seep Biology, Scripps.

Martin, R.A., Nesbitt, E.A. and Campbell, K.A., 2007. Carbon stable isotopic composition of benthic foraminifera from Pliocene cold methane seeps, Cascadia accretionary margin. Palaeogeography, Palaeoclimatology, Palaeoecology, 246: 260-277.

Martin, R.A., Nesbitt, E.A. and Campbell, K.A., 2009 online. The effects of anaerobic oxidation of methane on benthic foraminiferal assemblages and stable isotopes on the Hikurangi Margin of eaastern New Zealand. Marine Geology.

Maslin, M., Mikkelsen, N., Vilela, C. and Haq, B., 1998. Sea-level- and gas-hydrate-controlled catastrophic sediment failures of the Amazon Fan. Geology, 26(12): 1107 - 1110.

Nurnberg, D., Bijma, J. and Hemleben, C., 1996. Assessing the reliability of magnesium in foraminiferal calsite as a proxy for water mass temperatures. Geochimica et Cosmochimica Acta, 60: 803-814.

Panieri, G., 2006. Foraminiferal response to an active methane seep environment: A case study from the Adriatic Sea. Marine Micropaleontology, 61: 116-130.

Panieri, G., Camerlenghi, A., Conti, S., Pini, G.A. and Cacho, I., in press. Methane seepages recorded in benthic foraminifera from Miocene seep carbonates, Northern Apennines (Italy). Palaeoceanography, Palaeoclimatology, Palaeoecology.

Paull, C.K., Juli, A.J.T., Toolin, L.J. and Linick, T., 1985. Stable isotope evidence for chemosynthesis in an abyssal seep community. Nature, 317: 709-711.

Peckmann, J. and Thiel, V., 2004. Carbon cycling at ancient methane-seeps. Chemical Geology, 205: 443-467.

Rathburn, A.E. et al., 2003. Relationships between the distribution and stable isotopic composition of living benthic foraminifera and cold methane seep biogeochemistry in Monterey Bay, California. Geochemistry, Geophysics, Geosystems, 4(12): 1106, doi:10.1029/2003GC000595, 2003.

Roberts, H. and Whelan, T.W.I., 1975. Methane-derived carbonate cements in barrier and beach sands of a subtropical delta complex. Geochemica et Cosmochimica Acta, 19: 1085-1089.

Robinson, C.A., Bernhard, J.M., Levin, L.A., Mendoza, G.F. and Blanks, J., 2004. Surficial hydrocarbon seep infauna from the Blake Ridge (Atlantic Ocean, 2150m) and the Gulf of Mexico (690-2240 m). P.S.N.Z.: Marine Ecology, 25(4): 313-336.

Sample, J.C. and Reid, M.R., 1998. Contrasting hydrogeologic regimes along strike-slip and thrust faults in the Oregon convergent margin: Evidence from the chemistry of syntectonic carbonate cements and veins. Geological Society of America Bulletin, 110(1): 48-59.

Sassen, R. and MacDonald, I., 1998. Bacterial methane oxidation in sea-floor gas hydrate: Significance to life in extreme environments. Geology, 26: 851-854.

Schwalenberg, K., Haeckel, M., Poort, J. and Jegen, M., 2009 online. Evaluation of gas hydrate deposits in an active seep area using marine controlled source electromagnetics: results from the Wairarapa region, New Zealand. Marine Geology.

Sen Gupta, B.K., Platon, E., Bernhard, J.M. and Aharon, P., 1997. Foraminiferal colonization of hydrocarbon-seep bacterial mats and underlying sediment, Gulf of Mexico slope. Journal of Foraminiferal Research, 27(4): 292-300.

Sibuet, M. and Olu, K., 1998. Biogeography, biodiversity and fluid dependence of deep-sea cold-seep communities at active and passive margins. Deep-Sea Research II, 45: 517-567.

Smith, C.R. and Baco, A., 1998. Phylogenetic and functional affinities between whale-fall, seep and vent chemoautotrophic communities. Les Cahiers de Biologie Marine, 39: 345-346.

Snyder G.T., Dickens, G.R., Castellini, D.G., 2007. Labile barite contents and dissolved barium concentrations on Blake Ridge: New perspectives on barium cycling above gas hydrate systems. Journal of Geochemical Exploration Cold Seeps and Gas Hydrates 95 (1-3): 48-65.

Sommer, S., Linke, P., Pfannkuche, O., Niemann, H. and Treude, T., 2009 online. Benthic respiration in a novel seep habitat dominated by dense beds of

ampharetid polychaetes at the Hikurangi Margin (New Zealand). Marine Geology.

Teichert, B.M.A. et al., 2003. U/Th Systematics and ages of authigenic carbonates from Hydrate Ridge, Cascadia Margin: Recorders of fluid flow variations. Geochimica et Cosmochimica Acta, 67(20): 3845-3857.

Thauer, R.K., Kaster, A.-K., Seedorf, H., Buckel, W. and Hedderich, R., 2008. Methanogenic archaea: ecologically relevant differences in energy conservation. Nature Reviews Microbiology, 6: 579-591.

Torres, M., Bohrmann, G., Dube, T.E. and Poole, F.G., 2003a. Formation of modern and Paleozoic stratiform barite at cold methane seeps on continental margins. Geology, 31(10): 897-900.

Torres, M., Martin, R.A., Klinkhammer, G.P. and Nesbitt, E.A., submitted. Post depositional alteration of foraminifera shells in cold seep settings: New insights from Flow-Through analyses. Earth and Planetary Science Letters.

Torres, M. Mix, A.C., Kinports, K., Haley, B., Klinkhammer, G., McManus, J., and deAngelis, M.A., 2003b. Is methane venting at the seafloor recorded by the d13C of benthic foraminifera shells? Paleoceanography, 18: 1062-1075.

Torres, M.E. and Kastner, M., 2009. Data report: clues about carbon cycling in methane-bearing sediments using stable isotopes of the dissolved inorganic carbon. Proceedings of the Integrated Ocean Drilling Program, 311.

Tryon, M.D., Brown, K.M. and Torres, M.E., 2002. Fluid and chemical flux in and out of sediments hosting methane hydrate deposits on Hydrate Ridge, OR, II: Hydrological processes. Earth and Planetary Science Letters, 201: 541-557.

Valentine, D.L., 2002. Biogeochemistry and microbial ecology of methane oxidation in anoxic environments: a review. Antonie van Leeuwenhoek, 81: 271-282.

Watanabe, Y., Nakai, S., Hiruta, A., Matsumoto, R, Yoshida, K., 2008. U-Th dating of carbonate nodules from methane seeps off Joetsu, eastern margin of Japan Sea. Earth and Planetary Science Letters, Vol. 272 (1-2): 89-96

Wiedicke, M. and Weiss, W., 2006. Stable carbon isotope records of carbonates tracing fossil seep activity off Indonesia. Geochemistry, Geophysics, Geosystems, 7(11): Q11009, doi:10.1029/2006GC001292

.

Bibliography

Aharon, P., 2000. Microbial processes and products fueled by hydrocarbons at submarine seeps. In: R.E. Riding and S.M. Awramik (Editors), Microbial Sediments. Springer-Verlag, Berlin, Heidelberg, pp. 270-281.

Aharon, P. and Fu, B., 2000. Microbial sulfate reduction rates and sulfur and oxygen isotope fractionations at oil and gas seeps in deepwater Gulf of Mexico. Geochemica et Cosmochimica Acta, 64(2): 233-246.

Aharon, P., Schwarz, H.P. and Roberts, H., 1997. Radiometric dating of submarine hydrocarbon seeps in the Gulf of Mexico. GSA Bulletin, 109(5): 568-579.

Aharon, P. and Sen Gupta, B.K., 1994. Bathymetric reconstructions of the Miocene-age "calcari a Lucina" (Northern Apennines, Italy) from oxygen isotopes and benthic foraminifera. Geo-Marine Letters, 14: 219-230.

Aiello, I.W., In press. Fossil seep structures of the Monterey Bay region and tectonic/structural controls on fluid flow in an active transform margin. Palaeogeography, Palaeoclimatology, Palaeoecology.

Aiello, I.W., Garrison, R.E., Moore, J.C., Kastner, M. and Stakes, D.S., 2001. Anatomy and origin of carbonate structures in a Miocene cold-seep field. Geology, 29: 1111-1114.

Akimoto, K., Tanaka, T., Hattori, M. and Hotta, H., 1994. Recent benthic foraminiferal assemblages from the cold seep communities - A contribution to the methane gas indicator. In: R. Tsuchi (Editor), Pacific Neogene Events in Time and Space. University of Tokyo Press, Tokyo, pp. 11 - 25.

Allouc, J., 1990. Quaternary crusts on slopes of the Mediterranean Sea: a tentative explanation for their genesis. Marine Geology, 94(3): 205-238.

Aloisi, g. et al., 2002. CH_4-consuming microorganisms and the formation of carbonate crusts at cold seeps. Earth and Planetary Science Letters, 203: 195-203.

Aloisi, G. et al., 2000. Methane-related authigenic carbonates of eastern Mediterranean Sea mud volcanoes and their possible relation to gas hydrate destabilisation. Earth and Planetary Science Letters, 184: 321-338.

Aloisi, G. et al., 2004. The effect of dissolved barium on biogeochemical processes at cold seeps. Geochimica et Cosmochimica Acta, 8: 1735-1748.

Alperin, M.J., 1988. Carbon and hydrogen isotope fractionation resulting from anaerobic methane oxidation. Global Biogeochemical Cycles, 2(3): 279-288.

Alperin, M.J., 1992. Factors that control the stable carbon isotopic composition of methane produced in an anoxic marine sediment. Global Biogeochemical Cycles, 6(3): 271-291.

Alve, E. and Bernhard, J.M., 1995. Vertical migratory response of benthic foraminifera to controlled oxygen concentrations in an experimental mesocosm. Marine Ecology Progress Series, 116: 137-151.

Amano, K. and Little, C.T.S., 2004. Miocene whale-fall community from Hokkaido, northern Japan. Palaeogeography, Palaeoclimatology, Palaeoecology, 215: 345-356.

Armentrout, J.M., 1981. Correlation and ages of Cenozoic chronostratigraphic units in Oregon and Washington. Geological Society of America Special Paper, 184: 137-148.

Armentrout, J.M. and Berta, A., 1977. Eocene-Oligocene foraminiferal sequence from the northeast Olympic Peninsula, Washington. Journal of Foraminiferal Research, 7(3): 216-233.

Armentrout, J.M. and Suek, D.H., 1985. Hydrocarbon exploration in western Oregon and Washington. American Association of Petroleum Geologists Bulletin, 69: 627-643.

Ayala-Lopez, A. and Molina-Cruz, A., 1994. Micropalaeontology of the hydrothermal region in the Guaymas Basin, Mexico. Journal of Micropalaeontology, 13: 133-146.

Barbieri, R. and Panieri, G., 2004. How are benthic foraminiferal faunas influenced by cold seeps? Evidence from the Miocene of Italy. Palaeogeography, Palaeoclimatology, Palaeoecology, 204: 257-275.

Barbin, V. et al., 1991. Cathodoluminescence of Recent biogenic carbonates- an environmental and ontogenic fingerprint. Geological Magazine, 128(1): 19-26.

Barnard, W.D., 1978. The Washington continental slope: Quaternary tectonics and sedimentation. Marine Geology, 27: 79-114.

Barnes, P.M. et al., 2009 online. Tectonic and Geological Framework for Gas Hydrates and Cold Seeps on the Hikurangi Subduction Margin, New Zealand. Marine Geology.

Barry, J.P. et al., 19. Biologic and geologic characteristics of cold seeps in Monterey Bay, California. Deep-Sea Research I, 43: 1739-1762.

Bauch, e.a., 2003. Paleoceanographic Implications Neoglogoquadrina. Nature, 424.

Bayon, G. et al., 2007. Sr/Ca and Mg/Ca ratios in Niger Delta sediments: Implications for authigenic carbonate genesis in cold seep environments. Marine Geology, 241: 93-109.

Beal, E.J., House, C.H. and Orphan, V.J., 2009. Manganese- and iron-dependent marine methane oxidation. Science, 325: 184-187.

Beikman, H.M., Rau, W.W. and Wagner, H.C., 1967. The Lincoln Creek Formation, Grays Harbor Basin, southwestern Washington. United States Geological Survey Bulletin, 1244-1: 11-114.

Berndt, M.E., Allen, D.E. and Seyfried, W.E.J., 1996. Reduction of CO_2 during serpentinization of olivine at 300^{o}C and 500 bar. Geology, 24(4): 351-354.

Bernhard, J.M., 1986. Characteristic assemblages and morphologies of benthic foraminifera from anoxic, organic-rich deposits: Jurassic through Holocene. Journal of Foraminiferal Research(3): 207-215.

Bernhard, J.M., 1988. Postmortem vital staining in benthic foraminifera: Duration and importance in population and distributional studies. Journal of Foraminiferal Research, 18: 143-146.

Bernhard, J.M., 1992. Benthic foraminiferal distribution and biomass related to pore-water oxygen: central California continental slope and rise. Deep-Sea Research, 39: 585-605.

Bernhard, J.M., 2003. Potential symbionts in bathyal foraminifera. Science, 299: 861.

Bernhard, J.M. and Bowser, S.S., 1999. Benthic foraminifera of dysoxic sediments: chloroplast sequestration and functional morphology. Earth-Science Reviews, 46(1-4): 149-165.

Bernhard, J.M. and Bowser, S.S., 2008. Peroxisome proliferation in foraminifera inhabiting the chemocline: An adaptation to reactive oxygen species exposure? Journal of Eukaryotic Microbioloby, 55(3): 135-144.

Bernhard, J.M., Buck, K.R. and Barry, J.P., 2001. Monterey Bay cold-seep biota: Assemblages, abundance, and ultrastructure of living foraminifera. Deep-Sea Research Part I-Oceanographic Research Papers, 48: 2233-2249.

Bernhard, J.M., Ostermann, D.R., Williams, D.S. and Blanks, J.K., 2006. Comparisons of two methods to identify live benthic foraminifera: a test between Rose Bengal and Cell Tracker Green with implications for stable isotope paleoreconstructions. Paleoceanography, 21: doi: 10.1029/2006PA001290 (PA 4210).

Bernhard, J.M. and Reimers, C.E., 1991. Benthic foraminiferal population fluctuations related to anoxia: Santa Barbara Basin. Biogeochemistry: 127-149.

Bernhard, J.M., Sen Gupta, B.K., Borne, P.F., 1997. Benthic foraminiferal proxy to estimate dysoxic bottom-oxygen concentrations: Santa Barbara Basin, U.S. Pacific continental margin. Journal of Foraminiferal Research, 27: 301-310.

Billups, K., Kelly, C. and Pierce, E., 2008. The late Miocene to early Pliocene climate transition in the Southern Ocean. Palaeoceanography, Palaeoclimatology, Palaeoecology, 267: 31-40.

Billups, K. and Schrag, D.P., 2002. Paleotemperatures and ice volume of the past 27 Myr revisited with paired Mg/Ca and 18O/16O measurements on benthic foraminifera. Paleoceanography, 17(1).

Boetius, A. et al., 2000. A marine microbial consortium apparently mediating anaerobic oxidation of methane. Nature, 407: 623-626.

Boetius, A. and Suess, E., 2004. Hydrate Ridge: a natural laboratory for the study of microbial life fueled by methane from near-surface gas hydrates. Chemical Geology, 205: 291-310.

Bohrmann, G., Greinert, J., Suess, E. and Torres, M., 1998. Authigenic carbonates from the Cascadia subduction zone and their relation to gas hydrate stability. Geology, 26(7): 647-650.

Borowski, W.S., 2004. A review of methane and gas hydrates in the dynamic, stratified system of the Blake Ridge region, offshore southeastern North America. Chemical Geology, 205: 311-346.

Boulegue, J. and Mariotti, A., 1990. Carbonate cements and fluid circulation in intraplate deformation. In: J.R. Cochrane, D.A.V. Stow and e. al. (Editors), Proceedings of the Ocean Drilling Program, Scientific Results, pp. 135-139.

Boyle, E.A., 1981. Cadmium, zinc, copper and barium in foraminifera tests. Earth and Planetary Science Letters, 53: 11-35.

Boyle, E.A. and Keigwin, L., 1987. North Atlantic thermohaline circulation during the past 20,000 years linked to high-latitude surface temperature. Nature, 330: 35-40.

Brandon, M., Roden-Tice, M. and Garver, J., 1998. Late Cenozoic exhumation of the Cascadia

accretionary wedge in the Olympic Mountains, northwest Washington State. GSA Bulletin, 110(8): 985-1009.

Brocks, J.J., Buick, R., Summons, R.E. and Logan, G.A., 2003. A reconstruction of Archean biological diversity based on molecular fossils from the 2.78 to 2.45 billion-year-old Mount Bruce Supergroup, Hamersley Basin, Western Australia. Geochemica et Cosmochimica Acta, 67(22): 4321-4335.

Brocks, J.J., Logan, G.A., Buick, R. and Summons, R.E., 1999. Archean molecular fossils and the early rise of Eukaryotes. Science, 285: 1033-1036.

Brown, R.D. and Gower, H.D., 1958. Twin River Formation (Redefinition), Northern Olympic Peninsula, Washington. Bulletin American Association of Petroleum Geologists, 42(10): 2491-2512.

Bruckner, S. and Mackensen, A., 2008. Organic matter rain rates, oxygen availability, and vital effects from benthic foraminiferal d13C in the historic Skagerrak, North Sea. Marine Micropaleontology, 66: 192-207.

Budai, J.M., Martin, A.M., Walter, L.M. and Ku, T.C.W., 2002. Fracture-fill calcite as a record of microbial methanogenesis and fluid migration: a case study from the Devonian Antrim Shale, Michigan Basin. Geofluids, 2: 163-183.

Buffet, B.A., 2002. Clathrate Hydrates. Annual Review of Earth and Planetary Sciences, 28: 477-507.

Buick, R., 1991. Microfossil recognition in Archean rocks: An appraisal of spheroids and filaments from a 3500 M.Y. chert-barite unit at North Pole, Western Astralia. PALAIOS, 5: 441-459.

Buick, R., 1992. The antiquity of oxygenic photosynthesis: evidence from stromatolites in sulphate-deficient Archaean Lakes. Science, 255: 7-77.

Buick, R., Dunlop, J.S.R. and Groves, D.I., 1981. Stromatolite recognition in ancient rocks: An appraisal of irregularly laminated structures in an Early Archean chert-barite unit from North Pole, Western Australia. Alcheringa, 6: 161-181.

Burns, C., Campbell, K.A. and Mooi, R., 2005. Exceptional crinoid occurrences and associated cargonates of the Keasey Formation (lower Oligocene) at Mist, Oregon.

Buzas, M.A., 1979. The Measurement of Species Diversity. In: J.H. Lipps, W.H. Berger, M.A. Buzas, R.G. Douglas and C.A. Ross (Editors), Foraminiferal Ecology and Paleoecology. SEPM Short Course, pp. 3-10.

Buzas, M.A., Culver, S.J. and Jorissen, F.J., 1993 . A statistical evaluation of the microhabitats of living (stained) infaunal benthic foraminifera. Marine Micropaleontology, 20 : 311-320.

Buzas, M.A., Hayek, L.-A.C., Hayward, B.W., Grenfell, H.R. and Aswaq, T.S., 2007. Biodiversity and community structure of deep-sea foraminifera around New Zealand. Deep-Sea Research Part I, 154: 1641-1654.

Buzas-Stephens, P. and Buzas, M.A., 2005. Population dynamics and dissolution of foraminifera in Nueces Bay, Texas. Journal of Foraminiferal Research, 35(3): 248-258.

Caldwell, S.L. et al., 2008. Anaerobic oxidation of methane: Mechanisms, bioenergetics, and the ecology of associated microorganisms. Environmental Science and Technology, 42(18): 6791-6799.

Cameron, E.M., 1982. Sulphate and sulphate reduction in early Precambrian oceans. Nature, 296: 145-148.

Campbell, 1992. Recognition of a Mio-Pliocene cold seep setting from the Northeast Pacific convergent margin, Washington, U.S.A. Palaios, 7: 422-433.

Campbell, K.A., 2006. Hydrocarbon seep and hydrothermal vent paleonvironments and paleontology: Past developments and future research directions. Palaeogeography, Palaeoclimatology, Palaeoecology, 232: 362-407.

Campbell, K.A. and Bottjer, D.J., 1993. Fossil Cold Seeps. National Geographic Research & Exploration, 9(3): 326-242.

Campbell, K.A., Farmer, J.D. and Des Marais, D., 2002. Ancient hydrocarbon seeps from the Mesozoic convergent margin of California: geochemistry, fluids and palaeoenvironments. Geofluids, 2: 63-94.

Campbell, K.A., Francis, D.A., Collins, M., Gregory, M.R. and Aharon, P., 2008. Hydrocarbon seep-carbonates of a Miocene forearc (East Coast Basin) North Island, New Zealand. Sedimentary Geology, 204: 83-105.

Campbell, K.A. and Nesbitt, E.A., 2000. High resolution architecture and paleoecology of an active margin, storm-flood influenced estuary, Quinault Formation (Pliocene), Washington. Palaios, 15: 553-579.

Campbell, K.A. and Nesbitt, E.A., 2004. 92, 32nd International Geologic Congress, Abstracts. International Geological Congress, Florence, Italy, pp. 928.

Campbell, K.A. and Nesbitt, E.A., 2005. Characterizing seep ichnofabric and ichnological signatures, VII International Ichnofabrics Workshop, Auckland, New Zealand, pp. 15.

Campbell, K.A., Nesbitt, E.A. and Bourgeois, J., 2007. Signatures of storms, oceanic floods, and forearc tectonsim in marine shelf strata of the Quinault Formation (Pliocene), Washington, U.S.A. Geology.

Cannariato, K.G. and Kennett, J.P., 1999 . Biotic response to late Quaternary rapid climte switches in Santa Barbara Basin: Ecological and evolutionary implications. Geology, 27: 63-66.

Cannariato, K.G. and Stott, L.D., 2004. Evidence against clathrate-derived methane release to Santa Barbara Basin surface waters? Geochemistry, Geophysics, Geosystems, 5(5): Q05007, doi:10.1029/2003GC000600.

Cannariato, K.G. and Stott, L.D., 2004. Evidence against clathrate-derive methane release to Santa Barbara Basin surface waters? . Geochemistry, Geophysics, Geosystems, 5(5): 9 pages (Q05007, doi:10.1029/2003GC000600).

Carter, R.M. and Gammon, P., 2004. New Zealand Maritime glaciation: Millenial-scale southern climate change since 3.9 Ma. Science, 304: 1659-1662.

Carter, R.M. and Naish, T.R., 1998. A review of Wanganui Basin, New Zealand: global reference

section for shallow marine, Plio-Pleistocene (2.5-0 Ma) cyclostratigraphy. Sedimentary Geology, 122: 37-52.

Catling, D.C., Claire, M.W. and Zahnle, K.J., 2007. Anaerobic methanotrophy and the rise of atmospheric oxygen. Philosophical Transactions of the Royal Society, 365: 1867-1888.

Catling, D.C., Zahnle, K.J. and McKay, C.P., 2001. Biogenic methane, hydrogen escape, and the irreversible oxidation of Early Earth. Science, 293: 839-843.

Claypool, G.E. and Kaplan, I.R., 1974. The origin and distribution of methane in marine sediments. In: I.R.C. Kaplan (Editor), Natural Gases in Marine Sediments. Plenum, New York, pp. 99-139.

Claypool, G.E. et al., 2006. Microbial methane generation and gas transport in shallow sediments of an accretionary complex, southern Hydrate Ridge (ODP Leg 204), offshore Oregon, U.S.A. In: A.M. Trehu, G. Bohrmann, M. Torres and F.S. Colwell (Editors), Proceedings of the Ocean Drilling Program, Scientific Results, pp. 1-52.

Clift, P. and Vannuchi, P., 2004. Controls on tectonic accretion versus erosion in subduction zones: implications for the origin and recycling of the continental crust. Review of Geophysics, 42: 31 pp.

Conrad, R. and Schutz, H., 1988. Methods of studying methanogenic bacteria and methanogenic activities in aquatic envitonments. In: B. Austin (Editor), Methods in Aquatic Bacteriology. Wiley, Chichester, U.k., pp. 301-343.

Corliss, B.H., 1985. Microhabitats of benthic foraminifera within deep-sea sediments. Nature, 314: 435-438.

Corliss, B.H., 1991. Morphology and microhabitat preferences of benthic foraminigera from the northwest Atlantic Ocean. Marine Micropaleontology, 17: 195-236.

Corliss, B.H., McCorkle, D.C. and Higdon, D.M., 2002. A time series study of the carbon isotopic composition of deep-sea benthic foraminifera. Paleoceanography, 17 (3): 27 pages.

Cowen, J.P., Wen, X. and Popp, B.N., 2002. Methane in aging hydrothermal plumes. Geochimica et Cosmochimica Acta, 66(20): 3563-3571.

Cushman, J.A., 1945. Parallel evolution in the foraminifera. American Journal of Science, 243-A: 117-121.

Cushman, J.A. and Valentine, W.W., 1930. Shallow-water foraminifera from the Channel Islands of Southern California. Stanford University Dept. of Geology, Contr., 1(1): 7.

Dahlmann, A. and de Lange, G.J., 2003. Fluid-sediment interactions as Eastern Mediterranean mud volcanoes: a stable isotope study from ODP Leg 160. Earth and Planetary Science Letters, 212: 377-391.

Davidson, D.W. and Least, D.G., 1983. Oxygen-18 enrichment in the water of a clathrate hydrate. Geochimica et Cosmochimica Acta, 47: 2293-2295.

De Mets, C., Gordon, R.G., Argus, D.F. and Stein, S., 1990. Current plate motions. Geophysical Journal International, 101: 425-478.

DeJong, T.M., 1975. A comparison of three diversity indices based on their components of richness

and evennes. OIKOS, 26: 222-227.

Delaca, T.E. and Lipps, J.H., 1972. The mechanism and adaptive significance of attachment and substrate pitting in the foraminiferan *Rosalina globularis* d'Orbigny. Journal of Foraminiferal Research, 2(2): 68-72.

Dickens, G.R., 2001. Sulfate profiles and barium fronts in sediment on the Blake Ridge: Present and past methane fluxes through a large hydrate reservoir. Geochimica et Cosmochimica Acta, 65(4): 529-543.

Dickens, G.R., 2003a. A methane trigger for rapid warming? Science, 299: 1017.

Dickens, G.R., 2003b. Rethinking the global carbon cycle with a large, dynamic and microbially mediated gas hydrate capacitor. Earth and Planetary Science Letters, 213(3-4): 169-183.

Dickens, G.R., Castillo, M.M. and Walker, J.G.C., 1997. A blast of gas in the latest Paleoeocene: Simulating first-order effects of massive dissociation of oceanic methane hydrate. Geology, 25: 259-262.

Dickens, G.R., O'Neil, J.R., Rea, D.K. and Owen, R.M., 1995. Dissociation of oceanic methane hydrate as a cause of the carbon isotope excursion at the end of the Paleoeocene. Paleoceanography, 10: 965-971.

Dickinson, W.R. and Seely, D.R., 1979. Structure and stratigraphy of forecarc regions. American Association of Petroleum Geologists Bulletin, 63(1): 2-31.

Distel, D.L., 1998. Evolution of chemoautotrophic endosymbioses in bivalves. Bioscience, 48(4): 277-286.

Duncan, R.A., 1982. A captured island chain in the Coast Range of Oregon and Washington. Journal of Geophysical Research, 87(B13): 10827-10837.

Duncan, R.A. and Kulm, L.D., 1989. Plate tectonic evolution of the Cascades arc-subduction complex. In: E.L. Winterer, D.M. Hussong and R.W. Decker (Editors), The Eastern Pacific Ocean and Hawaii. The Geology of North America. Geological Society of America.

Dwyer, G.S. et al., 1995. North Atlantic deepwater temperature change during Late Pliocene and Late Quaternary clomatic cycles. Science, 270: 1347-1350.

Elderfield, H., Bertram, C. and Erez, J., 1996. A biomineralization model for the incorporation of trace elements into foraminiferal calcium carbonate. Earth and Planetary Science Letters, 142(409-423).

Elvert, M., Suess, E., Jens, G. and Whiticar, M., 2000. Archaea mediating anaerobic methane oxidation in deep-sea sediments at cold seeps of the eastern Aleutian subduction zone. Organic Geochemistry, 31: 1175-1187.

Emmanuel, S. and Ague, J.J., 2007. Implications of present-day abiogenic methane fluxes for the early Archaean atmosphere. Geophysical Research Letters, 34.

Erbacher, J. and Nelskamp, S., 2006. Comparison of benthic foraminifera inside and outside a sulphur-oxidizing bacterial mat from the oxygen-minimum zone off Pakistan (NE Arabian Sea). Deep-Sea Research I, 53: 751-775.

Erez, J., 2003. The source of ions for biomineralization in Foraminifera and their implications for paleoceanographic proxies. In: P.M. Dove, J.J. De Yoreo and S. Weiner (Editors), Biomineralization. Reviews in Mineralogy and Geochemistry. Mineralogical Society of America, Washington, pp. 115-149.
.

Ettwig, K.F. et al., 2008. denitrifying bacteria anaerobically oxidize methane in the absence of Archaea. Environmental Microbioloby, 10(11): 3164-3179.

Farr, L.C.J., 1989. Stratigraphy, diagenesis, and depositional environment of the Cowlitz Formation (Eocene) Northwest Oregon, Portland State University, Portland, 161 pp.

Faure, K. et al., 2006. Methane seepage and its relation to slumping and gas hydrate at the Hikurangi margin, New Zealand. New Zealand Journal of Geology and Geophysics, 49: 503-516.

Faure, K. et al., 2009 online. Methane seepage along the Hikurangi Margin of New Zealand: geochemical and physical evidence from the water column, sea surface and atmosphere.

Felbeck, H., 1983. Sulfide oxidation and carbon fixation by the gutless clam Solemya reidi: an animal-bacteria symbiosis. Journal of Comparative Physiology, 152(1): 3-11.

Ferguson, J.E., Henderson, G.M., Kucera, M. and Rickaby, R.E.M., 2008. Systematic change of foraminiferal Mg/Ca ratios across a strong salinity gradient. Earth and Planetary Science Letters, 265: 153-166.

Fiebig, J., Woodland, a.B., Spangenberg, J. and Oschmann, W., 2007. Natural evidence for rapid abiogenic hudrothermal generation of CH4. Geochimica et Cosmochimica Acta, 71: 3028-3039.

Fisher, C., Roberts, H., Cordes, E. and Bernard, B., 2007. Cold seeps and associated communities of the Gulf of mexico. Oceanography, 20: 118-129.

Formolo, M.J. et al., 2004. Quantifying carbon sources in the formation of authigenic carbonates at gas hydrate sites in the Gulf of Mexico. Chemical Geology, 205: 253-264.

Frank, D.J., Gormly, J.R. and Sackett, W.M., 1974. Re-evaluation of carbon-isotope compositions of natural methanes. Bulletin American Association Petroleum Geologists, 58(11): 2319-2325.

Frankel, L., 1974. Observations and speculations on the habitat and habits of *Trochammina ochracea* (Williamson) in subsurface sediments. Journal of Paleontology, 48(1): 143-147.

Fukuzaki, S., Nishio, N. and Nagai, S., 1990. Kinetics of methanogenic fermentation of acetate. Applied Environmental Microbiology, 56(10): 3158-3163.

Fuller, C.W., Willet, S.D. and Brandon, M.T., 2006. Formation of forearc basins and their influence on subduction zone earthquakes. Geology, 34(2): 65-68.

Gehlen, M., Bassinot, F.C., Chou, L. and McCorkle, D., 2005. Reassessing the dissolution of marine carbonates: I. Solubility. Deep-sea Research I, 52: 1445-1460.

Geslin, E., Heinz, P., Jorissen, F. and Hemleben, C., 2004. Migratory responses of deep-sea benthic foraminifera to variable oxygen conditions: laboratory investigations. Marine Micropaleontology, 53: 227-243.

Gieskes, J. et al., 2008. Systematic change of foraminiferal Mg/Ca ratios across a strong salinity gradient. Earth and Planetary Science Letters, 265(1-2): 153-166.

Goedert, J. and Benham, S.R., 1999. A new species of *Depressigyra?* (Gastropoda: Peltospiridae) from cold-seep carbonates in Eocene and Oligocene Rocks of Western Washington. The Veliger, 42(2): 112-116.

Goedert, J., Peckmann, J. and Reitner, J., 2000. Worm tubes in an allochthonous cold-seep carbonate from lower Oligocene rocks of Western Washington. Journal of Paleontology, 74(6): 992-999.

Goedert, J. and Squires, R., 1990. Eocene deep-sea communities in localized limestones formed by subduction-related methane seeps, southwestern Washington. Geology, 18(18): 1182-1185.

Goedert, J. et al., 2003. Late Eocene "Whiskey Creek" methane seep deposits (western Washington State) - Part I: Geology, Paleontology and Molecular Geobiology. Facies, 48: 223 - 240.

Goldfinger, C., Kulm, L.D., Yeats, R.S., McNeill, L. and Hummon, C., 1997. Oblique strike-slip faulting of the central Cascadia submarine forearc. Journal of Geophysical Research, 102(B4): 8217-8243.

Goldstein, S.T., 2002. Foraminifera: A biological overview. In: B.K. Sen Gupta (Editor), Modern Foraminifera. Kluwer Academic, Dordrecht/Boston/London, pp. 37-55.

Gradzinski, M., Tyszka, J., Uchman, A. and Jach, R., 2004. Large microbial-foraminiferal oncoids from condensed Lower-Middle Jurassic deposits: a case study from the Tatra Mountains, Poland. Palaeogeography, Palaeoclimatology, Palaeoecology, 213: 133-151.

Greinert, J., Bohrmann, G. and Elvert, M., 2002. Stromatolitic fabric of authigenic carbonate crusts: result of anaerobic methane ocidatin at cold seeps in 4,850 m water depth. International Journal of Earth Sciences, 91: 698-711.

Greinert, J., Bohrmann, G. and Suess, E., 2001. Gas hydrate-associated carbonates and methane-venting at Hydrate Ridge: classification, distribution, and origin of authigenic lithologies. In: C.K. Paull and W. Dillon (Editors), Natural Gas Hydrates: Occurrence, Distribution, and Detection. American Geophysical Union, Washington, D.C., pp. 99-113.

Greinert, J. and Derkachev, A., 2004. Glendonites and methane-derived Mg-calcites in the Sea of Okhotsk, Eastern Siberia: implications of a venting-related ikaite/glendonite formation. Marine Geology, 204: 129-144.

Gribaldo, S. and Brochier-Armanet, C., 2006. The origin and evolution of Archaea: a state of the art. Philosophical Transactions of the Royal Society, 361: 1007-1022.

Groeneveld, J. et al., 2008. Foraminiferal Mg/Ca increase in the Caribbean during the Pliocene: Western Atlantic Warm Pool formation, salinity influence, or diagenetic overprint? Geochemistry, Geophysics, Geosystems, 9(1).

Grossman, E.L., 1984. Carbon isotopic fractionation in live benthic foraminifera—comparison with inorganic precipitate studies. Geochimica et Cosmochimica Acta, 48: 1505-1512.
Grossman, E.L., 1987. Stable isotopes in modern benthic foraminifera: a study of vital effect. Journal of Foraminiferal Research, 17(1): 48-61.

Guilbault, J., Krautter, M., Conway, K.W. and Barrie, J.V., 2006. Modern foraminifera attached to hexactinellid sponge meshwork on the West Canadian shelf: comparison with Jurassic counterparts from Europe. Palaeontologia Electronica, 9(1): 3A:48p.

Haeckel, M., Boudreau, B. and Wallman, K., 2007. Bubble-induced porewater mixing: A 3-D model for deep porewater irrigation. Geochimica et Cosmochimica Acta, 71: 5135-5154.

Haeckel, M., Suess, E., Wallman, K. and Rickert, D., 2004. Rising methane gas bubbles form massive hydrate layers at the seafloor. Geochimica et Cosmochimica Acta, 68: 4335-4345.

Haese, R., Hensen, C. and de Lange, G.J., 2006. Pore water geochemistry of eastern Mediterranean mud volcanoes: Implications for fluid transport and fluid origin. Marine Geology, 225: 191-208.

Haeussler, P.J., Bradley, D.C., Wells, R.E. and Miller, M.L., 2003. Life and death of the Resurrection plate: Evidence for its existence and subduction in the northeastern Pacific in Paleocene-Eocene time. GSA Bulletin, 115(7): 867-880.

Haley, B. and Klinkhammer, G.P., 2002. Development of a flow-through system for cleaning and dissolving foraminiferal tests. Chemical Geology, 185: 51-69.

Haley, B.A., Klnikhammer, G.P. and Mix, a.C., 2005. Revisiting the rare earth elements in foraminiferal tests. Earth and Planetary Science Letters, 239: 79-97.

Hallock, P., 1999. Symbiont-bearing foraminifera. In: B.K. Sen Gupta (Editor), Modern Foraminifera. Kluwer Academic, Dordrecht, pp. 123-140.

Hallock, P. and Talge, H.K., 1994. A predatory foraminifer, *Floresina amphophaga*, n. sp., from the Florida Keys. Journal of Foraminiferal Research, 24(4): 210-213.

Hallock, P., Talge, H.K., Williams, D.E. and Harney, J.N., 1998. Borings in *Amphistegina* (Foraminiferida): Evidence of predation by *Floresina amphiphaga* (Foraminiferida). Historical Bioloby, 13: 73-76.

Hammond, P.E., 1998. Tertiary andesitic lava-flow complexes (stratovolcanoes) in the southern Cascade range of Washington- observations on tectonic processes within the Cascade arc. Washington Geology, 26(1): 20-30.

Han, M.W. and Suess, E., 1989. Subduction-induced pore fluid venting and the formation of authigenic carbonates along Cascadia continental margin: Implications for the global Ca-cycle. Palaeoceanography, Palaeoclimatology, Palaeoecology, 71: 97-118.

Han, X., Suess, E., Sahling, H. and Wallmann, K., 2004. Fluid venting activity on the Costa Rica margin: new results from authigenic carbonates. International Journal of Earth Sciences, 93: 596–611.

Hansen, H.J., 1999. Shell construction in modern calcareous foraminifera. In: B.K. Sen Gupta (Editor), Modern Foraminifera. Kluwer, Dordrecht/Boston/London, pp. 57-70.

Havach, S.M., Chandler, G.T., Wilson-Finelli, A. and Shaw, T.J., 2001. Experimental determination of trace element partition coefficients in cultured benthic foraminifera. Geochimica et Cosmochimica Acta, 65(8): 1277-1283.

Hawkes, A.D., Scott, D.B., Lipps, J.H. and Combellick, R., 2005. Evidence for possible precursor

events of megatrust earthquakes on the west coast of North America. GSA Bulletin, 117(7/8): 996-1008.

Hayes, J.M., 1994. Global methanotrophy at the Archean-Proterozoic transition. In: E. Bengtson (Editor), Early Life on Earth. Nobel Symposium, pp. 221-236.

Hayward, B.W., Carter, R., Grenfell, H.R. and Hayward, J.J., 2001. Depth distribution of Recent deep-sea benthic foraminifera east of New Zealand, and their potential for improving paleobathymetric assessments of Neogene microfaunas. New Zealand Journal of Geology and Geophysics, 44: 555-587.

Hayward, B.W., Grenfell, H.R., Reid, C.M. and Hayward, K.A., 1999. Recent New Zealand shallow-water benthic foraminifera: Taxonomy, ecologic distribution, biogeography, and use in paloeenvironmental assessment. Institute of Geological and Nuclear Sciences Monograph 21 (New Zealand Geological Survey paleontological bulletin 75): 258.

Heeschen, K.U. et al., 2005. Methane sources, distributions, and fluxes from cold vent sites at Hydrate Ridge, Cascadia Margin. Global Biogeochemical Cycles, 19.

Hein, C.R. and Koski, R.A., 1987. Bacterially mediated diagenetic origin for chert-hosted manganese deposits in the Franciscan Complex, California Coast Ranges. Geology, 15: 722-726.

Heinz, P., Sommer, S., Pfannkuche, O. and Hemleben, C., 2005. Living benthic foraminifera in sediments influenced by gas hydrates at the Cascadia convergent margin, NE Pacific. Marine Ecology Progress Series, 304: 77-89.

Heller, P.L., Tabor, R.W. and Suczek, C.A., 1987. Paleogeographic evolution of the United States Pacific Northwest during Paleogene time. Canadian Journal of Earth Science, 24: 1652-1667.

Hensen, C., Wallmann, K., Schmidt, M., Ranero, C.R. and Suess, E., 2004. Fluid expulsion related to mud extrusion off Costa Rica - A window to the subducting slab. Geology, 32(3): 201-204.

Hesse, R., 2003. Pore water anomalies of submarine gas-hydrate zones as tool to assess hydrate abundance and distribution in the subsurface. What have we learned in the past decade? Earth-Science Reviews, 61: 149-179.

Hickman, C.S., 1980. Paleogene marine gastropods of the Keasey Formation in Oregon. Bulletins of American Paleontology, 78: 1-112.

Hill, T.M., J.P., K. and Valentine, D.L., 2004a. Isotopic evidence for the incorporation of methane-derived carbon into foraminifera from modern methane seeps, Hydrate Ridge, Northeast Pacific. Geochimica et Cosmochimica Acta, 68(22): 4619-4627.

Hill, T.M., Kennett J.P. and Spero, H.J., 2003. Foraminifera as indicators of methane-rich environments: A study of modern methane seeps in Santa Barbara Channel, California. Marine Micropaleontology, 49: 123-138.

Hill, T.M., Kennett, J.P. and Spero, H.J., 2004b. High-resolution records of methane hydrate dissociation: ODP site 893, Santa Barbara Basin. Earth and Planetary Science Letters, 223: 127-140.

Hillgartner, H., Dupraz, C. and Hug, W., 2001. Microbially induced cementation of carbonate sands: are micritic meniscus cements good indicators of vadose diagenesis? Sedimentology, 48: 117-131.

Hinrichs, K.-U., Hayes, J.M., Sylva, S.P., Brewer, P.G. and DeLong, E.F., 1999. Methane-consuming archaebacteria in marine sediments. Nature, 398: 802-805.

Hintz, C.J. et al., 2006a. Minor element:calcium ratios in cultured benthic foraminifera. Part II: Ontogenetic variation. Geochimica et Cosmochimica Acta, 70: 1964-1976.

Hintz, C.J. et al., 2006b. Minor element:calcium ratios in cultured benthic foraminifera. Part I: Inter-species and inter-individual variability. Geochimica et Cosmochimica Acta, 70: 1952-1963.

Hoefs, J., 2004. Stable Isotope Geochemistry. Springer, Berlin, 244 pp.

Hoehler, T.M., Alperin, M.J., Albert, S.B. and Martens, C.S., 1994. Field and laboratory studies of methane oxidation in an anoxic marine sediment: Evidence for a methanogen-sulfate reducer consortium. Global Biogeochemical Cycles, 8(4): 451-463.

Horita, J. and Berndt, M., 1999. Abiogenic methane formation and isotopic fractionation under hydrothermal conditions. Science, 285: 1055-1057.

Hovland, M., 1992. Hydrocarbon seeps in northern marine waters - their occurrence and effects. Palaios, 7: 376-382.

Howard, N.J.B. and Haynes, J.R., 1976. *Chlamys opercularis* (Linnaeus) as a mobile substrate fo foraminifera. Journal of Foraminiferal Research, 6(1): 30-38.

Huber, B.T., Hodell, D.A. and Hamilton, C.P., 1995. Middle-Late Cretaceous climte of the southern high latitudes: Stable isogopic evidence for minimal equator-to-pole thermaal gradients. Geological Society of America Bulletin, 107(10): 1164-1191.

Ingle, J.C., Jr., 1967. Foraminiferal biofacies of Mio-Plio of Southern California. Bull. Am. Paleo 52, 52(236).

Ingle, J.C., Jr., 1976. Late Neogene paleobathymetry and paleoenvironments of the Humboldt River, northern California.

Ingle, J.C., Jr., 1980. Cenozoic paleobathymetry and depositional history of selected sequences withn the southern Calfornia continental borderland. Cushman Foundation Special Publication 19: 163-195.

Irving, A.J., Nesbitt, E.A. and Renne, P.R., 1996. Age constraints on earliest Cascade volcanism and Eocene marine biozones from a feldspar-rich tuff in the Cowlitz Formation southwestern Washington. ES Transactions American Geophysical Union, 77: F814.

Irwin, H., Curtis, C. and Coleman, M., 1977. Isotopic evidence for source of diagenetic carbonates formed during burial of organic-rich sediments. Nature, 269: 209-213.

Jenkins, R.G., Kaim, A., Hikida, Y. and Tanabe, K., 2007. Methane-flux-dependent lateral faunal changes in a Late Cretaceous chemosymbiotic assemblage from the Nakagawa area of Hokkaido, Japan. Geobiology.

Jiang, G., Kennedy, M.J. and Christie-Blick, N., 2003. Stable isotopic evidence for methane seeps in Neoproterozoic postglacial cap carbonates. Nature, 426: 822-826.

Jones, R.W., 1993. Preliminary observations on benthonic foraminifera associated with biogenic gas

seeps in the North Sea. In: D.G. Jenkins (Editor), Applied Micropaleontology. Kluwer Academic Publishers, Dordrecht, pp. 69-91.

Joye, S.B. et al., 2004. The anaerobic oxidation of methane and sulfate reduction in sediments from Gulf of Mexico cold seeps. Chemical Geology, 205: 219-238.

Judd, A.G., Hovland, M., Dimitrov, L.I., Gil, S.G. and Jukes, V., 2002. The geological methane budget at continental margins and its influence on climate change. Geofluids, 2: 109-126.

Karl, D., M, et al., 2008. Aerobic production of methane in the sea. Nature Geoscience, 1: 473-478.

Kasting, J.F., 2001. The rise of atmospheric oxygen. Science, 293: 819-820.

Kasting, J.F., 2005. Methane and climate during the Precambrian era. Precambrian Research, 137: 119-129.

Kasting, J.F. and Catling, D., 2003. Evolution of a habitable planet. Annual Review of Astronomy and Astrophysics, 41: 429-63.

Kastner, M., 2001. Gas hydrates in convergent margins: Formation, occurrence, geochemistry, and global significance. In: C.K. Paull and W. Dillon (Editors), Natural Gas Hydrates: Occurrence, Distribution, and Detection. American Geophysical Union Geophysical Monograph. American Geophysical Union, Washington, D.C., pp. 67-86.

Kastner, M., Elderfield, H., Jenkins, W.J., Gieskes, J.M. and Gamo, T., 1993. Geochemical and isotopic evidence of fluid flow in the western Nankai subduction zone, Japan. Proceedings of the Ocean Drilling Program, Scientific Results, 131: 397-413.

Kelley, D.S. and Fruh-Green, G., 1999. Abiogenic methane in deep-seated mid-ocean ridge environments: Insights from stable isotope analyses. Journal of Geophysical Research, 104(B5): 10,439-10460.

Kelley, D.S., Fruh-Green, G., Karson, J.A. and Ludwig, K., 2007. The Lost City hydrothermal field revisited. Oceanography, 20(4): 90-99.

Kennedy, M.J., Christie-Blick, N. and Sohl, L., 2001. Are Proterozoic cap carbonates and isotopic excursions a record of gas hydrate destabilization following Earth's coldest intervals? Geology, 29(5): 443-446.

Kennedy, M.J., Mrofka, D. and von der Borch, C., 2008. Snowball Earth termination by destabilization of equatorial permafrost methane clathrate. Nature, 453: 642-644.

Kennett, J.P., Cannariato, K.G., Hendy, I.L. and Behl, R.J., 2000. Carbon isotopic evidence for methane hydrate instability during Quaternary interstadials. Science, 288: 128-133.

Kennett, J.P., Cannariato, K.G., Hendy, I.L. and Behl, R.J., 2003. Methane Hydrates in Quaternary Climate Change: The Clathrate Gun Hypothesis. AGU Special Publication, 54, 216 pp.

Kennett, J.P. and Stott, L.D., 1991. Abrupt deep-sea warming, palaeoceanographic changes and benthic extinctions at the end of the Palaeocene. Nature, 353: 225-229.

Khusid, T.A., Domanov, M.M. and Svininnikov, A.M., 2006. Species composition and distribution of foraminifers in the Derygin Basin (Sea of Okhotsk). Biology Bulletin, 33(2): 172-178.

Kiel, S., 2006. New records and species of mollusks from Tertiary cold-sep carbonates in Washington State, USA. Journal of Paleontology, 80: 121-137.

Kiel, S. and Goedert, J.L., 2006. Deep-sea food bonanzas: early Cenozoic whale-fall communities resemble wood-fall rather than seep communities. Proceedings of the Royal Society B: doi:10.1098/rspb.2006.3620.

Kiel, S. and Peckmann, J., 2007. Chemosymbiotic bivalves and stable carbon isotopes indicate hydrocarbon seepae at four unusual Cenozoic fossil localities. Lethaia: 10.1111/j.1502-3931.2007.00033.x.

Klaucke, I., Weinrebe, W., Peterson, C. and Bowen, D., In press. Temporal variability of gas seeps offshore New Zealand: Multi-frequency geoacoustic imaging of the Wairarapa area, Hikurangi margin
. This issue.

Klinkhammer, G.P. and Haley, B., 2006. Multi-proxy relationships in foraminiferal tests as delineated from element-element plots of time-resolved flo-thru data. Geochimica et Cosmochimica Acta, 70: A325-A325.

Klinkhammer, G.P., Haley, B., Mix, A.C., Benway, H.M. and Cheseby, M., 2004. Further evaluation of flow-through as a method for cleaning and dissolving shells of planktonic foraminifera for Mg/Ca paleothermometry. Geochimica et Cosmochimica Acta, 68: A335-A335.

Klinkhammer, G.P., Mix, A.C. and Haley, B., 2009. Increased dissolved terestrial input to the coastal ocean during the last deglaciation. Geochemistry, Geophysics, Geosystems, 10(3).

Kohn, M.J., Riciputi, L.R., Stakes, D.S. and Orange, D.L., 1998. Sulfur isotope variability in biogenic pyrite: Reflections of heterogeneous bacterial colonization? American Mineralogist, 1454-1468.

Krabbenhoeft, A., Netzeband, G.L., Bialas, J. and Papenberg, C., 2009 online. Methane concentrations from ocean bottom stations and their relation to seismic structures. Marine Geology.

Kulm, L.D. and Suess, E., 1990. Relationship between carbonate deposits and fluid venting: Oregon accretionary prism. Journal of Geophysical Research, 95(B6): 8899-8915.

Kump, L.R. and Arthur, M.A., 1999. Interpreting carbon-isotope excursions: carboinates and organic matter. Chemical Geology, 161: 181-198.

Kunioka, D., Shirai, K., Takahata, N. and Sano, Y., 2006. Microdistribution of Mg/Ca, Sr/Ca, and Ba/Ca ratios in *Pulleniatina obliquiloculata* test by using a nanoSIMS: Implication for vital effect mechanism. Geochemistry, Geophysics, Geosystems, 7(12).

Kvenvolden, K.A., 1999. Potential effects of gas hydrate on human welfare. National Academy of Science Proceedings, 96: 3420-3426.

Langer, M., 1993. Epiphytic foraminifera. Marine Micropaleontology, 20: 235-265.

Law, C.S. et al., 2009 online. Geological, hydrodynamic and biogeochemical characterisation of a New Zealand deep-water methane cold seep during a three-year time-series study. Marine Geology.

Lea, D.W. and Martin, P.A., 1996. A rapid mass spectrometric method for the simultaneous analysis

of barium, cadmium and strontium in foraminifera shells. Geochimica et Cosmochimica Acta, 60(16): 3143-3149.

Lea, D.W., Mashiotta, T.A. and Spero, H.J., 1999. Controls on magnesium and strontium uptake in planktonic foraminifera determined by live culturing. 63(16): 2369-2379.

Leaist, D.G., Mashiotta, T.A. and Spero, H.J., 1999. Controls on magnesium and strontium uptake in planktonic foraminifera determined by live culturing. Geochimica et Cosmochimica Acta, 63(16): 2369-2379.

Lear, C.H., Elderfield, H. and Wilson, P.A., 2000. Cenozoic deep-sea temperatures and global ice volumes from Mg/Ca in benthic foraminiferal calcite. Science, 287: 269-272.

Lear, C.H., Rosenthal, Y. and Slowey, N., 2002. Benthic foraminiferal Mg/Ca-paleothermometry: A revised core-top calibration. Geochimica et Cosmochimica Acta, 66(19): 3375-3387.

Lear, C.H., Rosenthal, Y. and Wright, J.D., 2003. The closing of a seaway: ocean water masses and global climate change. Earth and Planetary Science Letters, 210: 425-436.

Lee, J.J. and Anderson, O.R., 1991. Symbiosis in foraminifera. In: J.J. Lee and O.R. Anderson (Editors), Biology of Foraminifera. Harcourt, Brace, Jovanovich, London, pp. 157-220.

Leefmann, T. et al., 2008. Miniaturized biosignature analysis reveals implications for the formation of cold seep carbonates at Hydrate Ridge. Biogeosciences, 5: 731-738.

Lescinsky, H.L., 1997. Epibiont communities: Recruitment and competition on North American Carboniferous brachiopods. Journal of Paleontology, 71(1): 34-52.

Levin, L.A., 2005. Ecology of cold seep sediments: Interactions of fauna with flow, chemistry, and microbes. Oceanography and Marine Biology, an Annual Review, 43: 1-46.

Levin, L.A. and Michener, R.H., 2002. Isotopic chemosynthesis-based nutrition of macrobenthos: the lightness of being at Pacific methane seeps. Limnology and oceanography, 47: 1336 - 1345.

Lewis, K.B. and Marshall, B.A., 1996. Seep faunas and other indicators of methane-rich dewatering on New Zealand convergent margins. New Zealand Journal of Geology and Geophysics, 39: 181-200.

Lewis, K.B. and Pettinga, J.R., 1993. The emerging, imbricate frontal wedge of the Hikurangi margin. In: P.F. Ballance (Editor), Sedimentary Basins of the World 2: Basins of the South West Pacific. Elsevier Science Publishers, Amsterdam, pp. 225-250.

Linke, P. and Lutze, G.F., 1993. Microhabitat preferences of benthic foraminifera - a static concept or a dynamic adaptation to optimize food acquisition? Marine Micropaleontology, 20: 215-234.

Lipps, J.H., 1973. Test structure in foraminifera. Annual reviews in microbiology, 27: 471-486.

Lobegeier, M.K. and Sen Gupta, B.K., 2008. Foraminifera of hydrocarbon seeps, Gulf of Mexico. Journal of Foraminiferal Research, 38(2): 93-116.

Lollar, B.S. et al., 2006. Unravelling abiogenic and biogenic sources of methane in the Earth's deep surface. Chemical Geology, 226: 328-339.

Lorenson, T.D. and Collett, T.S., 2000. Gas content and composition of gas hydrate from sediments of the southeastern North American continental margin. Procedings of the Ocean Drilling Program, Scientific Results, 164, 37-46 pp.

Luff, R. and Wallmann, K., 2003. Fluid flow, methane fluxes, carbonate precipitation and bigeochemical turnover in gas hydrate-bearing sediments at Hydrate Ridge, Cascadia Margin. Geochimica et Cosmochimica Acta, 67: 3403-3421.

Luff, R., Wallmann, K. and Aloisi, G., 2004. Numerical modeling of carbonate crust formation at cold vent sites: significance for fluid and methane budgets and chemosynthetic biological communities. Earth and Planetary Science Letters, 221: 337-353.

Lyons, T.W., Zhang, C.L. and Romanek, C.S., 2003. Isotopic records of microbially mediated processes. Chemical Geology, 195: 1-4.

Mackensen, A., Wollenburg, J. and Licari, l., 2006. Low $d^{13}C$ in tests of live epibenthic and endobenthic foraminifera at a site of active methane seepage. Paleoceanography, 21: PA2022, doi:10.1029/2005PA001196,2006.

Mackenson, A., Schumacher, S., Radke, J. and Schmidt, D.N., 2000. Microhabitat preferences and stable carbon isotopes of endobenthic foraminifera: clue to quantitative reconstruction of oceanic new production? Marine Micropaleontology, 40(233-258).

Madsen, J.K., Thorkelson, D.J. and Marshall, D.D., 2006. Cenozoic to Recent plate configuratio on the Pacific Basin: ridge subduction and slab window magnetism in western North America. Geosphere, 2: 11-34.

Majima, R., Nobuhara, T. and Kitazaki, T., 2005. Review of fossil chemosynthetic assemblages in Japan. Palaeogeography, Palaeoclimatology, Palaeoecology, 277(86 - 123).

Marshall, D.J., 1988. Cathodoluminescence of Geological Materials. Unwin Hayman, Boston, 146 pp.

Martin, J.B. et al., 2004. Relationships between the stable isotopic signatures of living and fossil foraminifera in Monterey Bay, California. Geochemistry, Geophysics, Geosystems, 5: Q04004, doi:10.1029/2003GC000629.

Martin, J.B., Orange, D.L., Lorenson, T.D. and Kvenvolden, K.A., 1997. Chemical and isotopic evidence of gas-influenced flow at a transform plate booundary: Monterey Bay, California. Journal of Geophysical Research, 102(B11): 24,903-24,915.

Martin, R.A., 2008. Foraminifers as hard substrates: An exaple from the Washington continental shelf of smaller foraminifers attached to larger, agglutinate foraminifers. Journal of Foraminiferal Research, 38(1): 3-10.

Martin, R.A. and Nesbitt, E.A., 2004. Benthic foraminiferal characteristics of a diffuse Pliocene mid-shelf hydrocarbon seep, Cascadia convergent margin, Geological Society of America, Denver, pp. 59.

Martin, R.A. and Nesbitt, E.A., 2005. Benthic foraminiferal characteristics of Cenozoic cold seeps on the Northeast Pacific margin, American Association of Petroleum Geologists, Calgary.

Martin, R.A., Nesbitt, E.A. and Caampbell, K.A., 2005. Benthic foraminiferal characterization of

two Cenozoic cold seeps, Cascadia accretionary margin, Third International Symposium on Hydrothermal Vent and Seep Biology, Scripps.

Martin, R.A., Nesbitt, E.A. and Campbell, K.A., 2007. Carbon stable isotopic composition of benthic foraminifera from Pliocene cold methane seeps, Cascadia accretionary margin. Palaeogeography, Palaeoclimatology, Palaeoecology, 246: 260-277.

Martin, R.A., Nesbitt, E.A. and Campbell, K.A., 2009 online. The effects of anaerobic oxidation of methane on benthic foraminiferal assemblages and stable isotopes on the Hikurangi Margin of eaastern New Zealand. Marine Geology.

Martin, W., Baross, J., Kelley, D. and Russell, M.J., 2008. Hydrothermal vents and the origin of life. Nature Reviews: Microbiology, 6: 805-814.

Maslin, M., Mikkelsen, N., Vilela, C. and Haq, B., 1998. Sea-level- and gas-hydrate-controlled catastrophic sediment failures of the Amazon Fan. Geology, 26(12): 1107 - 1110.

Mazzullo, S.J., 2000. Organogenic dolomitization in peritidal to deep-sea sediments. Journal of Sedimentary Research, 70(1): 10-23.

McCollom, T.C. and Seewald, J.S., 2006. Carbon isotope composition of organic compounds produced by abiotic synthesis under hydrothermal conditions. Earth and Planetary Science Letters, 243: 74-84.

McCorkle, D.C., Corliss, B.H. and Farnham, C.A., 1997. Vertical distributions and stable isotopic compositions of live (stained) benthic foraminifera from the North Carolina and California continental margins
. Deep-Sea Research I Oceanographic, 44(6): 983-1024.

McDougall, K., 1980. Paleoecological evaluation of late Eocene biostratigraphic zonations of the Pacific coast of North America. Journal of Paleontology Paleontological Monograph, 2: 1-46.

McElwain, J.C., Wade-Murphy, J. and Hesselbo, S.P., 2005. Changes in carbon diocide during an oceanic anoxic event linked to intrusion into Gondwana coals. Nature, 435(26): doi:10.1038/nature03618.

McNeill, L.C., Goldfinger, C., Kulm, L.D. and Yeats, R.S., 2000. Tectonics of the Neogene Cascadia forearc basin: Investigations of a deformed late Miocene unconformity. Geological Society of America Bulletin, 112(8): 1209-1224.

McQuay, E.L., Torres, M.E., Collier, R.W., Huh, D.-A. and McManus, J., 2008. Contribution of cold seep barite to the barium geochemical budget of a marginal basin. 55: 801-811.

Michaelis, W. et al., 2002. Microbial reefs in the Black Sea fueled by anaerobic oxidation of methane. Science, 297: 1013-1015.

Milkov, A.V. et al., 2003. In situ methane concentrations at Hydrate Ridge, offshore Oregon: New constraints on the global gas hydrate inventory from an active margin. Geological Society of America Bulletin, 31(10): 833-836.

Millo, C., Sarnthein, M. and Erlenkeuser, H., 2005a. Methane-driven late Pleistocene $\delta^{13}C$ minima and overflow reversals in the southwestern Greenland Sea. Geology, 33(11): 873-876.

Millo, C., Sarnthein, M., Erlenkheuser, H., Grootes, P.M. and Andersen, N., 2005b. Methane-induced early diagenesis of foraminiferal tests in the southwestern Greenland Sea. Marine Micropaleontology, 58: 1-12.

Mitsiguchi, T., Matsumoto, E., Abe, O., Uchida, T. and Isdale, P.J., 1996. Mg/Ca thermometry in coral skeletons. Science, 274: 961-962.

Moodley, L., van der Zwaan, G.J., Rutten, G.M.W., Boom, R.C.E. and Kempers, A.J., 1998. Subsurface activity of benthic foraminifera in relation to porewater oxygen content: laboratory experiments. Marine Micropaleontology, 34: 91-106.

Moore, E.J., 1999a. Diagenetic history of sequential calcite, barite, and quartz within the chambers of the Tertiary nautiloid *Aturia*, southwestern Washintgton. Saito Ho-on Kai Special Publication, Prof. T. Kotaka Commemorative Volume: 193-206.

Moore, J.C., 1999b. Fluid seeps at continental margins. Margins Newsletter, 4: 12-14.

Morse, J.W., Andersson, A.J. and Mackenzie, F.T., 2006. Initial responses of caronate-rich shelf sediments to rising atmospheric pCO_2 and "ocean adicification": Role of high Mg-calcites. Geochimica et Cosmochimica Acta, 70: 5814-5830.

Murray, J.W. and Bowser, S.S., 2000. Mortality, protoplasm decay rate, and reliability of staining techniques to recognize ‘‘living’’ Foraminifera. Journal of Foraminiferal Research, 30: 66-70.

Muyzer, G. and van der Kraan, G.M., 2008. Bacteria from hydrocarbon seep areas growing on short-chain alkanes. Trends in Microbiology, 16: 136-141.

Naehr, T.H. et al., 2007. Authigenic carbonate formation at hydrocarbon seeps in continental margins. Deep-Sea Research II, 54: 1268-1291.

Naehr, T.H. et al., 1998. Authigenic carbonates from the Cascadia subduction zone and their relation to gas hydrate stability. Geology, 26(7): 647 - 650.

Naehr, T.H., Rodriguez, N.M., Bohrmann, G., Paull, C.K. and Botz, R., 2000. Methane-derived authigenic carbonates associated with gas hydrate decomposition and fluid venting above the Blake Ridge diapir. Proceedings of the Ocean Drilling Program, Scientific Results, 164: 285-300.

Narayan, V.R., Barnes, C., R. and Johns, M., J., 2005. Taxonomy and biostratigraphy of Cenozoic foraminifers from Shell Canada well, Tofino Basin, offshore Vancouver Island, British Columbia. Micropaleontology, 51(2): 101-167.

Nesbitt, E.A. and Campbell, K.A., 2004a. Spatial and stratigraphic distribution of fossils from diffuse seeps in a Pliocene shelf setting, Cascadia convergent margin., Geological Society of America Abstracts with programs, Denver, pp. 314.

Nesbitt, E.A. and Campbell, K.A., 2004b. Trace fossil suite from diffuse seep carbonates in a storm and flood dominated mid-shelf setting, 32nd International Geological Congress Scientific Sessions: Abstracts. International Geological Congress, Florence, italy, pp. 930.

Nesbitt, E.A. and Campbell, K.A., 2005. Spatial and stratigraphic distribution of authigenic carbonates and trace and body fossils from diffuse seeps in a Pliocene inner to mid-shelf setting, Cascadia convergent margin, VII International Ichnofabrics Workshop, Auckland, New Zealand, pp. 27.

Nesbitt, E.A., Campbell, K.A. and Goedert, J.L. (Editors), 1994. Paleogene cold seeps and macroinvertebrate fauna in a forearc sequence of Oregon and Washington. Geological Society of America, Field Guides.

Nesbitt, E.A., Martin, R.A., Carroll, N. and Grieff, J., in revision. Reassessment of the Zemorrian foraminiferal Stage and Juanian molluscan Stage north of the Olympic Mountains, Washington State and Vancouver Island. Canadian Journal of Earth Sciences.

Nicol, A. et al., 2007. Tectonic evolution of the active Hikurangi subduction margin, New Zealand, since the Oligocene. Tectonics, 26(TC4002): doi:10.1029/2006TC002090,2007.

Nielsen, K.S.S., Nielsen, J.K. and Bromley, R.G., 2003. Palaeoecological and ichnological significance of microborings in Quaternary foraminifera. Palaeontologia Electronica, 6(2): 13pp.

Niemann, H. and Elvert, M., 2008. Diagnostic lipid biomarker and stable carbon isotope signatures of microbial communities mediating the anaerobic oxidation of methane with sulphate. Organic Geochemistry, 39: 1668-1667.

Nurnberg, D., Bjima, J. and Hemleben, C., 1996. Assessing the reliability of magnesium in foraminiferal calsite as a proxy for water mass temperatures. Geochimica et Cosmochimica Acta, 60: 803-814.

Orange, D.L. and Campbell, K.A., 1997. Modern and ancient cold seeps on the Pacific Coast - Monterey Bay, California, and offshore Oregon as modern-day analogs to the Hoh accretionary complex and Quinault Formation, Washington. Washington Geology, 25(4): 1--13.

Orange, D.L., Geddes, D.S. and Moore, J.C., 1993. Structural and fluid evolution of a young accretionary complex: The Hoh rock assemblage of the western Olympic Peninsula, Washington. Geological Society of America Bulletin, 105: 1053-1075.

Orange, D.L. et al., 1999. Widespread fluid expulsion on a translational continental margin; Mud volcanoes, fault zones, headless canyons, and organic-rich substrate in Monterey Bay, California. Geological Society of America Bulletin, 111(7): 992-1009.

Orcutt, B., Boetius, A., Elvert, M., Samarkin, V. and Joye, S., 2005. Molecular biogeochemistry of sulfate reduction, methanogenesis and the anaerobic oxidation of methane at Gulf of Mexico cold seeps. Geochimica et Cosmochimica Acta, 69(17): 4267-4281.

Orcutt, B.N. et al., 2004. Life at the edge of methane ice: microbial cycling of carbon and sulfur in Gulf of Mexico gas hydrates. Chemical Geology, 205: 239-251.

Orphan, V.J. et al., 2001a. Comparative analysis of methane-oxidizing archaea and sulfate-reducing bacteriain anoxic marine sediments. Applied and Environmental Microbiology, 67(4): 1922-1934.

Orphan, V.J., House, C.H., Hinrichs, K-U., McKeegan, K.D. and DeLong, E., 2001b. Methane-consuming archaea revealed by directly coupled isotopic and phylogenetic analysis. Science, 293: 484-487.

Orphan, V.J. et al., 2004. Geological, geochemical, and microbiological heterogeneity of the seafloor around methane vents in the Eel River Basin, offshore California. Chemical Geology, 205: 265-289.

Pagani, M., Freeman, K.H. and Arthur, M.A., 1999. Isotope analyses of molecular and total organic

carbon from Miocene sediments. Geochemica et Cosmochimica Acta, 64(1): 37-49.

Pagel, M., Barbin, V., Blanc, P. and Ohnenstetter, D. (Editors), 2000. Cathodoluminescence in Geosciences. Springer, Berlin, Heidelberg, New York, 514 pp.

Pancost, R.D. et al., 2000. Biomarker evidece for widespread anaerobic methane oxidation in Mediterranean sediments by a consortium of methanogenic archaea and bacteria. Applied and Environmental Microbiology, 66(3): 1126-1132.

Panieri, G., 2003. Benthic foraminifera response to methane release in an Adriatic Sea pockmark. Rivista Italiana di Paleontologia e Stratigrafia, 109(3).

Panieri, G., 2005. Benthic foraminifera associated with a hydrocarbon seep in the Rockall Trough (NE Atlantic). Geobios, 38(2): 247-255.

Panieri, G., 2006. Foraminiferal response to an active methane seep environment: A case study from the Adriatic Sea. Marine Micropaleontology, 61: 116-130.

Panieri, G., Camerlenghi, A., Conti, S., Pini, G.A. and Cacho, I., 2009. Methane seepages recorded in benthic foraminifera from Miocene seep carbonates, Northern Apennines (Italy). Palaeoceanography, Palaeoclimatology, Palaeoecology.

Panieri, G. and Sen Gupta, B.K., 2008. Benthic foraminifera of the Blake Ridge hydrate mound, Western North Atlantic Ocean. Marine Micropaleontology, 66(2): 91-102.

Parkes, R.J. et al., 2007. Biogeochemistry and biodiversity of methane cycling in subsurface marine sediments (Skagerrak, Denmark). Environmental Microbiology, 9(5): 1146-1161.

Paull, C.K., Buelow, W.J., Ussler, W., III and Borowski, W.S., 1996. Increased continental-margin slumping frequency during sea-level lowstands above gas hydrate-bearing sediments. Geology, 24: 143-146.

Paull, C.K., Chanton, J.P., Neumann, C., Coston, J.A. and Martens, C.S., 1992. Indicators of methane-derived carbonates and chemosynthetic organic carbon deposits: Examples from the Florida Escarpment. Palaios, 7: 361-375.

Paull, C.K. et al., 1984. Biological communities at the Florida Escarpment resemble hydrothermal vent taxa. Science, 226: 965-967.

Paull, C.K., Juli, A.J.T., Toolin, L.J. and Linick, T., 1985. Stable isotope evidence for chemosynthesis in an abyssal seep community. Nature, 317: 709-711.

Paull, C.K. et al., 2000. Isotopic composition of CH4, CO2 species, and sedimentary organic matter within samples from the Blake Ridge: Gas source implications. In: C.K. Paull, R. Matsumoto, P.J. Wallace and W.P. Dillon (Editors), Proceedings of the Ocean Drilling Program, pp. 67-78.

Paull, C.K. et al., 2007. Authigenic carbon entombed in methane-soaked sediments from the northeastern transform margin of the Guaymas Basin, Gulf of California. Deep-Sea Research Part II, 54: 1240-1267.

Pearson, P.N. et al., 2001. Warm tropical sea surface temperatures in the Late Cretaceous and Eocene epochs. Nature, 413: 481-487.

Peckmann, J. et al., 2003. The Late Eocene 'Whiskey Creek' mehtane-seep deposit (Western Washington State) part LL: petrology, stable isotopes, and biogeochemistry. Facies, 48: 241-254.

Peckmann, J., Goedert, J.L., Thiel, V., Michaelis, W. and Reitners, J., 2002. A comprehensive approach to the study of methane-seep deposits from the Lincoln Creek Formation, western Washington State, U.S.A. Sedimentology, 49: 855-873.

Peckmann, J. and Thiel, V., 2004. Carbon cycling at ancient methane-seeps. Chemical Geology, 205: 443-467.

Pena, D. et al., 2008. Characterization of contaminant phases in foraminifera carbonates by electron microprobe mapping. Geochemistry, Geophysics, Geosystems, 9(7).

Pfannkuche, O. and Linke, P., 2003. GEOMAR landers as long-term deep-sea observatories. Sea Technology, 44(9): 50-55.

Pohlman, J.W., 2006. Sediment biogeochemistry of northern Cascadia Margin shallow gas hydrate systems. Dissertation Thesis, College of William and Mary, 249 pp.

Pohlman, J.W. et al., 2005. The origin of thermogenic gas hydrates on the northern Cascadia Margin as inferred from isotopic (13C/12C and D/H) and molecular composition of hydrate and vent gas. Organic Geochemistry, 36: 703-716.

Price, G.D., Sellwood, B.W., Corfield, R.M., Clarke, L. and Cartlideg, J.E., 1998. Isotopic evidence for palaeotemperatures and depth stratification of Middle Cretaceous planktonic foraminifera from the Pacific Ocean. Geology Magazine, 135(2): 183-191.

Prothero, D.R. and Armentrout, J.M., 1985. Magnetostratigraphic sorrelation of the Lincoln Creek Formation, Wasington: Implications for the age of the Eocene/Oligocene boundary. Geology, 13(3): 208-211.

Prothero, D.R., Draus, E., Cockburn, T. and Nesbitt, E.A., 2008. Paleomagnetism and counterclockwise tectonic rotation of the Upper Oligocene Sooke Formation, Southern vancouver Island, British Columbia. Canadian Journal of Earth Sciences, 45(4): 499-507.

Prothero, D.R., Draus, E., Cockburn, T. and Nesbitt, E.A., 2009. Paleomagnetism and counterclockwise tectonic rotation of the Upper Oligocene Sooke Formation, Southern Vancouver Island, British Columbia. Newsletters on Stratigraphy, 43(2): 127-148.

Prothero, D.R. and Hankins, K.G., 2000. Magnetic stratigraphy and tectonic rotation of the Eocene-Oligocene Keasey Formation, northwest Oregon. Journal of Geophysical Research, 105(87): 16,473-16,480.

Raja, R., Saraswati, P.K., Rogers, K. and Iwao, K., 2005. Magnesium and strontium compositions of recent symbiont-bearing benthic foraminifera. Marine Micropaleontology, 58: 31-44.

Rakovan, J. and Waychunas, G., 1996. Luminiscence in minerals. Mineralogical Record, 27(1): 7-21.

Rathburn, A.E. and Corliss, B.H., 1994. The ecology of living (stained) deep-sea benthic foraminifera from the Sulu Sea. Paleoceanography, 9(1): 87-150.

Rathburn, A.E., Levin, L.A., Held, Z. and Lohmann, K.C., 2000. Benthic foraminifera associated

with cold methane seeps on the northern California margin: Ecology and stable isotopic composition. Marine Micropaleontology, 38: 247-266.

Rathburn, A.E. et al., 2003. Relationships between the distribution and stable isotopic composition of living benthic foraminifera and cold methane seep biogeochemistry in Monterey Bay, California. Geochemistry, Geophysics, Geosystems, 4(12): 1106, doi:10.1029/2003GC000595, 2003.

Rathmann, S., Hess, S., Kuhnert, H. and Muitza, S., 2004. Mg/Ca ratios of benthic foraminifera *Oridorsalis umbonatus* obtained by laser ablation from core top sediments: Relationship to bottom water temperature. Geochemistry, Geophysics, Geosystems, 5(12).

Rathmann, S. and Kuhnert, H., 2008. Carbonate isotope effect on Mg/Ca, Sr/Ca and stable isotopes on the benthic foraminifera *Oridorsalis umbonatus* off Namibia. Marine Micropaleontology, 66: 120-133.

Rau, W.W., 1966. Stratigraphy and Foraminifera of the Satsop River Area, southern Olympic Peninsula, Washington. State of Washington Division of Mines Geological Bulletin, 53: 66 pp.

Rau, W.W., 1970. Foraminifera, stratigraphy, and paleocology of the Quinault Formation, Point Grenville-Raft River coastal area, Washington. 41, 62: 41.

Rau, W.W., 1981. Pacific Northwest Tertiary benthic foraminiferal biostratigraphic framework; an overview. Geological Society of America Special Paper, 184: 67-84.

Reichert, G.-J., Jorissen, F., Anschutz, P. and Mason, P., 2003. Single foraminiferal test chemistry records the marine environment. Geology, 31: 355-358.

Reiners, P.W. et al., 2002. Late Miocene exhumation and uplift of the Washington Cascade Range. Geology, 30(9): 767-770.

Reitner, J. et al., 2005. Concretionary methane-seep carbonates and associated microbial communities in Black Sea sediments. Palaeogeography, Palaeoclimatology, Palaeoecology.

Rigby, J.K. and Goedert, J., 1996. Fossil sponges from a localized cold-seep limestone in Oligocene rocks of the Olympic Peninsula, Washington. Journal of Paleontology, 70(6): 900-908.

Roberts, H. and Whelan, T.W.I., 1975. Methane-derived carbonate cements in barrier and beach sands of a subtropical delta complex. Geochemica et Cosmochimica Acta, 19: 1085-1089.

Robinson, C.A., Bernhard, J.M., Levin, L.A., Mendoza, G.F. and Blanks, J., 2004. Surficial hydrocarbon seep infauna from the Blake Ridge (Atlantic Ocean, 2150 m) and the Gulf of Mexico (690-2240 m). P.S.N.Z.: Marine Ecology, 25(4): 313-336.

Rodland, D.L., Kowalewski, M., Carroll, M. and Simoes, M.G., 2004. Colonization of a 'Lost World': Encrustation Patterns in Modern Subtropical Brachiopod Assemblages. PALAIOS, 19: 381-395.

Rosenthal, Y., Boyle, E.A. and Slowey, N., 1997. Temperature control on the incorporation of magnesium, strontium, fluorine and cadmium into benthic foraminiferal shells from Little Bahama Bank. Geochimica et Cosmochimica Acta, 61(17): 3633-3643.

Rosenthal, Y., Lear, C.H., Oppo, D.W. and Braddock, K.L., 2006. Temperature and carbonate ion effects on Mg/Ca and Sr/Ca ratios in benthic foraminifera: Aragonitic species *Hoeglundina elegans*. Paleoceanography, 21.

Russell, A.D., Honisch, B., Spero, H.J. and Lea, D.W., 2004. Effects of seawater carbonate ion concentration and temperature on shell U, Mg, and Sr in cultured planktonic foraminifera. Geochimica et Cosmochimica Acta, 68(21): 4347-4361.

Sahling, H., Rickert, D., Lee, R.W., Linke, P. and Suess, E., 2002. Macrofaunal community structure and sulfide flux at gas hydrate deposits from the Cascadia convergent margin, NE Pacific. Marine Ecology Progress Series, 231: 121-138.

Sakai, H., Gamo, T., Ogawa, Y. and Boulegue, J., 1992. Stable isotope ratios and origins of the carbonates associated with cold seepage at the eastern Nankai Trough. Earth and Planetary Science Letters, 109: 391-404.

Sample, J.C. and Reid, M.R., 1998. Contrasting hydrogeologic regimes along strike-slip and thrust faults in the Oregon convergent margin: Evidence from the chemistry of syntectonic carbonate cements and veins. Geological Society of America Bulletin, 110(1): 48-59.

Sample, J.C., Reid, M.R., Tobin, H.J. and Moore, J.C., 1993. Carbonate cements indicate channeled fluid flow along a zone of vertical faults at the deformation front of the Cascadia accretionary wedge. Geology, 21: 507-510.

Sassen, R. and MacDonald, I., 1998. Bacterial methane oxidation in sea-floor gas hydrate: Significance to life in extreme environments. Geology, 26: 851-854.

Sassen, R. et al., 2004. Free hydrocarbon gas, gas hydrate, and authigenic minerals in chemosynthetic communities of the northern Gulf of Mexico continental slope: relation to microbial processes. Chemical Geology, 205: 195-17.

Schenck, H.G., 1927. Marine Oligocene of Oregon. Univeristy of California, Publications in Geological Sciences, 16 (12): 449-460.

Schidlowski, M., 2000. Carbon isotopes and microbial sediments. In: R.E. Riding and S.M. Awramik (Editors), Microbial Sediments. Springer-Verlag, Berlin
Heidelberg, pp. 84-95.

Schmeidl, G., Pfeilsticker, M., Hemleben, C. and Mackenson, A., 2004. Environmental and biological effects on the stable isotope composition of recent deep-sea benthic foraminifera from the western Mediterranean Sea. Marine Geology, 51: 129-152.

Schmidt, M. et al., 2002. Seeping hydrocarbons and related carbonate mineralisations in sediments south of Lihir Island (New Ireland fore arc basin, Papua New Guinea). Chemical Geology, 186: 249-264.

Schrag, D.P., DePaolo, D.J. and Richter, F.M., 1995. Reconstruction past sea surface temperatures: Correcting for diagenesis of bulk marine carbonate. Geochimica et Cosmochimica Acta, 59: 2265-2278.

Schulz, H., 1999. Short history and present trends of Fischer-Tropsch synthesis. Applied Catalysis A, General 186: 3-12.

Schwalenberg, K., Haeckel, M., Poort, J. and Jegen, M., 2009 online. Evaluation of gas hydrate deposits in an active seep area using marine controlled source electromagnetics: results from the Wairarapa region, New Zealand. Marine Geology.

Semrau, J.D., DiSpirito, A.A. and Murrell, J.C., 2008. Life in the extreme: thermoacidophilic methanotrophy. Trends in Microbiology, 16(5): 190-193.

Sen Gupta, B.K., 1999. Modern Foraminifera. Kluwerer, Boston, 371 pp.

Sen Gupta, B.K. and Aharon, P., 1994. Benthic foraminifera of bathyal hydrocarbon vents of the Gulf of Mexico: Initial report on communities and stable isotopes. Geo-Marine Letters, 14: 88-96.

Sen Gupta, B.K., Platon, E., Bernhard, J.M. and Aharon, P., 1997. Foraminiferal colonization of hydrocarbon-seep bacterial mats and underlying sediment, Gulf of Mexico slope. Journal of Foraminiferal Research, 27(4): 292-300.

Sen Gupta, B.K., Platon, E. and Lobegeier, M., 2002. Benthic Foraminifera of the Gulf of Mexoco, First International Palaeontological Congress. Geological Society of Australia Abstracts, Sudney, pp. 142-143.

Sen Gupta, B.K., Smith, L. and Lobegeier, M., 2007. Attachment of Foraminifera to vestimentiferan tubeworms at cold seeps: Refuge from seafloor hypoxia and sulfide toxicity. Marine Micropaleontology, 62: 1-6.

Sergeeva, N.G. and Gulin, M.B., 2007. Meiobenthos from an active methane seepage area in the NW Black Sea. Marine Ecology, 28: 152-159.

Shackleton, N.J., Wiseman, J.D. and Buckley, J.D., 1973. Non-equilibrium isotopic fractionation between sea-water and planktonic foraminifera. Nature, 242: 177-179..

Shapiro, R. and Spangler, E., 2009. Bacterial fossil record in whale-falls: Petrographic evidence of microbial sulfate reduction. Palaeogeography, Palaeoclimatology, Palaeoecology, 274: 196-203.

Shen, Y., Buick, R. and Canfield, D.E., 2001. Isotopic evidence for microbial sulphae reduction in the early Archaean era. 410: 77-81.

Shieh, Y.-T., You, C.-F., Shea, K.-S. and Horng, C.-S., 2002. Identification of diagenetic artifacts in foraminiferal shells using carbon and oxygen isotopes. Journal of Asian Earth Sciences, 21: 1-5.

Showers, W.J., Lent, R.M. and Margolis, S.V., 1987. BSEM evaluation of carbonate diagenesis: Benthic foraminifera from the Miocene Pungo River Formation, North Carolina. Geology, 15: 731-734.

Sibuet, M. and Olu, K., 1998. Biogeography, biodiversity and fluid dependence of deep-sea cold-seep communities at active and passive margins. Deep-Sea Research II, 45: 517-567.

Smith, C.R. and Baco, A., 1998. Phylogenetic and functional affinities between whale-fall, seep and vent chemoautotrophic communities. Les Cahiers de Biologie Marine, 39: 345-346.

Snavely, P.D. and Wells, R.E., 1996. Cenozoic evolution of the continental margin of Oregon and Washington. In: A.A. Rogers, T.J. Walsh, W.J. Kockelman and G.R. Priest (Editors), Assessing earthquake hazards and reducing risk in the Pacific Northwest: United States. United States Geological Survey Professional Paper. United States Government Printing Office, Washington, pp. 161-182.

Sommer, S., Linke, P., Pfannkuche, O., Niemann, H. and Treude, T., 2009 online. Benthic respiration in a novel seep habitat dominated by dense beds of ampharetid polychaetes at the Hikurangi Margin (New Zealand). Marine Geology.

Sommer, S. et al., 2006. Efficiency of the benthic filter: Biological control of the emission of dissolved methane from sediments containing shallow gas hydrates at Hydrate Ridge. Global Biogeochemical Cycles, 20(GB2019): doi:10.1029/2004GB002389.2006.

Spirakis, C.S. and Heyl, A.V., 1988. Possible effects of thermal degradation of organic matter on carbonate paragenesis and fluorite precipitation in Mississippi Valley-type deposits. Geology, 16: 1117-1120.

Squires, R. and Goedert, J., 1991. New Late Eocene mollusks from localized limestone deposits formed by subduction-related methane seeps, Southwestern Washington. Journal of Paleontology, 65(3): 412-416.

Stadnitskaia, A. et al., 2008. Carbonate formation by anaerobic oxidation of methane: Evidence from lipid biomarker and fossil 16S rDNA. Geochimica et Cosmochimica Acta, 72: 1824-1836.

Stakes, D.S., OrangeD.L., Paduan, J.B., Salamy, K.A. and Maher, N., 1999. Cold-seeps and authigenic carbonate formation in Monterey Bay, California. Marine Geology, 159: 93-109.

Stephenson, A.E. et al., 2008. Peptides enhance magnesium signature in calcite: Insight in origins of vital effects. Science, 322: 724-727.

Stewart, R.J., Brandon, M.T., Campbell, K.A., Nesbitt, E.A. and Pazzaglia, F.J., 2003. Tectonic Surfing: Evidence of Rapid Landward Transport in the Cascadia Subduction Wedge, NW Washington State, Eos Trans. AGU, 84(46), Fall Meet. Suppl., Abstract S42A-0146
.

Stewart, R.L. and Brandon, M.T., 2004. Detrital fission track ages for the "Hoh Formation": implications for late Cenozoic evolution of the Cascadia subduction wedge. Geological Society of America Bulletin, 116: 60-75.

Stott, L.D. et al., 2002. Does the oxidation of methane leave an isotopic fingerprint in the geologic record? Geochemistry, Geophysics, Geosystems, 3(2).

Stott, L.D. and Kennett, J.P., 1989. New constraints on early Tertiary palaeoproductivity from carbon isotopes in foraminifera. Nature, 342: 526-529.

Suess, E. et al., 1985. Biological communities at vent sites along the subduction zone off Oregon. In: M.L. Jones (Editor), The hydrothermal vents of the eastern Pacific: An Overview. Biological Society of Washington Bulletin, pp. 475-484.

Suess, E. et al., 2001. Sea floor methane hydrates at Hydrate Ridge, Cascadia Margin. In: C.K. Paull and W.P. Dillon (Editors), Natural Gas Hydrates: Occurrence, Distribution and Detection. American Geophysical Union Geophysical Monograph, Washington, D.C., pp. 87-98.

Suess, E. et al., 1999. Gas hydrate destabilization: enhanced dewatering, benthic material turnover and large methane plumes at the Cascadia convergent margin. Earth and Planetary Science Letters, 170: 1-15.

Suess, E. and Whiticar, M.J., 1989. Methane-derived CO2 in pore fluids expelled from the Oregon subduction zone. Palaeoceanography, Palaeoclimatology, Palaeoecology, 71: 119-136.

Svensen, H. et al., 2004. Release of methane from a volcanic basin as a mechanism for initial Eocene global warming. Nature: doi:10.1038/nature02566.

Taylor, P.D. and Wilson, M.A., 2003. Palaeoecology and evolution of marine hard substrate communities. Earth-Science Reviews, 62: 1-103.

Teichert, B.M.A., Bohrmann, G. and Suess, E., 2005. Chemoherms on Hydrate Ridge - Unique microbially-mediated carbonate build-ups growing into the water column. Paleogeography, Paleoclimatology, Paleoecology, 227: 67-85.

Teichert, B.M.A. et al., 2003. U/Th Systematics and ages of authigenic carbonates from Hydrate Ridge, Cascadia Margin: Recorders of fluid flow variations. Geochimica et Cosmochimica Acta, 67(20): 3845-3857.

Thauer, R.K., Kaster, A.-K., Seedorf, H., Buckel, W. and Hedderich, R., 2008. Methanogenic archaea: ecologically relevant differences in energy conservation. Nater Reviews Microbiology, 6: 579-591.

Thiel, V. et al., 2001. Molecular signals for anaerbic methane oxidation in Black Sea seep carbonates and a microbial mat. Marine Chemistry, 73: 97-112.
Thiel, V. et al., 1999. Highly isotopically depleted isoprenoids: Molecular markers for ancient methane venting. Geochimica et Cosmochimica Acta, 63: 3959-3966.

Thomas, D.J., Zachos, J.C., Bralower, T.J., Thomas, E. and Bohaty, S., 2002. Warming the fuel for the fire: Evidence for the thermal dissociation of methane hydrate during the Paleocene-Eocene thermal maximum. Geology, 30(12): 1067-1070.

Thurber, A.R., Kroeger, K., Neira, C., Wiklund, H. and Levin, L., 2009 online. Stable isotope signatures and methane use by New Zealand cold seep benthos. Marine Geology.

Tomaru, H., Lu, Z., Fehn, U., Muramatsu, Y. and Matsumoto, R., 2007a. Age variation of pore water iodine in the eastern Nankai Trough, Japan: Evidence for different methane sources in a large gas hydrate field. Geology, 35: 1015-1018.

Tomaru, H., Matsumoto, R., Torres, M.E. and Borowski, W.S., 2006. Geological and geochemical constraints on the isotopic composition of intersitial waters from the Hydrate Ridge region, Cascadia continental margin. In: A.m. Trehu, G. Bohrmann, M.E. Torres and F. Colwell, S. (Editors), Proceedings of the Ocean Drilling Program, Scientific Results, pp. 19 pp.

Tomaru, H., Zunli, L., Fehn, U., Muramatsu, Y. and Matsumoto, R., 2007b. Age variation of pore water iodine in the eastern Nankai Trough, Japan: Evidence for different methane sources in a large gas hydrate field. Geology, 35: 1015-1018.

Torres, M., Bohrmann, G., Dube, T.E. and Poole, F.G., 2003a. Formation of modern and Paleozoic stratiform barite at cold methane seeps on continental margins. Geology, 31(10): 897-900.

Torres, M. et al., Submitted-a. Methane feeding cold seeps on the shelf and upper continental slope off Central Oregon, USA.

Torres, M., Martin, R.A., Klinkhammer, G.P. and Nesbitt, E.A., submitted. Post depositional alteration of foraminifera shells in cold seep settings: New insights from Flow-Through analyses. Earth and Planetary Science Letters.

Torres, M. et al., 2003b. Is methane venting at the seafloor recorded by the d13C of benthic foraminifera shells? Paleoceanography, 18: 1062-1075.

Torres, M.E. and Kastner, M., 2009. Data report: clues about carbon cycling in methane-bearing sediments using stable isotopes of the dissolved inorganic carbon. Proceedings of the Integrated Ocean Drilling Program, 311.

Torres, M.E. et al., 2002. Fluid and chemical fluxes in and out of sediments hosting methane hydrate deposits on Hydrate ridge, OR, I: Hydrological provinces. Earth and Planetary Science Letters, 201: 525-540.

Trehu, A.M., Torres, M.E., Moore, G.F., Suess, E. and Bohrmann, G., 1999. Temporal and spatial evolution of a gas hydrate bearing accretionary ridge on the Oregon continental margin. Geology, 27(939-942).

Treude, T., Boetius, A., Knittel, K., Wallmann, K. and Jorgensen, B.B., 2003. Anaerobic oxidation of methane above gas hydrates at Hydrate Ridge, N.E. Pacific Ocean. Marine Ecology Progress Series, 264: 1-14.

Tryon, M.D. and Brown, K., 2001. Complex flow patterns through Hydrate Ridge and their impact on seep biota. Geophysical Research Letters, 28(14): 2863-2866.

Tryon, M.D. et al., 1999. Measurements of transience and downward fluid flow near episodic methane gas vents, Hydrate Ridge, Cascadia. Geology, 27: 1075-1078.

Tryon, M.D., Brown, K.M. and Torres, M.E., 2002. Fluid and chemical flux in and out of sediments hosting methane hydrate deposits on Hydrate Ridge, OR, II: Hydrological processes. Earth and Planetary Science Letters, 201: 541-557.

Tunnicliffe, V., 1992. The nature and origin of the modern hydrothermal vent fauna. Palaios, 7: 338-350.

Tunnicliffe, V., Juniper, S.K. and Sibuet, M., Reducing environments of the deep-sea floor, pp. 81-110.

Ueno, Y., Yamada, K., Yoshida, N., Maruyama, S. and Isozaki, Y., 2006. Evidence from fluid inclusions for microbial methanogenesis in the early Archaean era. Nature, 440: 516-519.

Ussler, W.I. and Paull, C.K., 1995. Effects of ion exclusion and isotopic fractionation on pore water geochemistry during gas hydrate formation and decomposition. Geo-Marine Letters, 15: 37-44.

Valentine, D.L., 2002. Biogeochemistry and microbial ecology of methane oxidation in anoxic environments: a review. Antonie van Leeuwenhoek, 81: 271-282.

Valentine, D.L. and Reesburgh, W.S., 2000. New perspectives on anaeroic methane oxidation. Environmental Microbiology, 2(5): 477-484.

Veizer, J., Godderis, Y. and Francois, L.M., 2000. Evidence for decoupling of atmospheric CO2 and global climate during the Phanerozoic eon. Nature, 408: 698-701.

Venec-Peyre, M.-T., 1996. Bioeroding foraminifera: a review. Marine Micropaleontology, 28: 19-30.

von Rad, U. et al., 1996. Authigenic carbonates derived from oxidized methane vented from the Makran accretionary prism off Pakistan. Marine Geology, 136: 55-77.

Watanabe, Y., Nakai, S.i., Hiruta, A., Matsumoto, R. and Yoshida, K., 2008. U-Th dating of carbonate nodules from methane seeps off Joetsu, Eastern margin of Japan Sea. Earth and Planetary Science Letters, 272: 89-96.

Wefer, G., Heinz, P.M. and Berger, W.H., 1994. Clues to ancient methane release. Nature, 369: 282.

Weiner, S. and Dove, P.M., 2003. An overview of biomineralization processes and the problem of the vital effect. In: P.M. Dove, J.J. De Yoreo and S. Weiner (Editors), Biomineralization. Reviews in Mineralogy and Geochemistry. Mineralogical Society of America, Washington, pp. 1-29.

Wells, R.E., Weaver, C.S. and Blakely, R.J., 1998. Fore-arc migration in Cascadia and its neotectonic significance. Geology, 26(8): 759-762.

Werne, J.P. et al., 2004. Life at cold seeps: a synthesis of biogeochemical and ecological data from Kazan mud volcano, eastern Mediterranean Sea. Chemical Geology, 205: 367-390.

Whiticar, M., 1994. Correlation of natural gases with their sources. In: L.B. Magoon and G. Dow (Editors), The petroleum system - from source to trap, pp. 261-283.

Whiticar, M.J., 1999. Carbon and hydrogen isotope systematics of bacterial formation and oxidation of methane. Chemical Geology, 161: 291-314.

Whiticar, M.J. and Faber, E., 1986. Methane oxidation in sediment and water column environments - isotope evidence. Organic Geochemistry, 10: 759-768.

Wiedicke, M. and Weiss, W., 2006. Stable carbon isotope records of carbonates tracing fossil seep activity off Indonesia. Geochemistry, Geophysics, Geosystems, 7(11): Q11009, doi:10.1029/2006GC001292
.

Wilson-Finelli, G.T., Chandler, G.T. and Spero, H.J., 1998. Stable isotope behavior in paleoceanographically important benthic foraminifera: results from microcosm culture experiments. Journal of Formaminiferal Research, 28(4): 312-320.

Wollenburg, J.E. and Mackensen, A., 2009. The ecology and distribution of benthic foraminifera at the Hakon Mosby muc volcano (SW Barents Sea slope). Deap-Sea Research I - Oceanographic Research Papers, 56(8): 1336-1370.

Zachos, J., Pagani, M., Sloan, L., Thomas, E. and Billups, K., 2001. Trends, rhythms, and aberrations in global climate 65 ma to present. Science, 292: 686-693
.

Zampi, M., Benocci, S. and Focardi, S., 1997. Epibiont foraminifera of *Sertella frigida* (Waters) (Bryozoa, Cheilostomata) from Terranova Bay, Ross Sea, Antarctica. Polar Biology, 17: 363-370.

Zeebe, R.E., 2007. Modeling CO_2 chemisty, $\delta^{13}C$, and oxidation of organic carbon and methane in sediment porewater: Implications for paleo-proxies in benthic foraminifera. Geochimica et Cosmochimica Acta, 71: 3238-3256.

Zhang, C.L. and Lanoil, B., 2004. Geomicrobiology and biogeochemistry of gas hydrates and cold seeps. Chemical Geology, 205: 187-194.

Zumwalt, G.S. and DeLaca, T.E., 1980. Utilization of brachiopod feeding currents by epizoic foraminifera. Journal of Paleontology, 54(2): 477-484.

Zyakun, A.M., 1992. Isotopes and their possible use as biomarkers of microbial products. In: R. Vially (Editor), Bacterial Gas. Editions Technip, Paris, pp. 27-46.

CURRICULUM VITA

PROFESSIONAL EXPERIENCE

2004-present University of Washington
- Graduate student
- Teaching assistant
  - Geobiology
  - Dinosaurs!
  - Evolution of Earth
- Research assistant
  - Collections reassessment, Vertebrate Paleontology, Burke Museum

1986-2004 Edmonds School District, Lynnwood, Washington
Teacher: Science, Health, and Mathematics at the middle school level
- Science Department chair, 1994 - 2003

1997-98 Antioch University, Seattle, Washington
Instructor: Science Teaching Methods for Elementary Teachers

1995-2005 University of Hawaii
Certified national trainer, Foundational Approaches in Science Teaching

1972 - 1982 University of Cape Town, Republic of South Africa
Research Officer, Marine Geoscience Unit
Lecturer: General Geology, Invertebrate paleontology, Geomorphology

PROFESSIONAL ACTIVITIES AND AFFILIATIONS

Member: Paleontological Society, Geological Society of America, Cushman Foundation for Foraminiferal Research, Micropalaeontological Society, National Science Teachers Association
Adjunct Instructor: Seattle Pacific University, Portland State University, University of Rio Grande, Ohio
Presenter: An Ocean of Air inquiry-based teacher workshops on weather and air pollution.
Institute for Systems Biology OEL Scientist

PUBLICATIONS

ABSTRACTS

Martin, R.A. and Nesbitt, E.A., 2004, *Benthic foraminiferal characteristics of a diffuse Pliocene mid-shelf hydrocarbon seep, Cascadia convergent margin,* Geological Society of America *Abstracts with Programs*, Vol. 36, No. 5, p. 59.

Martin, R.A. and Nesbitt, E.A., 2005. *Benthic foraminiferal characteristics of Cenozoic cold seeps, Northeast Pacific margin.* American Association of Petroleum Geologists, *Abstracts with Programs*. p. 76.

Martin, R.A., Nesbitt, E.A., Campbell, K.A., 2005. *Benthic foraminiferal characterization of two Cenozoic cold seeps, Cascadia accretionary margin*. Third International Symposium on Hydrothermal Vent and Seep Biology, *Abstracts with Programs*, p. 27.

Martin, R.A., Nesbitt, E.A., 2007. *Characteristics of methane-influenced fluid-flow in Oligocene-Miocene sediments of the Cascadia margin.* Geological Society of America. V. 39, No. 6, p. 304.

Boyd, S., Alfaro, A.C., Campbell, K.A., Gregory, M.R., Zemke-White, L., **Martin, R**., and Wallis, I., 2007. *Faunal assemblages and sediment characteristics of hydrocarbon seeps in the Hikurangi Margin, eastern North Island, New Zealand*. New Zealand Marine Sciences Society Annual Conference.

Martin, R.A., Torres, M., Klinkhammer, G., Campbell, K.A., Nesbitt, E.A., Sommer, S., 2008, *The effects of methane-influenced pore-waters on benthic foraminiferal assemblages from the*

Hikurangi Margin of eastern New Zealand. European Geosciences Union Annual Meeting, Vienna, April, 2008.

Martin, R.A., Nesbitt, E.A., Campbell, K.A., 2009. The effects of methane seepage on benthic foraminifera from the Hikurangi Margin of New Zealand. Geological Society of America *Abstracts with Programs*, Vol. 41, No. 7, p. 450

PAPERS

Martin, R.A., Nesbitt, E.A., Campbell, K.A., 2007. *Carbon stable isotopic composition of benthic foraminifera from Pliocene cold methane seeps, Cascadia accretionary margin*. submitted to *Palaeogeography, Palaeoclimatology, Palaeoecology.* V. 246: p. 260-277

Martin, R.A. 2008. *Foraminifers as hard substrates: an example from the Washington continental shelf of smaller foraminifers attached to larger, agglutinate foraminifers*. *Journal of Foraminiferal Research*. vol. 38, no. 1

Martin, R.A., Nesbitt, E. A., Campbell, K.A., 2009. *The effects of anaerobic oxidation of methane on benthic foraminiferal assemblages and stable isotopes from the Hikurangi Margin of eastern New Zealand. Marine Geology.* Online.

Torres, M.A., Martin, R.A., Klinkhammer, G., in prep. *Post depositional alteration of foraminifera shells in cold seep settings: New insights from Flow-Through analyses.* To be submitted to *Earth and Planetary Science Letters*.

Nesbitt, E.A., **Martin, R.A**., Carroll, N., Grieff, J., 2009. *Reassessment of the Zemorrian foraminiferal Stage and Juanian molluscan Stage north of the Olympic Mountains, Washington State and Vancouver Island. Newsletters on Stratigraphy.*

Nesbitt, E.A., **Martin, R.A**., Campbell, K.A., and Aharon, P., In prep. *Diffuse hydrocarbon seeps and organism signatures in the stratigraphic record*. to be submitted to *Palaeogeography, Palaeoclimatology, Palaeoecology*

Martin, R.A, 1981. *Benthic foraminifera from the Orange-Luderitz shelf, southern African continental margin*. Joint Geological Survey/University of Cape Town Marine Geoscience Unit Bulletin No. 11, 65 p.

Martin, R.A. 1980. *Benthic foraminifera from the west coast of southern Africa*. Joint Geological Survey/University of Cape Town Marine Geoscience Unit Technical Report No. 8, p. 23-45.

EDUCATION

Ph.D. (Earth and Space Sciences), 2010, University of Washington, Seattle, Washington
Teaching Certificate (K-8; Earth Science; General Science) 1991, Western Washington University.
Master of Science (Geology), University of Cape Town, Republic of South Africa, 1981
Bachelor of Science (Honours) (Geology), University of Cape Town, Republic of South Africa, 1972
Bachelor of Arts (Geology), 1969, Colorado College, Colorado Springs

HONORS

NAMS Student PosterAward/Travel Grant 2004
Presidential Award for Excellence in Science Teaching, 1998
Pacific Science Center/Ackerly Foundation Middle Level Teacher of the Year 1998
Chevron Best Classroom Practices Bright Idea Award 1997
Washington Science Teachers' Association Middle Level Teacher of the Year 1996
Washington State Department of Ecology Magic Apple Award 1994
Rocky Mountain Association of Petroleum Geologists Award 1969
Phi Beta Kappa, Magna cum laude 1969

RESEARCH ADVISOR

Dr. Elizabeth Nesbitt, Associate Professor, Department of Earth and Space Sciences, University of Washington; Curator of Vertebrate Paleontology, Burke Museum, University of Washington.
Telephone: 206-543-5949. E-mail: lnesbitt@u.washington.edu